BEILSTEIN JOURNAL OF ORGANIC CHEMISTRY

Copper catalysis: a constantly evolving field

Edited by Jaesook Yun and Elena Fernández

Imprint

Beilstein Journal of Organic Chemistry
www.bjoc.org
ISSN 1860-5397
Email: journals-support@beilstein-institut.de

The *Beilstein Journal of Organic Chemistry* is published by the Beilstein-Institut zur Förderung der Chemischen Wissenschaften.

Beilstein-Institut zur Förderung der Chemischen Wissenschaften
Trakehner Straße 7–9
60487 Frankfurt am Main
Germany
www.beilstein-institut.de

BEILSTEIN JOURNAL OF ORGANIC CHEMISTRY

Copper catalysis: a constantly evolving field

Elena Fernández[*1] and Jaesook Yun[*2]

Editorial

Open Access

Address:
[1]Departament de Química Física i Inorgànica, University Rovira i Virgili, Tarragona, Spain and [2]Department of Chemistry, Sungkyunkwan University, Suwon 16419, Republic of Korea

Email:
Elena Fernández[*] - mariaelena.fernandez@urv.net; Jaesook Yun[*] - jaesook@skku.edu

* Corresponding author

Keywords:
copper; copper catalysis

Beilstein J. Org. Chem. **2025,** *21,* 1477–1479.
https://doi.org/10.3762/bjoc.21.109

Received: 27 June 2025
Accepted: 02 July 2025
Published: 17 July 2025

This article is part of the thematic issue "Copper catalysis: a constantly evolving field".

Guest Editors: J. Yun and E. Fernández

Copper catalysis continues to thrive as one of the most dynamic and versatile areas of contemporary chemical research. Once viewed primarily as a cost-effective alternative to noble metals, copper has emerged as a powerful and versatile catalyst, capable of mediating a wide array of chemical transformations through both two-electron and single-electron pathways. This duality has enabled access to previously elusive molecular transformations, positioning copper at the center of modern synthetic strategy.

This thematic issue captures the dynamic nature of the field, featuring five insightful Review articles and five original research papers (three Full Research Papers and two Letters) contributed by scientists from Asia and Europe. The breadth of topics and the geographical diversity of the authors reflect the global interest in copper catalysis today.

The Review article by Yang and Fang focuses on copper-catalyzed yne–allylic substitution reactions [1]. In particular, the authors elaborate the concept and recent developments in this field, which allows access to enantioenriched chiral enynes. Interestingly, the article also illustrates the effects of the copper salt and the ligand employed, as well as the influence of the substrate substitution pattern on the regioselectivity and stereoselectivity of the reactions. A Review article by Papis and co-workers discusses various copper(II) triflate-catalyzed multicomponent reaction types [2]. Therein, the synthesis of cyclic and acyclic compounds, as well as three-component and four-component reactions, are separately debated. In addition, mechanistic insights into the reaction of heteropolycyclic systems, cycloadditions, and aza-Diels–Alder reactions are provided. This is important because multicomponent, one-pot reactions have gained interest as potentially more economic, efficient, and straightforward reactions. Complementarily, the Review article by Jang and Kim provides a deep understanding of recent advances in the combination of electrochemistry and copper catalysis for various organic transformations [3]. Their contribution elaborates various C–H functionalizations, olefin additions, decarboxylative functionalizations, and Chan–Lam coupling reactions. In doing so, the authors point out the combination of transition-metal catalysis and electrochemistry as an efficient, sustainable method for the oftentimes challenging formation of C–C and C–heteroatom bonds in complex molecules. Another Review by Son and co-workers illustrates recent advancements

in the use of dioxazolones in synthetic transformations with copper salts [4]. The authors remark that these catalytic systems, which employ dioxazolones as electrophilic amide sources, were applied for the preparation of diverse amidated products. In their contribution, Son et al. focus on transformations via the formation of copper nitrenoids, particularly amidations via oxidative insertion to N–O bonds and reductive elimination, and a small number of other reactions. The final Review by Cho, Lee, and co-workers is useful for the scientific community in that it elegantly reviews recent advances in allylation reactions of copper-catalyzed asymmetric allylic substitution reactions of chiral secondary alkylcopper species [5]. In summary, the contribution includes stereospecific transmetalations of organolithium and -boron compounds, copper hydride catalysis, and enantiotopic group-selective allylations of 1,1-diborylalkanes as core strategies. At the same time, the authors provide detailed mechanistic insights into the stereocontrol and provide a perspective on currently unresolved challenges in the field.

Concerning Full Research Papers, Burley, Watson, and co-workers present a new synthesis of germyl triazoles from germyl alkynes through a copper-catalyzed azide–alkyne cycloaddition (CuAAC) reaction [6]. The resulting Ge-substituted triazoles could be further diversified. For example, through chemoselective transition-metal-catalyzed cross-coupling reactions of bifunctional boryl- and germyl-containing compounds. On the other hand, a Full Research Paper presented by Lee and co-workers introduces a highly regioselective formal hydrocyanation method of allenes [7]. The strategy is based on a copper-catalyzed hydroalumination of allenes with diisobutylaluminum hydride, which is followed by the allylation with *p*-toluenesulfonyl cyanide in a regio- and stereoselective manner. They propose a new way to access accessing acyclic β,γ-unsaturated nitriles with α-all-carbon quaternary centers. In the process, they managed to achieve a yield of up to 99%, with excellent regio- and *E*-selectivities. The method could be used for functional-group transformations of amines, amides, and lactams, as well as for gram-scale syntheses, demonstrating synthetic usefulness and versatility. A complementary Full Research Paper by Martina and co-workers demonstrates that the efficient and green direct C–H amination of benzoxazoles can be catalyzed by copper chloride salts in acetonitrile in the absence of any acidic, basic, or oxidizing additives [8]. Both CuCl and $CuCl_2$ were found to be extremely efficient in promoting the reactions, which harness their Lewis-acidic and weakly oxidizing properties, respectively. In addition, microwave irradiation increases the reaction rate considerably. Furthermore, the use of a solid Cu(I) catalyst immobilized on an aminated silica support allows for a heterogeneous and cost-effective process, featuring straightforward workup and minimized free copper on solution. Due to this, the catalyst could be regenerated and reused in up to eight cycles. Upon optimization, this practical and versatile method could be used for the synthesis of several benzoxazole derivatives.

A Letter was contributed by D'Andrea and Jademyr, who focus on the preparation of phenethylamines and phenylisopropylamines via reduction of substituted β-nitrostyrenes using a system of sodium borohydride and copper(II) chloride [9]. The transformations are performed in one pot and proceed under mild conditions. The β-nitrostyrene products could be isolated quickly and in good yield, without the need for time-consuming purification steps. At the same time, no cumbersome precautions, such as an inert atmosphere, are necessary. Another fantastic Letter was contributed by Fañanás-Mastral and co-workers, in which a rare copper-catalyzed dimerization process of 4,4-dichloro-2-butenoic acid derivatives and bis(pinacolato)diboron is described [10]. The transformations feature excellent chemo-, regio-, and diastereoselectivities, and the resulting products are highly functionalized. Due to this, they were considered as versatile building blocks for the stereoselective synthesis of chlorocyclopropanes.

As guest editors, we are deeply grateful to all contributors for sharing their high-quality work and valuable perspectives. We also thank the referees for their thoughtful evaluations, which helped maintain the scientific rigor of this collection. We hope this collection inspires further exploration and innovation in this rapidly advancing field.

Elena Fernández and Jaesook Yun

Tarragona and Suwon, June 2025

Data Availability Statement

Data sharing is not applicable as no new data was generated or analyzed in this study.

References

1. Yang, S.; Fang, X. *Beilstein J. Org. Chem.* **2024,** *20,* 2739–2775. doi:10.3762/bjoc.20.232
2. Colombo, S.; Loro, C.; Beccalli, E. M.; Broggini, G.; Papis, M. *Beilstein J. Org. Chem.* **2025,** *21,* 122–145. doi:10.3762/bjoc.21.7
3. Kim, Y.; Jang, W. J. *Beilstein J. Org. Chem.* **2025,** *21,* 155–178. doi:10.3762/bjoc.21.9
4. Lee, S.; Kim, M.; Han, H.; Son, J. *Beilstein J. Org. Chem.* **2025,** *21,* 200–216. doi:10.3762/bjoc.21.12
5. Kim, M.; Kim, G.; Kim, D.; Lee, J. H.; Cho, S. H. *Beilstein J. Org. Chem.* **2025,** *21,* 639–658. doi:10.3762/bjoc.21.51
6. Halford-McGuff, J. M.; Richardson, T. M.; McKay, A. P.; Peschke, F.; Burley, G. A.; Watson, A. J. B. *Beilstein J. Org. Chem.* **2024,** *20,* 3198–3204. doi:10.3762/bjoc.20.265

7. Lim, S.; Kim, T.; Lee, Y. *Beilstein J. Org. Chem.* **2025,** *21,* 800–806. doi:10.3762/bjoc.21.63
8. Paraschiv, A.; Maruzzo, V.; Pettazzi, F.; Magliocco, S.; Inaudi, P.; Brambilla, D.; Berlier, G.; Cravotto, G.; Martina, K. *Beilstein J. Org. Chem.* **2025,** *21,* 1462–1476. doi:10.3762/bjoc.21.108
9. D'Andrea, L.; Jademyr, S. *Beilstein J. Org. Chem.* **2025,** *21,* 39–46. doi:10.3762/bjoc.21.4
10. Gómez-Roibás, P.; Chaves-Pouso, A.; Fañanás-Mastral, M. *Beilstein J. Org. Chem.* **2025,** *21,* 877–883. doi:10.3762/bjoc.21.71

License and Terms

BEILSTEIN JOURNAL OF ORGANIC CHEMISTRY

Copper-catalyzed yne-allylic substitutions: concept and recent developments

Shuang Yang* and Xinqiang Fang*

Review

Open Access

Address:
State Key Laboratory of Structural Chemistry, and Key Laboratory of Coal to Ethylene Glycol and Its Related Technology, Center for Excellence in Molecular Synthesis, Fujian Institute of Research on the Structure of Matter, University of Chinese Academy of Sciences, Fuzhou 350100, China

Email:
Shuang Yang* - yangshuang@fjirsm.ac.cn; Xinqiang Fang* - xqfang@fjirsm.ac.cn

* Corresponding author

Keywords:
copper-catalysis; copper vinyl allenylidene intermediate; 1,3-enyne; 1,4-enyne; yne-allylic substitution

Beilstein J. Org. Chem. **2024,** *20,* 2739–2775.
https://doi.org/10.3762/bjoc.20.232

Received: 09 July 2024
Accepted: 07 October 2024
Published: 31 October 2024

This article is part of the thematic issue "Copper catalysis: a constantly evolving field".

Guest Editor: J. Yun

Abstract

The catalytic (asymmetric) allylation and propargylation have been established as powerful strategies allowing access to enantioenriched α-chiral alkenes and alkynes. In this context, combining allylic and propargylic substitutions offers new opportunities to expand the scope of transition metal-catalyzed substitution reactions. Since its discovery in 2022, copper-catalyzed yne-allylic substitution has undergone rapid development and significant progress has been made using the key copper vinyl allenylidene intermediates. This review summarizes the developments and illustrates the influences of copper salt, ligand, and substitution pattern of the substrate on the regioselectivity and stereoselectivity.

Introduction

Copper is earth-abundant, inexpensive, relatively stable, and low toxic. Copper-catalyzed asymmetric allylic [1-22] and propargylic [23-32] substitutions are effective strategies for constructing new C–C and C–heteroatom bonds vicinal to alkenyl or alkynyl groups, which are highly valuable for downstream synthesis. At present, unstabilized nucleophiles [33-51] are commonly used in Cu-catalyzed allylic substitutions because of the inner-sphere mechanism and relatively harsh reaction conditions such as anhydrous, anaerobic, and low temperatures are usually required (Scheme 1a). Therefore, using stabilized nucleophiles in Cu-catalyzed allylic substitutions is a tremendous challenge. On the other hand, since the pioneering work of van Maarseveen [52] and Nishibayashi [53] groups in 2008, Cu-catalyzed asymmetric propargylic substitutions have made significant progress [54-60]. The protocol allows the use of stabilized nucleophiles via the outer-sphere mechanism, and

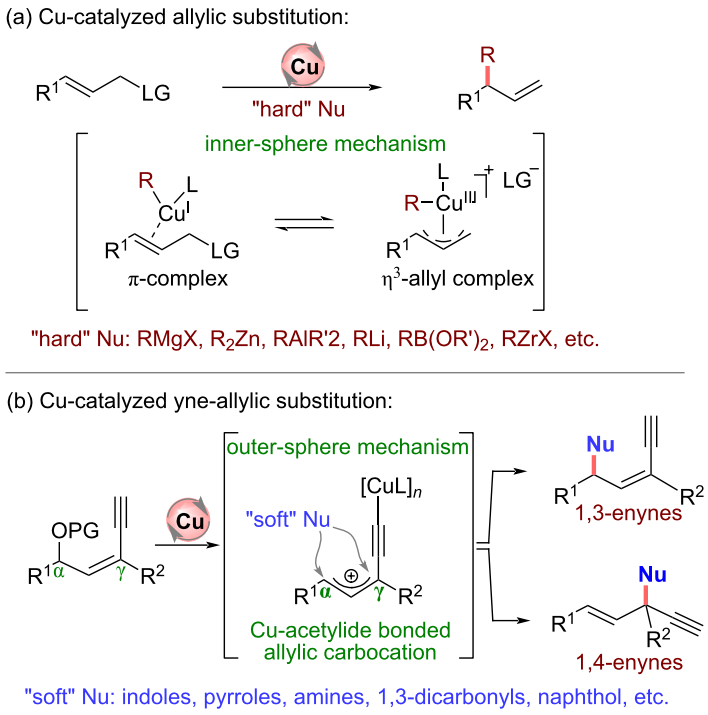

Scheme 1: Copper-catalyzed allylic and yne-allylic substitution.

the copper allenylidene intermediate formed by copper and terminal alkyne is the active species in the reactions. In this regard, merging the unique feature of Cu-catalyzed propargylic substitution with allylic substitution is a feasible solution to the challenge, which will represent a new sort of substitution reaction.

From 2022, the Cu-catalyzed yne-allylic substitution has emerged as a new and robust approach to achieve formal allylic substitution using stabilized nucleophiles. The copper acetylide-bonded allylic cation with copper vinyl allenylidene species as its resonance structure is key for the process, which can achieve the outer-sphere attack of nucleophiles (Scheme 1b). However, to achieve a highly selective yne-allylic substitution, a range of challenges must be addressed. First, how to achieve the regioselectivity under the coexistence of alkenyl and alkynyl units; second, how to realize the enantioselectivity control that is remote from the catalytic center; finally, the selectivity affording *E*-enyne and *Z*-enyne product is also an issue to be addressed, and possible side reactions need to be suppressed (Scheme 2).

In this review, we summarize the recent development of copper-catalyzed yne-allylic substitutions. It is worth noting that when we were preparing this review, another review on copper-catalyzed asymmetric propargylic substitution including some yne-

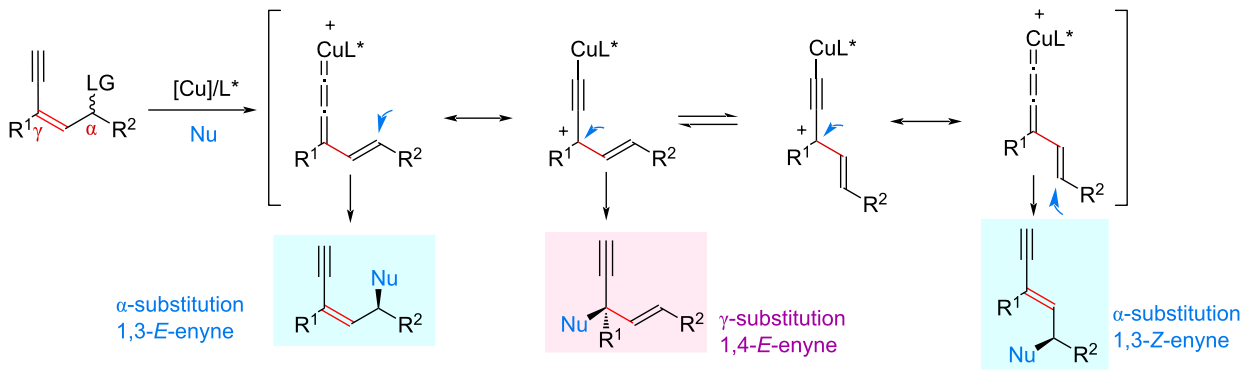

Scheme 2: Challenges in achieving highly selective yne-allylic substitution.

allylic substitutions was reported by Lin et al. [61]. We hope that this review can provide more guidance for the use of new nucleophiles and the development of new reaction modes related to yne-allylic substitutions.

Review

Copper-catalyzed yne-allylic substitutions affording 1,3- and 1,4-enynes

In 2022, Fang et al. [62] realized the copper-catalyzed yne-allylic substitution involving stabilized "soft" nucleophiles for the first time. Indoles and pyrroles with various substituents were found to be suitable for the reaction, delivering 1,3-enynes with medium to high yields and excellent regioselectivities (Scheme 3, **3a**–**e**, **3n**–**p**). Interestingly, when the 3-position of indole was blocked by a methyl group, the 2-position of indole underwent nucleophilic attack with an *E*/*Z* ratio of 2:1 (Scheme 3, **3e**). Carbonates with aryl or styryl residue can undergo the reaction smoothly (Scheme 3, **3f**–**k**), but alkyl-substituted substrates showed low yields (Scheme 3, **3l** and **3m**). Moreover, secondary amines with various substituents, acyclic amines, primary amines, or even the amine moieties in

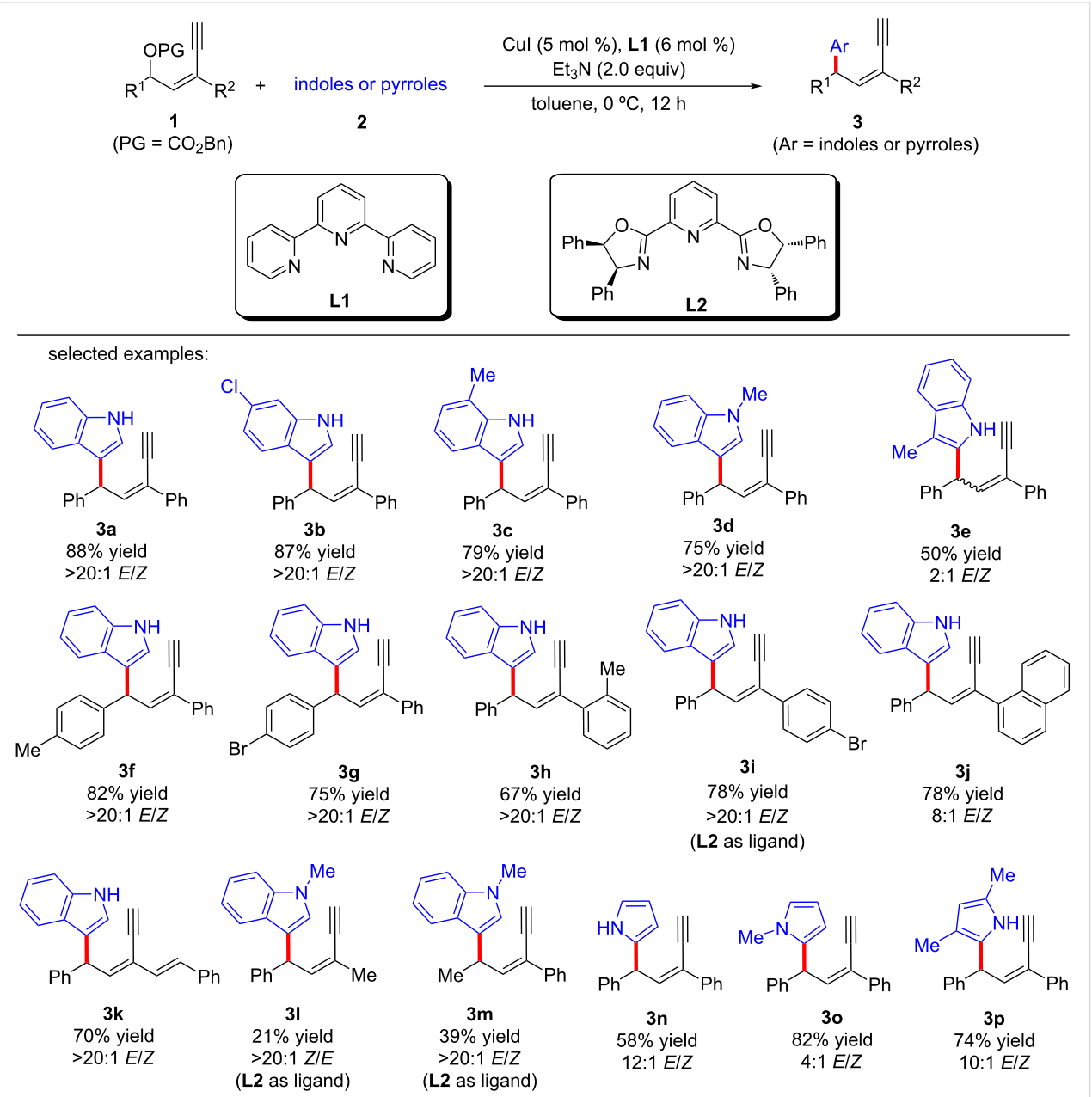

Scheme 3: Yne-allylic substitutions using indoles and pyroles.

drug molecules were all suitable nucleophiles (Scheme 4, **5a**–**k**). When R^2 is an H atom, the reactions occur at the γ-position, resulting in the formation of 1,4-enynes (Scheme 4, **6a**–**d**). Acyclic 1,3-dicarbonyls could also react with yne-allylic carbonates **1** at the γ-position because of the possible chelation interaction between the enolate derived from acyclic 1,3-dicarbonyl compounds and copper (Scheme 5, **8a**–**j**). Detailed control experiments indicate that the terminal alkyne moiety is critical and the reaction proceeds through an S_N1 mechanism. An outer-sphere nucleophilic attack through copper acetylide-bonded allylic cation as the key intermediate is proposed (Scheme 6a). It is worth noting that the nucleophilic attack favors a less sterically hindered site. Therefore, disubstituted alkene moiety prefers γ-attack while trisubstituted alkene moiety is inclined to α-attack (Scheme 6b).

Lin and He et al. [63,64] reported the first amine-mediated highly enantioselective copper-catalyzed asymmetric yne-allylic substitution, affording 1,4-enynes with up to 98% ee and >20:1 rr. A series of secondary amines can react smoothly and achieve good enantioselectivities and regioselectivities (Scheme 7, **6a**–**w**). Interestingly, both Cu(I) and Cu(II) can promote the reaction and the reaction is not sensitive to water (Scheme 7, **6g**). The intramolecular decarboxylative yne-allylic substitution can also be achieved (Scheme 8, **6a**–**u**). *O*-Nucleophiles and *C*-nucleophiles are all suitable reactants, yielding

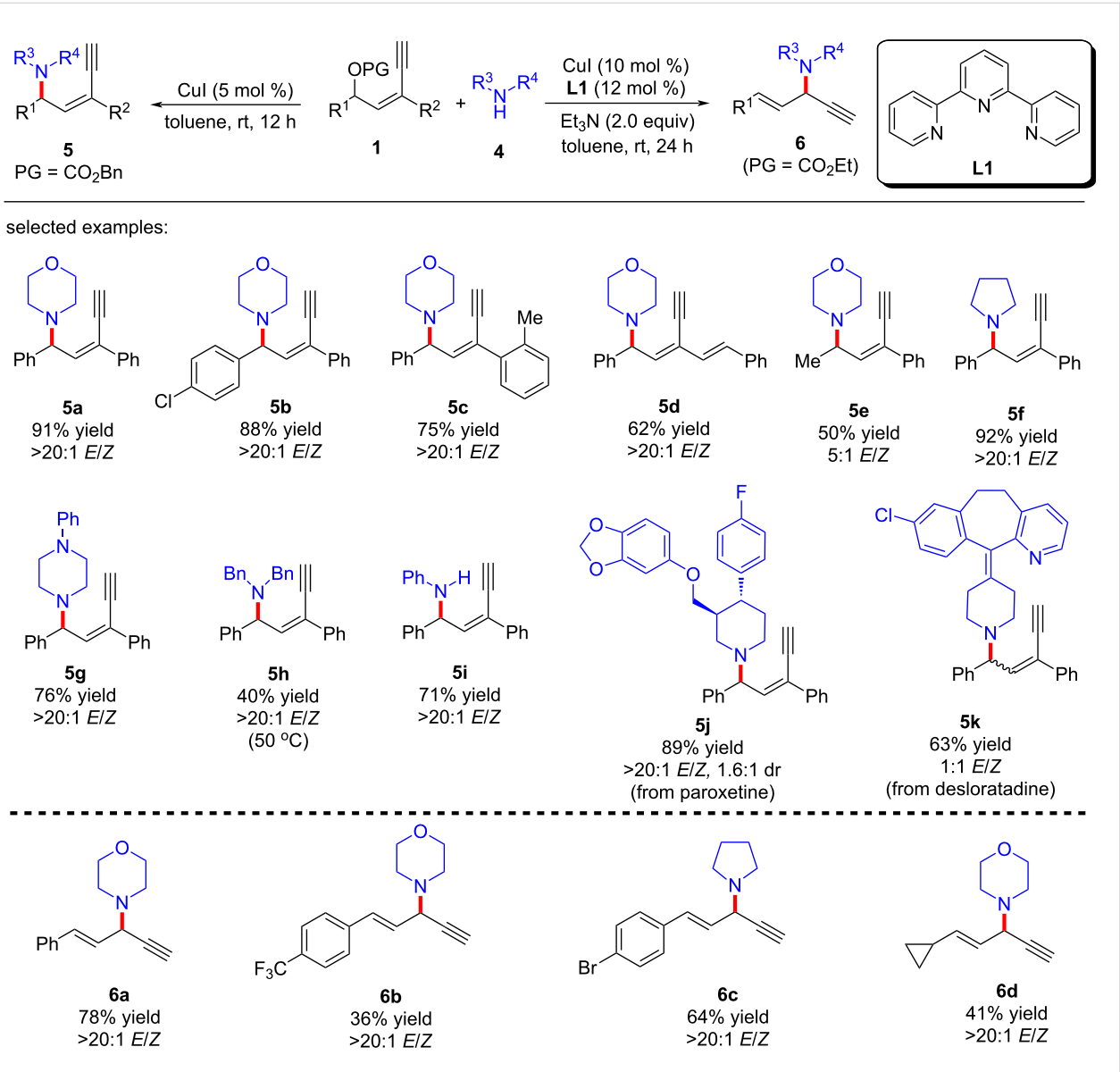

Scheme 4: Yne-allylic substitutions using amines.

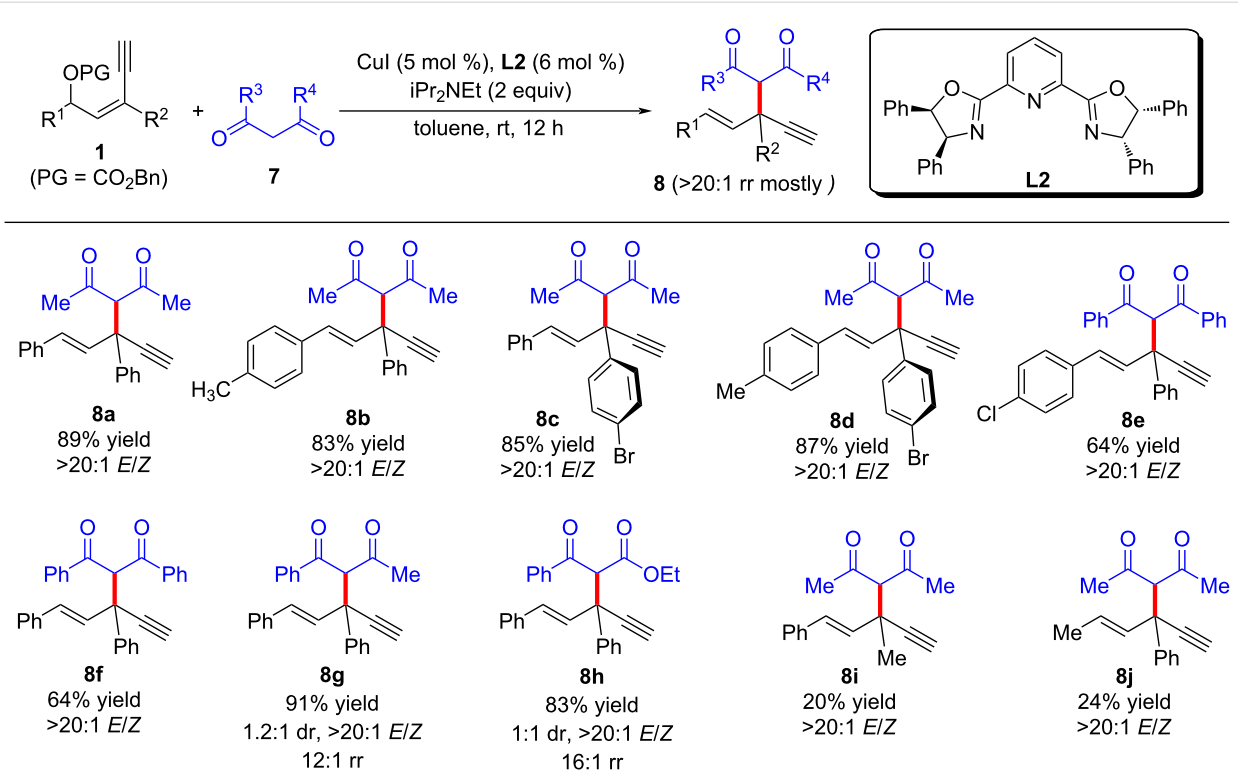

Scheme 5: Yne-allylic substitution using 1,3-dicarbonyls.

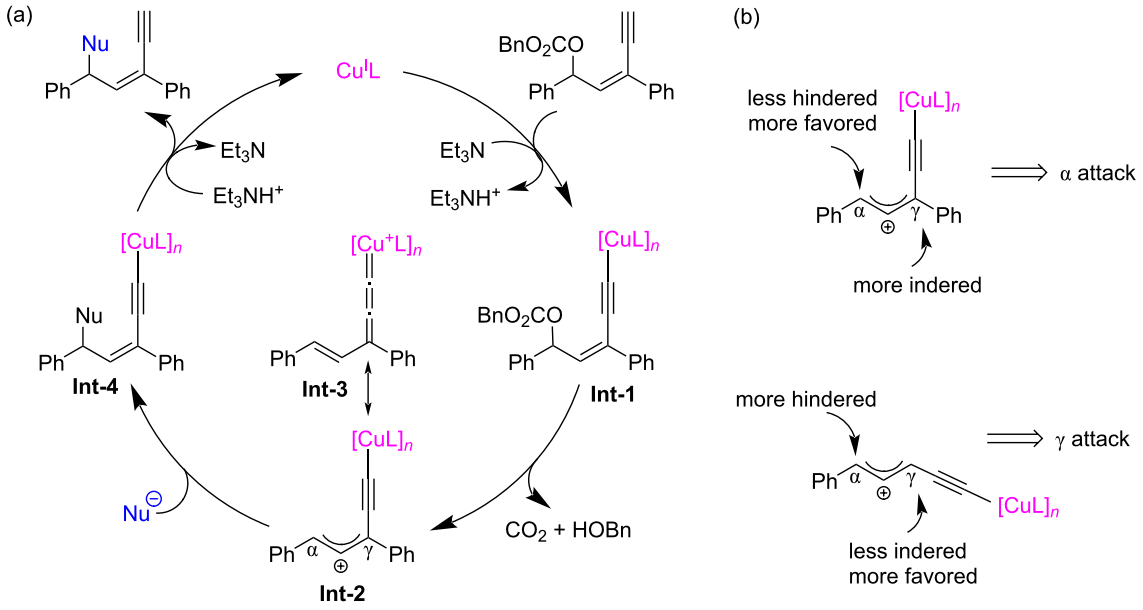

Scheme 6: Postulated mechanism via copper acetylide-bonded allylic cation.

alkoxylation and alkylation products with the assistance of Lewis acid as co-catalyst (Scheme 9). Starting from four different racemic substrates, the same product **6g** with 96% ee was obtained under standard conditions. This indicates that the reactions proceed through the same transition state and the stereocenter of the product is controlled by the catalyst. A single crystal of Cu(I) was investigated by X-ray and proved to be the dicopper complex, while the Cu(II) catalyst was revealed as

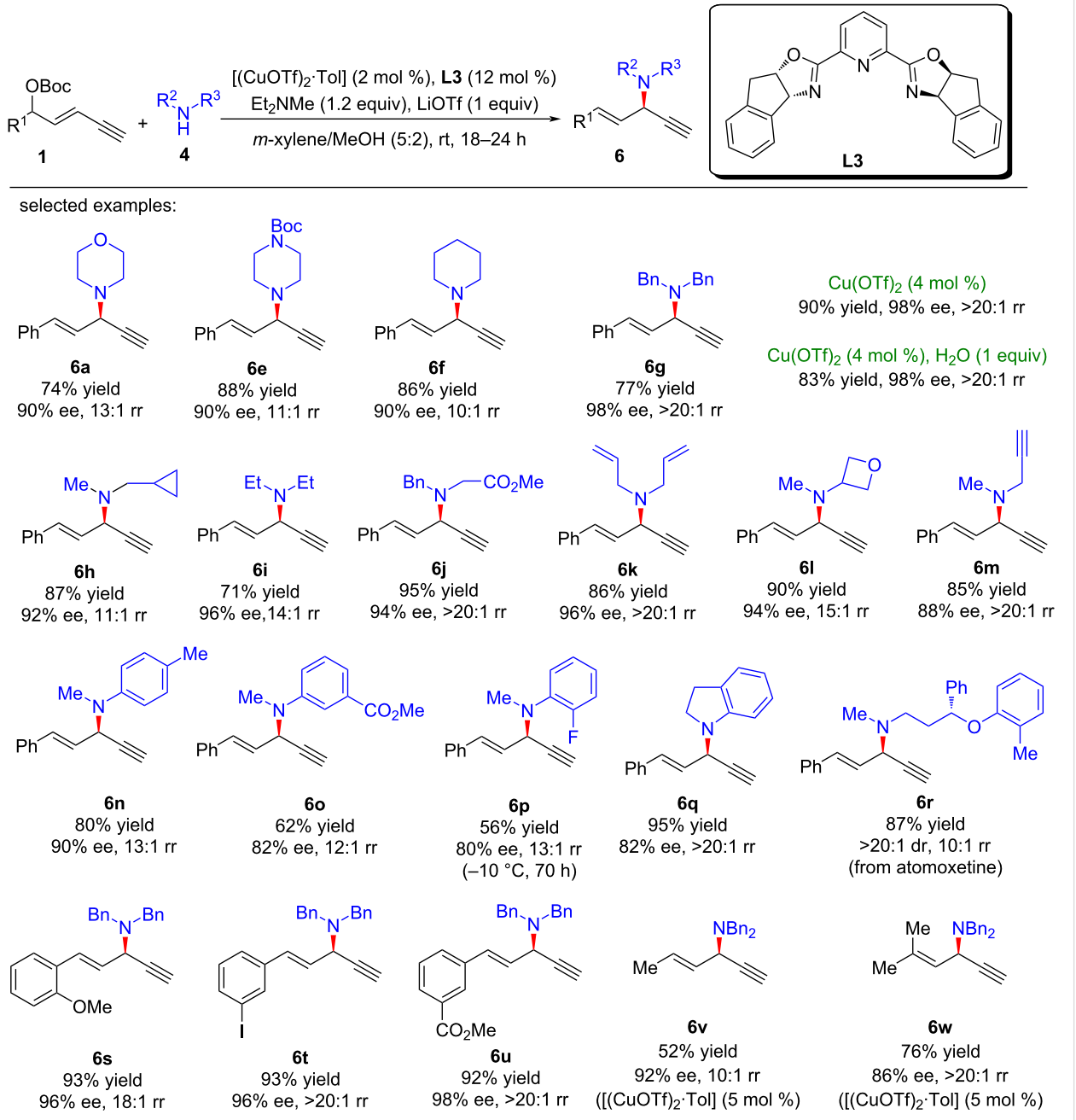

Scheme 7: Amine-participated asymmetric yne-allylic substitution.

mononuclear copper coordinated with two ligands. Further kinetic isotope experiments and nonlinear relationship studies for the Cu(I) system indicate that it is not the formation of alkynyl copper intermediate but the formation of active copper vinyl allenylidene intermediate is the rate-limiting step (Scheme 10).

Due to the gaseous nature of dimethylamine at room temperature, it needs to be stored in special solvents, which further limits the preparation of the related compounds. He et al. [65] used tetramethyldiaminomethane as a suitable surrogate of dimethylamine to achieve the asymmetric dimethylamination of yne-allylic esters, providing an efficient and convenient pathway for the synthesis of enantioenriched 1,4-enynes with dimethylamine moiety (Scheme 11, **6x** and **6y**). In addition to tetramethylenediaminomethane, other tetraalkyldiaminomethanes can also be used as supplants of dialkylamines, leading to products with dialkylamine units with high yields

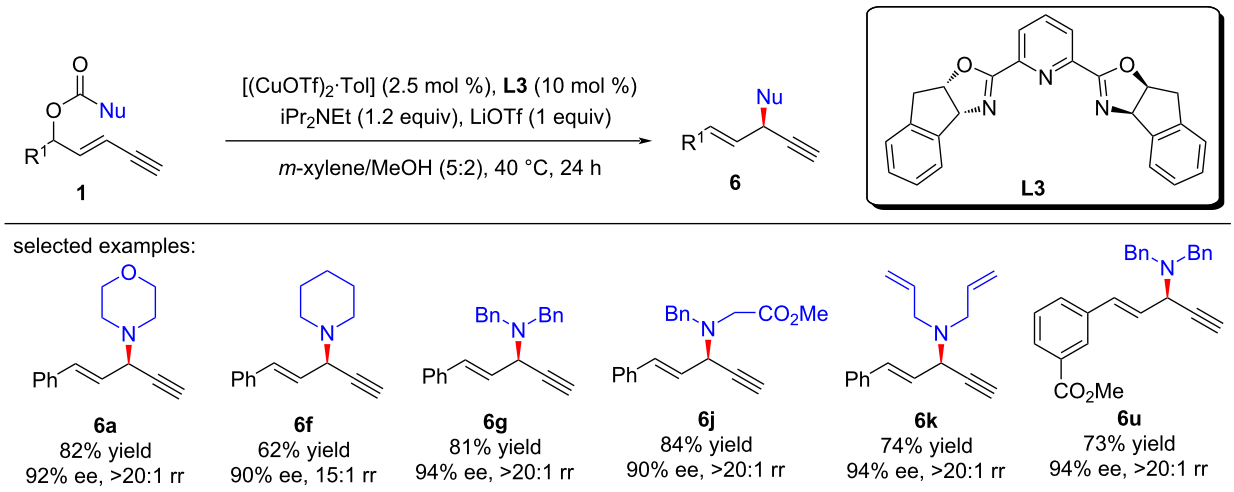

Scheme 8: Asymmetric decarboxylative yne-allylic substitution.

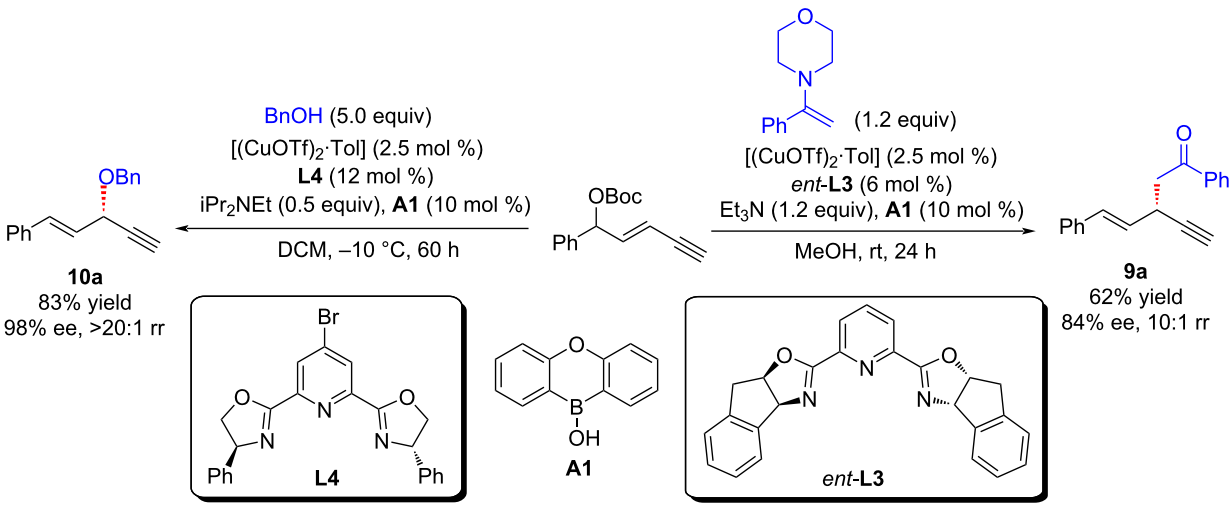

Scheme 9: Asymmetric yne-allylic alkoxylation and alkylation.

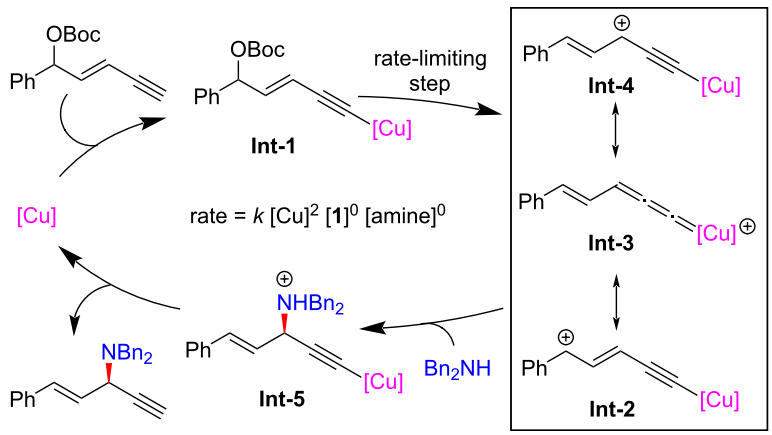

Scheme 10: Proposed mechanism for Cu(I) system.

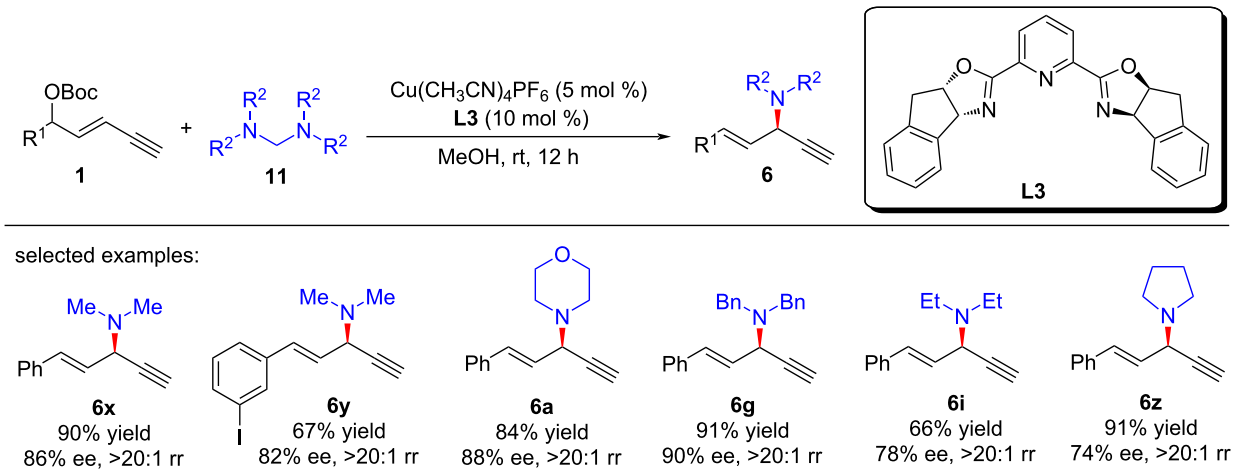

Scheme 11: Asymmetric yne-allylic dialkylamination.

and enantioselectivities (Scheme 11, **6a**, **6g**, **6i** and **6z**). Further control experiments and DFT calculations show that during the catalytic process, tertiary amine directly participates as a nucleophilic reagent to give the ammonium salt, which then releases dimethylaminium to provide the final product (Scheme 12).

Chiral allylic sulfone compounds can be easily transformed into a series of useful molecules, enabling them an important backbone in organic synthesis. Lin et al. [66] used sodium sulfinates as the nucleophiles to realize the asymmetric sulfonylation of yne-allylic esters. The reaction can be carried out under mild conditions with good to excellent regio-, stereo-, and enantioselectivities, resulting in a series of chiral yne-allylic sulfone compounds with different substituents (Scheme 13, **14a**–**q**). Due to the high steric hindrance of the γ-site, nucleophilic substitutions preferentially occur at the α-site. Through subsequent control experiments, they demon-

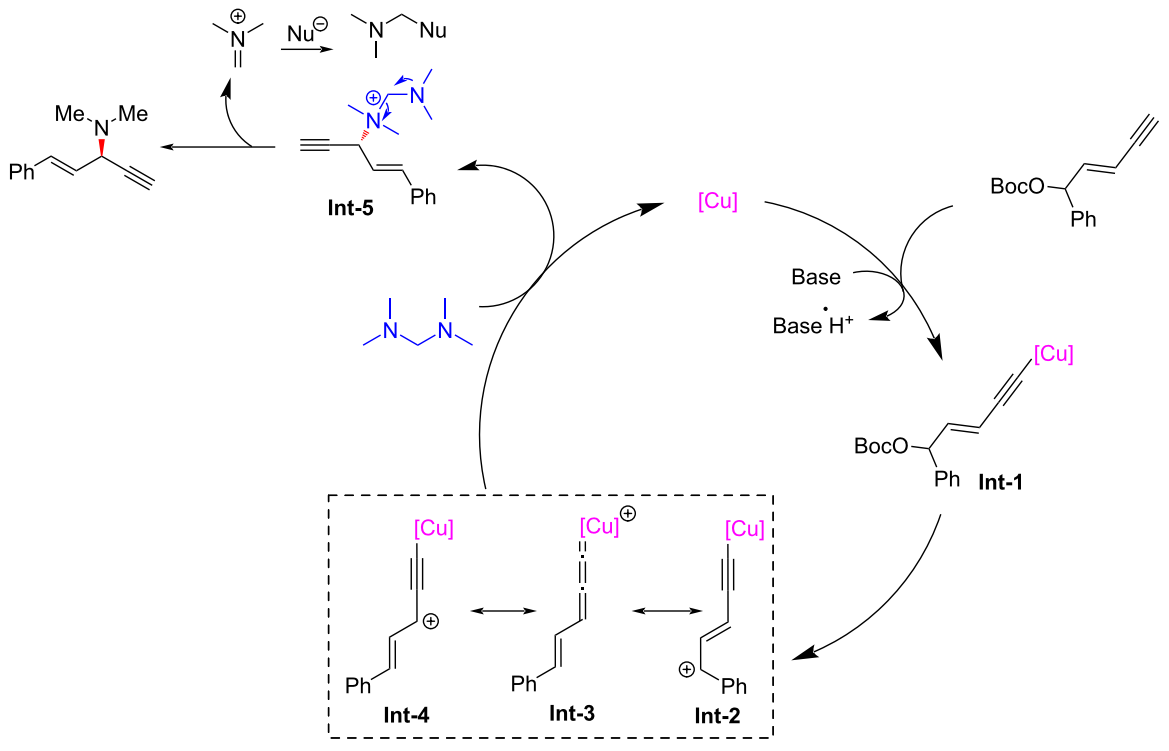

Scheme 12: Proposed mechanism of yne-allylic dialkylamination.

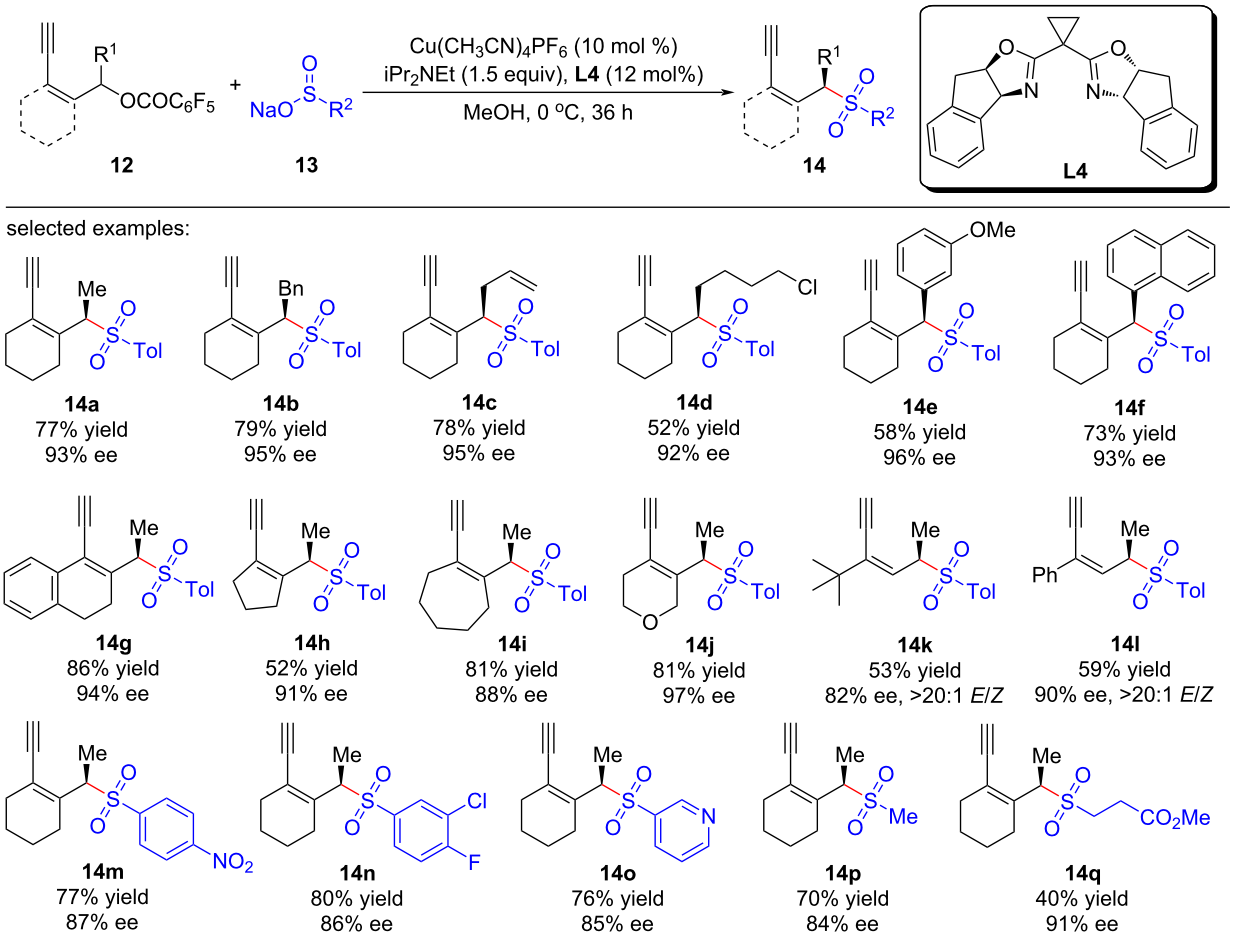

Scheme 13: Asymmetric yne-allylic sulfonylation.

strated that the terminal alkyne unit is crucial for the process and the reactions using different isomers all proceed via the same intermediate. Nonlinear relationship experiments proved that the active catalyst is a mono-copper complex containing one ligand. A catalytic cycle is proposed in which copper vinyl allenylidene is the key intermediate during the process (Scheme 14).

Recently, Fang et al. [67] used electron-rich arenes as the nucleophiles to achieve remote enantioselective control of yne-allylic substitutions. It is worth noting that when indoles or indolizines were used, the reactions yielded mono yne-allylic substituted products (Scheme 15, **3a**–**w**), but while pyrroles were used as nucleophiles, double yne-allylic substituted products can be obtained with high dr and ee values (Scheme 16, **15a**–**c**). They also demonstrated the importance of terminal alkyne through control experiments and confirmed that a copper–ligand monomer complex exists in the mechanism through nonlinear relationship experiments and kinetic studies (Scheme 17).

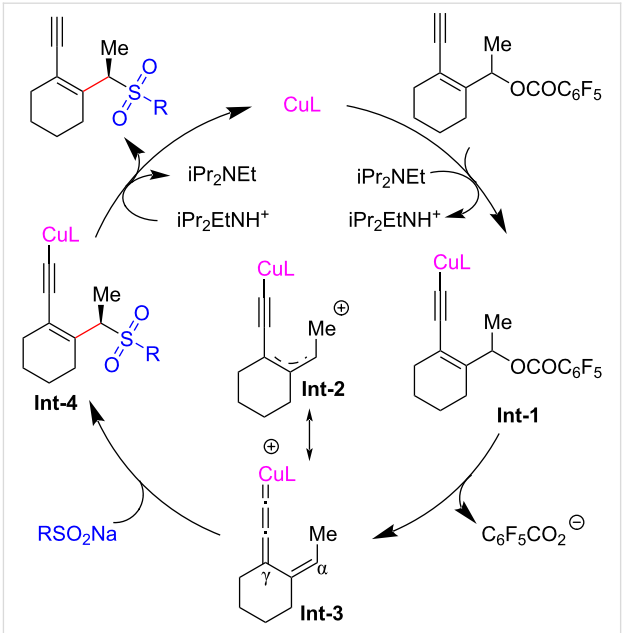

Scheme 14: Proposed mechanism of yne-allylic sulfonylation.

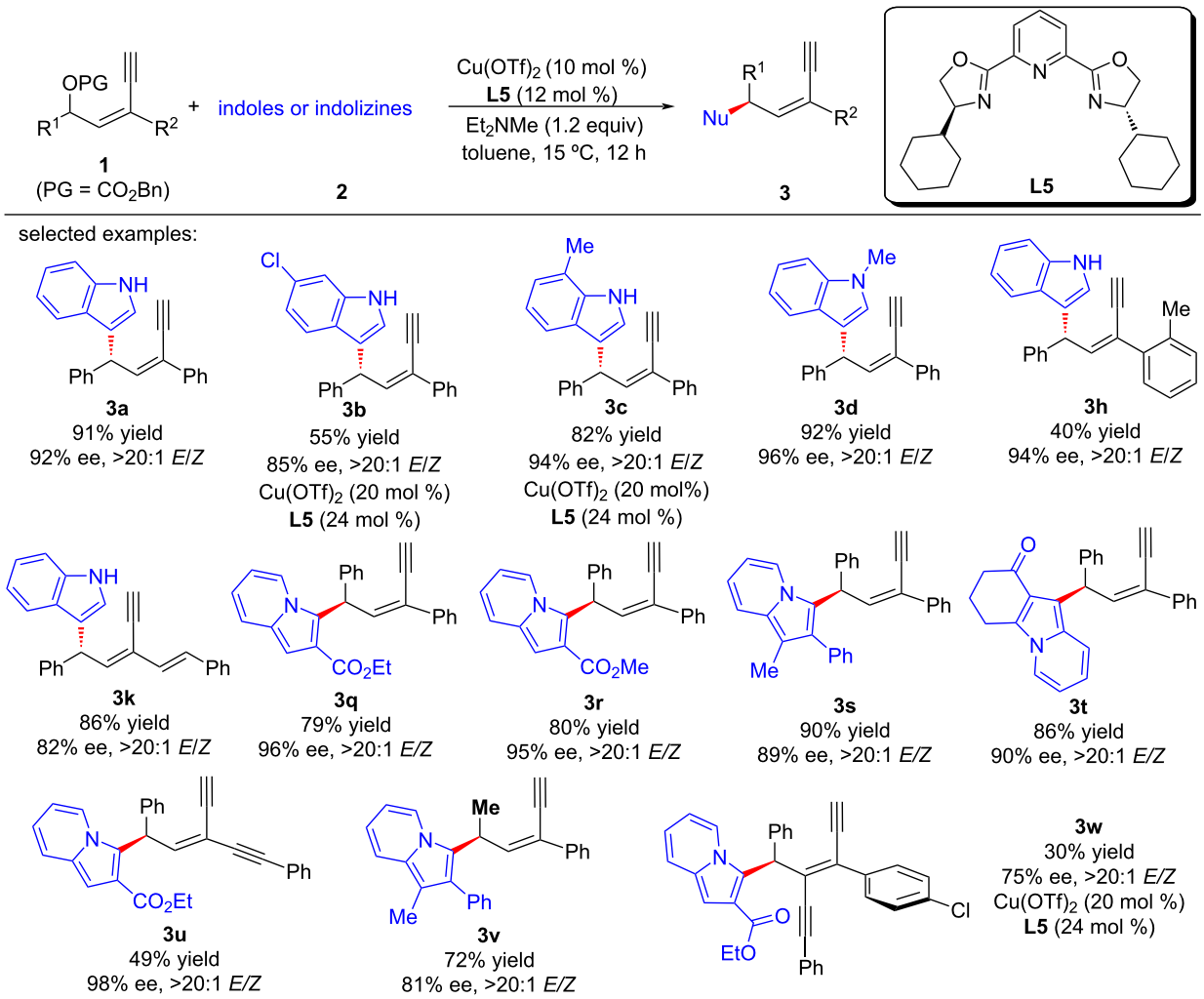

Scheme 15: Aymmetric yne-allylic substitutions using indoles and indolizines.

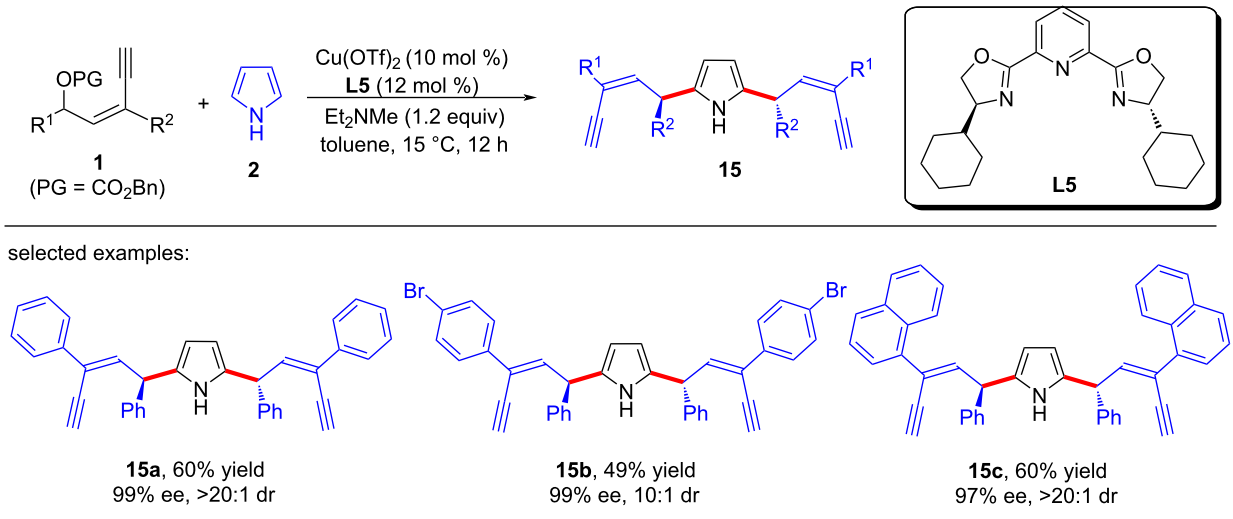

Scheme 16: Double yne-allylic substitutions using pyrrole.

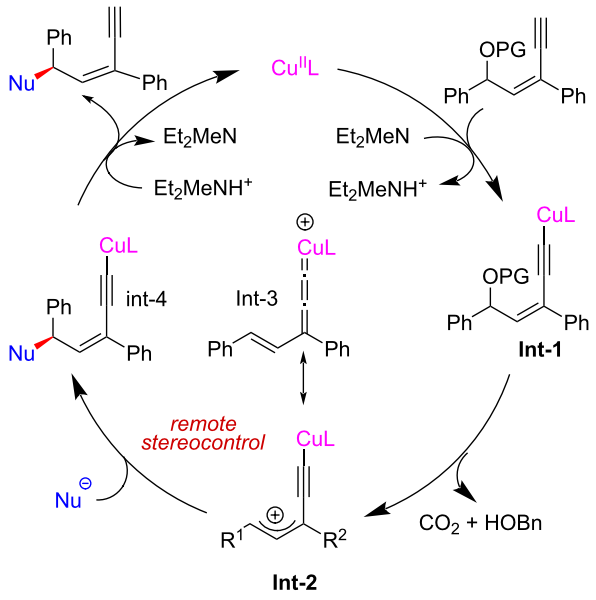

Scheme 17: Proposed mechanism of yne-allylic substitution using electron-rich arenes.

He et al. [68] developed the regio- and enantioselective monofluoroalkylation of yne-allylic esters using fluorinated malonates as the starting materials, giving rise to a series of differently substituted 1,4-enynes with monofluoroalkyl units in high yields and ee values (Scheme 18, **18a–i**). The reaction effectively overcomes the drawbacks of low activity of tertiary carbon nucleophiles and instability of fluorinated compounds. Preliminary mechanistic studies showed that the reaction exhibits a negative nonlinear effect, while the kinetic experiments indicate that a mono-copper catalyst might be involved in the rate-limiting step. They speculated that the observed nonlinear effect might arise from the existence of both the inactive homodimer of ligands and active mono-copper species in the enantiodetermining step (Scheme 19).

Lin et al. [69] achieved, for the first time, the asymmetric yne-allylic substitution using anthrones as the substrates by using a *p*-CF_3 substituted Pybox ligand, yielding 1,3-enynes containing

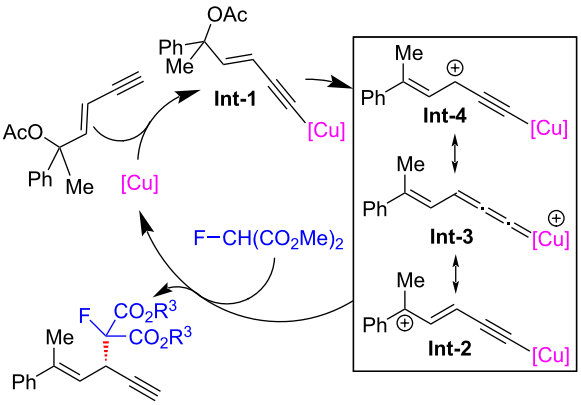

Scheme 19: Proposed mechanism.

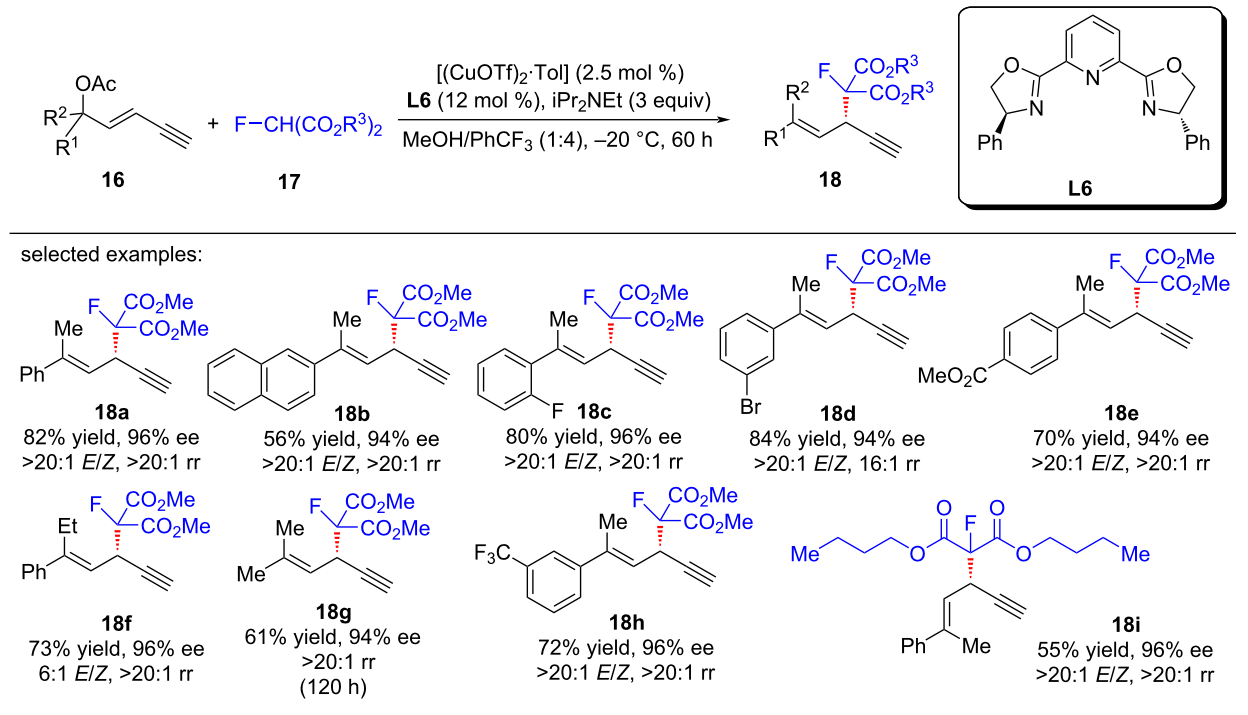

Scheme 18: Aymmetric yne-allylic monofluoroalkylations.

anthrone units with high regioselectivities and stereoselectivities (Scheme 20). The reaction tolerated various substituents in the yne-allylic esters (Scheme 20, **20a**–**h**), and showed good chiral induction effects for other multiring substrates (Scheme 20, **20i**–**k**) and linear substrates as well (Scheme 20, **20l**–**o**). A disubstituted yne-allylic ester was also a suitable substrate for the reaction (Scheme 20, **20p**). In addition, the presence of substituents such as hydroxy or chlorine groups on the anthrones had no impact on the reaction (Scheme 20, **20q**–**t**).

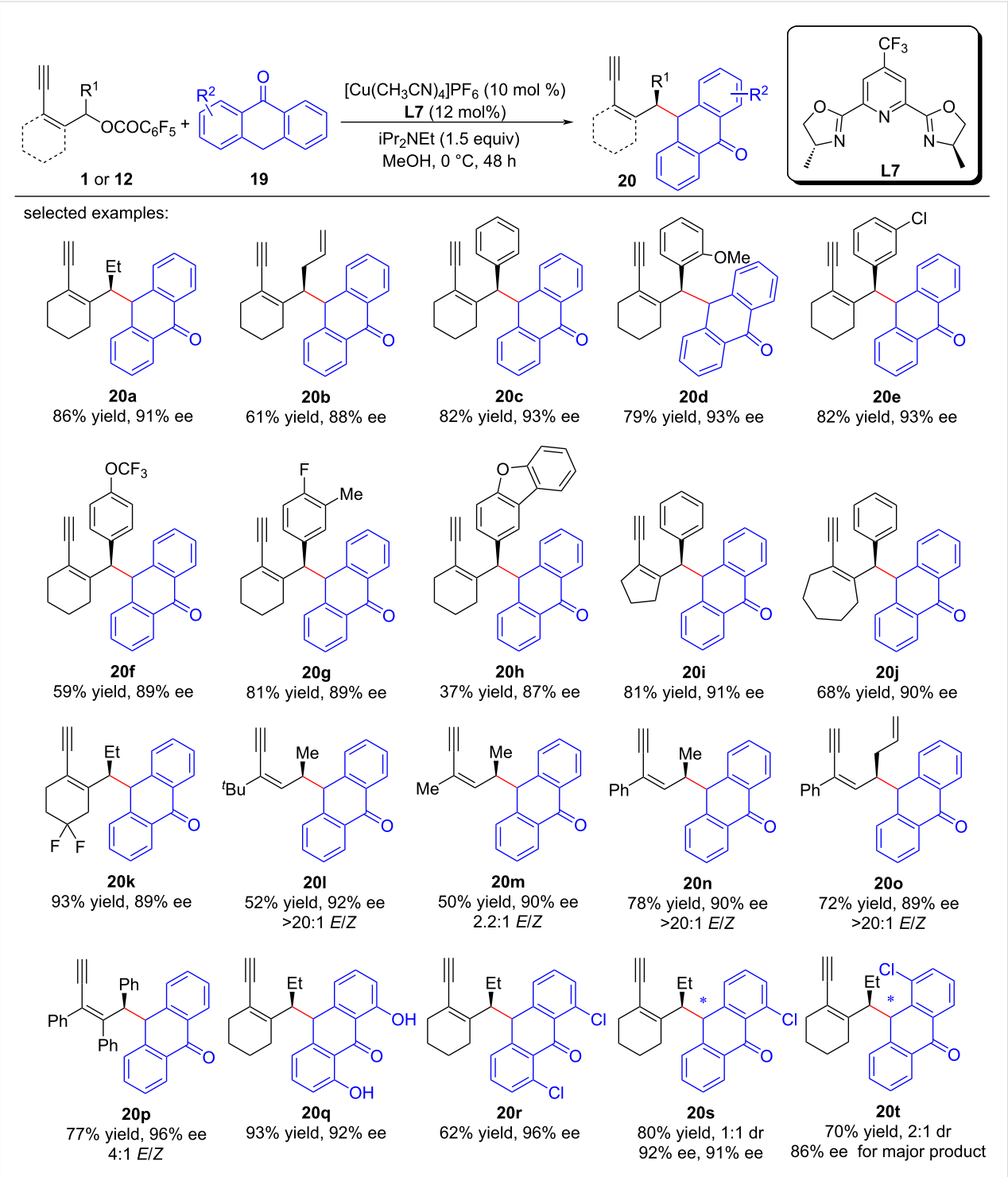

Scheme 20: Aymmetric yne-allylic substitution of yne-allylic esters with anthrones.

Chiral coumarins, renowned for their bioactive properties, form the cornerstone of numerous natural products and pharmaceutical prospects. Given their significance, the pursuit of efficient and direct synthetic routes to access functionalized chiral coumarins has garnered substantial interest. While the literature is abundant with reports on coumarin-based propargylic and allylic substitutions, the realm of yne-allylic substitution remains relatively unexplored. This scarcity of reports stems primarily from the inherent challenges posed by the presence of two unsaturated bonds in the substrates, which often complicates the control of regioselectivity. Additionally, the competition among various nucleophilic reagents further hampers the reactivity of coumarins. Xu, Peng and Feng et al. [70] introduce a groundbreaking dual remote enantioselective copper-catalyzed yne-allylic substitution methodology tailored specifically for coumarins (Scheme 21). This innovative approach facilitates the precise and highly regioselective construction of an array of novel chiral coumarin derivatives, characterized by

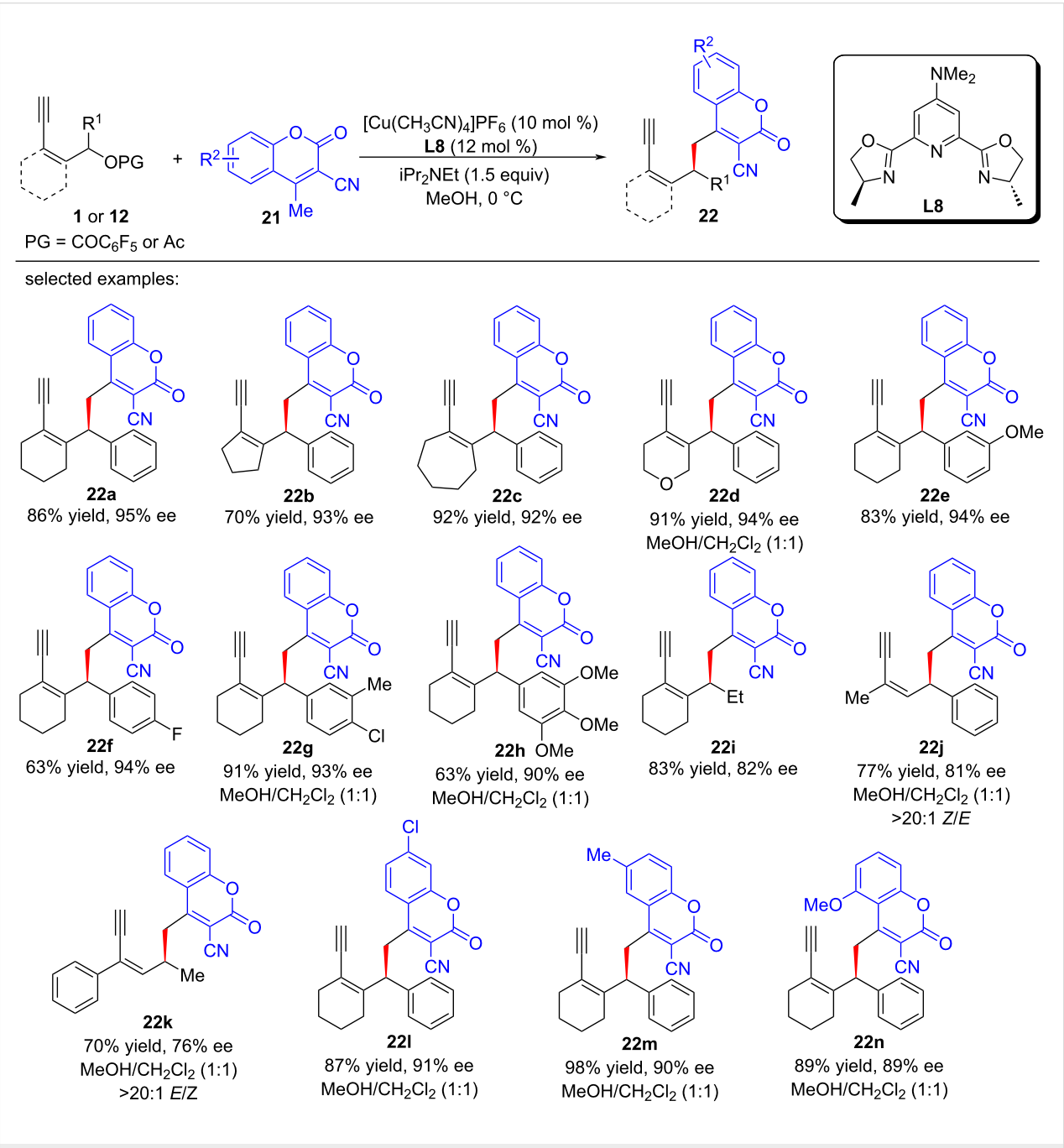

Scheme 21: Aymmetric yne-allylic substitution of yne-allylic esters with coumarins.

their exceptional synthetic efficiency and remarkable tolerance towards a broad spectrum of functional groups (Scheme 21, **22a**–**n**).

Almost at the same time, Lin et al. [71] also devised a copper-catalyzed protocol for the vinylogous yne-allylic substitution utilizing coumarins as substrates (Scheme 22). The methodolo-

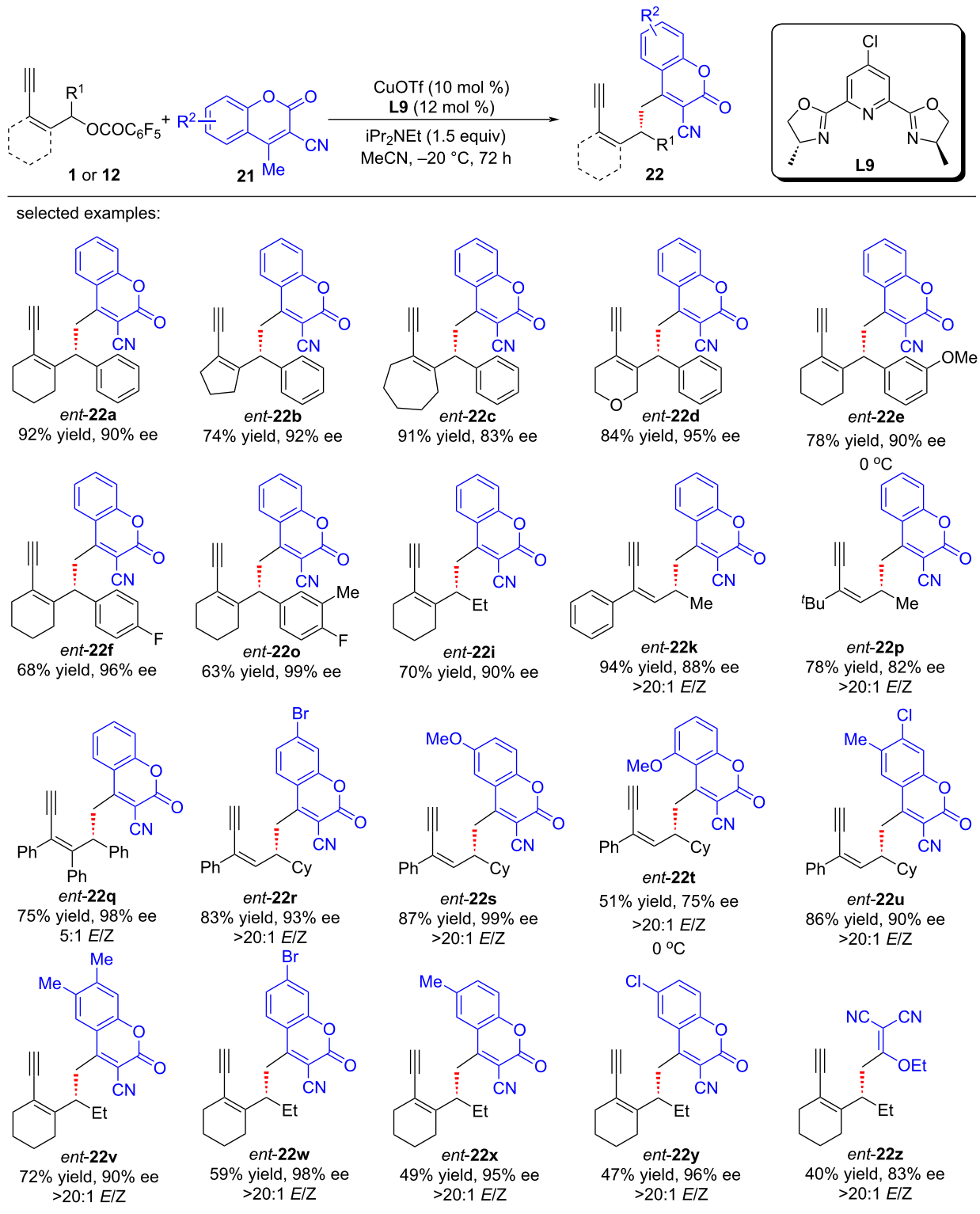

Scheme 22: Aymmetric yne-allylic substitution of with coumarins by Lin.

gy stands out for its exceptional regio and enantioselectivities, while employing readily available starting materials and mild reaction conditions, showcasing the robustness of the method to access structurally diverse chiral coumarin derivatives, which are of great interest in the fields of medicinal chemistry and synthetic organic chemistry (Scheme 22, **22a**–**y**). Moreover, the utilization of 2-(1-ethoxyethylidene)malononitrile as a γ-nucleophile yielded the desired product **22z** with a moderate 40% yield, but impressively high enantiomeric excess of 83%. To further validate the mechanistic pathway of the reaction, the authors conducted both radical trapping experiments and controlled experiments. These investigations conclusively demonstrated that the reaction did not proceed via a radical mechanism and the presence of terminal alkynes was found to be crucial for the smooth progression of the reaction, which suggested that the reaction proceeded through the same copper vinyl allenylidene intermediate (Scheme 23).

Yne-allylic substitutions through dearomatization and rearomatization

In 2023, Lin and He et al. [72] achieved the challenging dearomatization of heteroarenes through d-orbital electron of the transition-metal center and thus completed the asymmetric substitutions with remote stereoselective control induced by alkynylcopper. A newly electron-rich ligand was developed to enhance the back donation of d-orbital electron of copper, thereby achieving dearomatization and rearomatization with excellent yields and enantioselectivities. A series of synthesized useful diarylmethyl (Scheme 24, **24a**–**r**) and triarylmethyl (Scheme 25, **26a**–**l**) structures were obtained. Moreover, they also achieved the construction of C–N axis chirality through remote substitution/cyclization/1,5-H shift process (Scheme 26). The control experiments confirmed that the reaction requires the joint participation of copper and terminal alkyne, and the radical-capture experiment also ruled out a radical-involved mechanism. In addition, a positive nonlinear relationship between the product and ligand indicated that the dinuclear copper is the active catalyst, which was also proved by single crystal X-ray analysis. However, kinetic experiments showed the reaction is first-order on copper, implying that the dinuclear copper complex is the precursor of the active monocopper species which is involved in the turnover-limiting step (Scheme 27).

Subsequently, Zhu and Xu et al. [73] also achieved the distal enantioselective heteroarylation of yne-thiophene carbonates by applying a simpler *p*-OMe substituted pybox ligand (Scheme 28, **26a**–**m**). The thiophene unit of the carbonate could also be replaced by benzothiophene (Scheme 28, **26h**) or furan (Scheme 28, **26m**), and pyrrole (Scheme 28, **26j**), phenol

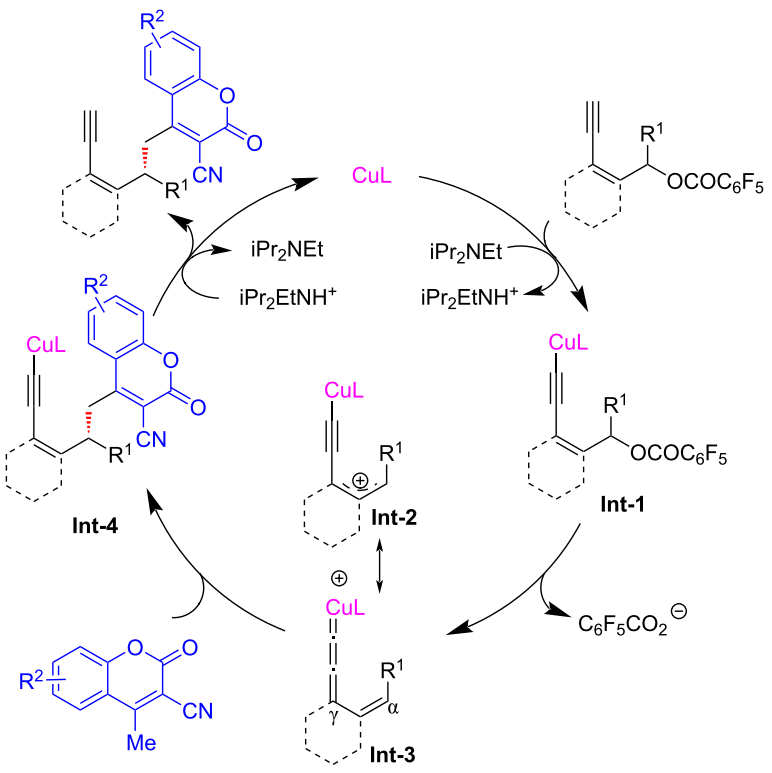

Scheme 23: Proposed mechanism.

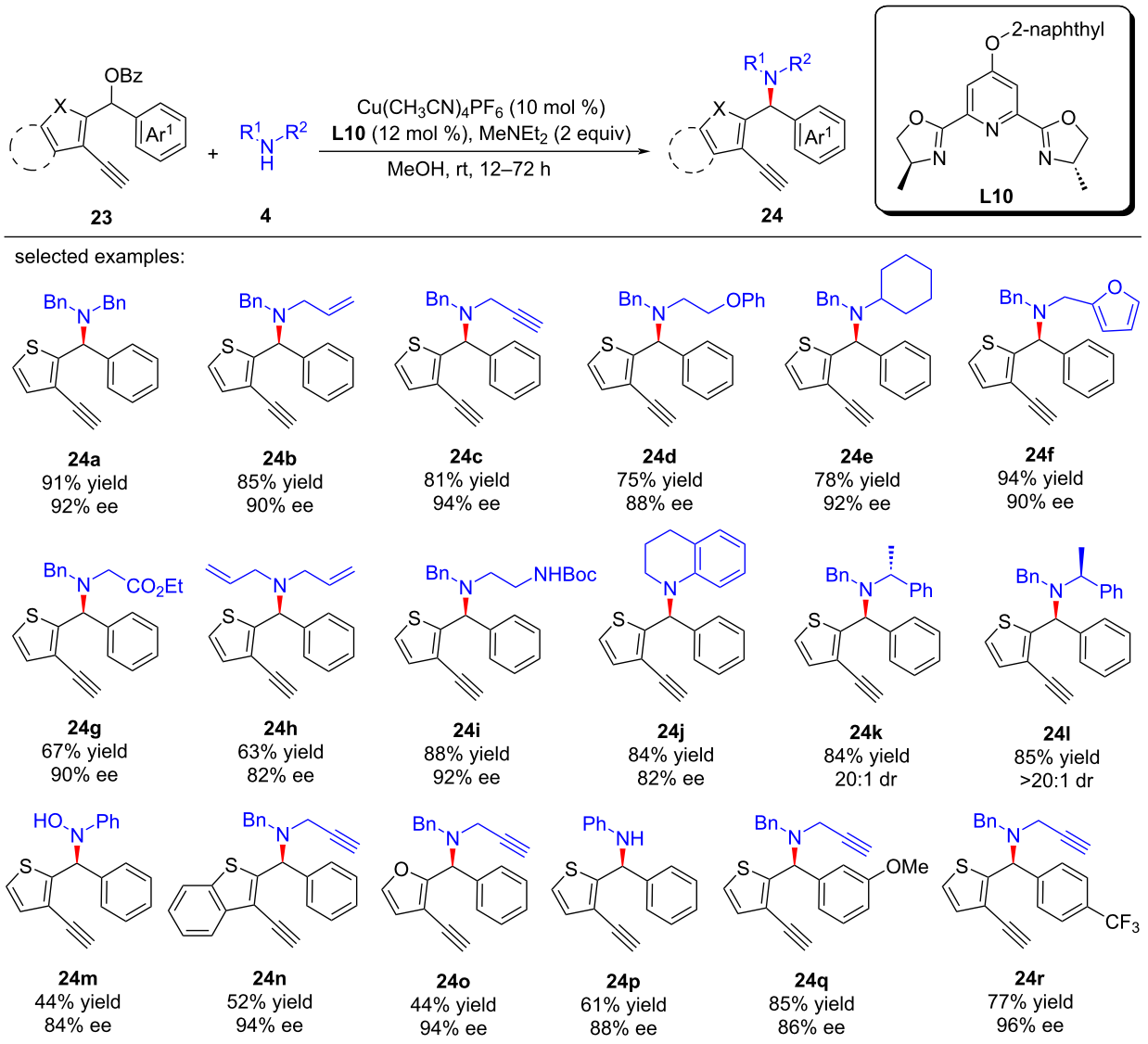

Scheme 24: Amination by alkynylcopper driven dearomatization and rearomatization.

(Scheme 28, **26k**); coumarin derivative (Scheme 28, **26n**), and dibenzylamine (Scheme 28, **24a**) could also undergo the reactions smoothly as nucleophilic reagents, producing the products with high enantioselectivities. They also conducted radical-trapping experiments and confirmed that the reaction does not involve a radical intermediate. Unlike the previous yne-allyllic substitutions, this reaction could be carried out without the presence of terminal alkyne, although no ee value was obtained. Therefore, they speculated that the direct substitution at the benzyl position is the key to causing the side reaction that affected the enantioselectivity.

Recently, Zhu and Xu et al. [74] achieved the η-nucleophilic substitutions of 5-ethynylthiophene esters. A series of C-, N-, O-, and S-nucleophiles could react smoothly to obtain various thiophene derivatives with different functional groups (Scheme 29, **28a–t**). Control experiments showed that terminal alkyne and copper catalysts are crucial for the smooth progress of the reaction. Therefore, they believe that the dearomatization caused by copper vinyl allenylidene intermediate remains a key step in the reaction (Scheme 30).

Copper-catalyzed yne-allylic substitution–annulation reactions

In the pioneering report [62], Fang et al. found that when cyclic 1,3-dicarbonyls such as Meldrum's acid and 1,3-dimethylbarbituric acid were used as the nucleophiles, the yne-allylic substitution products underwent further intramolecular cyclizations to

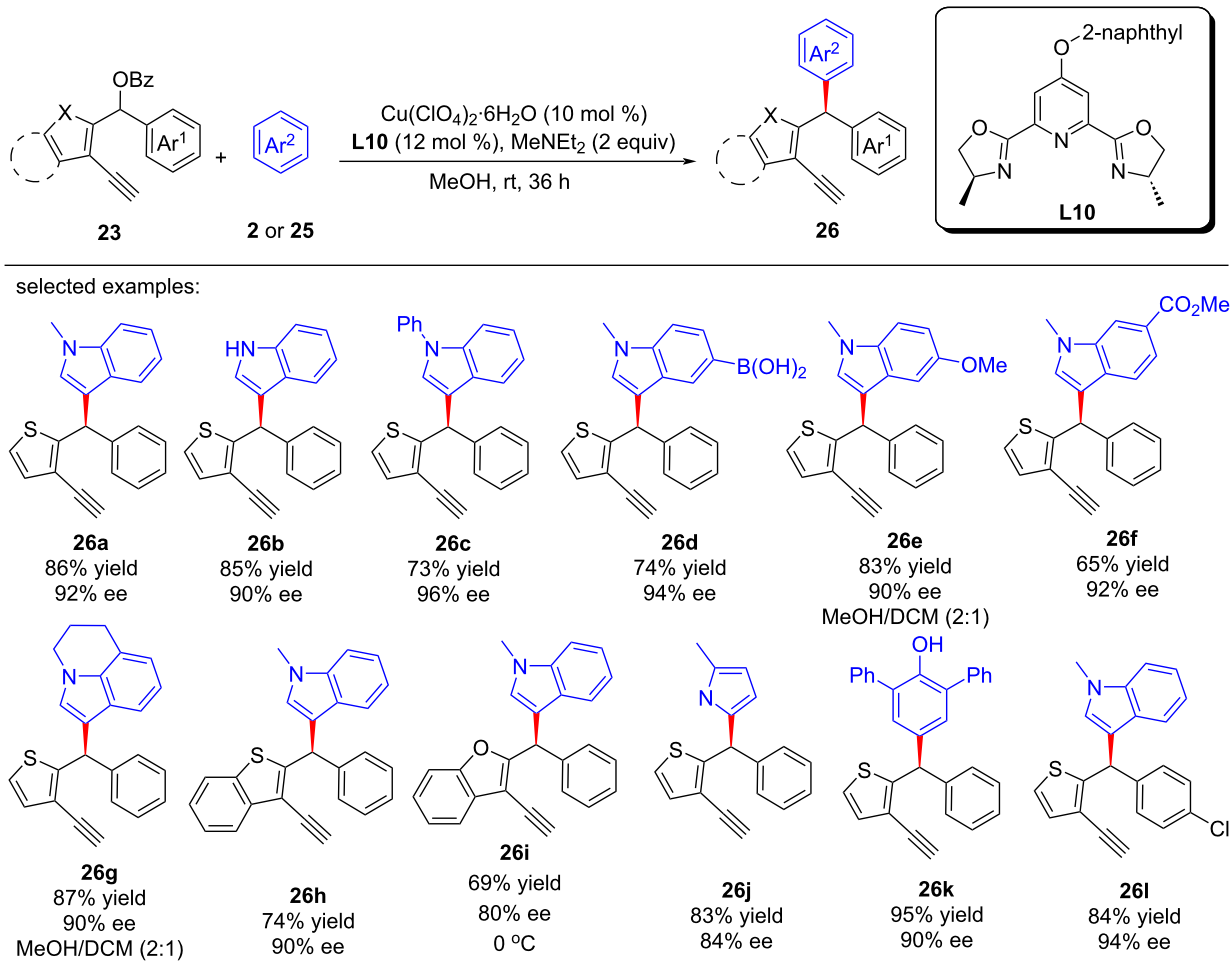

Scheme 25: Arylation by alkynylcopper driven dearomatization and rearomatization.

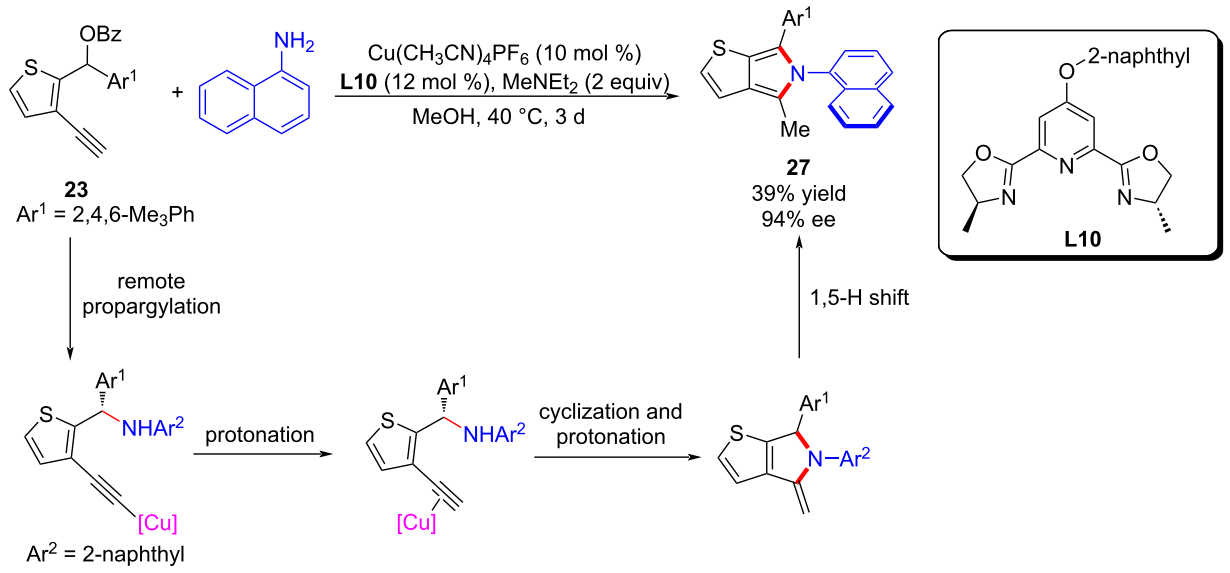

Scheme 26: Remote substitution/cyclization/1,5-H shift process.

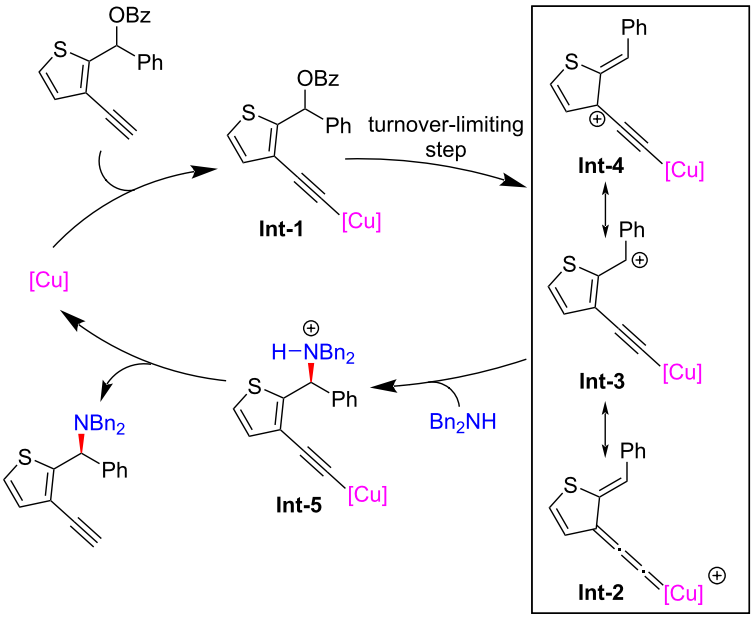

Scheme 27: Proposed mechanism.

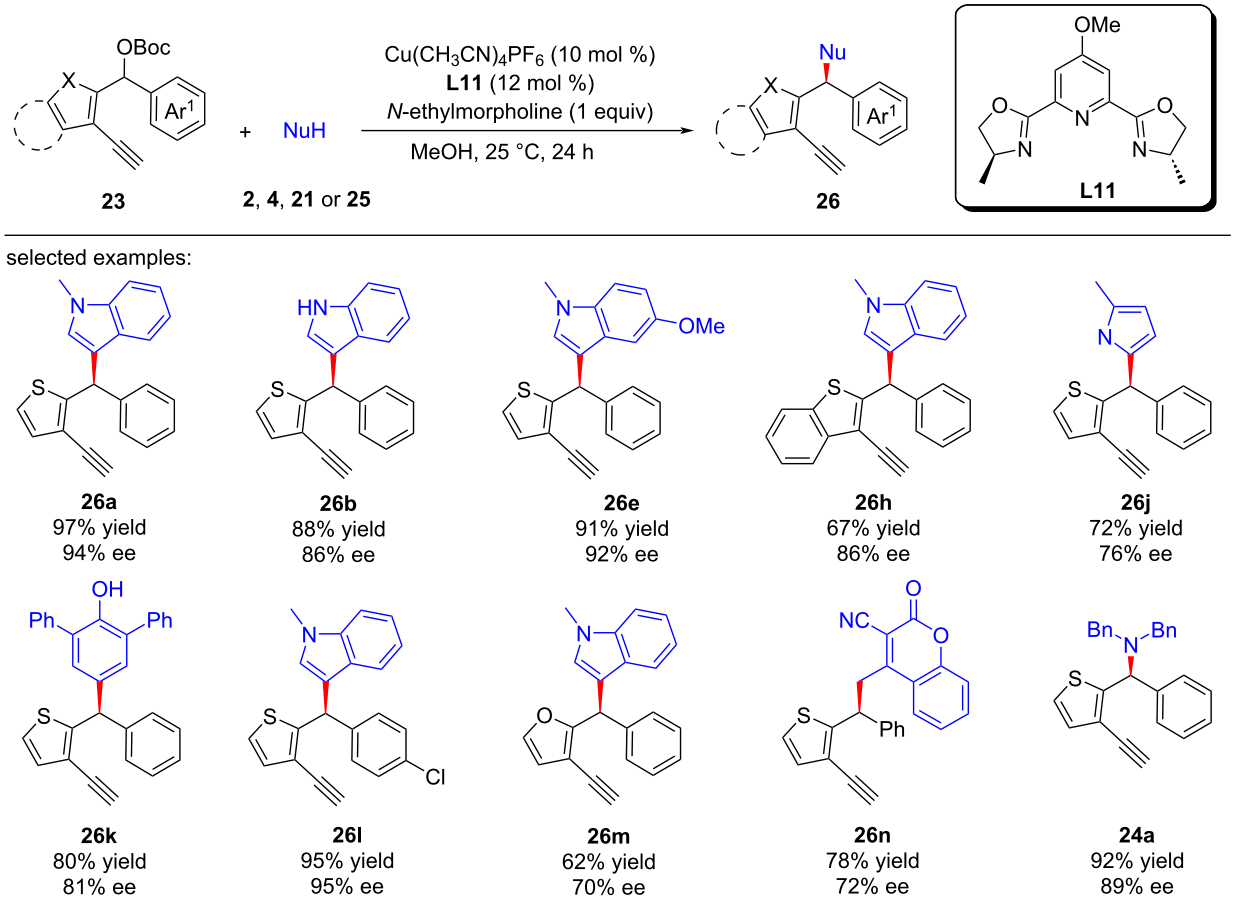

Scheme 28: Arylation or amination by alkynylcopper driven dearomatization and rearomatization.

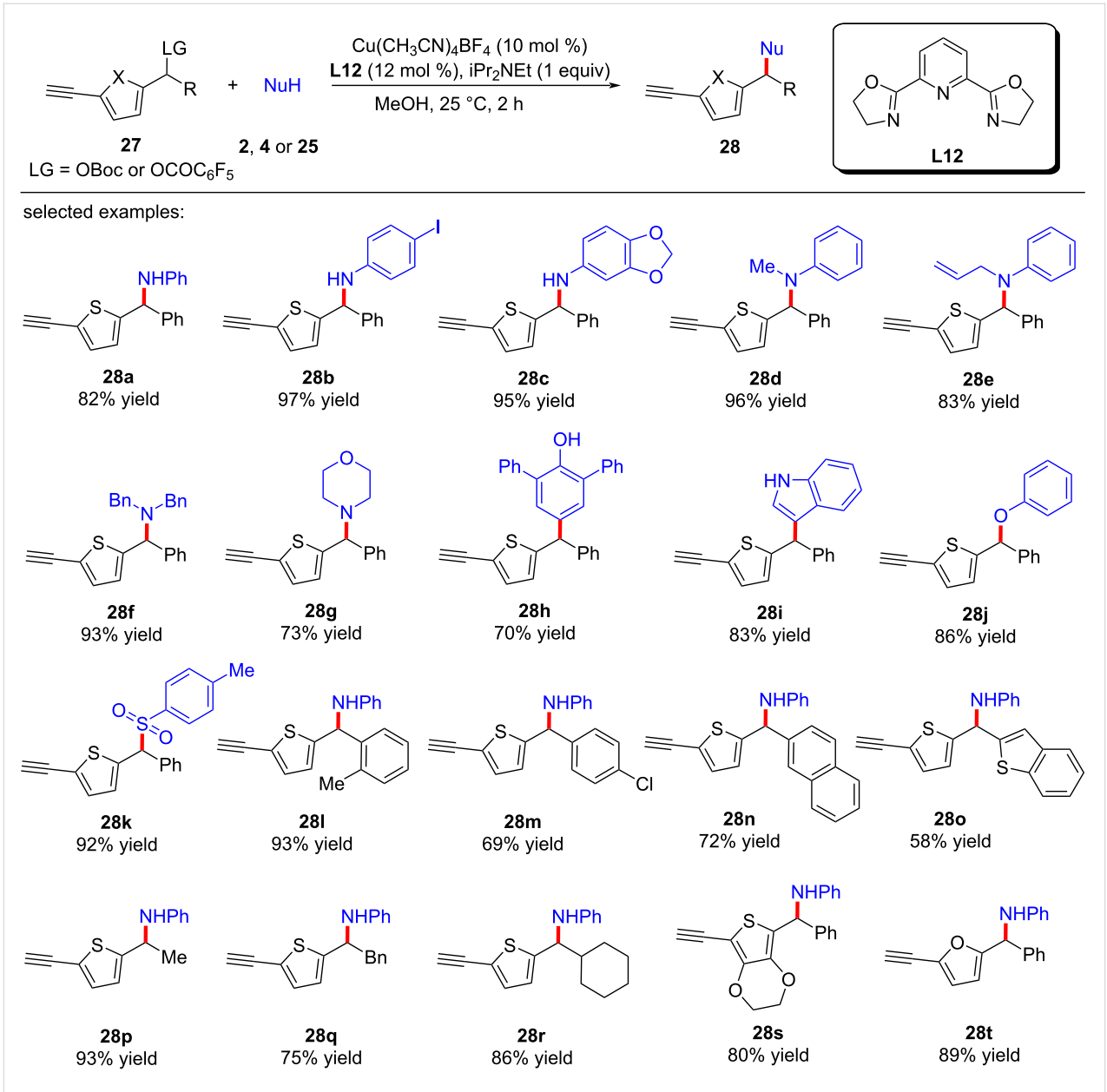

Scheme 29: Remote nucleophilic substitution of 5-ethynylthiophene esters.

give the spiro-cyclic products in high yields (Scheme 31, **30a**–**f**). The generation of products likely begins with an α-attack on the yne-allylic cation intermediate, followed by an intramolecular cyclization. The disparity in reactivity could stem from the chelation between acyclic 1,3-dicarbonyl enolates and the copper catalyst, enhancing γ-position attack in an intramolecular manner. Conversely, Meldrum's acid's rigid cyclic structure precludes stable copper-carbonyl interaction, favoring attack from a less hindered site.

Later, Qi and Xu et al. [75] achieved highly enantioselective copper-catalyzed [4 + 1] cyclization of yne-allylic esters and cyclic 1,3-dicarbonyls, achieving remote stereoselective control through copper vinyl allenylidene species. A series of differently substituted spiro-cyclic products can be obtained with high yields, regio- and stereoselectivities (Scheme 32, **30a**–**x**). Preliminary mechanistic studies indicated that the reaction first undergoes a substitution at the α-position of yne-allylic ester, followed by a Conia-ene cyclization. The absolute configuration of the products is controlled by the ligand, which further confirms the remote stereocontrol of the copper catalyst. They obtained a single crystal of dinuclear copper and confirmed that the catalytic efficiency of the single crystal is consistent with the standard reaction conditions. However, nonlinear effect ex-

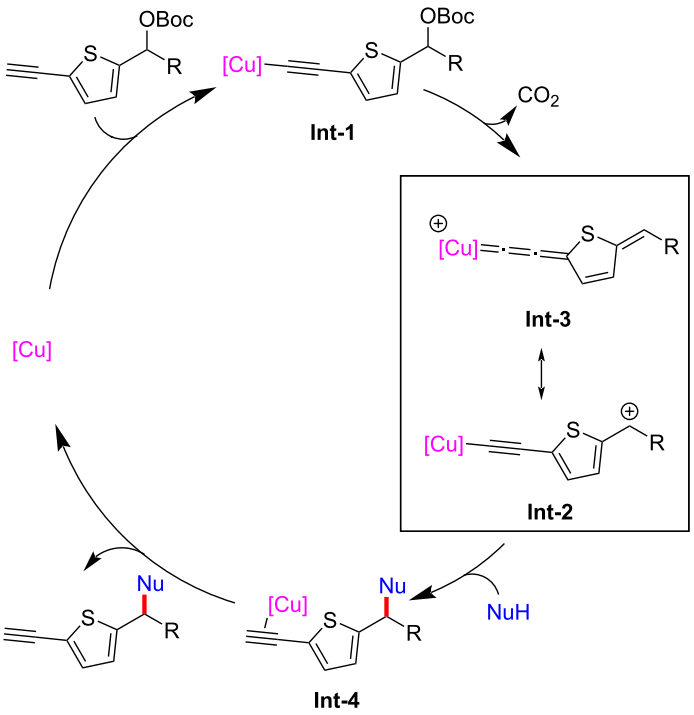

Scheme 30: Proposed mechanism.

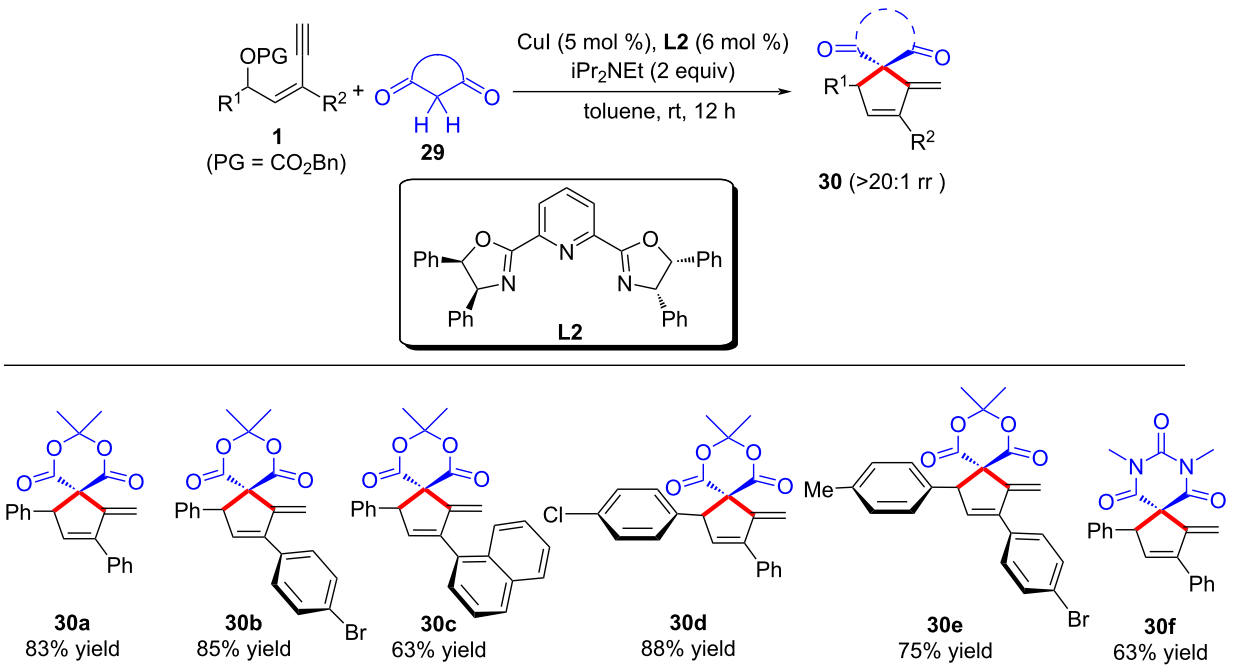

Scheme 31: [4 + 1] annulation of yne-allylic esters and cyclic 1,3-dicarbonyls.

periments confirmed that the active catalyst is a mono-copper species, so it is speculated that the dinuclear copper is the precursor of active single copper species (Scheme 33).

Fang et al. [67] achieved the first asymmetric [3 + 2] cyclization of yne-allylic esters and 2-naphthalenols, resulting in a range of allenyl dihydronaphthofuran products with high

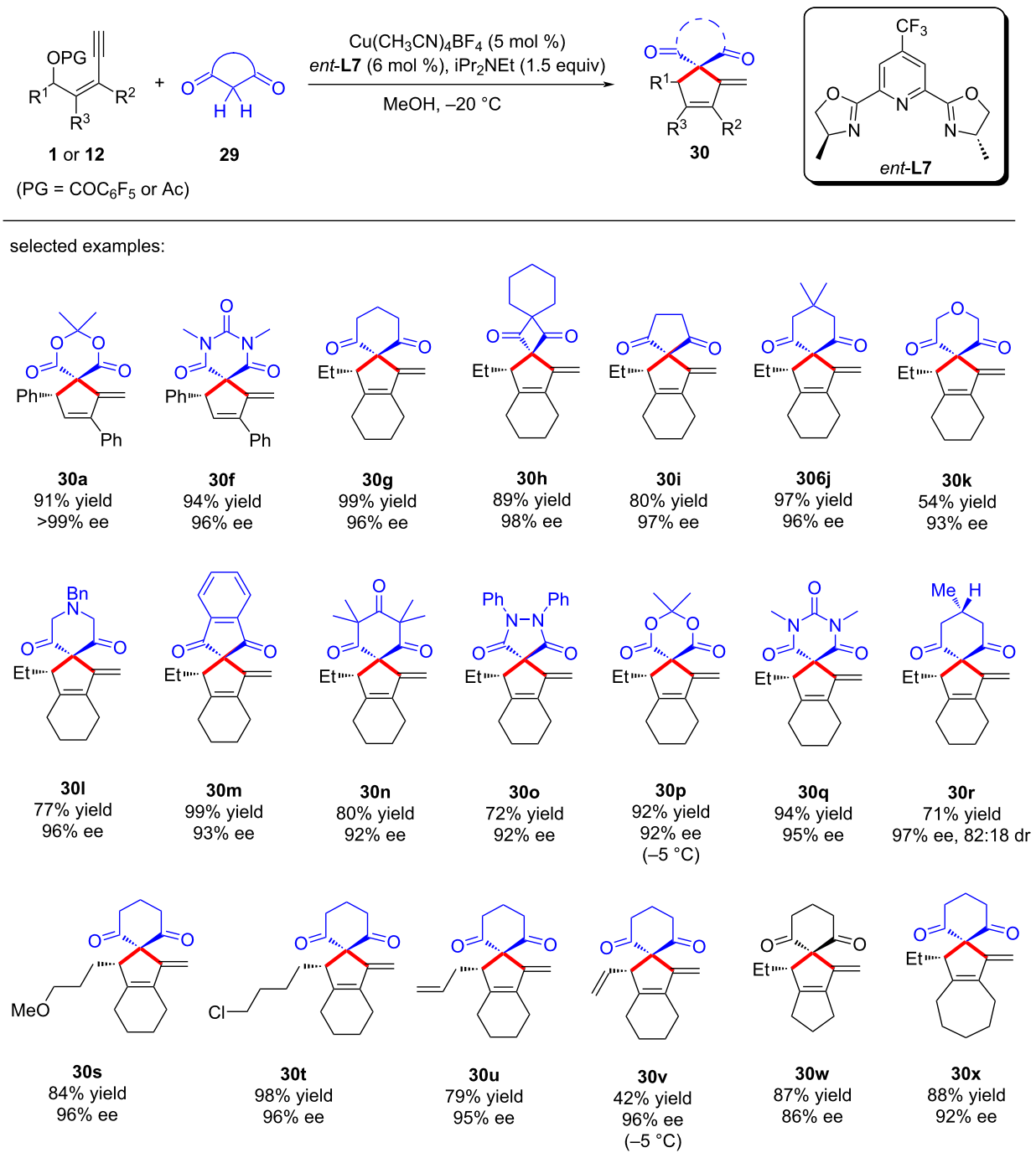

Scheme 32: Asymmetric [4 + 1] annulation of yne-allylic esters.

diastereo- and enantioselectivities (Scheme 34, **32a**–**h**). The attempt to separate the intermediate before cyclization failed, indicating that the following annulation and the formation of allene is very fast. It is speculated that in the formation of allene the copper catalyst still plays a key role in activating the alkyne unit (Scheme 35).

Han and Huang et al. [76] also achieved the yne-allylic substitution and Conia-ene cyclization process using vinyl ethynylethylene carbonates as the starting materials, thus completing their enantioselective formal [4 + 1] cycloadditions with cyclic 1,3-dicarbonyl compounds (Scheme 36, **34a**–**k**). They speculated that in the reaction mechanism, the key step is the formation of

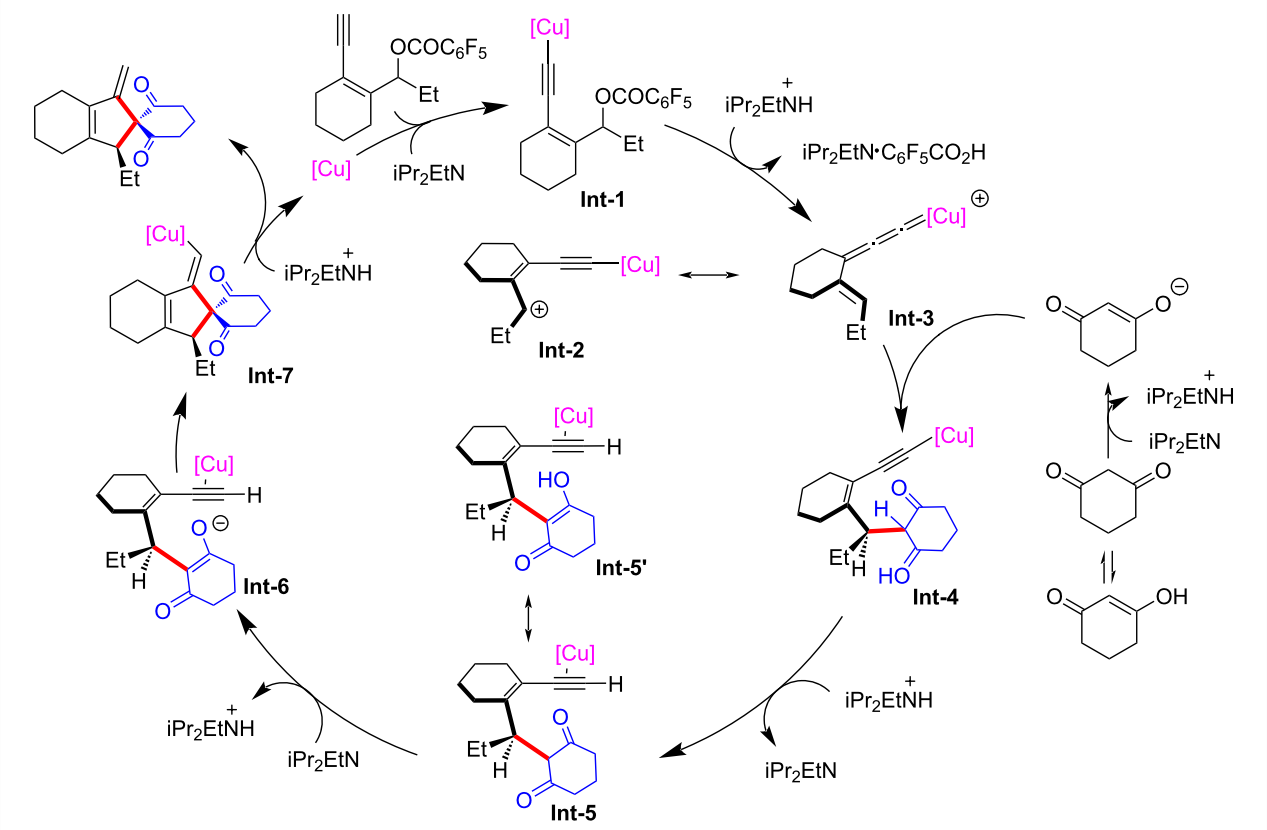

Scheme 33: Proposed mechanism.

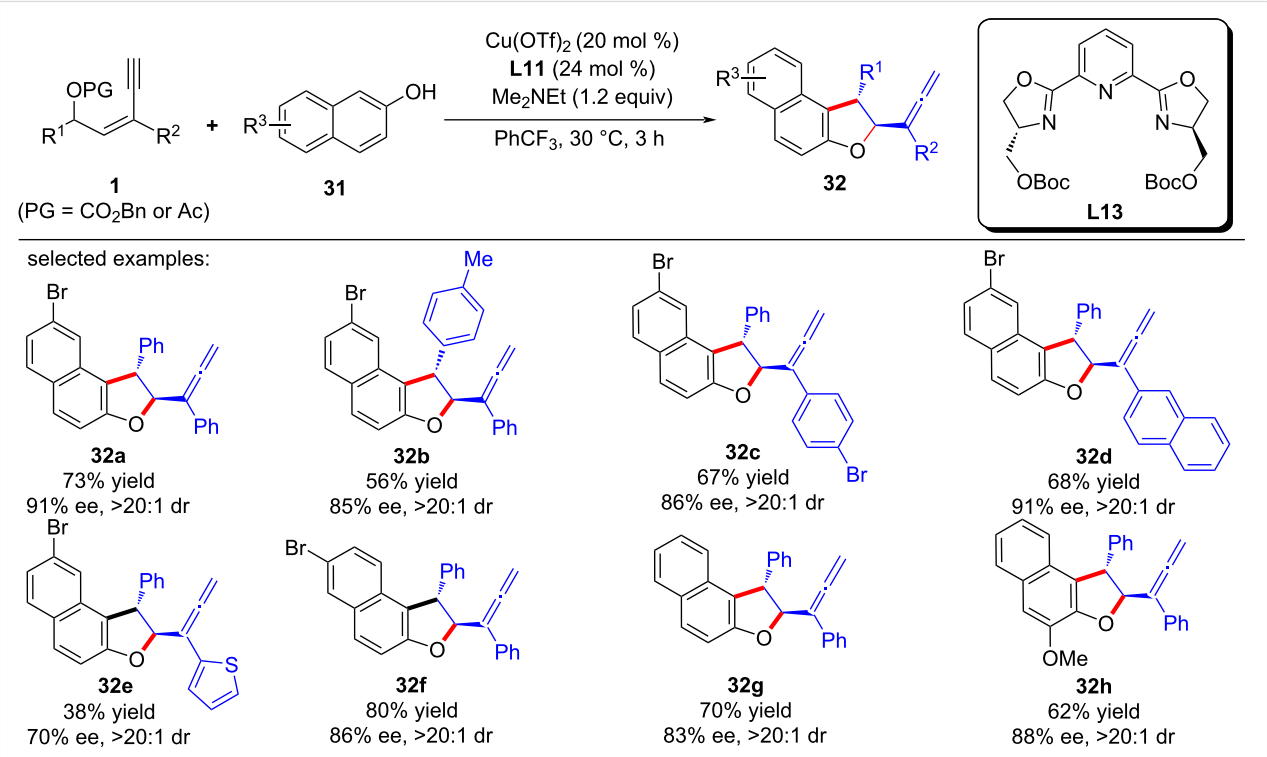

Scheme 34: Asymmetric [3 + 2] annulation of yne-allylic esters.

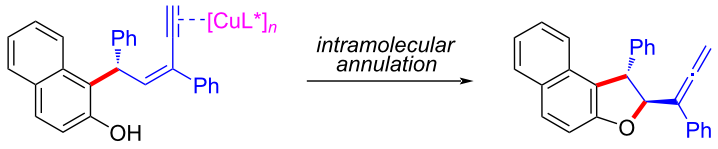

Scheme 35: Postulated annulation step.

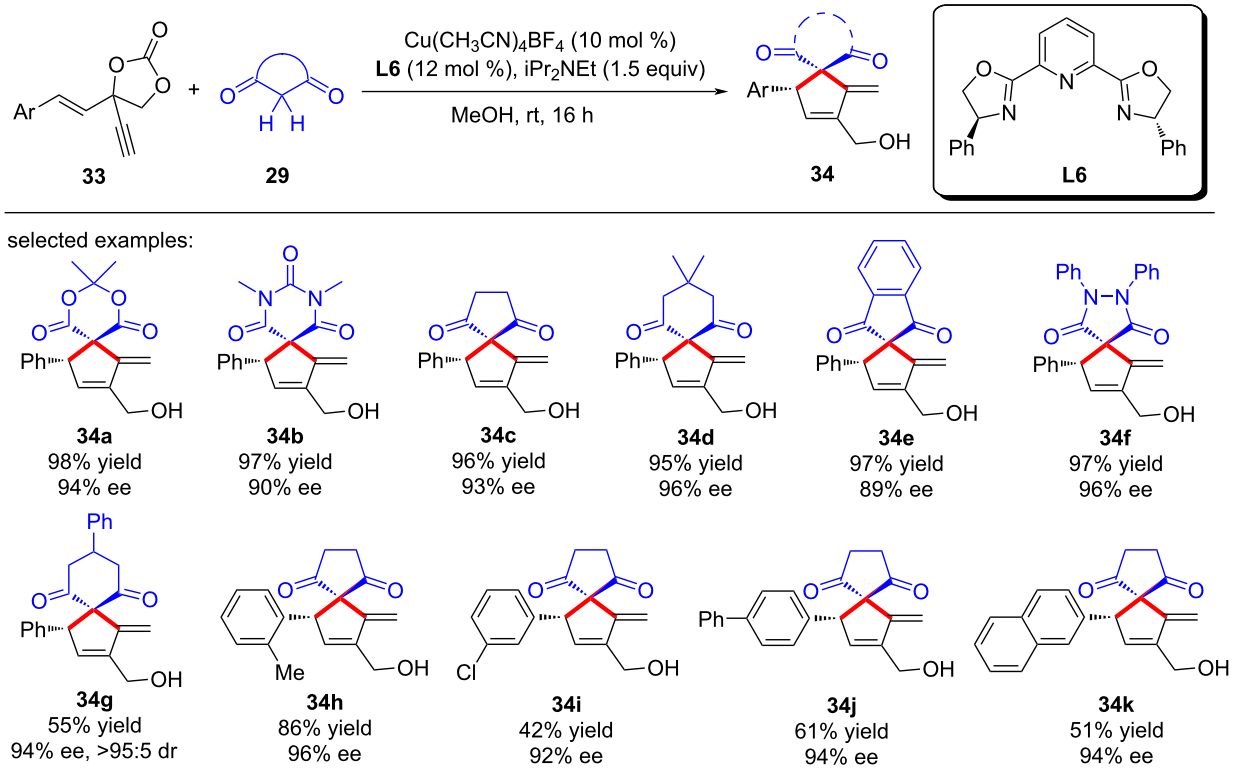

Scheme 36: [4 + 1] Annulations of vinyl ethynylethylene carbonates and 1,3-dicarbonyls.

the copper vinyl allenylidene intermediate from vinyl ethynylethylene carbonates and copper catalysts (Scheme 37).

He et al. [77] completed formal [4 + 1] and [4 + 2] annulations and obtained two types of seldomly studied heterocycles of thieno[2,3-*c*]pyrrole (Scheme 38, **36a**–**j**) and thieno[2,3-*d*]pyridazine (Scheme 39, **38a**–**h**) in high yields. It is worth noting that the formal [4 + 1] and [4 + 2] cyclizations were carried out through substitution by an alkynyl copper-driven dearomatization/rearomatization/cyclization/isomerization process (Scheme 40).

Li, Yu and Liu et al. [78] achieved the asymmetric catalyzed dearomative [4 + 1] spiroannulation of nonfunctionalized 1-naphthol by applying a new ligand **L14**, leading to the rapid construction of differently substituted chiral spirocyclic enones **40a**–**j** with high yields and enantioselectivities (Scheme 41). It is worth noting that when the C4 position of 1-naphthol was occupied, the reaction occurred at the C2 position, resulting in the C2-dearomatized naphthalenone products **41a**–**d** with high efficiency (Scheme 41). In addition, electron-rich phenols or nonfunctionalized 2-naphthols could also be used as nucleophiles, providing the desired chiral spirocycles **43a**–**e** and **44a**–**e** in good yields with excellent ee values (Scheme 42). Preliminary mechanistic studies have ruled out the 1,3-sigmatropic shift, indicating that the reaction proceeds through a nucleophilic substitution–annulation process of a reactive π-extended copper-allenylidene intermediate (Scheme 43).

At the same time, Qi and Xu et al. [79] also realized the dearomative spiroannulation of 2-naphthols or electron-enriched phenols under mild conditions with excellent regioselectivities,

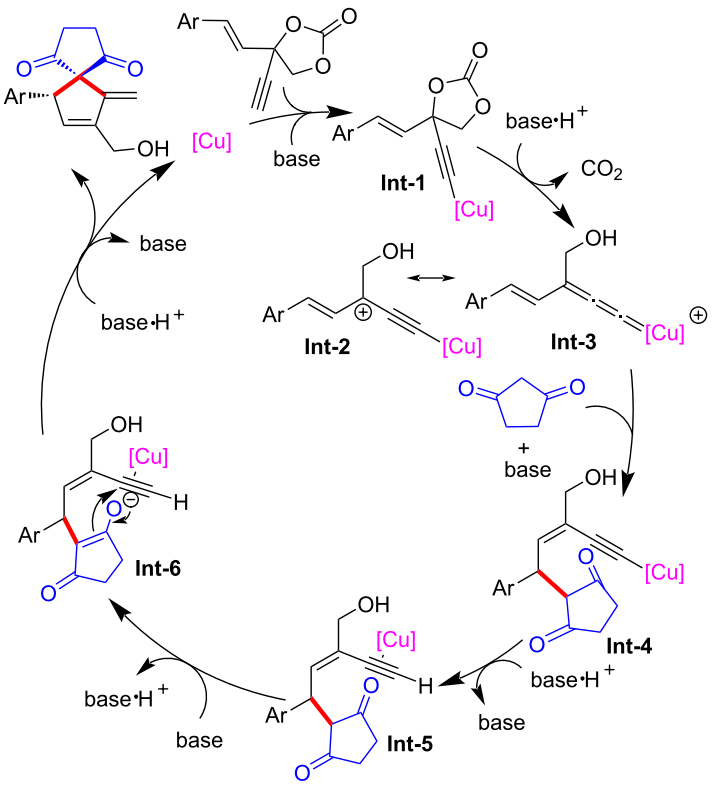

Scheme 37: Proposed mechanism.

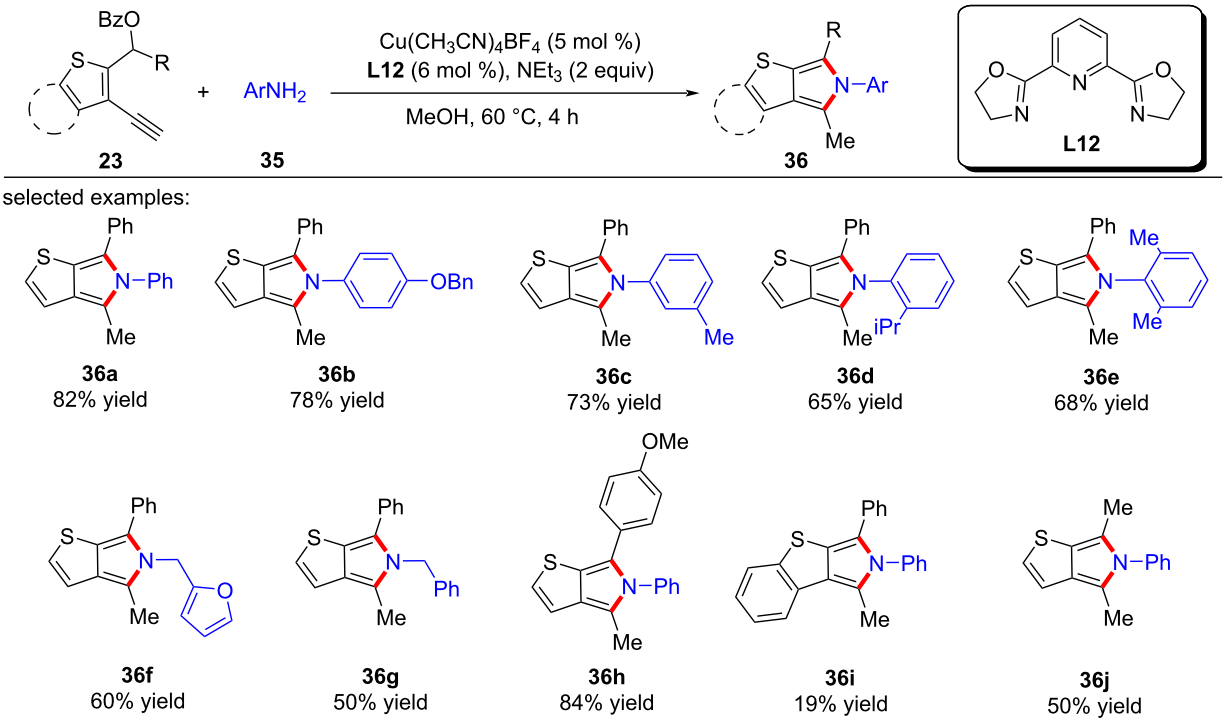

Scheme 38: Formal [4 + 1] annulations with amines.

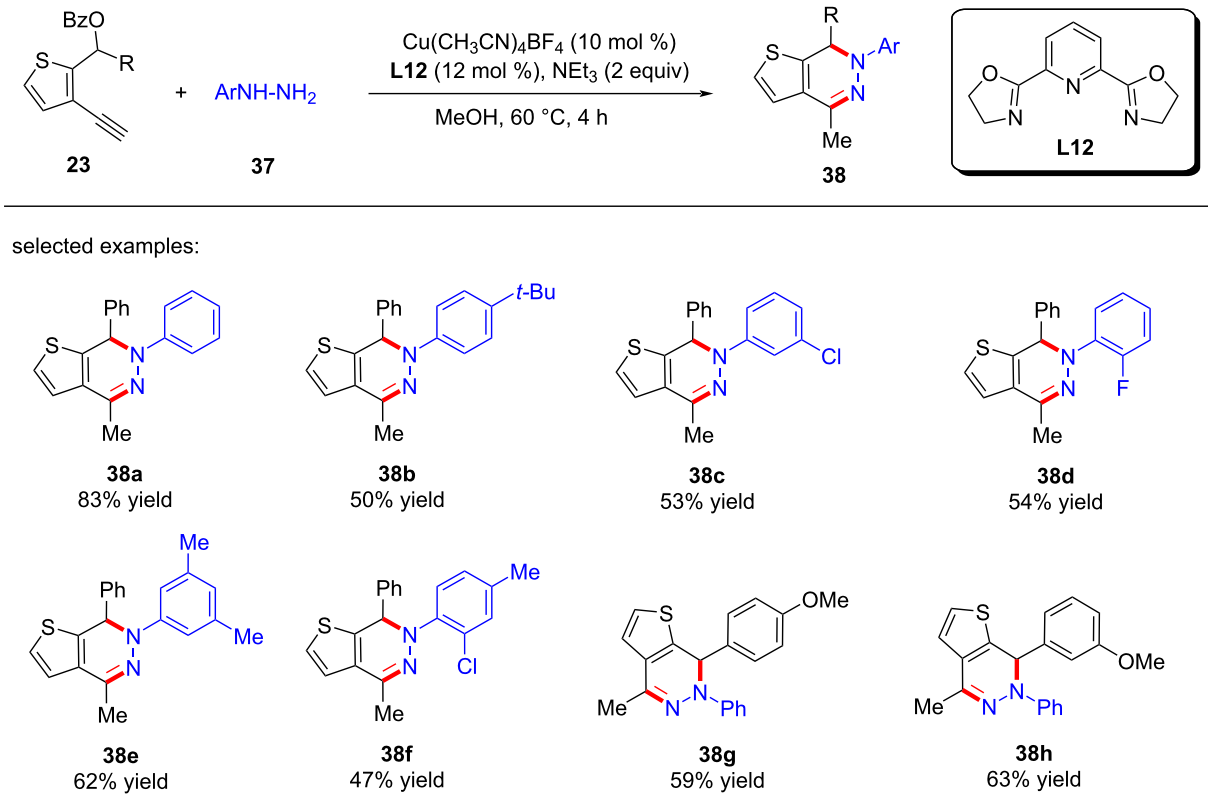

Scheme 39: Formal [4 + 2] annulations with hydrazines.

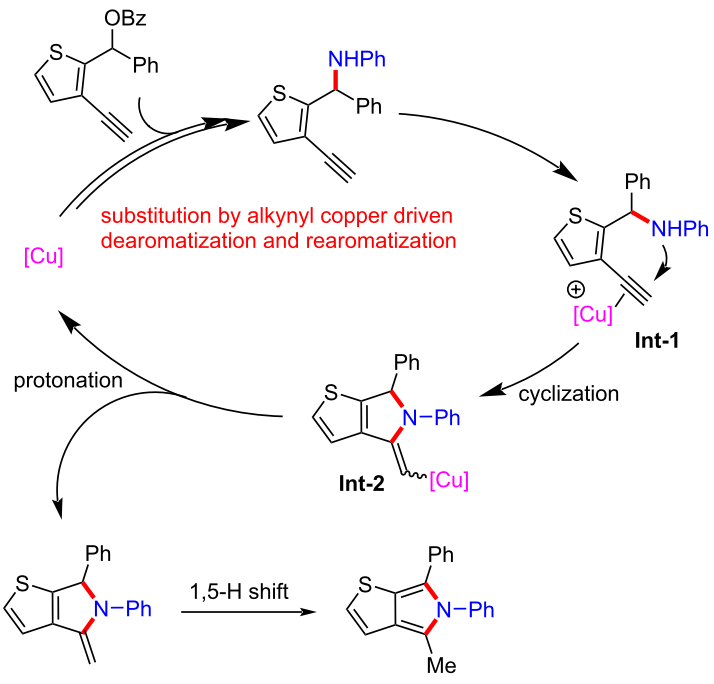

Scheme 40: Proposed mechanism.

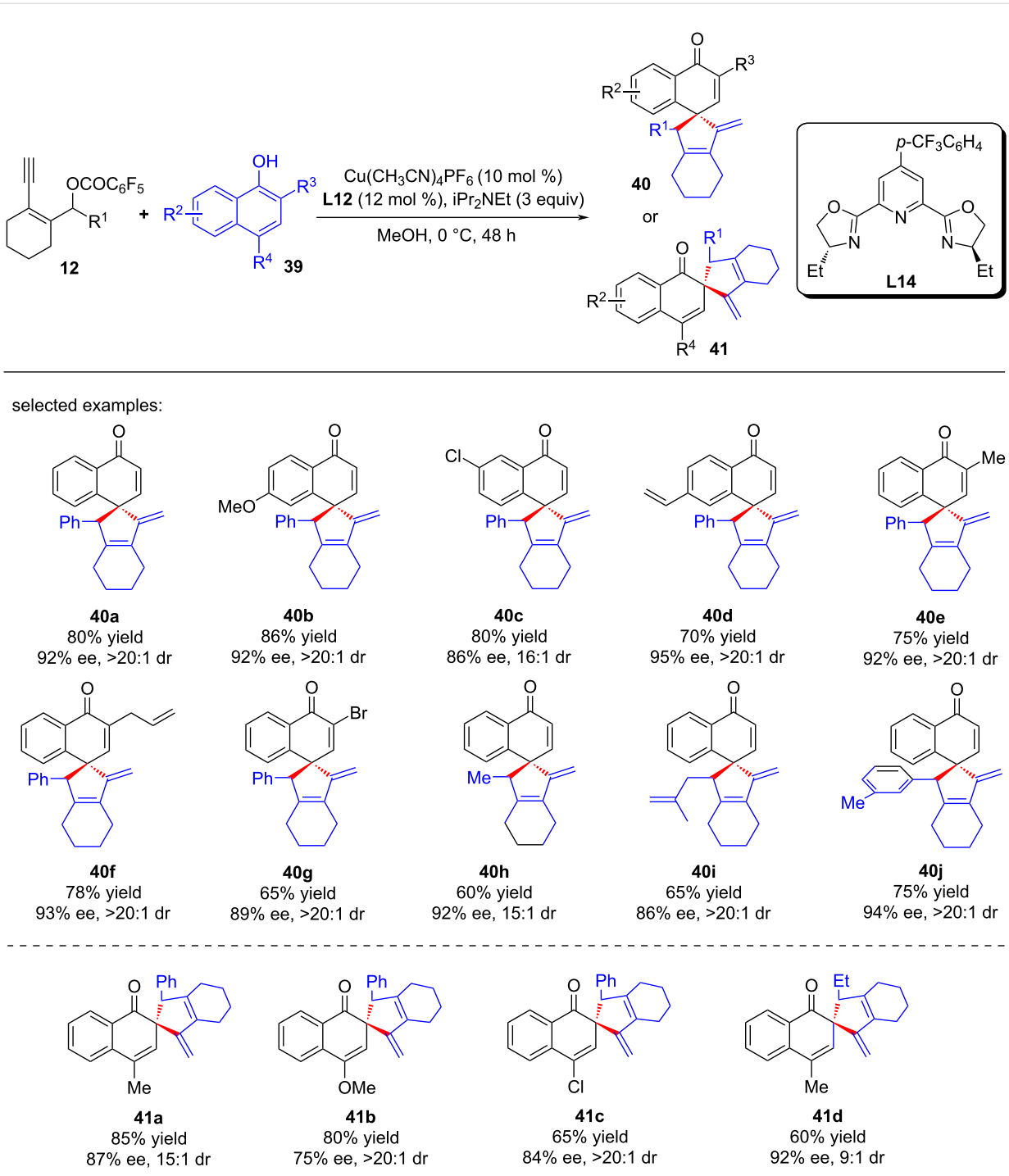

Scheme 41: Dearomative annulation of 1-naphthols and yne-allylic esters.

enantioselectivities and diastereoselectivities (Scheme 44, **43a**–**g**, **44a**–**q**). In addition, the nucleophilic substitution–dearomative cyclization process between indoles and yne-allylic esters can also proceed smoothly, resulting in spiroindolenine derivatives with high yields and ee values (Scheme 45, **45a**–**j**). They also conducted mechanism studies and believed that the designed cyclic *cis*-yne-allylic esters are crucial for the progress of the reaction. The distal yne-allylic substitution is considered to be the determining step for the enantioselectivity, while the diastereoselectivity is mainly induced by the chiral alkylated naphthol intermediate in the second annulation step (Scheme 46).

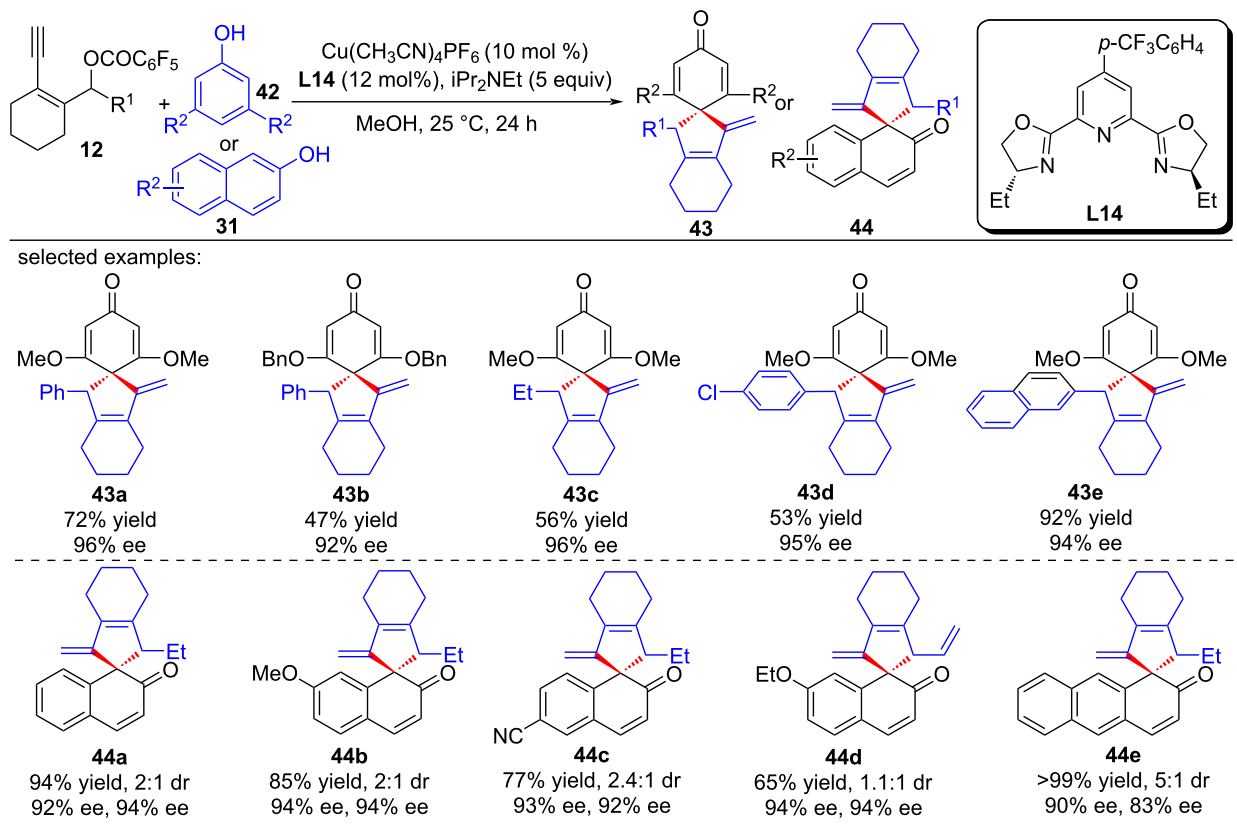

Scheme 42: Dearomative annulation of phenols or 2-naphthols and yne-allylic esters.

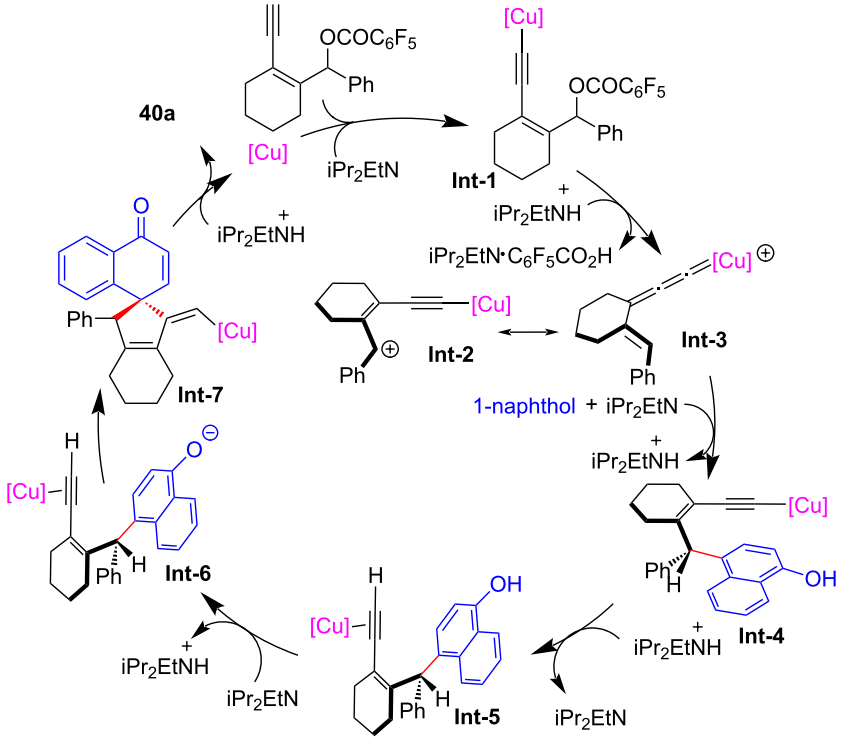

Scheme 43: Postulated annulation mechanism.

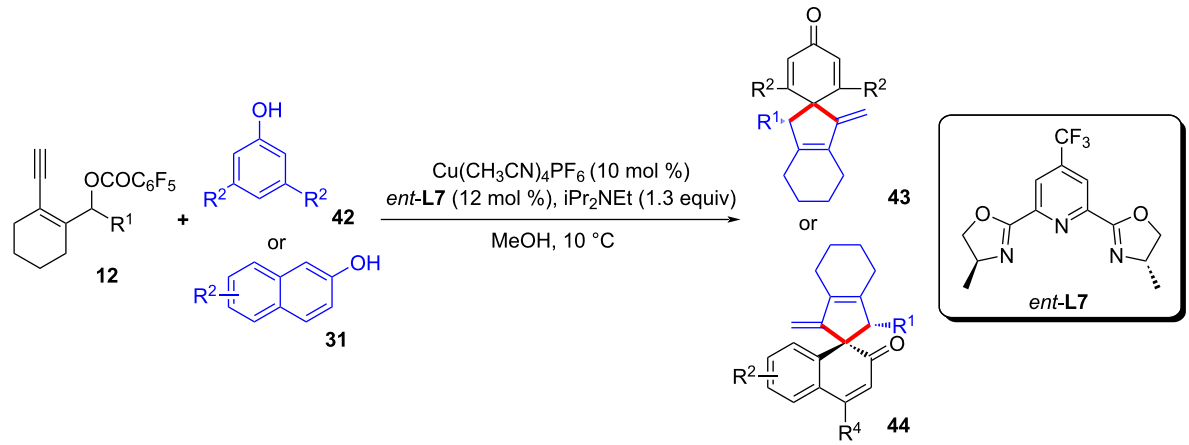

selected examples:

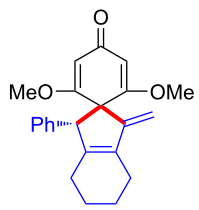

43a
90% yield
97% ee

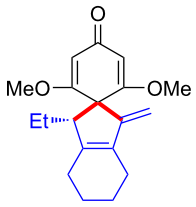

43c
97% yield
97% ee

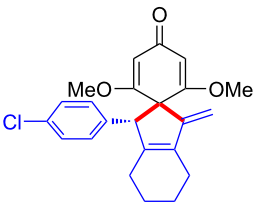

43d
99% yield
98% ee

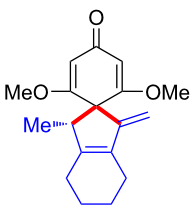

43f
87% yield
97% ee

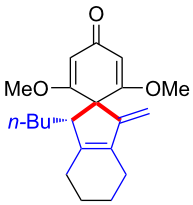

43g
98% yield
97% ee

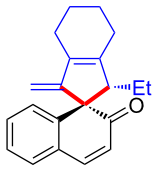

44a
92% yield, 88:12 dr
91% ee

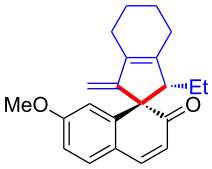

44b
97% yield, 81:19 dr
90% ee

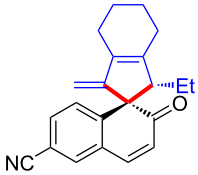

44c
52% yield, 73:27 dr
89% ee

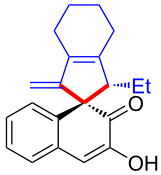

44f
62% yield, 79:21 dr
92% ee

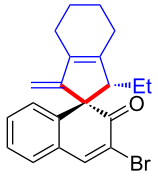

44g
88% yield, 91:9 dr
94% ee

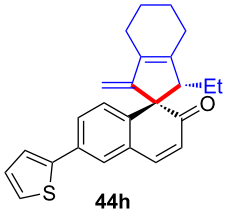

44h
67% yield, 84:16 dr
88% ee

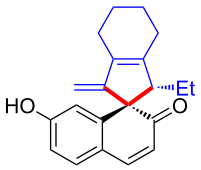

44i
83% yield, 84:16 dr
97% ee

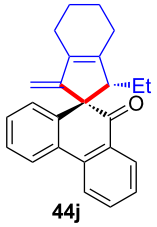

44j
54% yield, 75:25 dr
92% ee

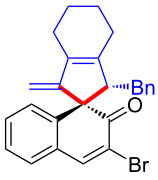

44k
85% yield, >20:1 dr
90% ee

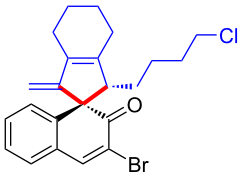

44l
91% yield, 92:8 dr
91% ee

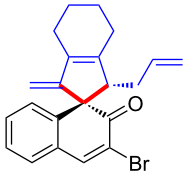

44m
94% yield, 92:8 dr
92% ee

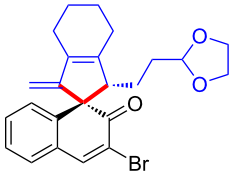

44n
94% yield, 89:11 dr
94% ee

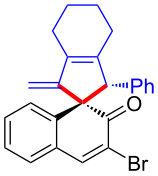

44o
70% yield, 76:24 dr
94% ee

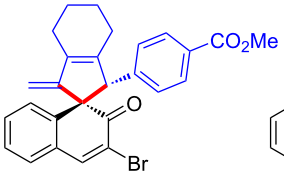

44p
99% yield, 83:17 dr
96% ee

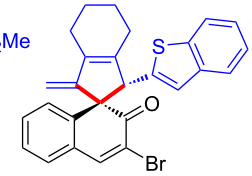

44q
92% yield, 88:12 dr
76% ee

Scheme 44: Dearomative annulation of phenols or 2-naphthols.

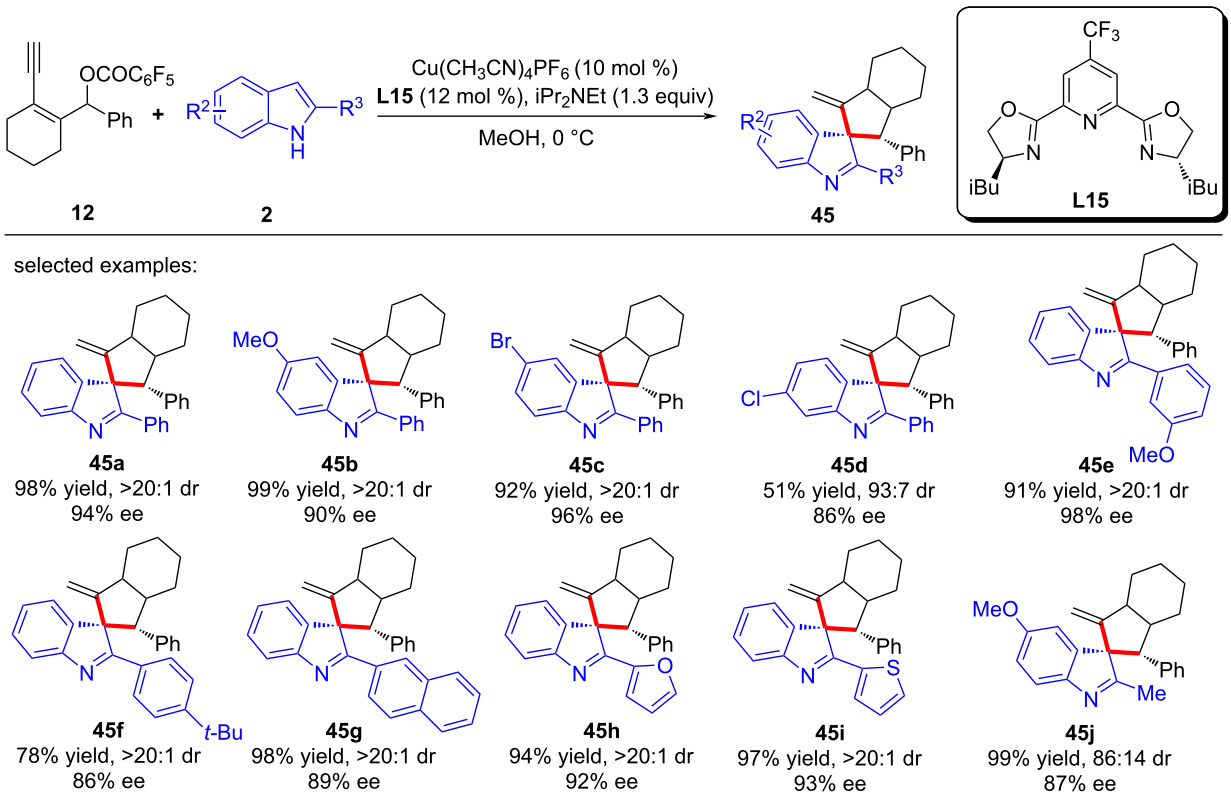

Scheme 45: Dearomative annulation of indoles.

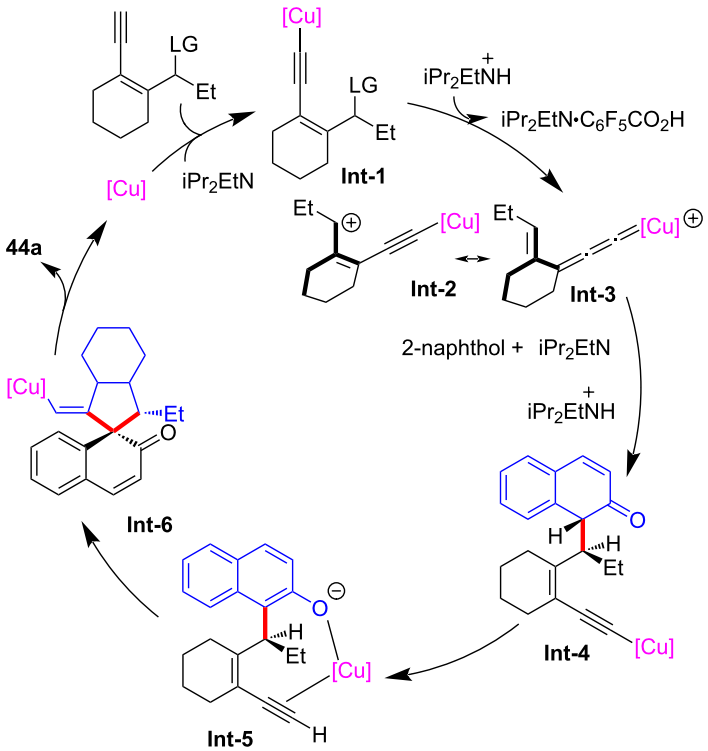

Scheme 46: Postulated annulation step.

Xu et al. [80] realized asymmetric [4 + 1] cyclization of yne-allylic esters with pyrazolones. This catalytic strategy provided direct access to a range of chiral spiropyrazolones in good to high yields, displaying moderate to excellent enantiomeric excess (Scheme 47, **47a–l**). The method represents a novel approach for the synthesis of enantioenriched spirocyclic compounds with structural complexity. Through control experiment, they have proposed a reaction mechanism where the formation of copper vinyl allenylidene and Conia-ene reaction are pivotal steps in the process (Scheme 48).

Crafting atropisomers, particularly for those with 1,2-diaxes, poses a formidable task owing to the intricate interplay of *ortho*-aryl steric hindrance. Recently, Xu et al. [81] presents a copper-catalyzed asymmetric [4 + 1] annulation strategy, utilizing remote stereocontrol substitution/annulation/aromatization to forge arylpyrroles with various C–C (Scheme 49, **48a–h**), C–N (Scheme 50, **49a–h**) or 1,2-di- (Scheme 51, **50a–l**) axial chirality in remarkable enantiopurities. Mechanistic studies and deuterium labeling experiments have revealed that the reaction proceeds in a stepwise manner without involv-

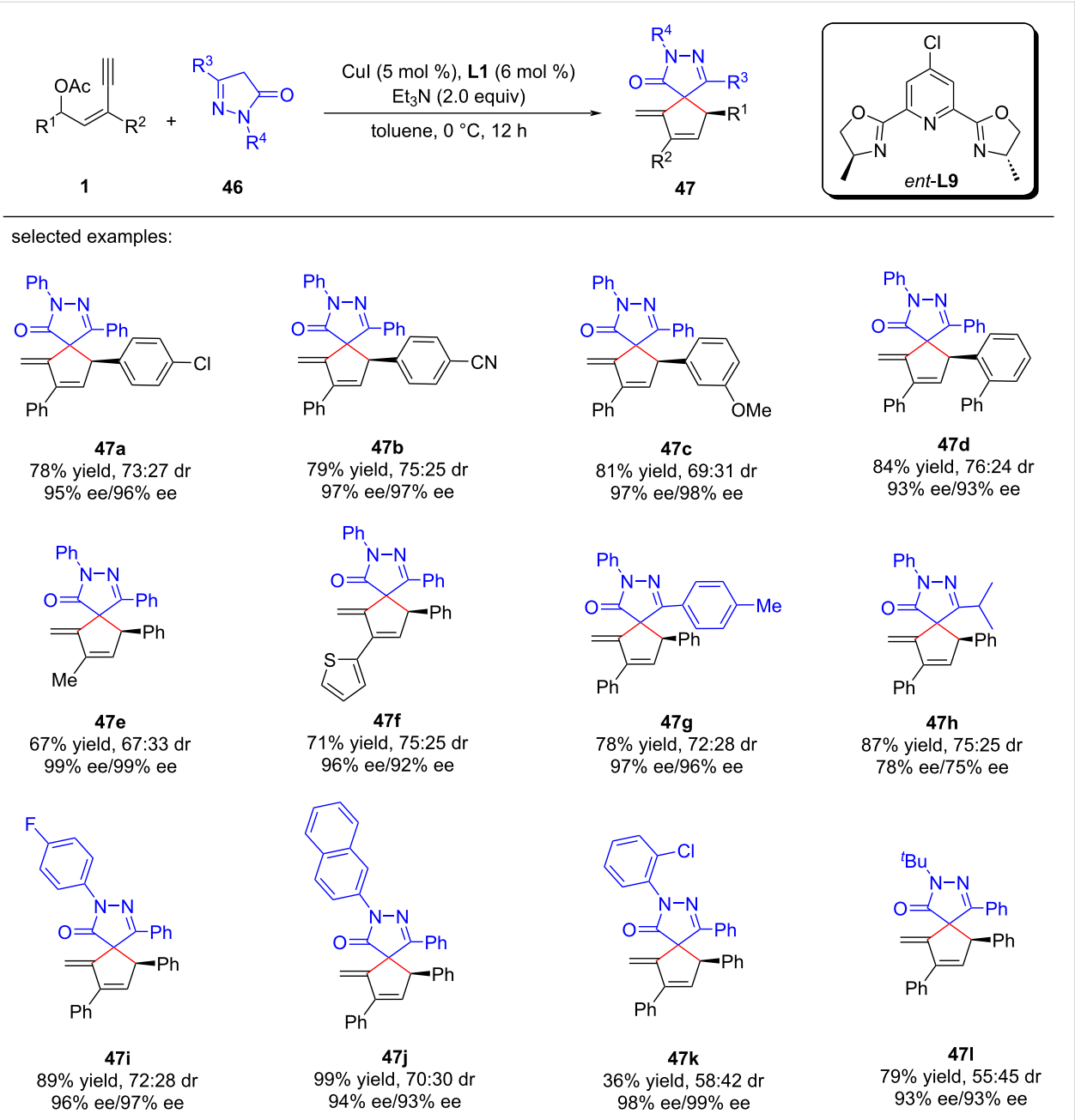

Scheme 47: Asymmetric [4 + 1] cyclization of yne-allylic esters with pyrazolones.

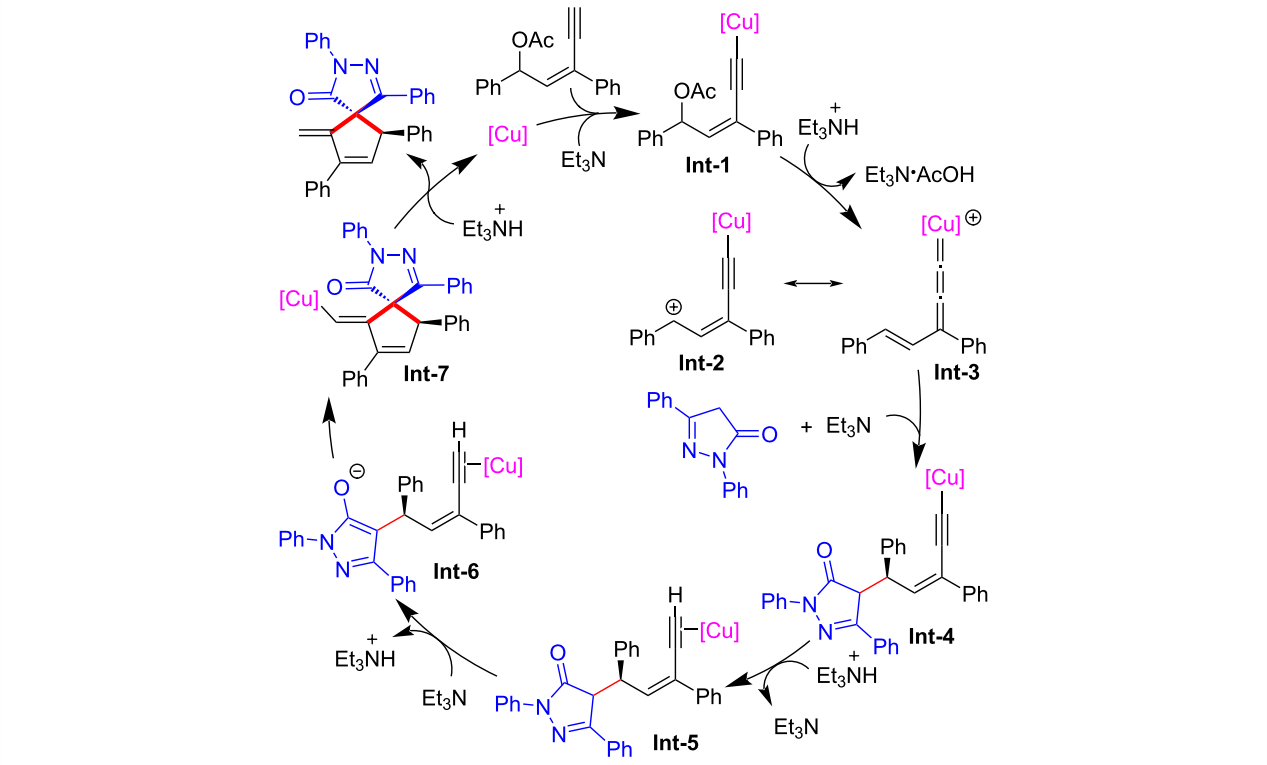

Scheme 48: Proposed mechanism.

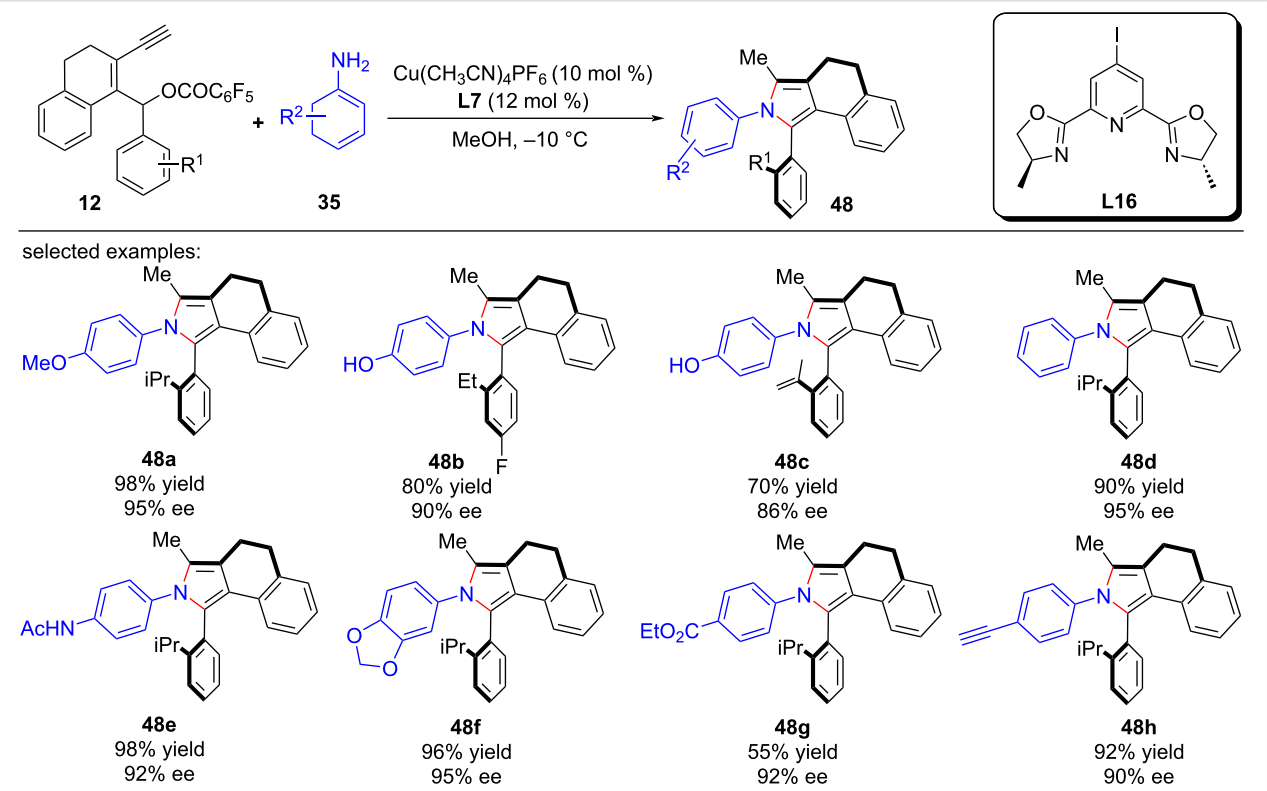

Scheme 49: Construction of C–C axially chiral arylpyrroles.

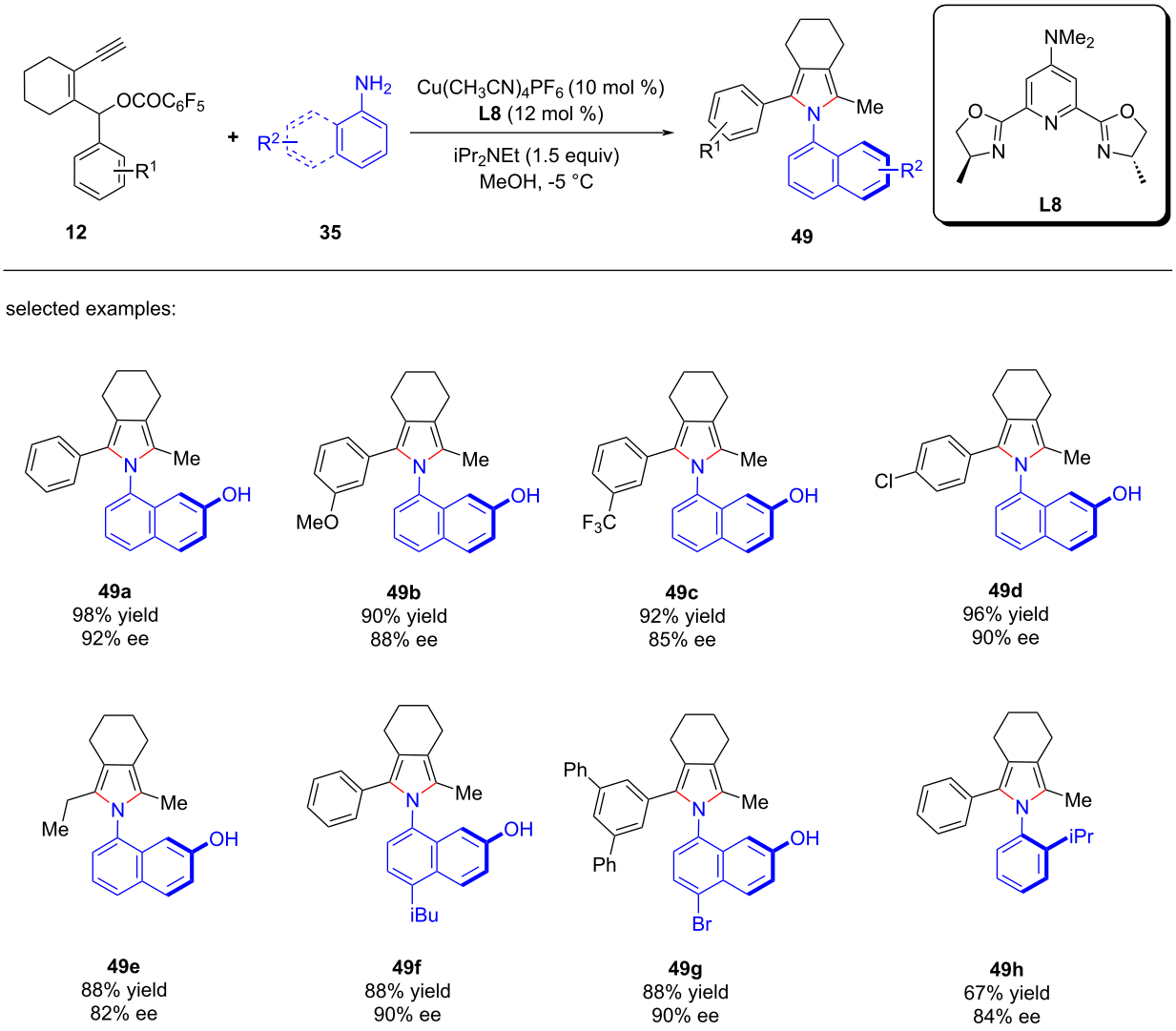

Scheme 50: Construction of C–N axially chiral arylpyrroles.

ing a 1,5-H migration process. Based on these findings, the authors have proposed a mechanism wherein the stereoselective aromatization serves as a pivotal step in the transfer of central chirality to axial chirality (Scheme 52).

To harness the full potential of CO_2 as a renewable and abundant carbon source, He et al. [82] proposed an innovative strategy that married asymmetric yne-allylic substitution with CO_2 shuttling (Scheme 53, **51a**–**k**). Furthermore, they established a Cu-catalyzed asymmetric multicomponent reaction for yne-allylic substitution, seamlessly integrating ^{13}C-labeled CO_2 into enantiomerically pure products (Scheme 54, **51a**, **51c**, **51f**, **51g**). This methodology enabled the synthesis of diverse, high-value oxazolidinones with exceptional yields and enantioselectivities. This not only addresses the challenge of CO_2 waste but also opens new avenues for the sustainable synthesis of complex molecules. Comprehensive mechanistic investigations underscored the pivotal role of DABCO in promoting CO_2 capture and indicated that the carboxylative cyclization is the rate-limiting step in the overall pathway (Scheme 55).

Conclusion

Since the first report in 2022, copper-catalyzed yne-allylic substitution has attracted intensive studies during the past two years. The protocol merges the features of both propargylic substitution and allylic substitution, but represents a new type of reaction mode, and greatly expands the scope of transition metal-catalyzed substitution reactions. Currently, yne-allylic substitutions affording 1,3- or 1,4-enynes, remote substitutions

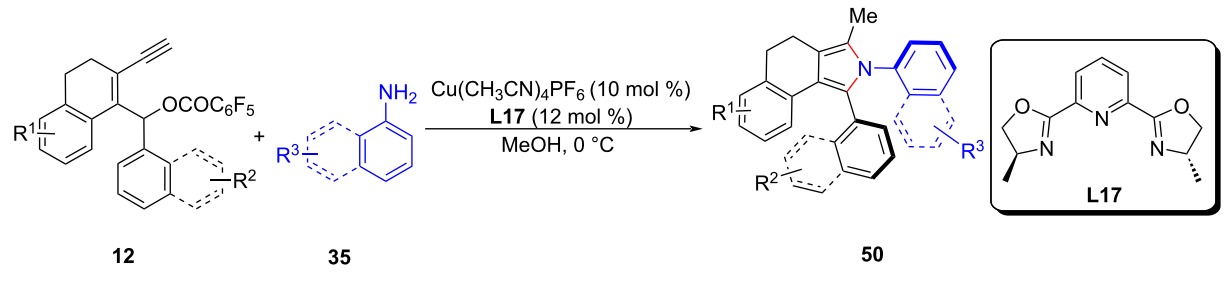

12 35 50

selected examples:

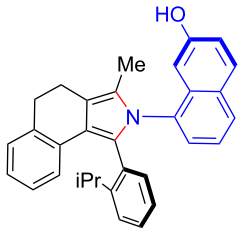

50a
92% yield, 99% ee
17:1 dr

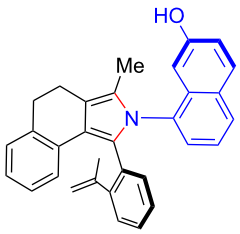

50b
85% yield, 97% ee
>20:1 dr

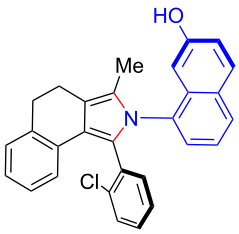

50c
97% yield, 93% ee
7.6:1 dr

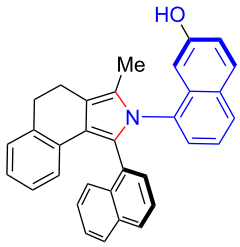

50d
88% yield, 98% ee
>20:1 dr

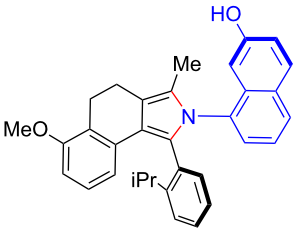

50e
75% yield, 97% ee
>20:1 dr

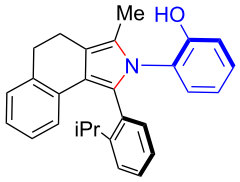

50f
95% yield, 97% ee
>20:1 dr

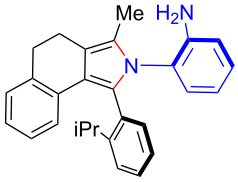

50g
68% yield, 90% ee
9:1 dr

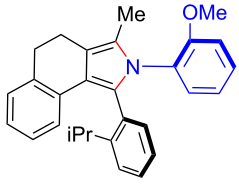

50h
99% yield, 86% ee
>20:1 dr

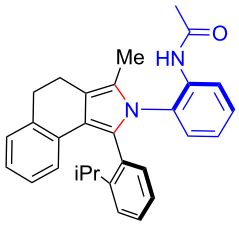

50i
47% yield, 93% ee
>20:1 dr

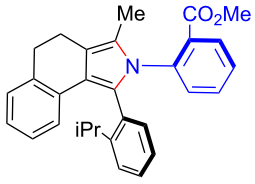

50j
36% yield, 86% ee
>20:1 dr

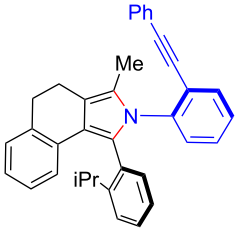

50k
84% yield, 80% ee
>20:1 dr

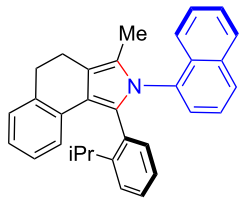

50l
99% yield, 95% ee
>20:1 dr

Scheme 51: Construction of chiral arylpyrroles with 1,2-di-axial chirality.

through dearomatization-rearomatization sequence, [4 + 1] and [3 + 2] annulations involving yne-allylic substitutions have been released. These studies have shown the huge potential of this protocol in affording diversified molecular scaffolds, and more studies will be expected to demonstrate the value of this reaction.

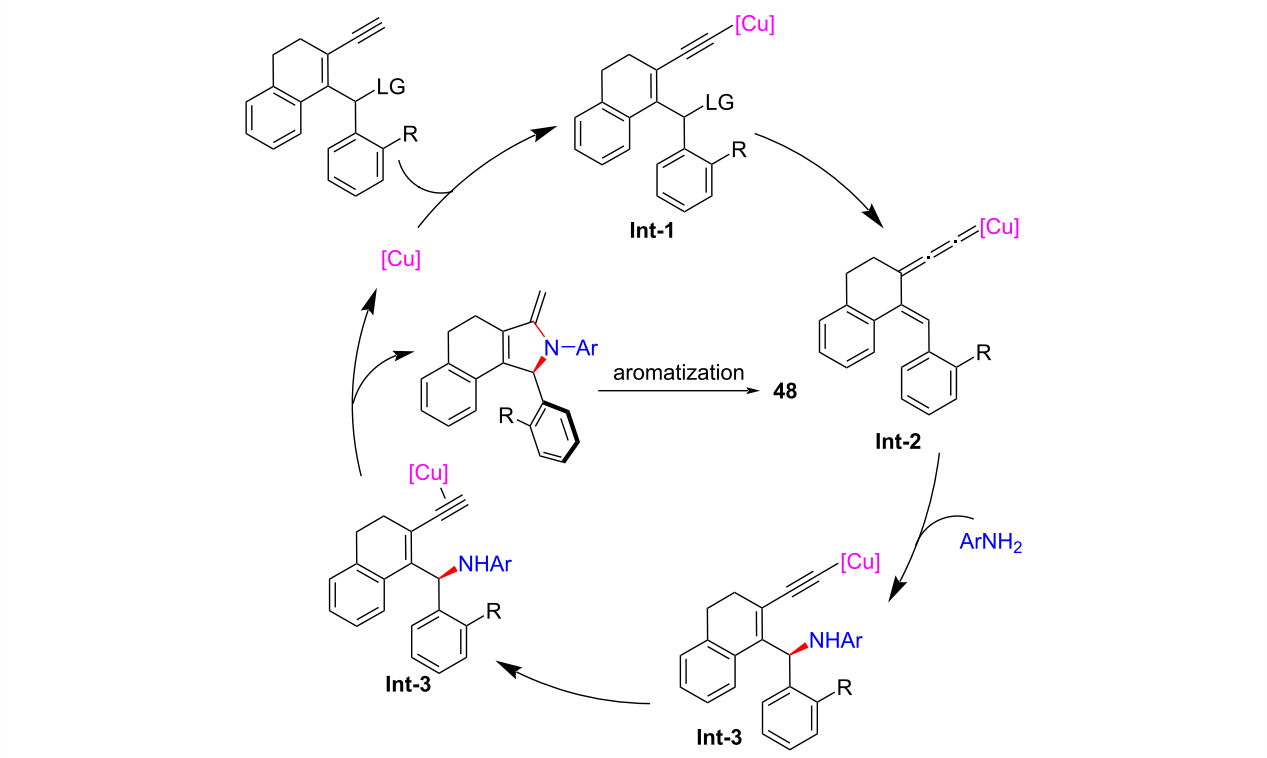

Scheme 52: Proposed mechanism.

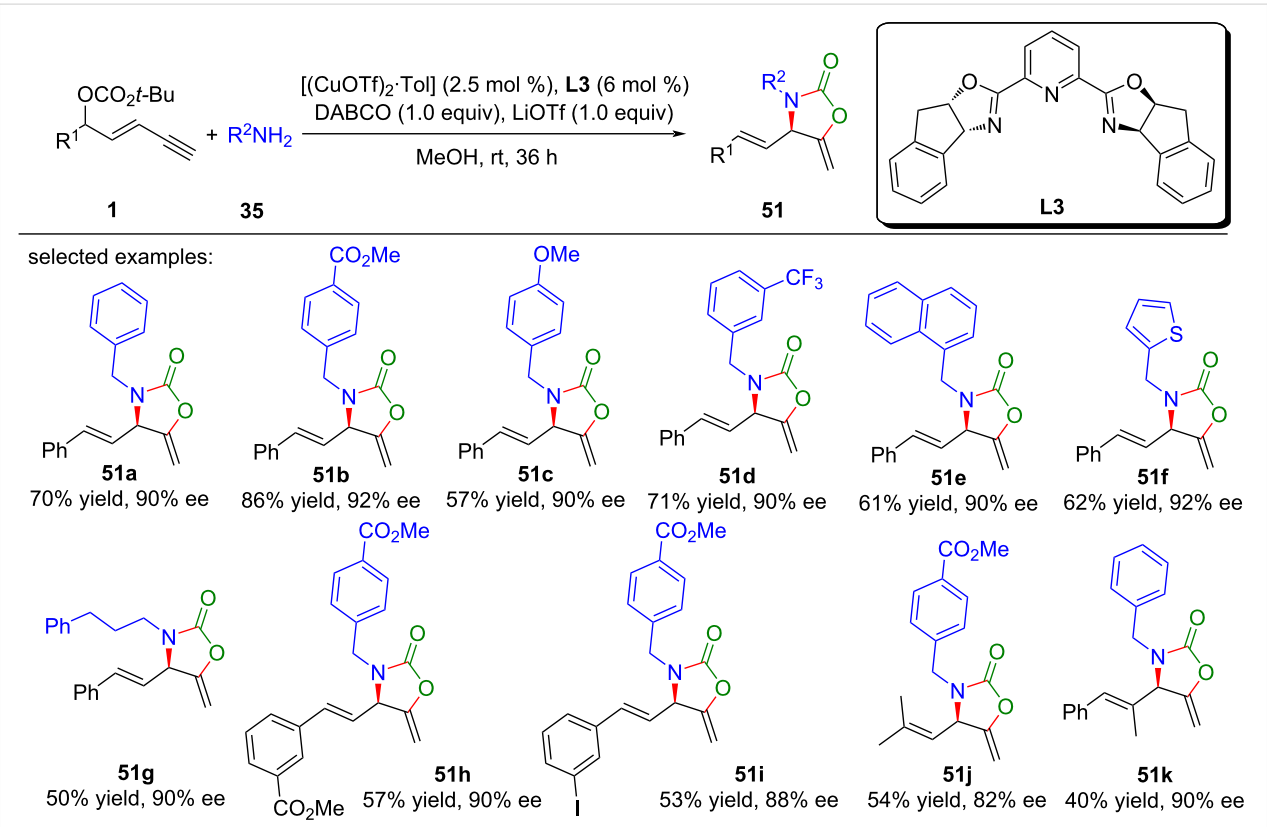

Scheme 53: CO_2 shuttling in yne-allylic substitution.

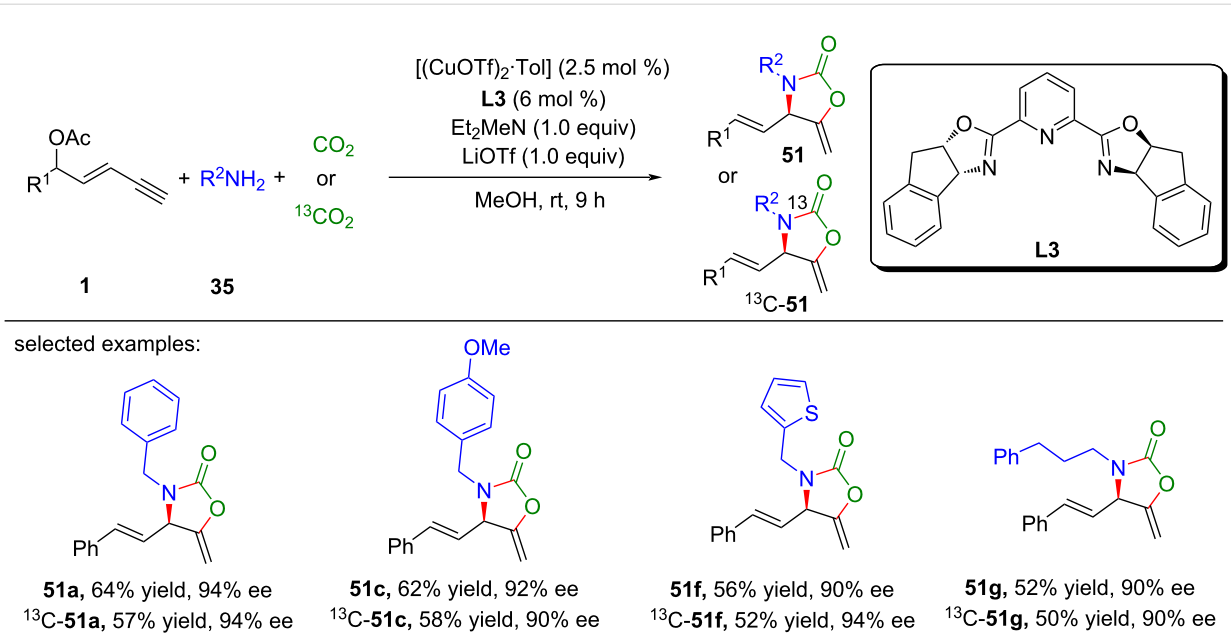

Scheme 54: CO_2 fixing in yne-allylic substitution.

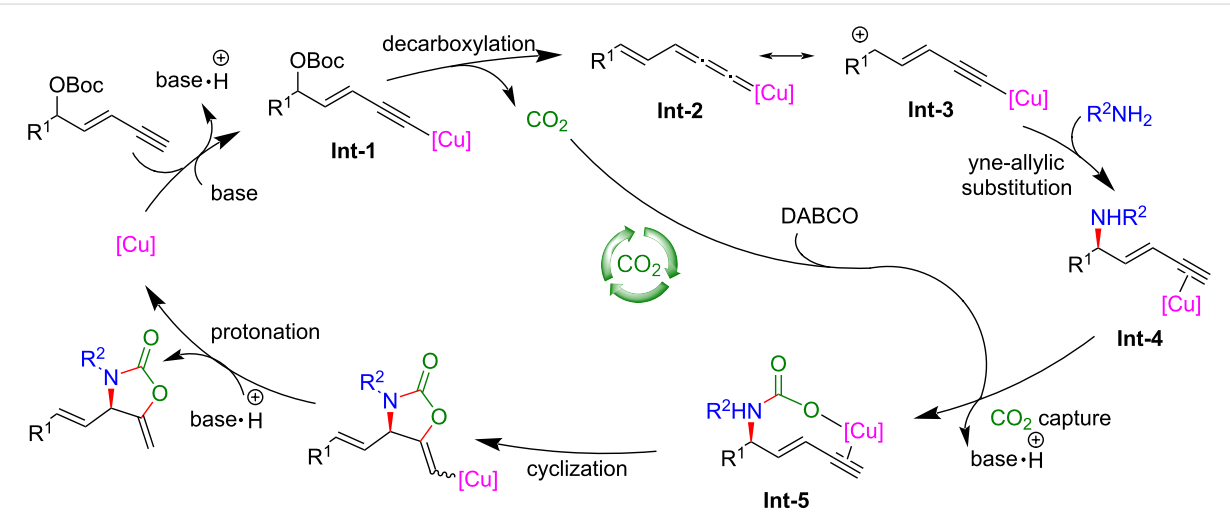

Scheme 55: Proposed mechanism.

Funding

This work was supported by the National Natural Science Foundation of China (Nos. 22071242 and 21871260), the Strategic Priority Research Program of the Chinese Academy of Sciences (No. XDB20000000), and the Fujian Natural Science Foundation (No. 2021J01522).

Author Contributions

Shuang Yang: writing – original draft. Xinqiang Fang: conceptualization; supervision; writing – review & editing.

ORCID® iDs

Xinqiang Fang - https://orcid.org/0000-0001-8217-7106

Data Availability Statement

Data sharing is not applicable as no new data was generated or analyzed in this study.

References

1. Trost, B. M.; Van Vranken, D. L. *Chem. Rev.* **1996,** *96,* 395–422. doi:10.1021/cr9409804

2. Harutyunyan, S. R.; den Hartog, T.; Geurts, K.; Minnaard, A. J.; Feringa, B. L. *Chem. Rev.* **2008,** *108,* 2824–2852. doi:10.1021/cr068424k
3. Alexakis, A.; Bäckvall, J. E.; Krause, N.; Pàmies, O.; Diéguez, M. *Chem. Rev.* **2008,** *108,* 2796–2823. doi:10.1021/cr0683515
4. Hartwig, J. F.; Stanley, L. M. *Acc. Chem. Res.* **2010,** *43,* 1461–1475. doi:10.1021/ar100047x
5. Trost, B. M.; Crawley, M. L. *Top. Organomet. Chem.* **2011,** *38,* 321–340. doi:10.1007/3418_2011_13
6. Kazmaier, U., Ed. *Transition Metal Catalyzed Enantioselective Allylic Substitution in Organic Synthesis;* Topics in Organometallic Chemistry, Vol. 38; Springer, 2012. doi:10.1007/978-3-642-22749-3
7. Yoshikai, N.; Nakamura, E. *Chem. Rev.* **2012,** *112,* 2339–2372. doi:10.1021/cr200241f
8. Zhuo, C.-X.; Zheng, C.; You, S.-L. *Acc. Chem. Res.* **2014,** *47,* 2558–2573. doi:10.1021/ar500167f
9. Butt, N. A.; Zhang, W. *Chem. Soc. Rev.* **2015,** *44,* 7929–7967. doi:10.1039/c5cs00144g
10. Hornillos, V.; Gualtierotti, J.-B.; Feringa, B. L. Asymmetric Allylic Substitutions Using Organometallic Reagents. *Progress in Enantioselective Cu(I)-catalyzed Formation of Stereogenic Centers;* Topics in Organometallic Chemistry, Vol. 58; Springer International Publishing: Cham, Switzerland, 2016; pp 1–39. doi:10.1007/3418_2015_165
11. Qu, J.; Helmchen, G. *Acc. Chem. Res.* **2017,** *50,* 2539–2555. doi:10.1021/acs.accounts.7b00300
12. Cheng, Q.; Tu, H.-F.; Zheng, C.; Qu, J.-P.; Helmchen, G.; You, S.-L. *Chem. Rev.* **2019,** *119,* 1855–1969. doi:10.1021/acs.chemrev.8b00506
13. Zhang, M.-M.; Wang, Y.-N.; Lu, L.-Q.; Xiao, W.-J. *Trends Chem.* **2020,** *2,* 764–775. doi:10.1016/j.trechm.2020.06.002
14. Xue, W.; Oestreich, M. *ACS Cent. Sci.* **2020,** *6,* 1070–1081. doi:10.1021/acscentsci.0c00738
15. Li, G.; Huo, X.; Jiang, X.; Zhang, W. *Chem. Soc. Rev.* **2020,** *49,* 2060–2118. doi:10.1039/c9cs00400a
16. Huang, H.-M.; Bellotti, P.; Glorius, F. *Chem. Soc. Rev.* **2020,** *49,* 6186–6197. doi:10.1039/d0cs00262c
17. Hoveyda, A. H.; Zhou, Y.; Shi, Y.; Brown, M. K.; Wu, H.; Torker, S. *Angew. Chem., Int. Ed.* **2020,** *59,* 21304–21359. doi:10.1002/anie.202003755
18. Zheng, C.; You, S.-L. *ACS Cent. Sci.* **2021,** *7,* 432–444. doi:10.1021/acscentsci.0c01651
19. Dutta, S.; Bhattacharya, T.; Werz, D. B.; Maiti, D. *Chem* **2021,** *7,* 555–605. doi:10.1016/j.chempr.2020.10.020
20. Pàmies, O.; Margalef, J.; Cañellas, S.; James, J.; Judge, E.; Guiry, P. J.; Moberg, C.; Bäckvall, J.-E.; Pfaltz, A.; Pericàs, M. A.; Diéguez, M. *Chem. Rev.* **2021,** *121,* 4373–4505. doi:10.1021/acs.chemrev.0c00736
21. Süsse, L.; Stoltz, B. M. *Chem. Rev.* **2021,** *121,* 4084–4099. doi:10.1021/acs.chemrev.0c01115
22. Wright, T. B.; Evans, P. A. *Chem. Rev.* **2021,** *121,* 9196–9242. doi:10.1021/acs.chemrev.0c00564
23. Ljungdahl, N.; Kann, N. *Angew. Chem., Int. Ed.* **2009,** *48,* 642–644. doi:10.1002/anie.200804114
24. Detz, R. J.; Hiemstra, H.; van Maarseveen, J. H. *Eur. J. Org. Chem.* **2009,** 6263–6276. doi:10.1002/ejoc.200900877
25. Miyake, Y.; Uemura, S.; Nishibayashi, Y. *ChemCatChem* **2009,** *1,* 342–356. doi:10.1002/cctc.200900214
26. Ding, C.-H.; Hou, X.-L. *Chem. Rev.* **2011,** *111,* 1914–1937. doi:10.1021/cr100284m
27. Nishibayashi, Y. *Synthesis* **2012,** 489–503. doi:10.1055/s-0031-1290158
28. Adeleke, A. F.; Brown, A. P. N.; Cheng, L.-J.; Mosleh, K. A. M.; Cordier, C. J. *Synthesis* **2017,** *49,* 790–801. doi:10.1055/s-0036-1588405
29. Li, T.-R.; Wang, Y.-N.; Xiao, W.-J.; Lu, L.-Q. *Tetrahedron Lett.* **2018,** *59,* 1521–1530. doi:10.1016/j.tetlet.2018.02.081
30. Roy, R.; Saha, S. *RSC Adv.* **2018,** *8,* 31129–31193. doi:10.1039/c8ra04481c
31. Roh, S. W.; Choi, K.; Lee, C. *Chem. Rev.* **2019,** *119,* 4293–4356. doi:10.1021/acs.chemrev.8b00568
32. Nishibayashi, Y. *Chem. Lett.* **2021,** *50,* 1282–1288. doi:10.1246/cl.210126
33. Li, H.; Alexakis, A. *Angew. Chem., Int. Ed.* **2012,** *51,* 1055–1058. doi:10.1002/anie.201107129
34. Hornillos, V.; Pérez, M.; Fañanás-Mastral, M.; Feringa, B. L. *J. Am. Chem. Soc.* **2013,** *135,* 2140–2143. doi:10.1021/ja312487r
35. Giannerini, M.; Fañanás-Mastral, M.; Feringa, B. L. *J. Am. Chem. Soc.* **2012,** *134,* 4108–4111. doi:10.1021/ja300743t
36. Kacprzynski, M. A.; May, T. L.; Kazane, S. A.; Hoveyda, A. H. *Angew. Chem., Int. Ed.* **2007,** *46,* 4554–4558. doi:10.1002/anie.200700841
37. McGrath, K. P.; Hoveyda, A. H. *Angew. Chem., Int. Ed.* **2014,** *53,* 1910–1914. doi:10.1002/anie.201309456
38. Dabrowski, J. A.; Gao, F.; Hoveyda, A. H. *J. Am. Chem. Soc.* **2011,** *133,* 4778–4781. doi:10.1021/ja2010829
39. Pérez, M.; Fañanás-Mastral, M.; Bos, P. H.; Rudolph, A.; Harutyunyan, S. R.; Feringa, B. L. *Nat. Chem.* **2011,** *3,* 377–381. doi:10.1038/nchem.1009
40. Goh, S. S.; Guduguntla, S.; Kikuchi, T.; Lutz, M.; Otten, E.; Fujita, M.; Feringa, B. L. *J. Am. Chem. Soc.* **2018,** *140,* 7052–7055. doi:10.1021/jacs.8b02992
41. You, H.; Rideau, E.; Sidera, M.; Fletcher, S. P. *Nature* **2015,** *517,* 351–355. doi:10.1038/nature14089
42. Makida, Y.; Takayama, Y.; Ohmiya, H.; Sawamura, M. *Angew. Chem., Int. Ed.* **2013,** *52,* 5350–5354. doi:10.1002/anie.201300785
43. Harada, A.; Makida, Y.; Sato, T.; Ohmiya, H.; Sawamura, M. *J. Am. Chem. Soc.* **2014,** *136,* 13932–13939. doi:10.1021/ja5084333
44. Ito, H.; Kunii, S.; Sawamura, M. *Nat. Chem.* **2010,** *2,* 972–976. doi:10.1038/nchem.801
45. Yamamoto, E.; Takenouchi, Y.; Ozaki, T.; Miya, T.; Ito, H. *J. Am. Chem. Soc.* **2014,** *136,* 16515–16521. doi:10.1021/ja506284w
46. Delvos, L. B.; Vyas, D. J.; Oestreich, M. *Angew. Chem., Int. Ed.* **2013,** *52,* 4650–4653. doi:10.1002/anie.201300648
47. Zhou, Y.; Shi, Y.; Torker, S.; Hoveyda, A. H. *J. Am. Chem. Soc.* **2018,** *140,* 16842–16854. doi:10.1021/jacs.8b10885
48. Sun, Y.; Zhou, Y.; Shi, Y.; del Pozo, J.; Torker, S.; Hoveyda, A. H. *J. Am. Chem. Soc.* **2019,** *141,* 12087–12099. doi:10.1021/jacs.9b05465
49. Zhang, Q.; Zhou, S.-W.; Shi, C.-Y.; Yin, L. *Angew. Chem., Int. Ed.* **2021,** *60,* 26351–26356. doi:10.1002/anie.202110709
50. Wang, Y.-M.; Buchwald, S. L. *J. Am. Chem. Soc.* **2016,** *138,* 5024–5027. doi:10.1021/jacs.6b02527
51. Han, J. T.; Jang, W. J.; Kim, N.; Yun, J. *J. Am. Chem. Soc.* **2016,** *138,* 15146–15149. doi:10.1021/jacs.6b11229
52. Detz, R. J.; Delville, M. M. E.; Hiemstra, H.; van Maarseveen, J. H. *Angew. Chem., Int. Ed.* **2008,** *47,* 3777–3780. doi:10.1002/anie.200705264

53. Hattori, G.; Matsuzawa, H.; Miyake, Y.; Nishibayashi, Y. *Angew. Chem., Int. Ed.* **2008,** *47,* 3781–3783. doi:10.1002/anie.200800276
54. Zhang, D.-Y.; Hu, X.-P. *Tetrahedron Lett.* **2015,** *56,* 283–295. doi:10.1016/j.tetlet.2014.11.112
55. Hattori, G.; Sakata, K.; Matsuzawa, H.; Tanabe, Y.; Miyake, Y.; Nishibayashi, Y. *J. Am. Chem. Soc.* **2010,** *132,* 10592–10608. doi:10.1021/ja1047494
56. Nakajima, K.; Shibata, M.; Nishibayashi, Y. *J. Am. Chem. Soc.* **2015,** *137,* 2472–2475. doi:10.1021/jacs.5b00004
57. Li, R.-Z.; Tang, H.; Yang, K. R.; Wan, L.-Q.; Zhang, X.; Liu, J.; Fu, Z.; Niu, D. *Angew. Chem., Int. Ed.* **2017,** *56,* 7213–7217. doi:10.1002/anie.201703029
58. Cheng, L.-J.; Brown, A. P. N.; Cordier, C. J. *Chem. Sci.* **2017,** *8,* 4299–4305. doi:10.1039/c7sc01042g
59. Gómez, J. E.; Cristòfol, À.; Kleij, A. W. *Angew. Chem., Int. Ed.* **2019,** *58,* 3903–3907. doi:10.1002/anie.201814242
60. Li, R.-Z.; Liu, D.-Q.; Niu, D. *Nat. Catal.* **2020,** *3,* 672–680. doi:10.1038/s41929-020-0462-9
61. Li, M.-D.; Wang, X.-R.; Lin, T.-Y. *Tetrahedron Chem* **2024,** *11,* 100082. doi:10.1016/j.tchem.2024.100082
62. Niu, S.; Luo, Y.; Xu, C.; Liu, J.; Yang, S.; Fang, X. *ACS Catal.* **2022,** *12,* 6840–6850. doi:10.1021/acscatal.2c00911
63. Ma, J.-S.; Lu, H.-Y.; Chen, Y.-W.; Zhao, W.-C.; Sun, Y.-Z.; Li, R.-P.; Wang, H.-X.; Lin, G.-Q.; He, Z.-T. *Nat. Synth.* **2023,** *2,* 37–48. doi:10.1038/s44160-022-00176-4
64. van Maarseveen, J. H. *Nat. Synth.* **2023,** *2,* 11–12. doi:10.1038/s44160-022-00192-4
65. Luo, S.-Y.; Lin, G.-Q.; He, Z.-T. *Org. Chem. Front.* **2024,** *11,* 690–695. doi:10.1039/d3qo01749d
66. Li, M.-D.; Wang, Z.-H.; Zhu, H.; Wang, X.-R.; Wang, J.-R.; Lin, T.-Y. *Angew. Chem., Int. Ed.* **2023,** e202313911. doi:10.1002/anie.202313911
67. Luo, D.; Niu, S.; Gong, F.; Xu, C.; Lan, S.; Liu, J.; Yang, S.; Fang, X. *ACS Catal.* **2024,** *14,* 2746–2757. doi:10.1021/acscatal.3c06146
68. Lu, H.-Y.; Li, Z.-H.; Lin, G.-Q.; He, Z.-T. *Chem. Commun.* **2024,** *60,* 4210–4213. doi:10.1039/d4cc00371c
69. Lin, T.-Y.; Li, M.-D.; Wang, R.; Wang, X. *Org. Lett.* **2024,** *26,* 5758–5763. doi:10.1021/acs.orglett.4c01916
70. Yin, T.; Zhao, C.; Yao, C.; Qian, H.-D.; Yuan, Z.; Peng, H.; Feng, Y.; Xu, H. *Org. Lett.* **2024,** *26,* 5961–5965. doi:10.1021/acs.orglett.4c02012
71. Wang, X.-R.; Li, M.-D.; Wang, Z.-H.; Zhu, H.; Wang, J.-R.; Wei, Y.-Y.; Lin, T.-Y. *Org. Lett.* **2024,** *26,* 6407–6412. doi:10.1021/acs.orglett.4c02199
72. Sun, Y.-Z.; Ren, Z.-Y.; Yang, Y.-X.; Liu, Y.; Lin, G.-Q.; He, Z.-T. *Angew. Chem., Int. Ed.* **2023,** e202314517. doi:10.1002/anie.202314517
73. Qian, H.-D.; Li, X.; Yin, T.; Qian, W.-F.; Zhao, C.; Zhu, C.; Xu, H. *Sci. China: Chem.* **2024,** *67,* 1175–1180. doi:10.1007/s11426-023-1922-5
74. Li, X.; Qian, H.-D.; Qiao, X.; Zhao, C.; Lu, Y.; Zhu, C.; Xu, H. *Org. Chem. Front.* **2024,** *11,* 3962–3967. doi:10.1039/d4qo00602j
75. Kong, H.-H.; Zhu, C.; Deng, S.; Xu, G.; Zhao, R.; Yao, C.; Xiang, H.-M.; Zhao, C.; Qi, X.; Xu, H. *J. Am. Chem. Soc.* **2022,** *144,* 21347–21355. doi:10.1021/jacs.2c09572
76. Zhu, H.; Xu, L.; Zhu, B.; Liao, M.; Li, J.; Han, Z.; Sun, J.; Huang, H. *Org. Lett.* **2023,** *25,* 9213–9218. doi:10.1021/acs.orglett.3c03871
77. Sun, Y.-Z.; Lin, G.-Q.; He, Z.-T. *Synlett* **2024,** in press. doi:10.1055/a-2294-5395
78. Li, X.; Guo, J.-X.; Zhang, J.; Chen, Q.-Y.; He, Y.-J.; Sha, F.; Xiang, H.; Yu, P.; Liu, P.-N. *ACS Catal.* **2024,** *14,* 9244–9253. doi:10.1021/acscatal.4c01563
79. Zhao, R.; Deng, S.; Huang, R.; Kong, H.-H.; Lu, Y.; Yin, T.; Wang, J.; Li, Y.; Zhu, C.; Pan, F.; Qi, X.; Xu, H. *ACS Catal.* **2024,** *14,* 9254–9264. doi:10.1021/acscatal.4c01756
80. Xu, G.; Zhu, C.; Li, X.; Zhu, K.; Xu, H. *Chin. Chem. Lett.* **2024,** in press. doi:10.1016/j.cclet.2024.110114
81. Yao, C.; Li, D.-R.; Xiang, H.-M.; Li, S.-J.; Lu, Y.; Wang, Z.; Yin, T.; Wang, J.; Feng, K.; Zhu, C.; Xu, H. *Nat. Commun.* **2024,** *15,* 6848. doi:10.1038/s41467-024-50896-8
82. Li, Z.-H.; Ma, J.-S.; Lu, H.-Y.; Lin, G.-Q.; He, Z.-T. *ACS Catal.* **2024,** *14,* 11646–11656. doi:10.1021/acscatal.4c02333

License and Terms

BEILSTEIN JOURNAL OF ORGANIC CHEMISTRY

Germanyl triazoles as a platform for CuAAC diversification and chemoselective orthogonal cross-coupling

John M. Halford-McGuff[1], Thomas M. Richardson[1], Aidan P. McKay[1], Frederik Peschke[2], Glenn A. Burley[*2] and Allan J. B. Watson[*1]

Full Research Paper

Open Access

Address:
[1]EaStCHEM, School of Chemistry, University of St Andrews, North Haugh, St Andrews, Fife, KY16 9ST, UK and [2]Department of Pure & Applied Chemistry, University of Strathclyde, Glasgow, G1 1XL, UK

Email:
Glenn A. Burley[*] - glenn.burley@strath.ac.uk; Allan J. B. Watson[*] - aw260@st-andrews.ac.uk

* Corresponding author

Keywords:
chemoselectivity; click chemistry; copper; germanium; triazole

Beilstein J. Org. Chem. **2024,** *20,* 3198–3204.
https://doi.org/10.3762/bjoc.20.265

Received: 23 August 2024
Accepted: 25 November 2024
Published: 05 December 2024

This article is part of the thematic issue "Copper catalysis: a constantly evolving field".

Guest Editor: J. Yun

Abstract

We report the synthesis of germanyl triazoles formed via a copper-catalysed azide–alkyne cycloaddition (CuAAC) of germanyl alkynes. The reaction is often high yielding, functional group tolerant, and compatible with complex molecules. The installation of the Ge moiety enables further diversification of the triazole products, including chemoselective transition metal-catalysed cross-coupling reactions using bifunctional boryl/germyl species.

Introduction

Since its inception, click chemistry has been established as a powerful approach for molecule synthesis. Strategies within click chemistry include several widely used reactions such as the (hetero-)Diels–Alder reaction [1,2], alkene hydrothiolation [3], and an array of amide-bond-forming chemistries [4]. However, by virtue of the access to alkyne and azide precursors and the formation of a single 1,4-disubstituted triazole product, the copper-catalysed azide–alkyne cycloaddition (CuAAC) remains the archetypal click reaction (Scheme 1) [5].

The reaction has shown applicability on small and large scale, as well as under flow conditions [6], and extensive scope across a range of benign solvent conditions [7-10]. In addition, the CuAAC reaction uses inexpensive Cu catalysts [11], is insensitive towards oxygen and water [12,13], and consistently delivers high yields and (where relevant) enantioselectivities [8-10,14-19]. As such, the reaction has been used extensively throughout drug discovery [20,21], chemical biology [22,23], and materials science [24-27]. Orthogonal alkyne reactivity can also be observed under certain systems [28-30]. The reaction typically uses a Cu(II) pre-catalyst, which is converted to a mechanistically-required Cu(I) species in situ through the addition of a reductant (e.g., sodium ascorbate, NaAsc) [31,32], or via Glaser–Hay alkyne homocoupling [33,34].

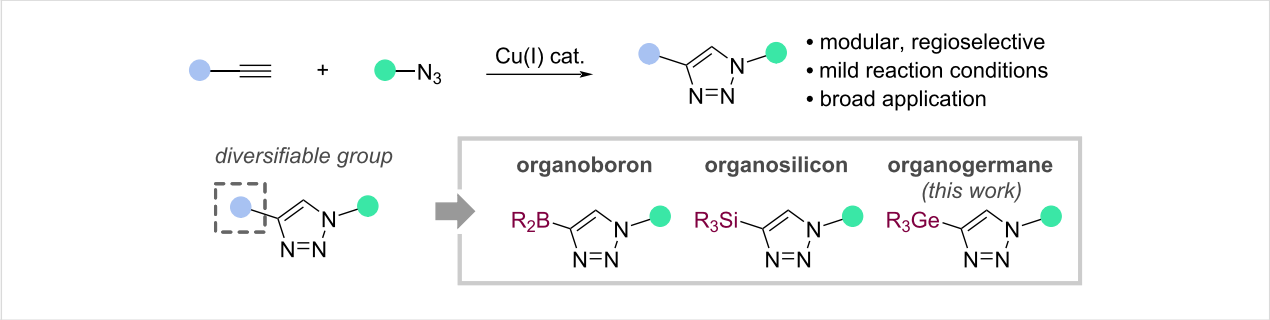

Scheme 1: The CuAAC reaction and installation of functional groups for product diversification.

The mild and accessible nature of the CuAAC reaction has allowed the use of azide or alkyne components that bear functional groups for subsequent product diversification (Scheme 1). For example, protected alkynylboron reagents can be employed [35-37], such as *N*-methyliminodiacetic acid (MIDA)boronate esters [38], potassium trifluoroborates [39], and others [40-42]. Similarly, organosilicon reagents have proven useful in various Cu- and Pd-catalysed C–X-bond-forming strategies [43-51], including widespread use across several CuAAC methodologies [52-54].

Germanium-based functional groups have recently emerged as highly useful components for transition-metal-catalysed cross-couplings. Schoenebeck and co-workers have shown that Ge-based compounds are versatile reagents within chemoselective cross-coupling processes for the formation of a variety of C–C and C–X bonds [55-63]. Importantly, these transformations can take place in the presence of borylated functional groups, allowing orthogonal cross-coupling, whilst also offering excellent stability compared to boron-based reagents [57-67].

Based on their utility and stability, germanium units could therefore be useful within CuAAC reactions and offer potential as functional handles for downstream elaboration of CuAAC products. To date, the main use of germanyl alkynes in (3 + 2) cycloadditions has been limited to a small number of Huisgen (non-Cu-catalysed) reactions [68,69]. Zaitsev and co-workers reported the synthesis and CuAAC reactions of a dialkynyl germane to access 1,2-bis(triazolyl)tetraphenyldigermanes [70]. Here, we report the development of germanyl alkynes as CuAAC components, with exploration of their scope and downstream diversification.

Results and Discussion

We undertook an exploratory survey of CuAAC reaction conditions using benzyl azide and triethylgermanyl acetylene (see Supporting Information File 1). The most effective conditions were found to be based on the classical combination of $CuSO_4$/NaAsc, with optimisation (see Supporting Information File 1) delivering the general conditions shown in Scheme 2. These afforded a clean conversion to the desired triazole products **1**–**21** without any observable degermylation or other side reactions that could be anticipated based on transmetalation to Cu [43].

The generality of the CuAAC process was explored using a range of azides (Scheme 2a), with variation of the germanyl alkyne motif (Scheme 2b), and with variation of both components (Scheme 2c). In general, the CuAAC process worked effectively, tolerating the functional groups for which the CuAAC is well-known – in all cases the remaining mass balance was accounted for by the germanyl acetylene, suggesting sluggish CuAAC reactivity compared to other alkynes, which typically require much shorter reaction times. Extending the reaction time provided a higher conversion to the product **14**. Yields were observed to be greater for aryl azides (e.g., **4** vs **6**). Heterocycles such as pyridine (**1**), pyrimidine (**10**), phenothiazine (**11**), and chromene (**12**) were tolerated. Benzylic azides were accommodated including those bearing nitro (**2**), iodo (**3**), and boronic ester groups (**5**, **21**). Strained rings were effective including cubane (**18**) and bicyclopentane (**20**). While **18** and **20** were isolated in lower yield, no evidence of ring opening was observed and the starting material could be recovered in each case, consistent with observations by Lam and MacMillan [71,72]. Variation of the steric and electronic parameters of the germanyl acetylene was straightforward (**14**–**17**; Scheme 2b). Several limitations were observed (Scheme 2d): benzyl azides displaying an arylboronic acid and MIDA ester (**22** and **23**) gave no reaction, side reactions were observed with a dialkynyl germane (**24**), and the product derived from azide **25** was unstable to purification.

To further demonstrate the compatibility and utility of germanyl alkynes in CuAAC reactions, we applied the CuAAC process to more challenging substrates. Using fluorophore- and cholesterol-derived azides, coupling with the triethylgermanyl alkyne delivered the expected products **26** and **27**, respectively, in good yield, enabling possible downstream diversification of these

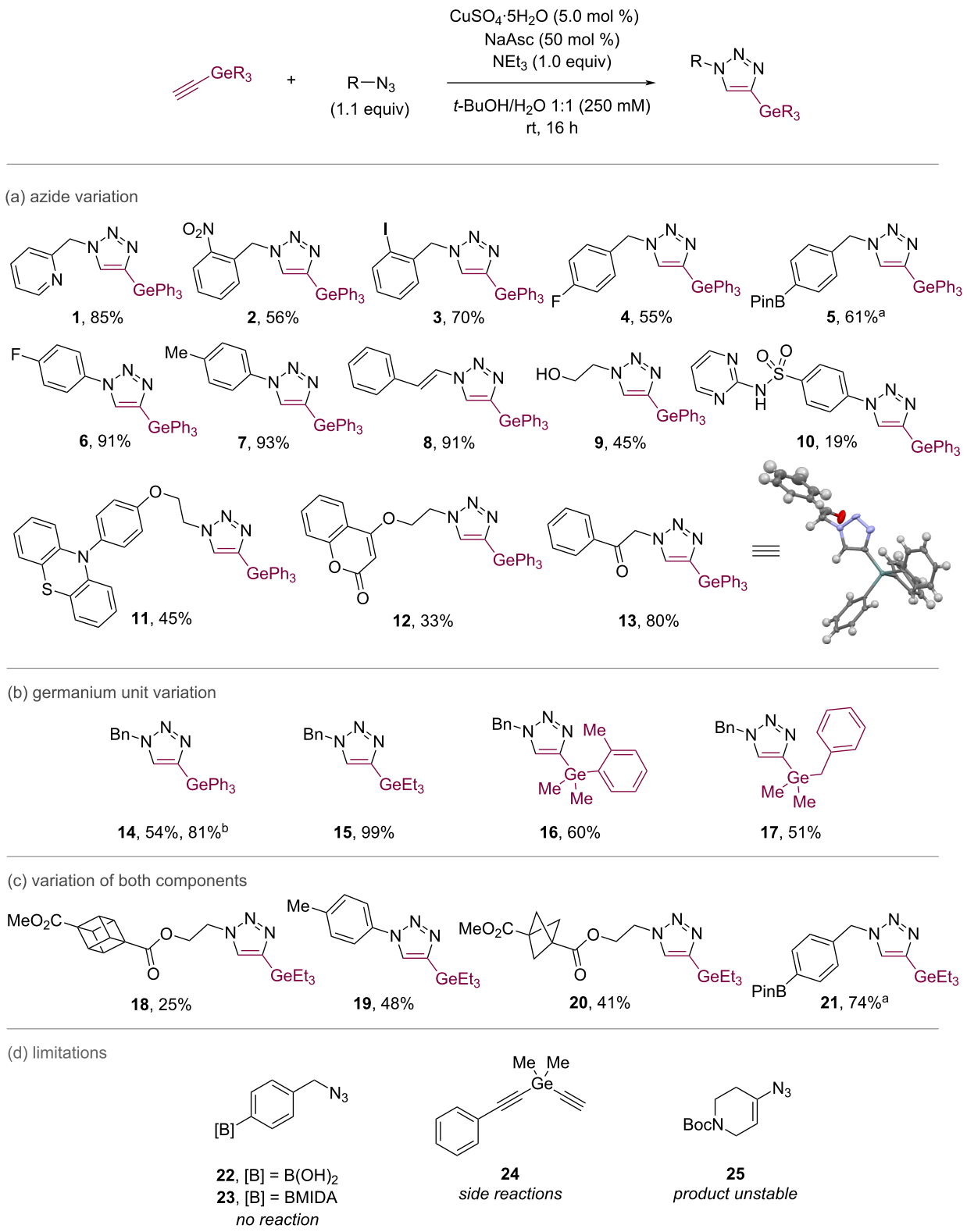

Scheme 2: Scope of germanyl acetylene CuAAC. Alkyne (1.0 equiv), azide (1.1 equiv), $CuSO_4·5H_2O$ (5.0 mol %), NaAsc (50 mol %), NEt_3 (1.0 equiv), *t*-BuOH/H_2O 1:1 (250 mM), N_2, rt, 16 h. Isolated yields. [a]Reaction performed with CsF (2.0 equiv) as an additive. [b]Reaction performed at rt for 64 h.

functional molecules of relevance to chemical biology (Scheme 3a).

The utility of the germanyl triazole products was then assessed by subsequent derivatisation of exemplar compounds **15** and **21** (Scheme 3b). Chemoselective Suzuki–Miyaura cross-coupling of the BPin moiety in **21** was straightforward, giving **28** in excellent yield [73]. Similarly, cross-coupling of the $GeEt_3$ moiety in **15** under conditions developed by Schoenebeck and co-workers gave **29** [57]. Bromodegermanylation using NBS employing conditions from Schoenebeck gave bromotriazoles **30** and **31** in moderate to excellent yield [62]. These could then undergo Suzuki–Miyaura cross-coupling to give **32** or chemoselective Negishi coupling to give **33** [74]. Finally, BPin **21** could be oxidised to the phenol derivative **34** or cross-coupled with piperidine under Chan–Lam conditions to give the aniline derivative **35** in good yield [75].

Conclusion

In summary, we have developed a general method towards the synthesis of germanyl triazoles. These reagents are generally compatible but seem to be less reactive than other classes of alkyne. The germanyl alkyne CuAAC is applicable to functional group-rich molecules, opening opportunities for downstream diversification by chemoselective functionalisation strategies [76]. The germanyl group installed in the triazole products can be used as a reactive handle for further diversification including cross-coupling reactions.

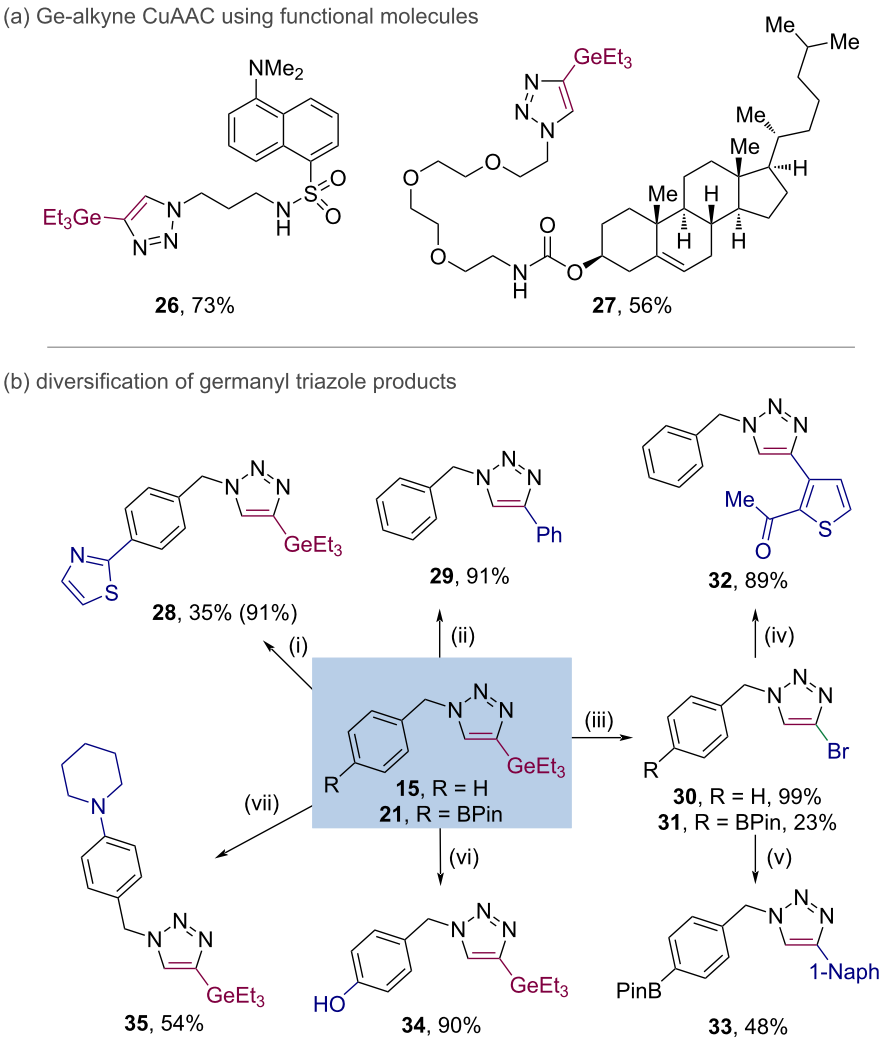

Scheme 3: (a) Application of Ge-alkyne CuAAC to functional molecules. (b) Functionalisation of germylated triazoles. Isolated yields unless stated. (i) $Pd(PPh_3)_4$ (10 mol %), 2-bromothiazole (1.2 equiv), KCl (3.0 equiv), PhMe/EtOH 4:1, N_2, 100 °C, 16 h. NMR yield in parentheses. (ii) $Pd_2(dba)_3$ (2.5 mol %), iodobenzene (1.5 equiv), $AgBF_4$ (1.5 equiv), DMF, N_2, 80 °C, 16 h. (iii) NBS (2.0 equiv), DMF, air, rt, 2 h. (iv) $Pd(dtbpf)Cl_2$ (10 mol %), 2-acetylthiophen-3-ylboronic acid (1.2 equiv), K_3PO_4 (2.0 equiv), iPrOH/H_2O 3:4, N_2, 85 °C, 16 h. (v) $Pd(dtbpf)Cl_2$ (2.0 mol %), 1-naphthylzinc bromide (1.2 equiv), THF, N_2, 45 °C, 16 h. (vi) $Cu(OAc)_2{\cdot}H_2O$ (30 mol %), $B(OH)_3$ (2.0 equiv), DBU (2.0 equiv), MeCN, air, 70 °C, 24 h. (vii) $Cu(OAc)_2{\cdot}H_2O$ (30 mol %), $B(OH)_3$ (2.0 equiv), piperidine (2.0 equiv), MeCN, air, 70 °C, 24 h. See Supporting Information File 1 for full details.

Supporting Information

The research data supporting this publication can be accessed at https://doi.org/10.17630/53959471-068e-483e-bcd4-920e6761926b and CCDC 2355570 contains the supplementary crystallographic data for this study.

Supporting Information File 1

Characterization data and copies of NMR spectra.
[https://www.beilstein-journals.org/bjoc/content/supplementary/1860-5397-20-265-S1.pdf]

Supporting Information File 2

Crystallographic information file (cif) for compound **13**.
[https://www.beilstein-journals.org/bjoc/content/supplementary/1860-5397-20-265-S2.cif]

Supporting Information File 3

Checkcif file for compound **13**.
[https://www.beilstein-journals.org/bjoc/content/supplementary/1860-5397-20-265-S3.pdf]

Acknowledgements

We thank Dr. Aitor Maestro for assistance with starting material synthesis.

Funding

J.M.H.-M. thanks the EPSRC Centre for Doctoral Training EaSI-CAT for a Ph.D. studentship. T.M.R. thanks the EPSRC and the University of St Andrews for Ph.D. studentship. G.A.B., F.P., and A.J.B.W. thank the Leverhulme Trust (RPG-2020-380). A.J.B.W. thanks the Leverhulme Trust for a Research Fellowship (RF-2022-014) and the EPSRC Programme Grant ‘‘Boron: Beyond the Reagent’’ (EP/W007517/1) for support.

Author Contributions

John M. Halford-McGuff: conceptualization; data curation; formal analysis; investigation; validation; writing – original draft; writing – review & editing. Thomas M. Richardson: data curation; formal analysis; investigation; validation; writing – original draft; writing – review & editing. Aidan P. McKay: formal analysis; investigation. Frederik Peschke: formal analysis; investigation; methodology; writing – original draft; writing – review & editing. Glenn A. Burley: conceptualization; data curation; formal analysis; funding acquisition; project administration; resources; supervision; writing – original draft; writing – review & editing. Allan J. B. Watson: conceptualization; data curation; formal analysis; funding acquisition; project administration; resources; supervision; writing – original draft; writing – review & editing.

ORCID® iDs

John M. Halford-McGuff - https://orcid.org/0009-0009-4529-6988
Aidan P. McKay - https://orcid.org/0000-0002-8578-7054
Allan J. B. Watson - https://orcid.org/0000-0002-1582-4286

Data Availability Statement

Data generated and analyzed during this study is openly available at https://doi.org/10.17630/53959471-068e-483e-bcd4-920e6761926b.

Preprint

A non-peer-reviewed version of this article has been previously published as a preprint: doi:10.26434/chemrxiv-2024-s7dht

References

1. Tasdelen, M. A. *Polym. Chem.* **2011,** *2,* 2133–2145. doi:10.1039/c1py00041a
2. Eschenbrenner-Lux, V.; Kumar, K.; Waldmann, H. *Angew. Chem., Int. Ed.* **2014,** *53,* 11146–11157. doi:10.1002/anie.201404094
3. Hoyle, C. E.; Bowman, C. N. *Angew. Chem., Int. Ed.* **2010,** *49,* 1540–1573. doi:10.1002/anie.200903924
4. Li, H.; Aneja, R.; Chaiken, I. *Molecules* **2013,** *18,* 9797–9817. doi:10.3390/molecules18089797
5. Kolb, H. C.; Finn, M. G.; Sharpless, K. B. *Angew. Chem., Int. Ed.* **2001,** *40,* 2004–2021. doi:10.1002/1521-3773(20010601)40:11<2004::aid-anie2004>3.0.co;2-5
6. Hatit, M. Z. C.; Reichenbach, L. F.; Tobin, J. M.; Vilela, F.; Burley, G. A.; Watson, A. J. B. *Nat. Commun.* **2018,** *9,* 4021. doi:10.1038/s41467-018-06551-0
7. Melo, A.; Monteiro, L.; Lima, R. M. F.; de Oliveira, D. M.; de Cerqueira, M. D.; El-Bachá, R. S. *Oxid. Med. Cell. Longevity* **2011,** 467180. doi:10.1155/2011/467180
8. Meldal, M.; Tornøe, C. W. *Chem. Rev.* **2008,** *108,* 2952–3015. doi:10.1021/cr0783479
9. Haldón, E.; Nicasio, M. C.; Pérez, P. J. *Org. Biomol. Chem.* **2015,** *13,* 9528–9550. doi:10.1039/c5ob01457c
10. García-Álvarez, J.; Díez, J.; Gimeno, J. *Green Chem.* **2010,** *12,* 2127–2130. doi:10.1039/c0gc00342e
11. Wang, K.; Bi, X.; Xing, S.; Liao, P.; Fang, Z.; Meng, X.; Zhang, Q.; Liu, Q.; Ji, Y. *Green Chem.* **2011,** *13,* 562–565. doi:10.1039/c0gc00848f
12. Fu, F.; Martinez, A.; Wang, C.; Ciganda, R.; Yate, L.; Escobar, A.; Moya, S.; Fouquet, E.; Ruiz, J.; Astruc, D. *Chem. Commun.* **2017,** *53,* 5384–5387. doi:10.1039/c7cc02504a
13. Nebra, N.; García-Álvarez, J. *Molecules* **2020,** *25,* 2015. doi:10.3390/molecules25092015
14. Vala, D. P.; Vala, R. M.; Patel, H. M. *ACS Omega* **2022,** *7,* 36945–36987. doi:10.1021/acsomega.2c04883
15. Cook, T. L.; Walker, J. A.; Mack, J. *Green Chem.* **2013,** *15,* 617–619. doi:10.1039/c3gc36720g
16. Girard, C.; Önen, E.; Aufort, M.; Beauvière, S.; Samson, E.; Herscovici, J. *Org. Lett.* **2006,** *8,* 1689–1692. doi:10.1021/ol060283l

17. Chtchigrovsky, M.; Primo, A.; Gonzalez, P.; Molvinger, K.; Robitzer, M.; Quignard, F.; Taran, F. *Angew. Chem., Int. Ed.* **2009,** *48,* 5916–5920. doi:10.1002/anie.200901309
18. Zhu, R.-Y.; Chen, L.; Hu, X.-S.; Zhou, F.; Zhou, J. *Chem. Sci.* **2020,** *11,* 97–106. doi:10.1039/c9sc04938j
19. Liu, E.-C.; Topczewski, J. J. *J. Am. Chem. Soc.* **2019,** *141,* 5135–5138. doi:10.1021/jacs.9b01091
20. Lal, K.; Yadav, P.; Kumar, A.; Kumar, A.; Paul, A. K. *Bioorg. Chem.* **2018,** *77,* 236–244. doi:10.1016/j.bioorg.2018.01.016
21. Rani, A.; Singh, G.; Singh, A.; Maqbool, U.; Kaur, G.; Singh, J. *RSC Adv.* **2020,** *10,* 5610–5635. doi:10.1039/c9ra09510a
22. Wright, M. H.; Sieber, S. A. *Nat. Prod. Rep.* **2016,** *33,* 681–708. doi:10.1039/c6np00001k
23. Sapienza, P. J.; Currie, M. M.; Lancaster, N. M.; Li, K.; Aubé, J.; Goldfarb, D.; Cloer, E. W.; Major, M. B.; Lee, A. L. *ACS Chem. Biol.* **2021,** *16,* 2766–2775. doi:10.1021/acschembio.1c00617
24. Döhler, D.; Michael, P.; Binder, W. H. *Acc. Chem. Res.* **2017,** *50,* 2610–2620. doi:10.1021/acs.accounts.7b00371
25. Meldal, M. *Macromol. Rapid Commun.* **2008,** *29,* 1016–1051. doi:10.1002/marc.200800159
26. Pacini, A.; Nitti, A.; Vitale, M.; Pasini, D. *Int. J. Mol. Sci.* **2023,** *24,* 7620. doi:10.3390/ijms24087620
27. Zaccaria, C. L.; Cedrati, V.; Nitti, A.; Chiesa, E.; Martinez de Ilarduya, A.; Garcia-Alvarez, M.; Meli, M.; Colombo, G.; Pasini, D. *Polym. Chem.* **2021,** *12,* 3784–3793. doi:10.1039/d1py00737h
28. Hatit, M. Z. C.; Sadler, J. C.; McLean, L. A.; Whitehurst, B. C.; Seath, C. P.; Humphreys, L. D.; Young, R. J.; Watson, A. J. B.; Burley, G. A. *Org. Lett.* **2016,** *18,* 1694–1697. doi:10.1021/acs.orglett.6b00635
29. Hatit, M. Z. C.; Seath, C. P.; Watson, A. J. B.; Burley, G. A. *J. Org. Chem.* **2017,** *82,* 5461–5468. doi:10.1021/acs.joc.7b00545
30. Seath, C. P.; Burley, G. A.; Watson, A. J. B. *Angew. Chem., Int. Ed.* **2017,** *56,* 3314–3318. doi:10.1002/anie.201612288
31. Rodionov, V. O.; Fokin, V. V.; Finn, M. G. *Angew. Chem., Int. Ed.* **2005,** *44,* 2210–2215. doi:10.1002/anie.200461496
32. Rostovtsev, V. V.; Green, L. G.; Fokin, V. V.; Sharpless, K. B. *Angew. Chem., Int. Ed.* **2002,** *41,* 2596–2599. doi:10.1002/1521-3773(20020715)41:14<2596::aid-anie2596>3.0.co;2-4
33. Hein, J. E.; Fokin, V. V. *Chem. Soc. Rev.* **2010,** *39,* 1302–1315. doi:10.1039/b904091a
34. Bunschoten, R. P.; Peschke, F.; Taladriz-Sender, A.; Alexander, E.; Andrews, M. J.; Kennedy, A. R.; Fazakerley, N. J.; Lloyd Jones, G. C.; Watson, A. J. B.; Burley, G. A. *J. Am. Chem. Soc.* **2024,** *146,* 13558–13570. doi:10.1021/jacs.4c03348
35. Huang, J.; Macdonald, S. J. F.; Harrity, J. P. A. *Chem. Commun.* **2009,** 436–438. doi:10.1039/b817052e
36. Huang, J.; Macdonald, S. J. F.; Cooper, A. W. J.; Fisher, G.; Harrity, J. P. A. *Tetrahedron Lett.* **2009,** *50,* 5539–5541. doi:10.1016/j.tetlet.2009.07.085
37. Dai, C.; Cheng, Y.; Cui, J.; Wang, B. *Molecules* **2010,** *15,* 5768–5781. doi:10.3390/molecules15085768
38. Grob, J. E.; Nunez, J.; Dechantsreiter, M. A.; Hamann, L. G. *J. Org. Chem.* **2011,** *76,* 10241–10248. doi:10.1021/jo201973t
39. Jung, S. h.; Choi, K.; Pae, A. N.; Lee, J. K.; Choo, H.; Keum, G.; Cho, Y. S.; Min, S.-J. *Org. Biomol. Chem.* **2014,** *12,* 9674–9682. doi:10.1039/c4ob01967a
40. Zu, B.; Guo, Y.; He, C. *J. Am. Chem. Soc.* **2021,** *143,* 16302–16310. doi:10.1021/jacs.1c08482
41. Van Belois, A.; Maar, R. R.; Workentin, M. S.; Gilroy, J. B. *Inorg. Chem.* **2019,** *58,* 834–843. doi:10.1021/acs.inorgchem.8b02966
42. Li, J.; Tanaka, H.; Imagawa, T.; Tsushima, T.; Nakamoto, M.; Tan, J.; Yoshida, H. *Chem. – Eur. J.* **2024,** *30,* e202303403. doi:10.1002/chem.202303403
43. Lam, P. Y. S.; Deudon, S.; Hauptman, E.; Clark, C. G. *Tetrahedron Lett.* **2001,** *42,* 2427–2429. doi:10.1016/s0040-4039(01)00203-9
44. Denmark, S. E.; Smith, R. C.; Chang, W.-T. T.; Muhuhi, J. M. *J. Am. Chem. Soc.* **2009,** *131,* 3104–3118. doi:10.1021/ja8091449
45. Denmark, S. E.; Regens, C. S. *Acc. Chem. Res.* **2008,** *41,* 1486–1499. doi:10.1021/ar800037p
46. Hirabayashi, K.; Mori, A.; Kawashima, J.; Suguro, M.; Nishihara, Y.; Hiyama, T. *J. Org. Chem.* **2000,** *65,* 5342–5349. doi:10.1021/jo000679p
47. Nakao, Y.; Takeda, M.; Matsumoto, T.; Hiyama, T. *Angew. Chem., Int. Ed.* **2010,** *49,* 4447–4450. doi:10.1002/anie.201000816
48. Hagiwara, E.; Gouda, K.-i.; Hatanaka, Y.; Hiyama, T. *Tetrahedron Lett.* **1997,** *38,* 439–442. doi:10.1016/s0040-4039(96)02320-9
49. Hatanaka, Y.; Hiyama, T. *J. Org. Chem.* **1988,** *53,* 918–920. doi:10.1021/jo00239a056
50. Denmark, S. E.; Wehrli, D. *Org. Lett.* **2000,** *2,* 565–568. doi:10.1021/ol005565e
51. Denmark, S. E.; Choi, J. Y. *J. Am. Chem. Soc.* **1999,** *121,* 5821–5822. doi:10.1021/ja9908117
52. Yamamoto, K.; Kanezashi, M.; Tsuru, T.; Ohshita, J. *Polym. J.* **2017,** *49,* 401–406. doi:10.1038/pj.2016.128
53. Venkatesh, G. B.; Hari Prasad, S. *Phosphorus, Sulfur Silicon Relat. Elem.* **2015,** *190,* 335–341. doi:10.1080/10426507.2014.947405
54. Li, L.; Shang, T.; Ma, X.; Guo, H.; Zhu, A.; Zhang, G. *Synlett* **2015,** *26,* 695–699. doi:10.1055/s-0034-1379970
55. Fricke, C.; Schoenebeck, F. *Acc. Chem. Res.* **2020,** *53,* 2715–2725. doi:10.1021/acs.accounts.0c00527
56. Rogova, T.; Ahrweiler, E.; Schoetz, M. D.; Schoenebeck, F. *Angew. Chem., Int. Ed.* **2024,** *63,* e202314709. doi:10.1002/anie.202314709
57. Fricke, C.; Sherborne, G. J.; Funes-Ardoiz, I.; Senol, E.; Guven, S.; Schoenebeck, F. *Angew. Chem., Int. Ed.* **2019,** *58,* 17788–17795. doi:10.1002/anie.201910060
58. Dahiya, A.; Schoetz, M. D.; Schoenebeck, F. *Angew. Chem., Int. Ed.* **2023,** *62,* e202310380. doi:10.1002/anie.202310380
59. Dahiya, A.; Gevondian, A. G.; Schoenebeck, F. *J. Am. Chem. Soc.* **2023,** *145,* 7729–7735. doi:10.1021/jacs.3c01081
60. Dahiya, A.; Fricke, C.; Schoenebeck, F. *J. Am. Chem. Soc.* **2020,** *142,* 7754–7759. doi:10.1021/jacs.0c02860
61. Sherborne, G. J.; Gevondian, A. G.; Funes-Ardoiz, I.; Dahiya, A.; Fricke, C.; Schoenebeck, F. *Angew. Chem., Int. Ed.* **2020,** *59,* 15543–15548. doi:10.1002/anie.202005066
62. Fricke, C.; Deckers, K.; Schoenebeck, F. *Angew. Chem., Int. Ed.* **2020,** *59,* 18717–18722. doi:10.1002/anie.202008372
63. Kaithal, A.; Sasmal, H. S.; Dutta, S.; Schäfer, F.; Schlichter, L.; Glorius, F. *J. Am. Chem. Soc.* **2023,** *145,* 4109–4118. doi:10.1021/jacs.2c12062
64. Luo, Y.; Tian, T.; Nishihara, Y.; Lv, L.; Li, Z. *Chem. Commun.* **2021,** *57,* 9276–9279. doi:10.1039/d1cc03907e
65. Xu, Q.-H.; Xiao, B. *Org. Chem. Front.* **2022,** *9,* 7016–7027. doi:10.1039/d2qo01467j

66. Li, W.-F.; Xu, Q.-H.; Miao, Q.-Y.; Xiao, B. *J. Org. Chem.* **2024,** *89,* 16269–16281. doi:10.1021/acs.joc.3c02348
67. Han, A.-C.; Xiao, L.-J.; Zhou, Q.-L. *J. Am. Chem. Soc.* **2024,** *146,* 5643–5649. doi:10.1021/jacs.3c14386
68. Piterskaya, Y. L.; Khramchikhin, A. V.; Stadnichuk, M. D. *Zh. Obshch. Khim.* **1996,** *66,* 1188–1194.
69. Demina, M. M.; Nguyen, T. L. H.; Shaglaeva, N. S.; Mareev, A. V.; Medvedeva, A. S. *Russ. J. Org. Chem.* **2012,** *48,* 1582–1584. doi:10.1134/s1070428012120196
70. Zaitsev, K. V.; Veshchitsky, G. A.; Oprunenko, Y. F.; Kharcheva, A. V.; Moiseeva, A. A.; Gloriozov, I. P.; Lermontova, E. K. *Chem. – Asian J.* **2023,** *18,* e202300753. doi:10.1002/asia.202300753
71. Smith, E.; Jones, K. D.; O'Brien, L.; Argent, S. P.; Salome, C.; Lefebvre, Q.; Valery, A.; Böcü, M.; Newton, G. N.; Lam, H. W. *J. Am. Chem. Soc.* **2023,** *145,* 16365–16373. doi:10.1021/jacs.3c03207
72. Wiesenfeldt, M. P.; Rossi-Ashton, J. A.; Perry, I. B.; Diesel, J.; Garry, O. L.; Bartels, F.; Coote, S. C.; Ma, X.; Yeung, C. S.; Bennett, D. J.; MacMillan, D. W. C. *Nature* **2023,** *618,* 513–518. doi:10.1038/s41586-023-06021-8
73. Pérez-Perarnau, A.; Preciado, S.; Palmeri, C. M.; Moncunill-Massaguer, C.; Iglesias-Serret, D.; González-Gironès, D. M.; Miguel, M.; Karasawa, S.; Sakamoto, S.; Cosialls, A. M.; Rubio-Patiño, C.; Saura-Esteller, J.; Ramón, R.; Caja, L.; Fabregat, I.; Pons, G.; Handa, H.; Albericio, F.; Gil, J.; Lavilla, R. *Angew. Chem., Int. Ed.* **2014,** *53,* 10150–10154. doi:10.1002/anie.201405758
74. Wang, C.; Tobrman, T.; Xu, Z.; Negishi, E.-i. *Org. Lett.* **2009,** *11,* 4092–4095. doi:10.1021/ol901566e
75. Vantourout, J. C.; Miras, H. N.; Isidro-Llobet, A.; Sproules, S.; Watson, A. J. B. *J. Am. Chem. Soc.* **2017,** *139,* 4769–4779. doi:10.1021/jacs.6b12800
76. Peschke, F.; Taladriz-Sender, A.; Andrews, M. J.; Watson, A. J. B.; Burley, G. A. *Angew. Chem., Int. Ed.* **2023,** *62,* e202313063. doi:10.1002/anie.202313063

License and Terms

BEILSTEIN JOURNAL OF ORGANIC CHEMISTRY

Facile one-pot reduction of β-nitrostyrenes to phenethylamines using sodium borohydride and copper(II) chloride

Laura D'Andrea[*1,2] and Simon Jademyr[1,3]

Letter

Open Access

Address:
[1]Department of Drug Design and Pharmacology, Faculty of Health and Medical Sciences, University of Copenhagen, Universitetsparken 2, 2100 København Ø, Denmark, [2]current address: Department of Chemistry and Bioscience, Aalborg University, Fredrik Bajers Vej 7H, 9220 Aalborg, Denmark and [3]current address: Centre for Analysis and Synthesis, Lund University, Naturvetarvägen 14, 223 62 Lund, Sweden

Email:
Laura D'Andrea[*] - laurad@bio.aau.dk

* Corresponding author

Keywords:
2C-X; $CuCl_2$; $NaBH_4$; β-nitrostyrene; phenethylamine

Beilstein J. Org. Chem. **2025,** *21,* 39–46.
https://doi.org/10.3762/bjoc.21.4

Received: 10 May 2024
Accepted: 18 December 2024
Published: 07 January 2025

This article is part of the thematic issue "Copper catalysis: a constantly evolving field".

Guest Editor: J. Yun

Abstract

Phenethylamines and phenylisopropylamines of scientific relevance can be prepared with a $NaBH_4/CuCl_2$ system in 10 to 30 minutes via reduction of substituted β-nitrostyrenes. This one-pot procedure allows the quick isolation of substituted β-nitrostyrene scaffolds with 62–83% yield under mild conditions, without the need for special precautions, inert atmosphere, and time-consuming purification techniques.

Introduction

The phenethylamine scaffold represents a recurring motif among natural and synthetic drug molecules. The latter are mainly constituted by a varied class of substituted phenylethylamines exhibiting psychoactive properties, and typically employed for medical and recreational use [1,2]. Representative examples include CNS stimulants (amphetamine), antidepressants and antiparkinson's agents (e.g., L-deprenyl) [3], hallucinogens and entactogens (e.g., 2,5-dimethoxy-4-iodoamphetamine (DOI) and 3,4-methylenedioxy-*N*-methylamphetamine (MDMA)) [4,5], nasal decongestants (e.g., levomethamphetamine), and appetite suppressants (e.g., phentermine) [6].

Phenethylamines can be produced via numerous different procedures [7]. One of the oldest methods involves the reduction of benzyl cyanide with H_2 in liquid ammonia with Raney-Nickel catalyst at 130 °C, and high pressure [8]. Another known method is based on the reductive amination of phenyl-2-propanone by use of Al/Hg amalgam. The latter procedure

involves numerous drawbacks, such as environmental concerns for the use of mercury, contamination of the final products, the need of special safety precautions, and adequate disposal techniques [9,10].

One of the most studied and inexpensive routes to synthesize substituted phenethylamines focuses on the reduction of their α,β-unsaturated nitroalkene analogue (β-nitrostyrene), where both the double bond and the nitro group need to be reduced to deliver the corresponding primary amine. Their reduction can be accomplished via catalytic hydrogenation, involving stepwise reactions and workup, use of additional reagents, and reaction time between 3 and 24 hours [11,12]. Most commonly, metal hydrides are employed, typically lithium aluminum hydride [13-18], requiring an inert atmosphere, special precautions, and with isolated yields up to 60% [14,15]. Due to the formation of side products, final purification of the amino derivatives requires the use of either multiple separation techniques, chromatography, or distillation [15-18] (Scheme 1).

Differently from lithium aluminum hydride, sodium borohydride is a non-pyrophoric and easy-to-handle reducing agent. Since the first attempts in 1967, $NaBH_4$ has been employed to reduce β-nitrostyrene scaffolds to the corresponding nitroalkanes [19-21]. Several catalysts have been combined with $NaBH_4$ to facilitate full reduction of β-nitrostyrenes to phenethylamines, however, to date, no effective method for converting α,β-unsaturated nitroalkenes into aminoalkanes have been developed using $NaBH_4$ as reducing agent [21,22].

The number of procedures reported in the literature regarding the reduction of β-nitrostyrenes is limited, since a $NaBH_4$/transition metal salt system is mostly used to reduce nitroarenes [23-26].

One of the reported methods takes advantage of titanium(IV) isopropoxide as a catalyst to prepare varied β-phenethylamine analogues. Despite its simplicity, the reaction time is quite prolonged (from 18 to 20 hours), and this procedure is not used to prepare α-phenethylamines [27].

In view of the limitations associated with conventional methods, we report our findings on an improved approach for reducing β-nitrostyrenes to their corresponding substituted phenethylamines. We demonstrate that the $NaBH_4/CuCl_2$ system effectively facilitates this transformation and provide an account of its application to the β-nitrostyrene examples presented in Figure 1.

Result and Discussion

Herein, we demonstrate that $NaBH_4$, in combination with catalytic amounts of $CuCl_2$, is a simple and higher yielding method

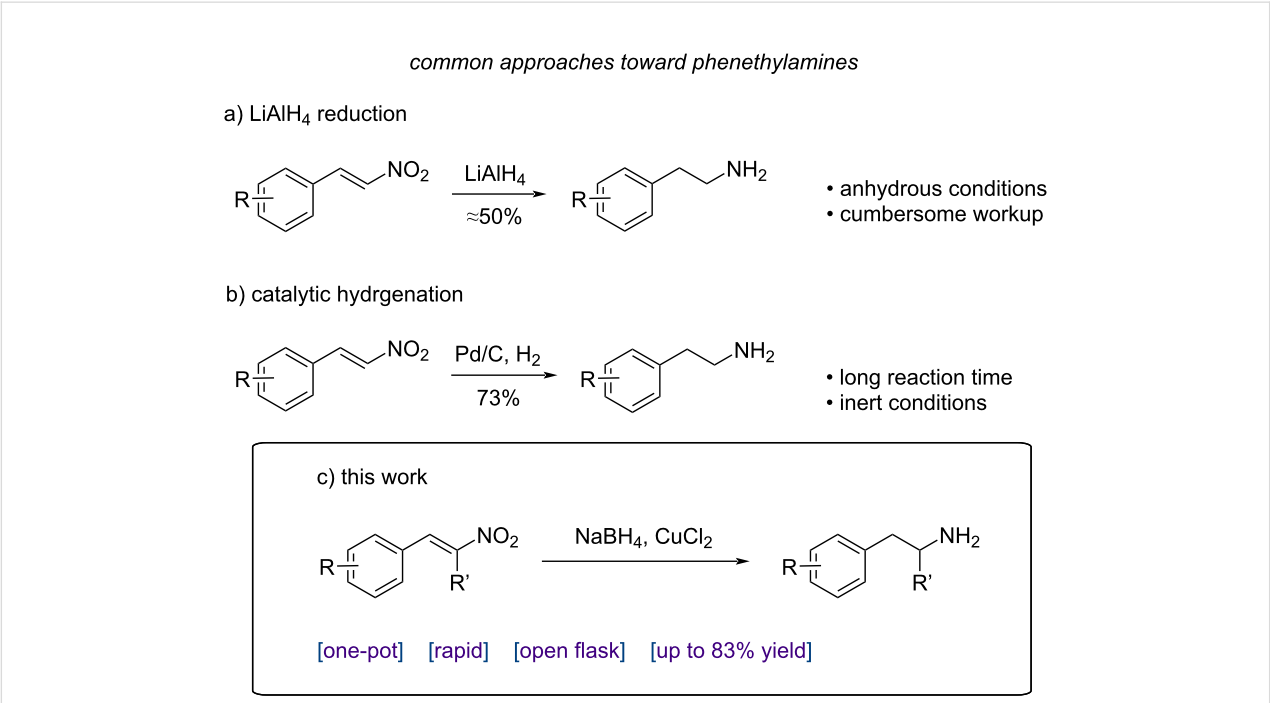

Scheme 1: Brief comparison between the main traditional synthetic routes for the preparation of substituted phenethylamines from β-nitrostyrene scaffolds and our work.

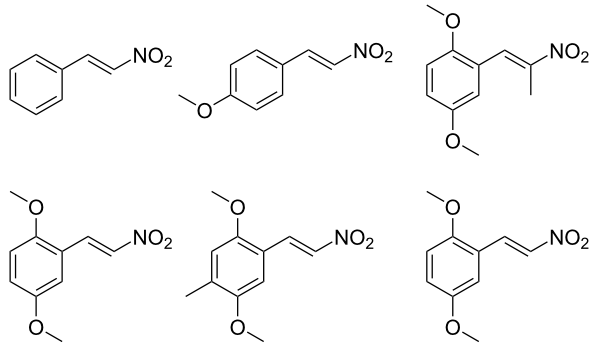

Figure 1: The β-nitrostyrene analogues used in this work.

to synthesize phenethyl- and phenylisopropylamines from the corresponding nitroalkenes [15,17]. Representatively substituted β-nitrostyrene analogues were reduced via this method at 80 °C, including 2,5-dimethoxy-β-methyl-β-nitrostyrene (**3a**), precursor of amphetamines, and 2,5-dimethoxy-β-nitrostyrene (**4a**), precursor of most of the hallucinogenic 2C-X family (Table 1).

This method was also tested on other types of scaffolds to investigate its potential general applications and effects on other substituents. As sodium borohydride per se does not reduce ester nor nitro functionalities [15-22,28,29], the presence of the copper salt results in overcoming this issue and leads to isolated yields above 90% (**7**–**9**) (Scheme 2).

Table 1: The reduced β-nitrostyrene scaffolds with their corresponding products (entries 1–6). The isolated product yields were obtained by performing the reactions at 80 °C for the time indicated beside each product. For more details, see the experimental section below.

Entry	Substrate	Product	Time (min)	Yield (%)
1	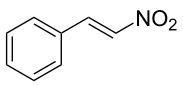 **1a**	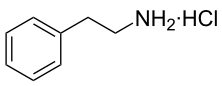 **1b**	15	83
2	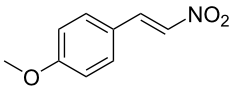 **2a**	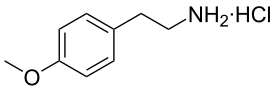 **2b**	10	82
3	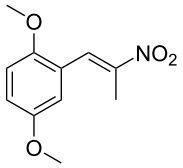 **3a**	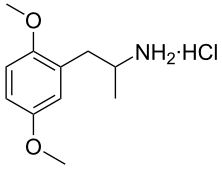 **3b**	30	62
4	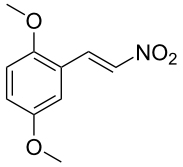 **4a**	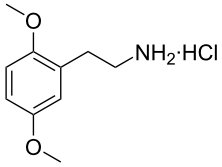 **4b**	10	82
5	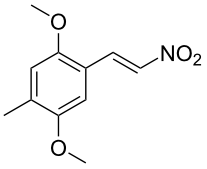 **5a**	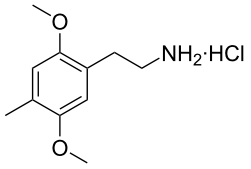 **5b**	30	65
6	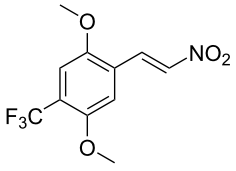 **6a**	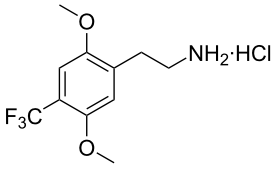 **6b**	30	71

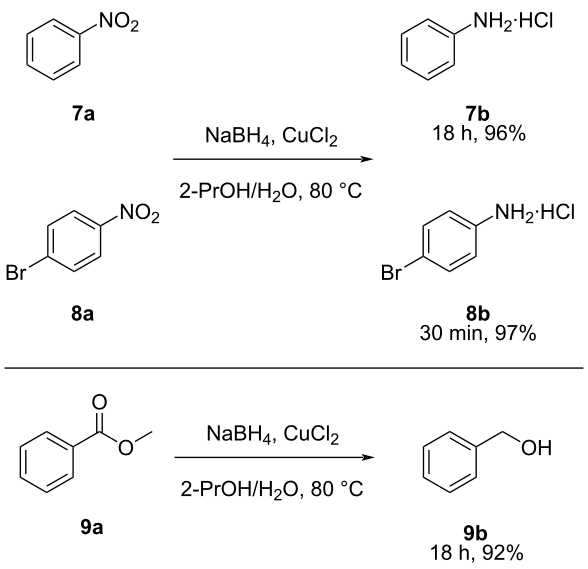

Scheme 2: Additional products obtained via this method: nitrobenzene and methyl benzoate are reduced in excellent yields.

Therefore, the $NaBH_4/CuCl_2$ system was proved to work on aromatic ester, nitro, and α,β-unsaturated nitroalkene functionalities.

Our work demonstrates that, up to 24 hours, this method shows some degree of functional group tolerance, as the amido and carboxylic acid functionalities of benzamide and benzoic acid, were left untouched, and the starting materials were finally fully recovered.

1-Bromo-4-nitrobenzene (**8a**) and 3-chlorophenol were used to test the potential effects on halogenated aromatic structures and no dehalogenation was detected up to 24 hours stirring. The retention of halogen atoms on aryl halides distinguishes this procedure from traditional techniques, such as those involving $LiAlH_4$, which can cause dehalogenation [30,31].

The role of the $CuCl_2$ salt is pivotal to the success of this method. Studies on the reduction of $CuCl_2$ by $NaBH_4$ suggest that copper(II) is promptly reduced to free Cu(0), composing up to 96% of the products. The remaining 4% consist of Cu_2O and negligible amounts of other copper species [32,33]. Consistently, once the chloride is added, the reduction to free Cu(0) is visually indicated by the immediate disappearance of the blue color of the copper(II) solution, and the formation of a fine suspended black powder. The latter, as metallic copper particles, acts as the actual catalyst.

Time plays a crucial role in the synthesis of phenethylamine analogues via this method. Dithering before the addition of the copper solution leads to the formation of Micheal adducts, which decrease the product yields. This phenomenon is due to the nature of β-nitrostyrenes, displaying considerable delocalization towards the nitro group, which makes them highly susceptible to Michael addition [34].

While being stirred with the borohydride, the substrate progressively forms an α-carbanion in the newly formed nitroalkane, which ultimately leads to Michael addition to the nitrostyrene.

Furthermore, studies to identify the highest yielding reaction times (reaction stopped at 10, 15, 30, 45, 60, 75, and 90 minutes) revealed that longer stirring when heating is applied is not beneficial. In general, soon after the optimal reaction times indicated in Table 1, the yield progressively decreases when the reaction stirring time increases. MS analyses on **4b** showed consistently that, while the product mass decreases over time, high molecular mass compounds form increasingly (MS data for **4b** can be found in Supporting Information File 1).

Over the course of the reaction to form **1b**, MS analyses indicated the prompt formation of numerous intermediate species at $T = 0$, unstable enough to decompose and deliver the desired product (Figure 2).

These species were not present in the crude mixture after 15 minutes of stirring. We could speculate that this phenomenon might indicate that the reduction proceeds via Haber or

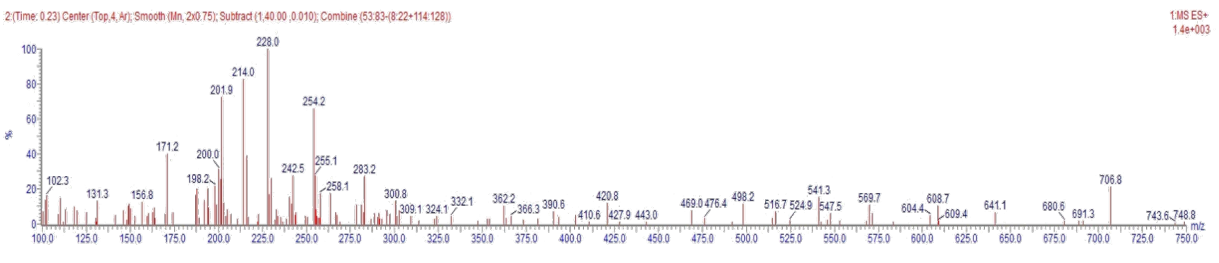

Figure 2: Numerous masses (*m*/*z*) were detected by ESI-MS at $T = 0$ upon mixing all the reagents to produce **1b**.

Jackson mechanisms (product (**a**)), which, to date, were only associated to the catalytic hydrogenation of nitrobenzene analogues [35-37] (Figure 3).

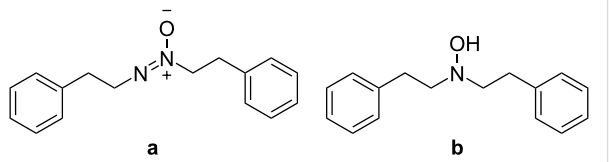

Figure 3: Structures of proposed adducts. Their masses, 254.2 and 242.2, respectively, were found at T = 0 by UPLC-MS investigation.

An attempt to identify the higher molecular masses observed by MS was made, and two intermediate structures are proposed in Figure 3. Together with (**a**), *N*,*N*-diphenethylhydroxylamine (**b**) as second product is proposed. The latter may be produced from the reaction of 2-phenylacetaldehyde (**e**) and the reduced amino product **d** via reductive alkylation [38-40] (Scheme 3).

Further research is required to clarify the formation of high molecular weight structures both prior to and following the production of the target compounds.

The application of mild heating is crucial to reach full conversion of the starting materials in the times indicated in Table 1. However, conversion to the desired products is also achievable at room temperature over 18 hour stirring with minor yield loss. Increasing the heating temperature up to 110 °C does not lead to increased product yields (for more information on the optimization process, see Supporting Information File 1, page S19).

The use of diethylenetriamine (DETA) was also investigated to evaluate its impact on the extraction process and copper(II) removal. However, the addition of DETA led to decreased yields and a deterioration of the phase separation. It was observed that using a 20% aqueous sodium hydroxide solution, instead of 35%, negatively impacted phase separation, making the extraction process more time-consuming. Additionally, the effect of the addition order of the reagents was evaluated, and the results are also provided in Supporting Information File 1.

Furthermore, methanol, 2-propanol, and water were independently tested as reaction solvents. Solubility issues, which lead to the formation of dense suspensions and precipitation of the starting materials, make these solvents unsuitable for this reaction and the isolation of the products troublesome. The use of 2-propanol/water (2:1), together with the application of heat, ensures optimal solubility of the species involved. Moreover, the workup procedure is simplified thanks to the ability of 2-propanol to partition from the sodium hydroxide aqueous solution, which allows prompt extraction of the products.

Once 2-propanol is evaporated, the products can also be isolated as free amines by dissolving the residue in diethyl ether, decanting it into another flask, and concentrating in vacuo.

Scalability was briefly investigated, and the procedure ensures minor yield loss up to 10 mmol scale of the starting material.

Conclusion

In summary, the presented procedure represents a simple, higher-yielding, and faster alternative to the conventional reductive methods used to date for the synthesis of substituted phenethylamines from their α,β-unsaturated nitroalkene analogues. Furthermore, the $NaBH_4/CuCl_2$ system is effective at

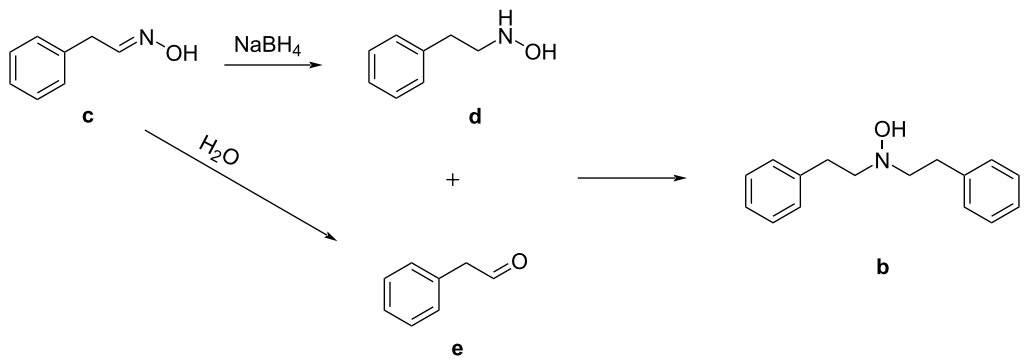

Scheme 3: Proposed mechanism for the formation of the hydroxylamine side product **b**. *N*-Phenethylhydroxylamine (**d**), originated during the reduction process, reacts with the acetaldehyde **e** resulting from the hydrolysis of the aldoxime precursor **c**.

reducing nitro and ester functionalities on aromatic structures, while leaving intact benzoic acid, amido- and halogenated aromatic compounds.

Experimental

NMR spectra were recorded on Bruker Avance 400 MHz or Bruker Avance III HD 600 MHz spectrometers. Residual solvent peaks ($CDCl_3$, D_2O, CD_3OD, $(CD_3)_2SO$) were used as internal standard (7.26, 4.79, 3.31, and 2.50 ppm for ^1H, and 77.16, 49, and 39.52 ppm for ^{13}C, respectively). UPLC-MS analyses were performed on a Waters Acquity H-class UPLC with a Sample Manager FTN and a TUV dual wavelength detector coupled to a QDa single quadrupole analyzer using electrospray ionization (ESI). UPLC separation was achieved with a C18 reversed-phase column (Acquity UPLC BEH C18, 2.1 mm × 50 mm, 1.7 µm) operated at 40 °C, using a linear gradient of the binary solvent system of buffer A (Milli-Q H_2O/MeCN/formic acid, 95:5:0.1 v/v) to buffer B (MeCN/formic acid, 100:0.1 v/v) from 0 to 100% B in 3.5 min, then 1 min at 100% B, flow rate: 0.8 mL/min. Data acquisition was controlled by MassLynx ver. 4.1 and data analysis was done using Waters OpenLynx browser ver. 4.1.

Solvents were commercial HPLC grade and used without further purification. The substrates **2a**, **7a**, and **8a** were commercially available and used without further purification. The substituted β-nitrostyrenes **1a** and **3a**–**6a** were prepared as described in the literature [41]. **9a** was prepared by modification of the literature [42].

General procedure

The desired substrate (**1a**–**9a**) (2 mmol, 1 equiv) was added in small portions to a stirring suspension of $NaBH_4$ (15 mmol, 7.5 equiv) in 2-PrOH/H_2O (8 mL, 2:1). 0.1 mL of a freshly prepared $CuCl_2$ 2 M solution were added dropwise but rapidly to the vessel. The reaction was monitored by TLC and refluxed at 80 °C in either oil bath or heating mantle for the time indicated in Table 1.

General workup procedure of the amino products (1b–8b): Once cooled to room temperature, a 35% solution of NaOH (10 mL) was added under stirring. The mixture was extracted with 2-PrOH (3 × 10 mL), and the organic extracts were combined, thoroughly dried over $MgSO_4$, and filtered.

(I): The residue was concentrated under reduced pressure and dissolved in a large amount of diethyl ether. The amino products were precipitated under stirring with an excess of 2 N HCl in diethyl ether solution and the vessel was cooled to 5 °C. The solid was filtered, washed with cold diethyl ether, and dried under reduced pressure as the amine hydrochloride salt.

(II) An excess of 4 N HCl in dioxane solution was added and the filtrate was stirred for 30 minutes. The residue was concentrated under reduced pressure, suspended in dry cold acetone, and stirred vigorously for 1 hour. The suspension was filtered and washed with a minimum amount of cold acetone to deliver the product as hydrochloride salt.

2-Phenylethan-1-amine hydrochloride (1b): The product was isolated by use of (II) as an amorphous white solid (83%). ^1H NMR (600 MHz, CD_3OD) δ 2.97 (m, J = 5.18 Hz, 2H), 3.18 (m, J = 5.24 Hz, 2H), 7.28 (m, J = 5.0 Hz, 3H), 7.35 (m, J = 7.6 Hz, 2H); ^{13}C NMR (151 MHz, CD_3OD) δ 34.55, 41.98, 128.26, 129.77, 129.99, 137.92; ESI-MS m/z: $[M + 1]^+$ 121.1; found, 121.0; mp 220–221 °C.

2-(4-Methoxyphenyl)ethan-1-amine hydrochloride (2b): The product was isolated by use of (I) as a white solid (82%). ^1H NMR (600 MHz, CD_3OD) δ 2.89 (t, J = 7.7 Hz, 2H), 3.13 (t, J = 7.7 Hz, 2H), 3.78 (s, 3H), 6.91 (ddd, J = 8.4, 2.8, 0.2 Hz, 2H), 7.19 (ddd, J = 8.4, 2.5, 0.2 Hz, 2H); ^{13}C NMR (151 MHz, CD_3OD) δ 33.75, 42.14, 55.71, 115.42, 129.60, 130.78, 160.47; ESI-MS m/z: $[M + 1]^+$ 151.1; found, 152.1; mp 214–216 °C.

1-(2,5-Dimethoxyphenyl)propan-2-amine hydrochloride (3b): The product was isolated by use of (II) as a white solid (62%). ^1H NMR (600 MHz, CD_3OD) δ 1.26 (d, J = 6.60 Hz, 3H), 2.82 (m, J = 6.92 Hz, 1H), 2.95 (m, J = 6.60 Hz, 1H), 3.56 (m, J = 6.51 Hz, 1H), 3.75 (s, 3H), 3.81 (s, 3H), 6.79 (m, J = 2.94 Hz, 1H), 6.84 (dd, J = 2.43, 8.85 Hz, 1H), 6.93 (m, J = 8.94 Hz, 1H); ^{13}C NMR (151 MHz, CD_3OD) δ 18.56, 36.85, 49.22, 56.12, 56.24, 112.81, 114.06, 118.63, 126.24, 153.17, 155.14; ESI-MS m/z: $[M + 1]^+$ 135.1; found, 136.2; mp 115–117 °C.

2-(2,5-Dimethoxyphenyl)ethan-1-amine hydrochloride (4b): The product was isolated by use of (I) as a white solid (82%). ^1H NMR (600 MHz, $(CD_3)_2SO$) δ 2.81 (t, J = 7.8 Hz, 2H), 2.97 (t, J = 7.8 Hz, 2H), 3.70 (s, 3H), 3.75 (s, 3H), 6.78 (m, J = 3.1 Hz, 1H), 6.81 (dd, J = 3.09, 8.82 Hz, 1H), 6.92 (m, J = 8.9 Hz, 1H); ^{13}C NMR (151 MHz, $(CD_3)_2SO$) δ 28.14, 38.65, 55.32, 55.79, 111.78, 112.18, 116.45, 126.03, 151.25, 153.05; ESI-MS m/z: $[M + 1]^+$ 181.1; found, 182.2; mp 138–140 °C.

2-(2,5-Dimethoxy-4-methylphenyl)ethan-1-amine hydrochloride (5b): The product was isolated by use of (II) as a white solid (65%). ^1H NMR (600 MHz, CD_3OD) δ 2.18 (s, 3H), 2.92 (t, J = 7.38 Hz, 2H), 3.12 (t, J = 7.38 Hz, 2H), 3.78 (s, 3H), 3.80 (s, 3H), 6.76 (s, 1H), 6.81 (s, 1H); ^{13}C NMR (151 MHz, CD_3OD) δ 16.27, 29.81, 41.07, 56.33, 56.48, 114.24, 114.96, 123.38, 127.73, 152.65, 153.22; ESI-MS m/z: $[M + 1]^+$ 195.1; found, 196.2; mp 213–215 °C.

2-(2,5-Dimethoxy-4-(trifluoromethyl)phenyl)ethan-1-amine hydrochloride (6b): The product was isolated by use of (II) as a white solid (71%). ^{1}H NMR (400 MHz, CD_3OD) δ 3.03 (t, J = 7.38 Hz, 2H), 3.18 (m, J = 3.76 Hz, 2H), 3.87 (s, 3H), 3.88 (s, 3H), 7.10 (s, 1H), 7.16 (s, 1H); ^{13}C NMR (151 MHz, CD_3OD) δ 29.96, 40.85, 56.11, 56.26, 112.74, 113.86, 113.87, 117.99, 126.84, 153.15, 155.24; ESI-MS m/z: $[M + 1]^+$ 249.1; found, 250.1; mp 260–261 °C.

Aniline hydrochloride (7b): The product formation was monitored by TLC using Hex/EtOAc/TEA (3:7:0.1). The product was isolated by use of (I) as a white solid (96%). ^{1}H NMR (600 MHz, D_2O) δ 7.40 (m, J = 2.96 Hz, 2H), 7.51 (m, J = 1.66 Hz, 1H), 7.56 (m, J = 1.79 Hz, 2H); ^{13}C NMR (151 MHz, D_2O) δ 109.59, 122.50, 128.67, 130.07; ESI-MS m/z: $[M + 1]^+$ 93.1; found, 94,2; mp 196–197 °C.

***p*-Bromoaniline hydrochloride (8b):** The product formation was monitored by TLC using pure pentane. The product was isolated by use of (I) as a bright white powder (97%). ^{1}H NMR (600 MHz, D_2O) δ 7.31 (ddd, J = 8.5, 2.6, 0.3 Hz, 2H), 7.66 (ddd, J = 8.5, 2.6, 0.3 Hz, 2H); ^{13}C NMR (151 MHz, D_2O) δ 122.41, 124.77, 129.01, 133.06; ESI-MS m/z: $[M + 1]^+$ 171.0; found, 171.1; mp 190–191 °C.

Benzyl alcohol (9b): The product formation was monitored by TLC using Hex/EtOAc (6:1). Once cooled to room temperature, the mixture was acidified with 20% HCl solution and extracted with DCM (3 × 15 mL). The organic extracts were combined, dried over $MgSO_4$, and concentrated under reduced pressure to deliver **9b** as colorless liquid (92%). ^{1}H NMR (400 MHz, $CDCl_3$) δ 1.87 (br, 1H), 4.69 (s, 2H), 7.31 (m, J = 2.67 Hz, 1H), 7.37 (m, J = 2.30 Hz, 4H); ^{13}C NMR (151 MHz, $CDCl_3$) δ 65.48, 127.12, 127.79, 128.69, 140.97; ESI-MS m/z: $[M + 1]^+$ 108.1; found, 109.1.

Supporting Information

Supporting Information File 1

^{1}H and ^{13}C NMR spectra of the synthesized compounds, the optimization table, and ESI-MS spectra for the synthesis of **4b**.
[https://www.beilstein-journals.org/bjoc/content/supplementary/1860-5397-21-4-S1.pdf]

Acknowledgements

The authors acknowledge the Ph.D. thesis of L.D'A., titled "Design and Synthesis of beta-Arrestin-Biased 5HT2AR Agonists".

Funding

L.D'A. acknowledges the EU Horizon 2020, Innovative Training Network SAFER (765657).

Conflict of Interest

The authors declare no conflicts of interest.

ORCID® iDs

Laura D'Andrea - https://orcid.org/0000-0002-2186-7880
Simon Jademyr - https://orcid.org/0009-0003-3648-6073

Data Availability Statement

All data that supports the findings of this study is available in the published article and/or the supporting information of this article.

Preprint

A non-peer-reviewed version of this article has been previously published as a preprint: doi:10.26434/chemrxiv-2023-nwn3x-v4

References

1. Shulgin, A. T. Basic pharmacology and effects. *Hallucinogens: a forensic drug handbook;* Academic Press: London, UK, 2003; pp 67–138.
2. Chackalamannil, S.; Rotella, D.; Ward, S. E. *Comprehensive Medicinal Chemistry III;* Elsevier: Amsterdam, Netherlands, 2017.
3. Youdim, M. B. H.; Bakhle, Y. S. *Br. J. Pharmacol.* **2006,** *147* (Suppl. 1), S287–S296. doi:10.1038/sj.bjp.0706464
4. Berquist, M. D.; Fantegrossi, W. E. *Behav. Pharmacol.* **2021,** *32,* 382–391. doi:10.1097/fbp.0000000000000628
5. Mitchell, J. M.; Ot'alora G, M.; van der Kolk, B.; Shannon, S.; Bogenschutz, M.; Gelfand, Y.; Paleos, C.; Nicholas, C. R.; Quevedo, S.; Balliett, B.; Hamilton, S.; Mithoefer, M.; Kleiman, S.; Parker-Guilbert, K.; Tzarfaty, K.; Harrison, C.; de Boer, A.; Doblin, R.; Yazar-Klosinski, B.; MAPP2 Study Collaborator Group. *Nat. Med.* **2023,** *29,* 2473–2480. doi:10.1038/s41591-023-02565-4
6. Barkholtz, H. M.; Hadzima, R.; Miles, A. *ACS Pharmacol. Transl. Sci.* **2023,** *6,* 914–924. doi:10.1021/acsptsci.3c00019
7. Shulgin, A. T. *J. Psychedelic Drugs* **1979,** *11,* 41–52. doi:10.1080/02791072.1979.10472091
8. Robinson, J. C., Jr.; Snyder, H. R. *Org. Synth.* **1943,** *23,* 68.
9. Wassink, B. H. G.; Duijndam, A.; Jansen, A. C. A. *J. Chem. Educ.* **1974,** *51,* 671. doi:10.1021/ed051p671
10. Kunalan, V.; Nic Daéid, N.; Kerr, W. J.; Buchanan, H. A. S.; McPherson, A. R. *Anal. Chem. (Washington, DC, U. S.)* **2009,** *81,* 7342–7348. doi:10.1021/ac9005588
11. Patil, R. D.; Dutta, M.; Pratihar, S. *Organometallics* **2022,** *41,* 2432–2447. doi:10.1021/acs.organomet.2c00229
12. Martín, N.; Cirujano, F. G. *Org. Biomol. Chem.* **2020,** *18,* 8058–8073. doi:10.1039/d0ob01571g
13. Martins, D.; Gil-Martins, E.; Cagide, F.; da Fonseca, C.; Benfeito, S.; Fernandes, C.; Chavarria, D.; Remião, F.; Silva, R.; Borges, F. *Pharmaceuticals* **2023,** *16,* 1158. doi:10.3390/ph16081158
14. Efange, N. M.; Lobe, M. M. M.; Yamthe, L. R. T.; Pekam, J. N. M.; Tarkang, P. A.; Ayong, L.; Efange, S. M. N. *Antimicrob. Agents Chemother.* **2022,** *66,* e00607-22. doi:10.1128/aac.00607-22

15. d'Andrea, L. Design and synthesis of beta-Arrestin-biased 5HT2AR agonists. Ph.D. Thesis, Aalborg University, Aalborg, Denmark, 2023. doi:10.54337/aau528157052
16. Jademyr, S. Synthesis of Conformationally Restrained Serotonin 2A Agonists, M.Sc. Thesis, University of Gothenburg, Gothenburg, Sweden, 2018.
17. Shulgin, A.; Shulgin, A. *PiHKAL: a Chemical Love Story;* Transform Press:: Berkeley, CA, USA, 1991.
18. Kupriyanova, O. V.; Shevyrin, V. A.; Shafran, Y. M.; Lebedev, A. T.; Milyukov, V. A.; Rusinov, V. L. *Drug Test. Anal.* **2020,** *12,* 1154–1170. doi:10.1002/dta.2859
19. Letort, S.; Lejeune, M.; Kardos, N.; Métay, E.; Popowycz, F.; Lemaire, M.; Draye, M. *Green Chem.* **2017,** *19,* 4583–4590. doi:10.1039/c7gc01622k
20. Varma, R. S.; Kabalka, G. W. *Synth. Commun.* **1985,** *15,* 151–155. doi:10.1080/00397918508076821
21. Li, J.; Sun, L.; Zhao, Y.; Shi, C. *Chin. J. Org. Chem.* **2023,** *43,* 4168–4187. doi:10.6023/cjoc202306008
22. Hu, Z.-N.; Liang, J.; Ding, K.; Ai, Y.; Liang, Q.; Sun, H.-b. *Appl. Catal., A* **2021,** *626,* 118339. doi:10.1016/j.apcata.2021.118339
23. Fountoulaki, S.; Daikopoulou, V.; Gkizis, P. L.; Tamiolakis, I.; Armatas, G. S.; Lykakis, I. N. *ACS Catal.* **2014,** *4,* 3504–3511. doi:10.1021/cs500379u
24. Zeynizadeh, B.; Mohammadzadeh, I.; Shokri, Z.; Hosseini, S. A. *J. Colloid Interface Sci.* **2017,** *500,* 285–293. doi:10.1016/j.jcis.2017.03.030
25. Hu, Z.-N.; Liang, J.; Ding, K.; Ai, Y.; Liang, Q.; Sun, H.-b. *Appl. Catal., A* **2021,** *626,* 118339. doi:10.1016/j.apcata.2021.118339
26. Yan, Z.; Xie, X.; Song, Q.; Ma, F.; Sui, X.; Huo, Z.; Ma, M. *Green Chem.* **2020,** *22,* 1301–1307. doi:10.1039/c9gc03957k
27. Bhattacharyya, S.; Chatterjee, A.; Williamson, J. S. *Synlett* **1995,** 1079–1080. doi:10.1055/s-1995-5175
28. Hansen, M.; Phonekeo, K.; Paine, J. S.; Leth-Petersen, S.; Begtrup, M.; Bräuner-Osborne, H.; Kristensen, J. L. *ACS Chem. Neurosci.* **2014,** *5,* 243–249. doi:10.1021/cn400216u
29. Smith, M. B. Functional Group Exchange Reactions: Reductions. *Organic synthesis,* 4th ed.; Academic Press: San Diego, CA, USA, 2016; pp 313–316.
30. Trevoy, L. W.; Brown, W. G. *J. Am. Chem. Soc.* **1949,** *71,* 1675–1678. doi:10.1021/ja01173a035
31. Smith, M. B. Functional Group Exchange Reactions: Reductions. *Organic synthesis,* 4th ed.; Academic Press: San Diego, CA, USA, 2016; pp 319–329.
32. Hohnstedt, L. F.; Miniatas, B. O.; Waller, M. C. *Anal. Chem. (Washington, DC, U. S.)* **1965,** *37,* 1163–1164. doi:10.1021/ac60228a028
33. Glavee, G. N.; Klabunde, K. J.; Sorensen, C. M.; Hadjipanayis, G. C. *Langmuir* **1994,** *10,* 4726–4730. doi:10.1021/la00024a055
34. Meyers, A. I.; Sircar, J. C. *J. Org. Chem.* **1967,** *32,* 4134–4136. doi:10.1021/jo01287a116
35. Serna, P.; Corma, A. *ACS Catal.* **2015,** *5,* 7114–7121. doi:10.1021/acscatal.5b01846
36. Song, J.; Huang, Z.-F.; Pan, L.; Li, K.; Zhang, X.; Wang, L.; Zou, J.-J. *Appl. Catal., B* **2018,** *227,* 386–408. doi:10.1016/j.apcatb.2018.01.052
37. Gelder, E. A.; Jackson, S. D.; Lok, C. M. *Chem. Commun.* **2005,** 522–524. doi:10.1039/b411603h
38. Hutchins, R. O.; Hutchins, M. K. Reduction of C=N to CHNH by Metal Hydrides. In *Comprehensive Organic synthesis;* Trost, B. M.; Fleming, I., Eds.; Pergamon Press: New York, NY, USA, 1991; Vol. 8, pp 60–70. doi:10.1016/b978-0-08-052349-1.00218-3
39. Guy, M.; Freeman, S.; Alder, J. F.; Brandt, S. D. *Cent. Eur. J. Chem.* **2008,** *6,* 526–534. doi:10.2478/s11532-008-0054-z
40. Beckett, A. H.; Coutts, R. T.; Ogunbona, F. A. *J. Pharm. Pharmacol.* **1973,** *25,* 708–717. doi:10.1111/j.2042-7158.1973.tb10052.x
41. Hansen, M. Design and Synthesis of Selective Serotonin Receptor Agonists for Positron Emission Tomography Imaging of the Brain. Ph.D. Thesis, University of Copenhagen, Copenhagen, Denmark, 2010.
42. Williamson, K. L.; Masters, K. M. *Macroscale and microscale organic experiments,* 7th ed.; Cengage Learning: Boston, MA, USA, 2016.

License and Terms

BEILSTEIN JOURNAL OF ORGANIC CHEMISTRY

$Cu(OTf)_2$-catalyzed multicomponent reactions

Sara Colombo[1], Camilla Loro[1], Egle M. Beccalli[2], Gianluigi Broggini[1] and Marta Papis[*1]

Review

Open Access

Address:
[1]Dipartimento di Scienza e Alta Tecnologia, Università degli Studi dell'Insubria, Via Valleggio 9, 22100, Como, Italy and [2]DISFARM, Sezione di Chimica Generale e Organica "A. Marchesini", Università degli Studi di Milano, Via Venezian 21, 20133, Milano, Italy

Email:
Marta Papis[*] - mpapis@uninsubria.it

* Corresponding author

Keywords:
cascade process; copper catalysis; heteropolycycles; multicomponent reactions; one-pot reaction

Beilstein J. Org. Chem. **2025,** *21,* 122–145.
https://doi.org/10.3762/bjoc.21.7

Received: 21 October 2024
Accepted: 19 December 2024
Published: 14 January 2025

This article is part of the thematic issue "Copper catalysis: a constantly evolving field".

Guest Editor: J. Yun

Abstract

This review reports the achievements in copper(II) triflate-catalyzed processes concerning the multicomponent reactions, applied to the synthesis of acyclic and cyclic compounds. In particular, for the heteropolycyclic systems mechanistic insights were outlined as well as cycloaddition and aza-Diels–Alder reactions were included. These strategies have gained attention due to their highly atom- and step-economy, one-step multi-bond forming, mild reaction conditions, low cost and easy handling.

Introduction

Copper has gained a relevant role in organic synthesis as an alternative to precious metals due to its low toxicity, ease of handling, high catalytic activity, and cost-effectiveness [1,2]. In recent years, $Cu(OTf)_2$ has significantly emerged among copper catalysts because it can act as a precursor to triflic acid in addition to a powerful copper-catalytic effect. Indeed, $Cu(OTf)_2$ has proven to be an excellent surrogate for triflic acid compared with other metal triflates because it is inexpensive and exhibits high activity with low toxicity [3-7].

Multicomponent reactions are one of the most effective methods to assemble multiple reagents, thus facilitating access to the target molecules more quickly, due to atom/step economy, short reaction times, and eco-friendly benefits. Combining multicomponent reactions with transition-metal catalysts provides synthetic tools even more advantageously. Copper has also become very interesting in this field, mainly in processes aimed at synthesizing heterocyclic compounds. Among the various catalysts, $Cu(OTf)_2$ stands out in heterocyclic synthesis and ring transformations due to its dual activity as a metal catalyst as well as a Lewis acid [8-11]. However, in many cases, the role of copper is not clear and both activities often work synergistically. In all other cases, copper's activity is due to the coordination/complexation with unsaturated systems, but it is rarely possible to exclude its action also as Lewis acid. Confirming this dual activity, it should be noted that copper triflate can rarely be replaced by other copper salts or complexes to obtain the same results. In general, catalyst switching does not work with copper triflate, thus supporting its unique behavior or reactivity properties. The ambiguity related to the role of $Cu(OTf)_2$

is particularly relevant for cycloaddition reactions, where it is even more difficult to justify the activation of the copper species as a Lewis acid or metal catalyst [12-14].

The reaction mechanism involved can be ionic or radical (Figure 1). The latter is typically operative when the reaction is carried out under oxidative conditions, usually in the presence of O_2 and TEMPO, involving the formation of radical species through single-electron transfer (SET) from a copper catalyst to a precursor. Subsequent addition to multiple C–C bonds generates extended carbon radicals capable of giving further functionalization.

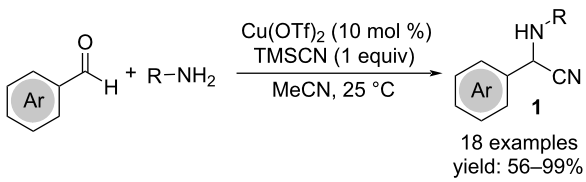

Ar = Ph, 4-Cl-C_6H_4, 4-OMe-C_6H_4, 4-CN-C_6H_4, 4-OH-C_6H_4, 4-NO_2-C_6H_4, 2-OH-C_6H_4, 3-NO_2-C_6H_4, 3,4-$(OMe)_2$-C_6H_3, 3,4-$(O\text{-}CH_2\text{-}O)_2$-$C_6H_3$, 2,4-(*t*-Bu)$_2$-6-(OMe)-$C_6H_2$, 2-OMe-naphthyl, *trans*-cinnamyl, 2-furyl, *n*-C_9H_{19}

R = 4-OMe-C_6H_4, Bn, α-methylbenzyl, Ph

Scheme 1: Synthesis of α-aminonitriles **1**.

Regarding the ionic mechanism, the key step generally comprises the complexation with the unsaturated substrate leading to activation of the alkenyl/alkynyl moiety towards a nucleophilic attack. In some cases, activation of a carbonyl group by the copper catalyst to facilitate nucleophilic attack has also been reported. Moreover, both activations can be operative simultaneously. Since copper shows affinity either for multiple C–C bonds or polar functional groups, it seems the ideal tool for this type of reaction.

Review

Three-component reactions

Several three-component procedures have been successfully carried out using $Cu(OTf)_2$ as a catalyst. These processes have been exploited mainly to access nitrogen compounds endowed with various structures, in a faster and more sustainable way than reactions conducted step by step.

Providing acyclic compounds

A three-component Strecker-type condensation of aromatic aldehydes, amines, and cyanides under mild reaction conditions furnishes α-aminonitriles **1** in good to high yields (Scheme 1) [15]. The reaction failed only in the case of acetophenone. Among various Lewis acids, only $Cu(OTf)_2$ in combination with TMSCN was effective or a valuable alternative was the use of acetone cyanohydrin combined with a catalytic amount of TEA (5 mol %). The mechanism involves the formation of an imine facilitating the addition of the nitrile group.

Among the known processes, a particular Mannich-type reaction was realized in water in the presence of a dendritic 2,2'-bipyridine ligand **2** and $Cu(OTf)_2$ (Scheme 2) [16]. The hydrophobic ligand surrounding the metal revealed to be essential for the organic synthesis in water, thus increasing the reaction yields.

The Mannich reaction with aromatic aldehydes and cyclic amines was performed efficiently on 2-naphthol, by using SiO_2-supported copper triflate under solvent-free conditions, without an additional co-catalyst or additive (Scheme 3) [17].

The treatment of stoichiometric amounts of arylaldehydes, secondary aliphatic or aromatic amines and thiols in the presence of catalytic $Cu(OTf)_2$ (1 mol %) in aqueous media was proven to be a sustainable procedure to access thioaminals **5**, avoiding high temperatures and/or hazardous reagents required by classical conditions (Scheme 4) [18].

The 1,2-difunctionalization of alkenes carried out with carbazates (*N*-aminocarbamates) and (hetero)arene nucleophiles or amines exploiting *N*-(*tert*-butyl)-*N*-fluoro-3,5-bis(trifluoromethyl)benzenesulfonamide (NFBS) as intermolecular hydrogen-atom-transfer reagent results in alkylarylation processes (Scheme 5) [19]. The reaction proceeds through an initial single-electron transfer from NFBS assisted by the active copper species, followed by intermolecular hydrogen-atom transfer from the carbazate. The nitrogen radical intermediate **I**

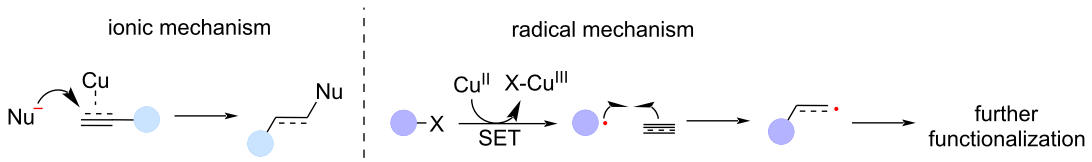

Figure 1: Plausible general catalytic activation for ionic or radical mechanisms.

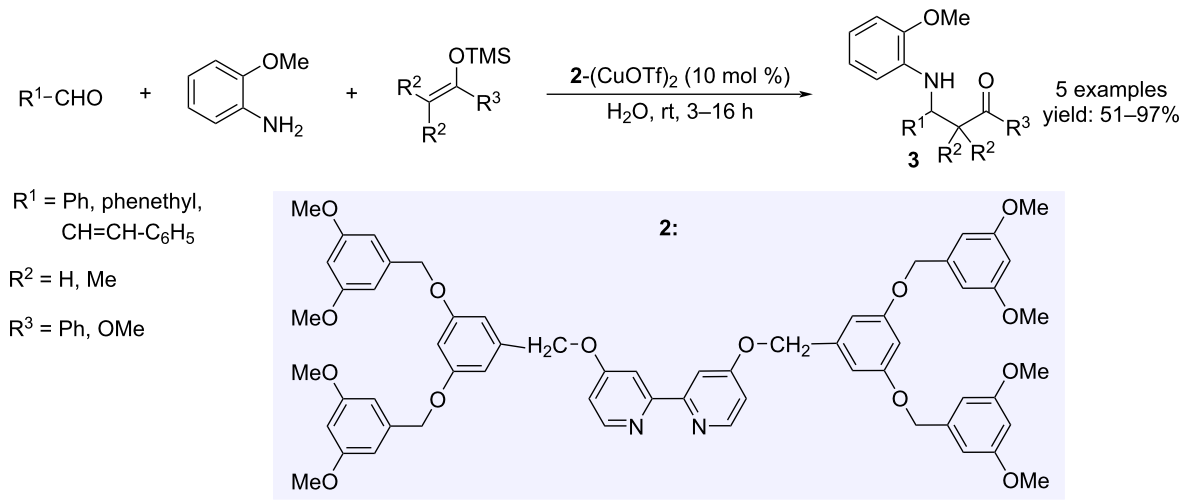

Scheme 2: Synthesis of β-amino ketone or β-amino ester derivatives **3**.

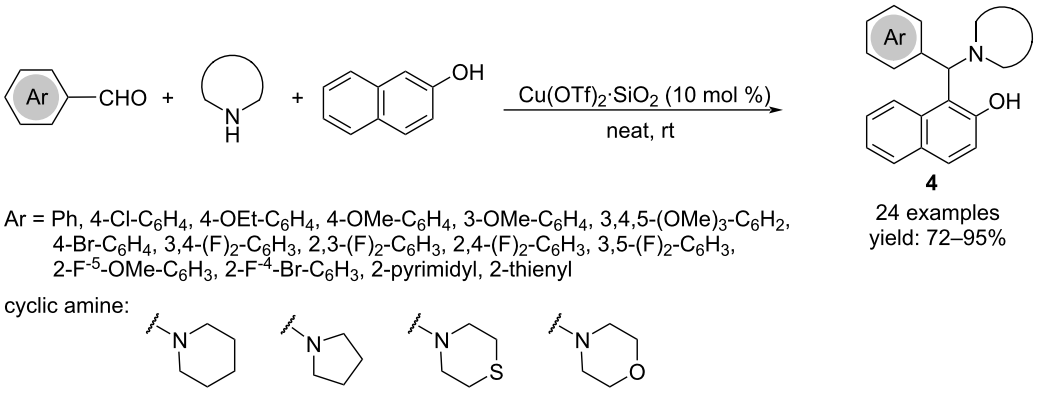

Scheme 3: Synthesis of 1-(α-aminoalkyl)-2-naphthol derivatives **4**.

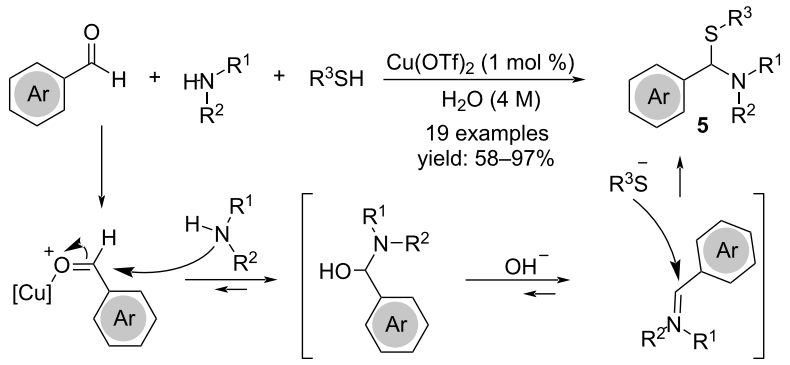

Scheme 4: Synthesis of thioaminals **5**.

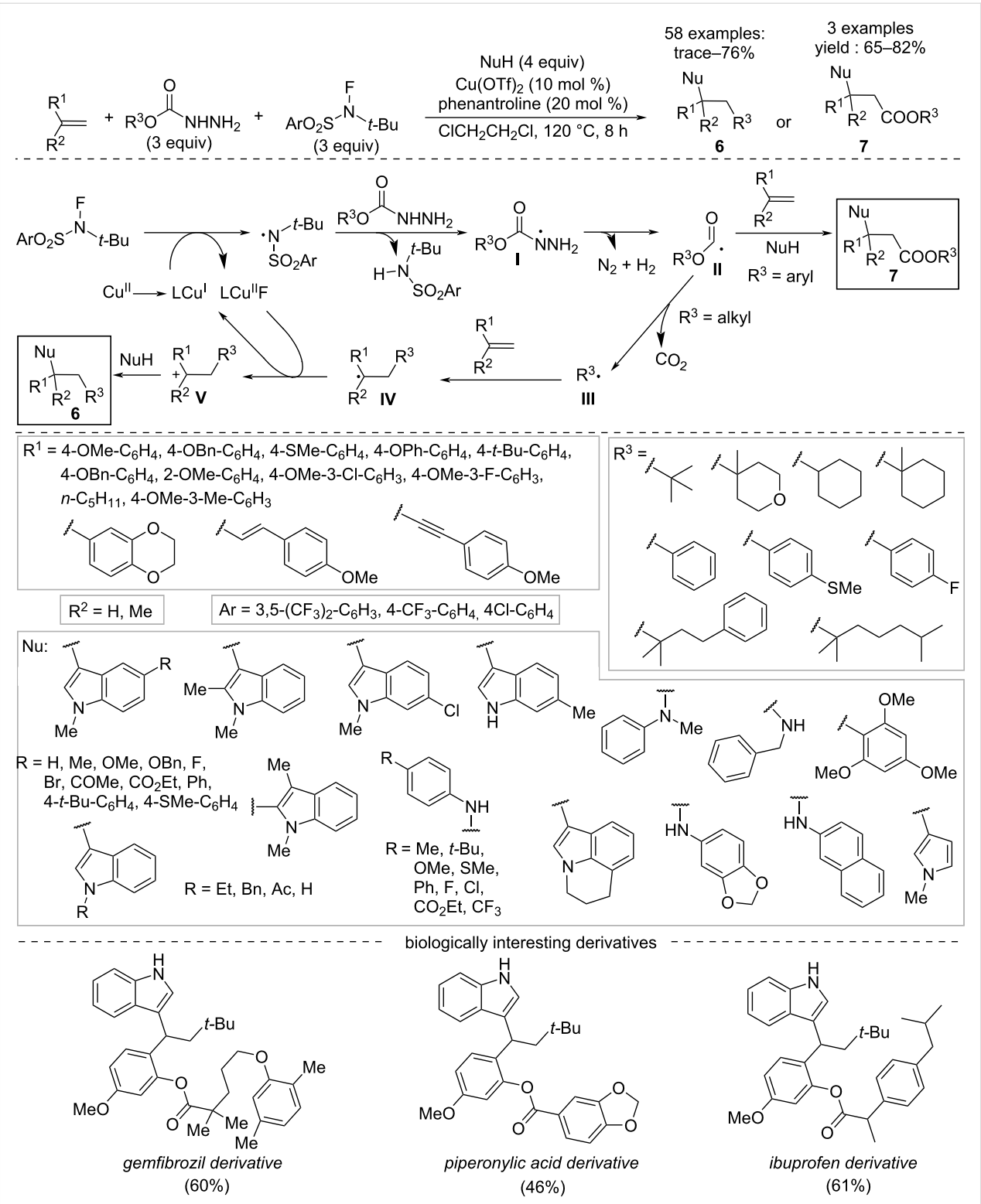

Scheme 5: Synthesis of aryl- or amine-containing alkanes **6** and **7**.

thus formed is decomposed into the acyl or alkyl radical intermediates **II** and **III**, respectively. The latter interacts with the alkene generating an alkyl radical **IV** that converts to the cationic intermediate **V** by single-electron oxidation by the Cu(II) species. Finally, the attack of the nucleophile leads to the desired products **6**. Starting from aryl carbazates, intermediate

II, adds directly to the alkene, then reacts with the nucleophile to afford product **7**.

The regioselective 1,2-difunctionalization of allyl alcohol has been developed as a three-component cascade reaction using arenes and sulfonamides as nucleophiles to achieve arylation/hydroamination processes. The reaction involves a Friedel–Crafts alkylation of the arene followed by hydroamination (Scheme 6) [5]. The mechanism plausibly starts with the in situ formation of triflic acid from $Cu(OTf)_2$ which leads to protonation of the oxygen atom of the alcohol with generation of the activated allyl alcohol. This latter gives the allyl carbenium ion **VI** through the loss of a molecule of water, then undergoes a Friedel–Crafts alkylation by attack of the aromatic partner. The outcome of the reaction proceeds through a Markovnikov protonation of the allylated arene **VII** by triflic acid, which generates the carbocation intermediate **VIII**. At this stage, the amido–copper complex **IX** selectively attacks the intermediate providing the 1-aryl-2-sulfonamidopropane **8**. This procedure is a valuable alternative to a similar approach for the synthesis of amphetamine derivatives **9** from allyl carbamates that requires excess of $Cu(OTf)_2$ [6].

Three-component coupling of amines, aldehydes or ketones, and terminal alkynes catalyzed by $Cu(OTf)_2$ is a fruitful tool for the production of α-substituted propargylamines **10** (Scheme 7)

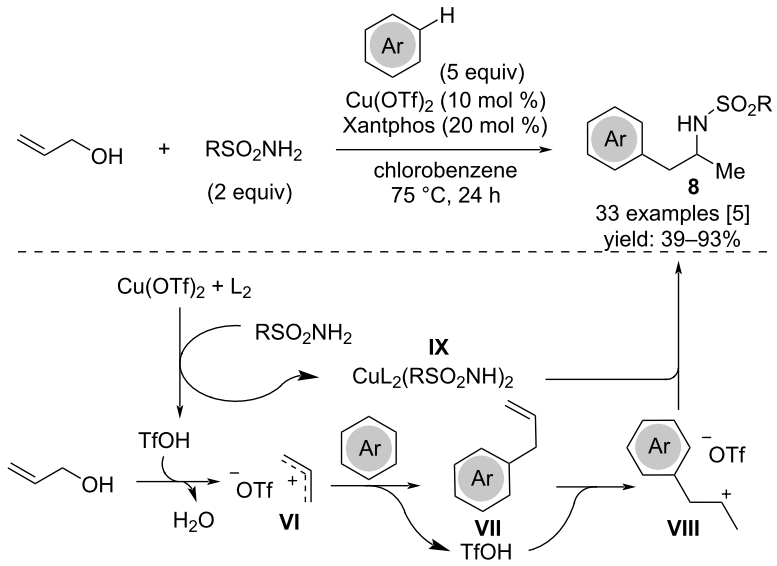

R = Ph, 4-Me-C_6H_4, 4-NO_2-C_6H_4, 4-Cl-C_6H_4, 4-CF_3-C_6H_4, 2-Me-C_6H_4, 2-NO_2-C_6H_4, 3-OMe-C_6H_4

Ar = Mes, 2,3,5,6-$(Me)_4$-C_6H_1, 2,3,4,5,6-$(Me)_5$-C_6, 2,5-$(Me)_2$-C_6H_3, 2,4,6-$(OMe)_3$-C_6H_2, 2,5-$(OMe)_2$-C_6H_3, 2-OMe-5-Me-C_6H_3, 2-OMe-5-Cl-C_6H_3, 2-OMe-5-Br-C_6H_3, 2-OMe-4-Br-C_6H_3, 2-OMe-C_6H_4, 4-OMe-C_6H_4, 2-thienyl, 3-thienyl

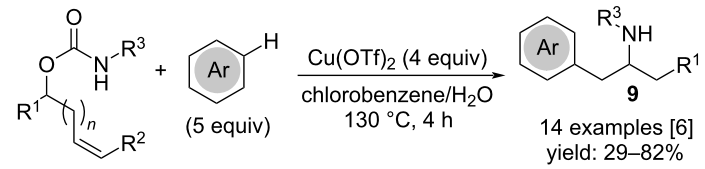

n = 0, 1

$R^1 = R^2$ = H, Me

R^3 = 4-Me-C_6H_4, 2-NO_2-C_6H_4

Ar = Ph, Mes, 2,3,5,6-$(Me)_4$-C_6H_1, 2,5-$(Me)_2$-C_6H_3, 3,4-$(Me)_2$-C_6H_3, 2,6-$(Me)_2$-C_6H_3, 2,3-$(Me)_2$-C_6H_3, 2,4-$(Me)_2$-C_6H_3, 2-Me-C_6H_4, 4-Me-C_6H_4, 2,4,6-$(Et)_3$-C_6H_2, 2,4,6-$(Me)_3$-3-Br-C_6H_1, 2-OMe-5-Me-C_6H_3, 2-OMe-5-Br-C_6H_3, 2,4,6-$(OMe)_3$-C_6H_2

Scheme 6: Synthesis of 1-aryl-2-sulfonamidopropanes **8**.

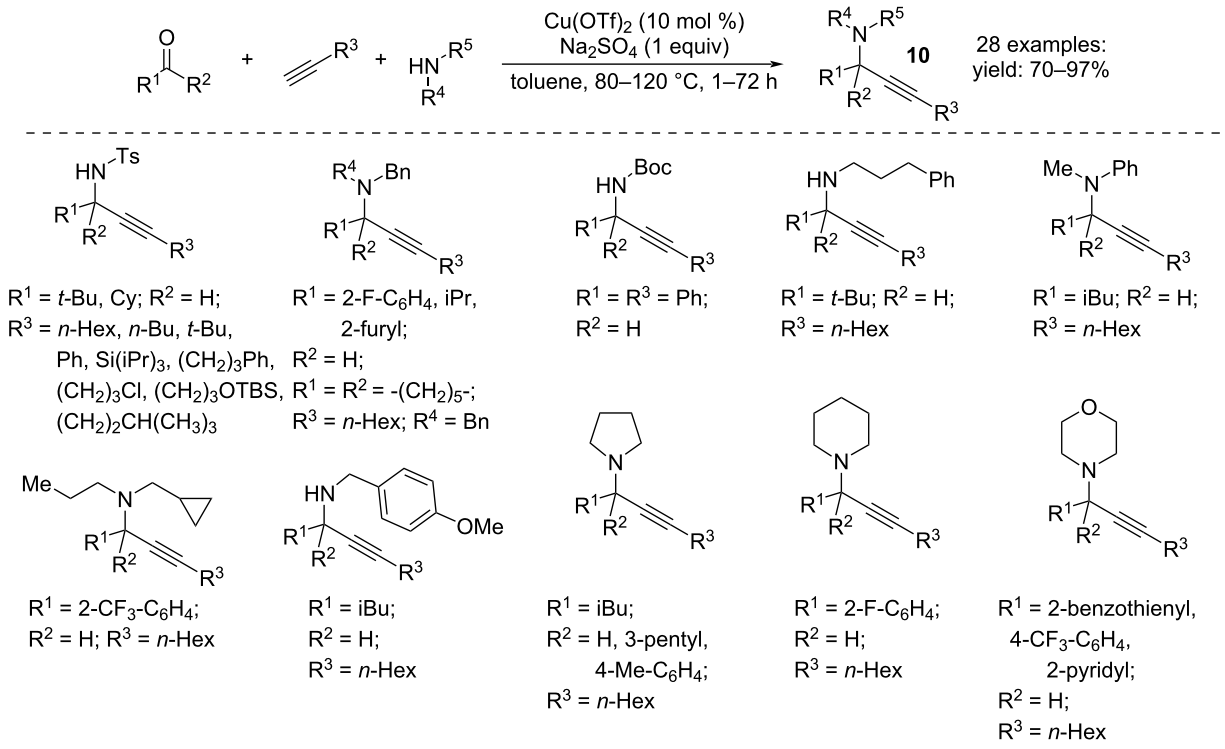

Scheme 7: Synthesis of α-substituted propargylamines **10**.

[20]. The reaction involves the alkynylation of the corresponding imines formed in situ and provides higher yields than the two-step reactions. The addition of Na_2SO_4 facilitates the formation of the products, while $MgSO_4$ or molecular sieves were found to be irrelevant to the reaction rate. It should be noted that this three-component process is promoted by the specific combination of Cu(II) with the triflate counteranion.

The use of a carbamate among the substrates instead of the amine allowed the synthesis of propargylcarbamates **11**. This reaction, effective only for the aromatic aldehydes, did not require other co-catalysts or ligands (Scheme 8) [21].

Three-component reactions of alkynes, alkyltrifluoroborates and sulfur dioxide afforded vinyl sulfones with excellent regio- and stereoselectivity (Scheme 9) [22]. The authors used $DABCO(SO_2)_2$ to generate sulfur dioxide, and visible light irradiation and the mandatory presence of a photocatalyst for this transformation suggested a radical mechanism. The inhibition of the reaction in the presence of TEMPO confirmed this hypothesis. The copper catalyst assisted in the addition step of the alkylsulfonyl radical **X** to the alkyne. The presence of 2-iodopropane as additive improved the yields. The role was unclear, but it might facilitate the conversion of the alkyltrifluoroborate into its corresponding alkyl radical.

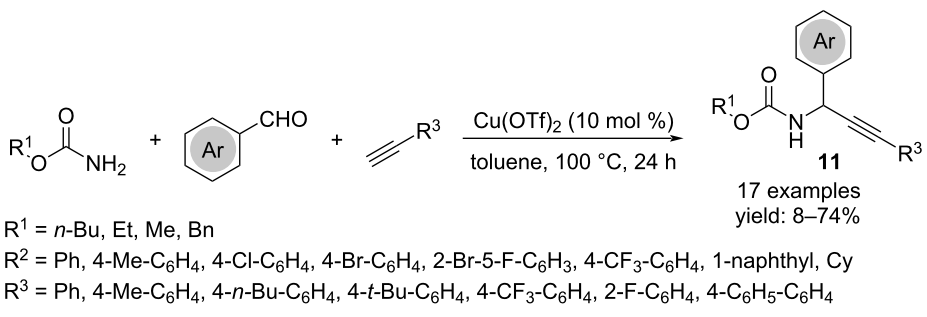

Scheme 8: Synthesis of *N*-propargylcarbamates **11**.

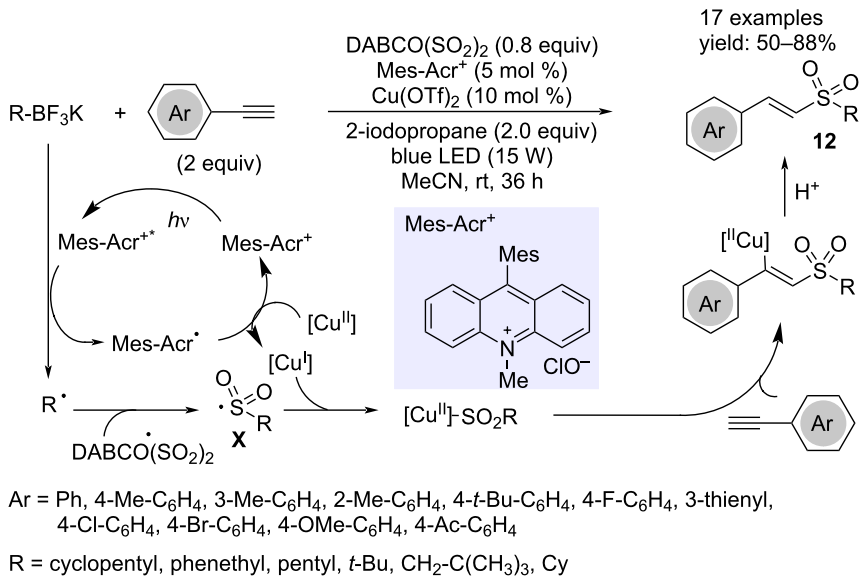

Scheme 9: Synthesis of (*E*)-vinyl sulfones **12**.

o-Halo-substituted aryl selenides and sulfides **13** can be achieved by a three-component coupling reaction performed with an aryne precursor, potassium halides and electrophilic chalcogen species as reactants, in the presence of $Cu(OTf)_2$ (Scheme 10) [23]. Under these conditions the reaction between aryl thiosulfonates with arynes to give sulfones is competitive. $Cu(OTf)_2$ is essential to remove the sulfinate anions in the reaction medium, avoiding side reactions arising from their attack to the electrophilic arynes. The so-obtained products are susceptible of Pd-catalyzed cross-coupling reactions, allowing the formation of C–C and C–N bonds in the *o*-position of the aryl chalcogen compounds.

α-Aminophosphonates **14** were the result of a one-pot condensation of an aldehyde, a primary amine and phosphite $P(OMe)_3$ with copper triflate acting as Lewis acid. Electron-poor and electron-rich aromatic aldehydes gave good results, whereas aliphatic aldehydes gave moderate yields (Scheme 11) [24].

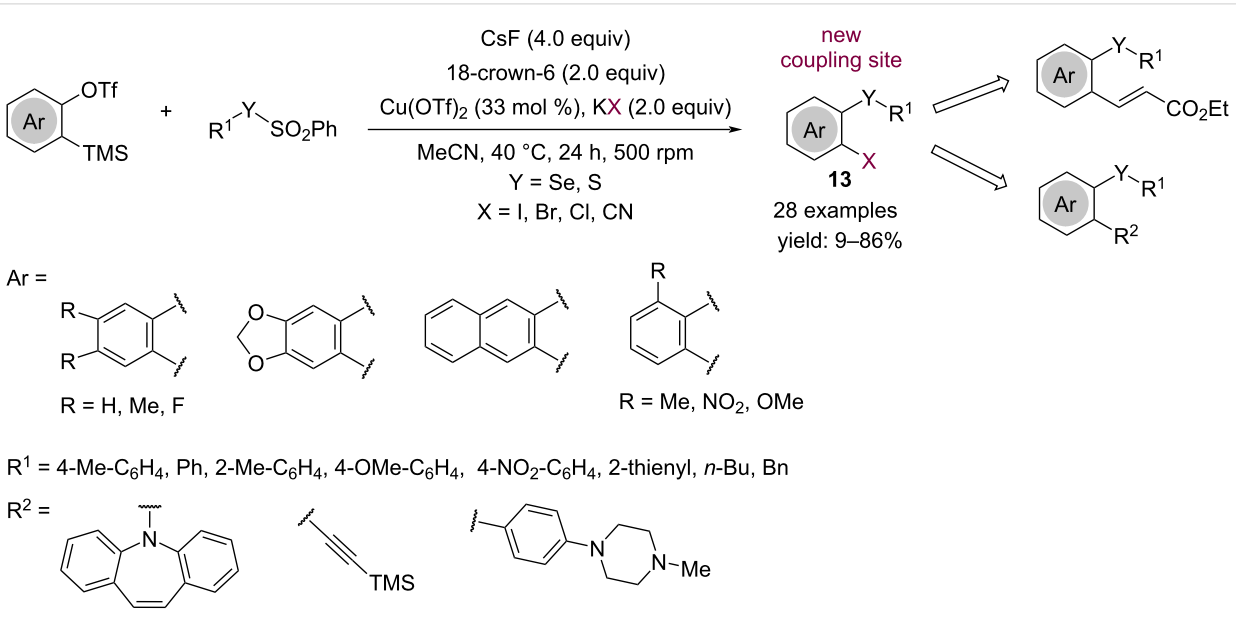

Scheme 10: Synthesis of *o*-halo-substituted aryl chalcogenides **13**.

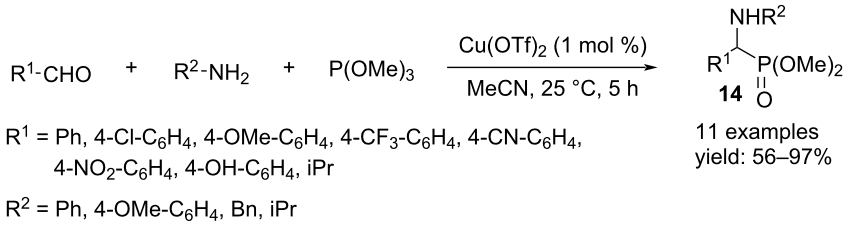

Scheme 11: Synthesis of α-aminophosphonates **14**.

The asymmetric conjugate addition of dialkylzinc and benzaldehyde to unsaturated carbonyls under copper catalysis in the presence of optically pure phosphanes was realized with high diastereo- and enantioselectivities (Scheme 12) [25].

Providing cyclic compounds

For more than a century, Biginelli's reaction has been known as an effective tool for the construction of dihydropyrimidines through a three-component process by condensation in an acidic medium of an aldehyde, urea and a 1,3-dicarbonyl compound [26,27]. In these reactions, the use of catalytic $Cu(OTf)_2$ proved to be an excellent triflate surrogate, also revealing a remarkable reuse activity. The first example of a Biginelli reaction carried out with $Cu(OTf)_2$ catalysis was reported by Sudalai and co-workers in 2003 (Scheme 13) [28]. Working in acetonitrile at room temperature, very high yields were obtained with recycling of the catalyst with negligible loss of activity. The reaction is successful also by operating it in ethanol as a solvent under microwave irradiation [29]. More recently, the Biginelli reaction was carried out starting from salicylaldehyde providing hydroxyphenyl-substituted dihydropyrimidines **18** [30]. Subsequently, the regioselective oxidation of the dihydropyrimidine ring in the presence of CAN allowed the formation of new pyrimidinone derivatives **19**.

The efficacy of $Cu(OTf)_2$ as a catalyst in three-component processes was also demonstrated in three-component reactions involving alkynes, amines and α,β-unsaturated aldehydes to obtain 1,4-dihydropyridines **20** (Scheme 14) [31]. By using terminal alkynes, 2,6-unsubstituted products were achieved. Concerning the mechanism, it is plausible to assume as the key step for ring formation an aza-Diels–Alder reaction be-

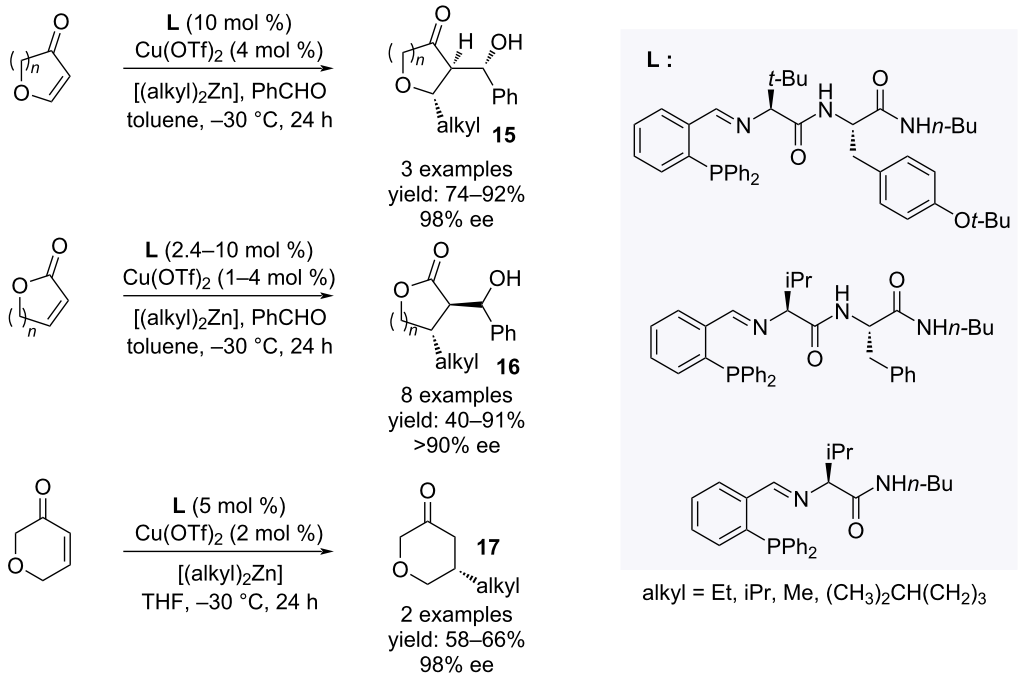

Scheme 12: Synthesis of unsaturated furanones and pyranones **15**–**17**.

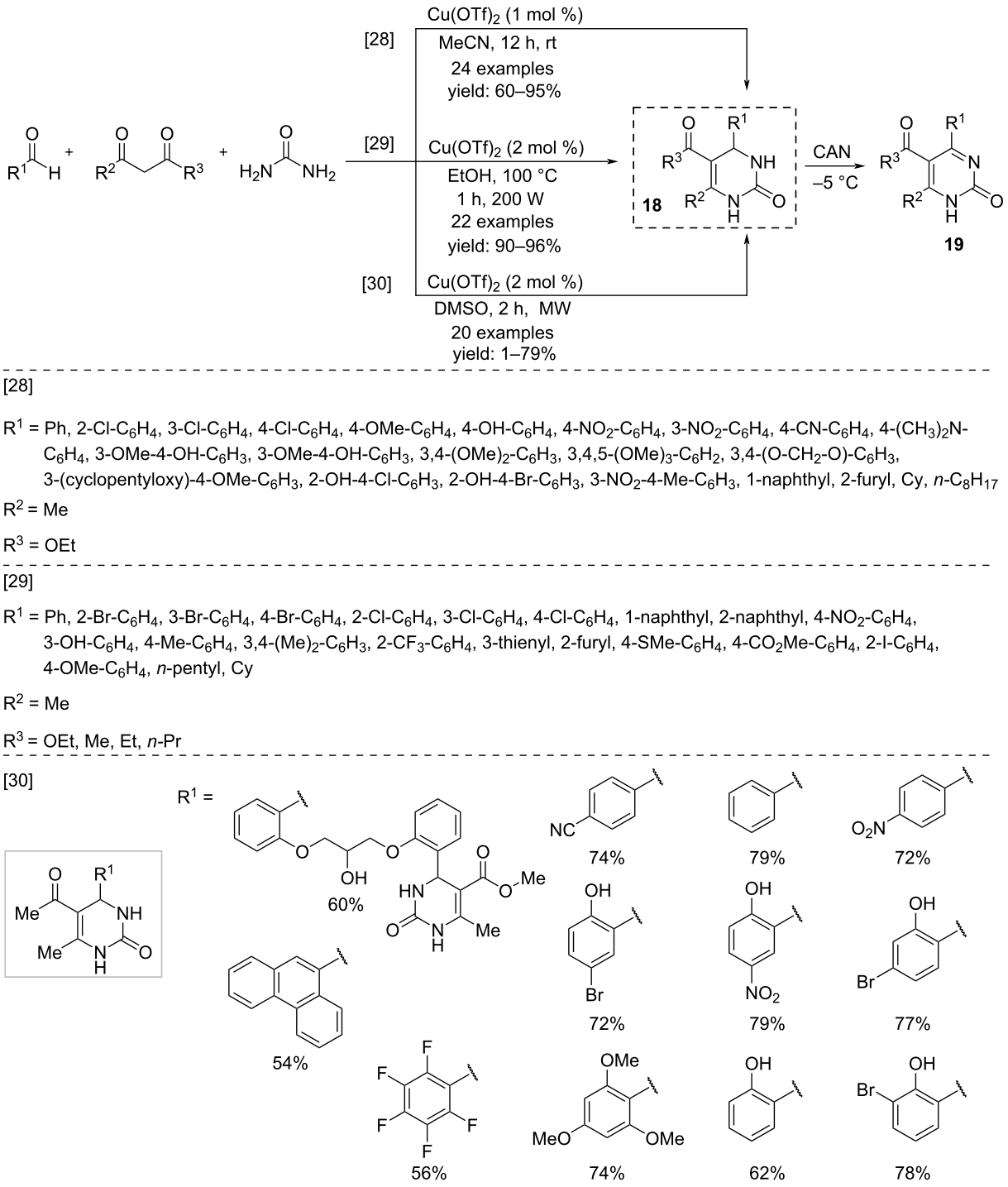

Scheme 13: Synthesis of substituted dihydropyrimidines **18**.

tween the alkyne and the imine generated by dehydration between the aldehyde and aniline. The catalyst promotes the formation of the imine **XI**, while the high regioselectivity is ascribable to the favored orientation between the electron-rich nitrogen of the diene and the electron-poor carbon of the alkyne.

A different one-pot procedure affording tetrahydropyridines was developed employing two molecules of aromatic aldehydes, ethyl acetoacetate and two molecules of aniline. The copper triflate catalyst acts in the initial formation of imine **XII** and enamine **XIII**, reacting each other in a mechanism that involved two Mannich-type reactions (Scheme 15) [32].

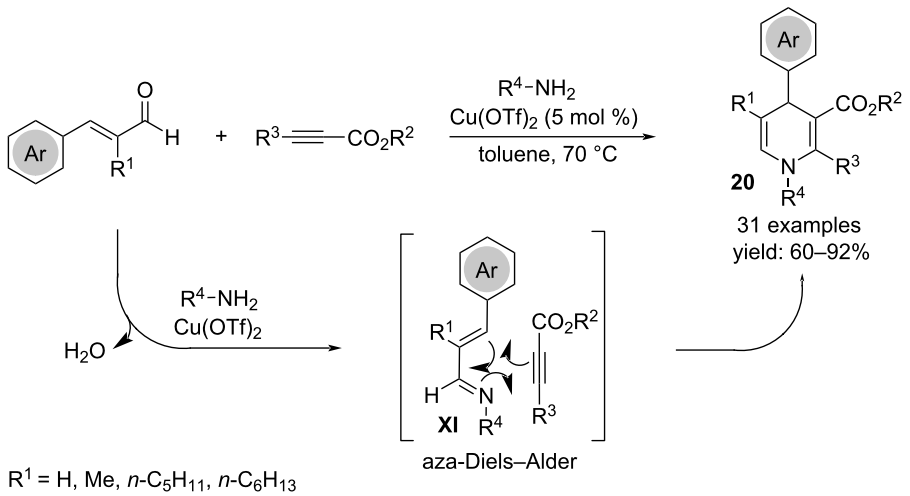

R^1 = H, Me, *n*-C_5H_{11}, *n*-C_6H_{13}

R^2 = Me, Et

R^3 = H, CO_2R^2; R^4 = Ph, 4-F-C_6H_4, 4-Cl-C_6H_4, 3-Cl-C_6H_4, 3,5-$(Cl)_2$-C_6H_3, 2-Cl-C_6H_4, 4-Br-C_6H_4, 4-I-C_6H_4, 4-CF_3-C_6H_4, 4-NO_2-C_6H_4, 4-OMe-C_6H_4, 4-OCF_3-C_6H_4, 4-Me-C_6H_4, 3-Me-C_6H_4, 3,5-Me-C_6H_3, 2-Me-C_6H_4, 4-iPr-C_6H_4, Bn, Cy

Ar = Ph, 4-Me-C_6H_4, 4-OMe-C_6H_4, 4-Br-C_6H_4, 4-Cl-C_6H_4, 4-F-C_6H_4, 3-F-C_6H_4

Scheme 14: Regioselective synthesis of 1,4-dihydropyridines **20**.

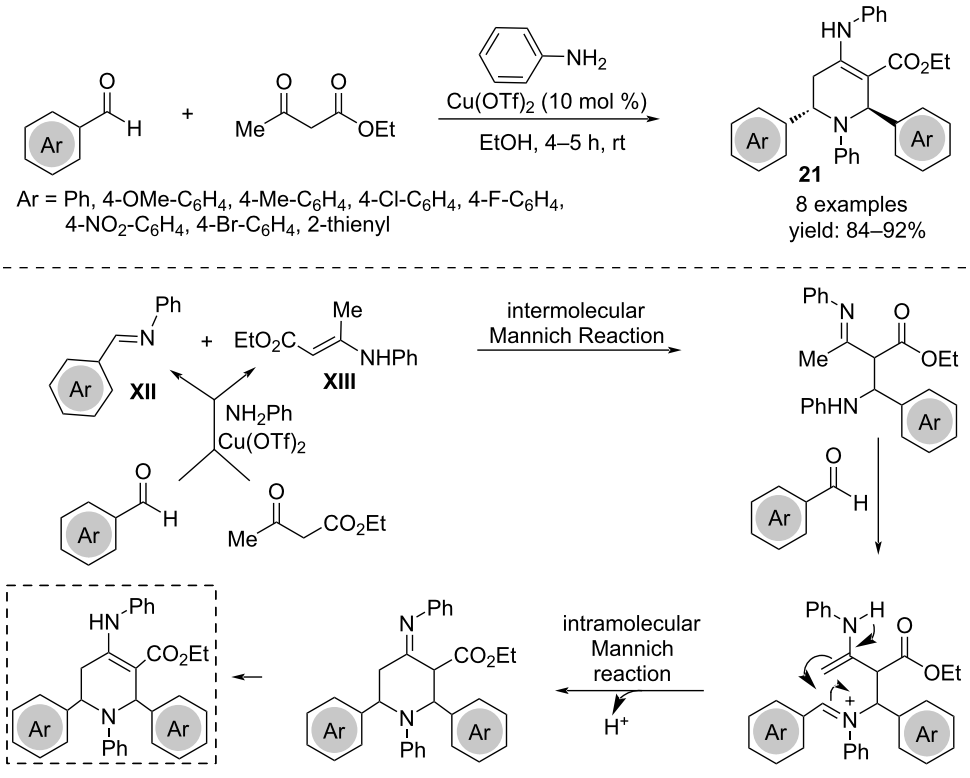

Scheme 15: Synthesis of tetrahydropyridines **21**.

Activation of terminal alkynes with $Cu(OTf)_2$ is the key step for the preparation of furoquinoxalines **22** from *o*-phenylenediamine and ethyl glyoxylate (Scheme 16) [33]. The reaction, which occurs with formation of C–C, C–N and C–O bonds, involves a nucleophilic addition of the activated alkyne **XIV** to the in situ-generated iminium ion **XV**, followed by cyclization to form a quinoxalin-2-one intermediate **XVI**. A subsequent 5-*endo-dig* cyclization involving the triple bond furnishes the furo-ring and the final oxidation affords the tricyclic product **22**.

Substituted quinolines **23** were obtained in a convenient solvent-free multicomponent reaction starting from electron-rich or electron-poor anilines, alkyl or arylaldehydes and terminal alkynes, performing the coupling with copper triflate as catalyst, without ligand, co-catalyst or other additives. The reaction involved the formation of the imine **XVII** followed by alkynylation to propargylamine **XVIII**, cyclization, and oxidation to quinoline **23** (Scheme 17) [34].

Three component oxidative annulation to obtain cyclic ether-fused tetrahydroquinolines **24** has been reported starting from secondary anilines, cyclic ethers and paraformaldehyde (Scheme 18) [35]. In addition to $Cu(OTf)_2$ as a catalyst, the most effective reaction conditions required a substoichiometric amount of *p*-nitrobenzoic acid as an additive. Some control experiments support a mechanism whose key intermediates are the formation of the iminium ion **XIX**, originated from aniline with formaldehyde which serves as the C1 building block, and the generation of the cyclic α,β-unsaturated ethers **XX** by $Cu(OTf)_2$-catalyzed dehydrogenation of the corresponding saturated compounds. Subsequent nucleophilic addition of the cyclic vinyl ether to the iminium salt generates an intermediate **XXI** susceptible of intramolecular electrophilic attack to give a tricyclic structure **XXII**. The final deprotonation provides the desired product **24**.

The multicomponent reaction was also fruitful to obtain 1,2-dihydroisoquinolines **25** starting from 2-alkynylbenzaldehydes, primary amines and allylic or benzyl bromide, in the presence of zinc and using the combination of $Mg(ClO_4)_2$/$Cu(OTf)_2$ as catalyst. The use of a mixture THF/DCE 1:20 as solvent was mandatory, because THF was crucial for the formation of the organozinc reagent (Scheme 19) [36].

Spiro-2,3-dihydroquinazolinones **26** were formed exploiting a one-pot multicomponent reaction, using isatoic anhydride, ketones and primary amines. The isolation of the amide intermediate **XXIII** obtained by the copper-catalyzed reaction between the anhydride and the amine suggested the subsequent reaction with the ketone to give an imine intermediate **XXIV**. This latter can undergo intramolecular nucleophilic attack affording the quinazolinone derivative **26** (Scheme 20) [37].

Polysubstituted pyrroles **27** were obtained in a cascade process by using α-diazoketones, nitroalkenes and primary amines, in the presence of air as oxidant. The mechanism involved the for-

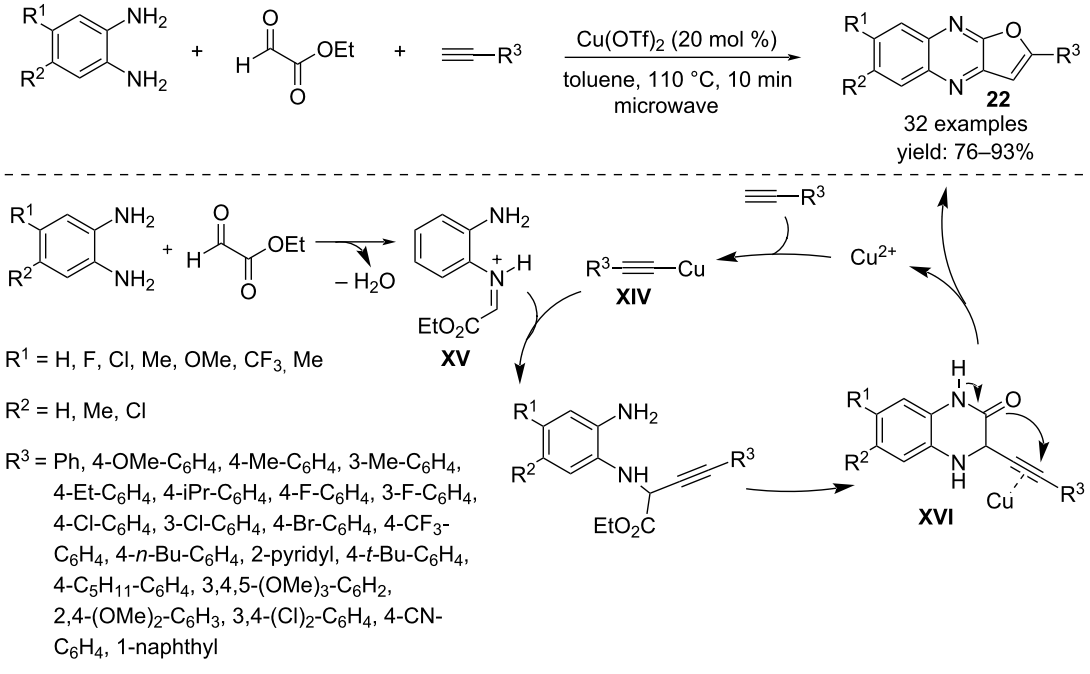

Scheme 16: Synthesis of furoquinoxalines **22**.

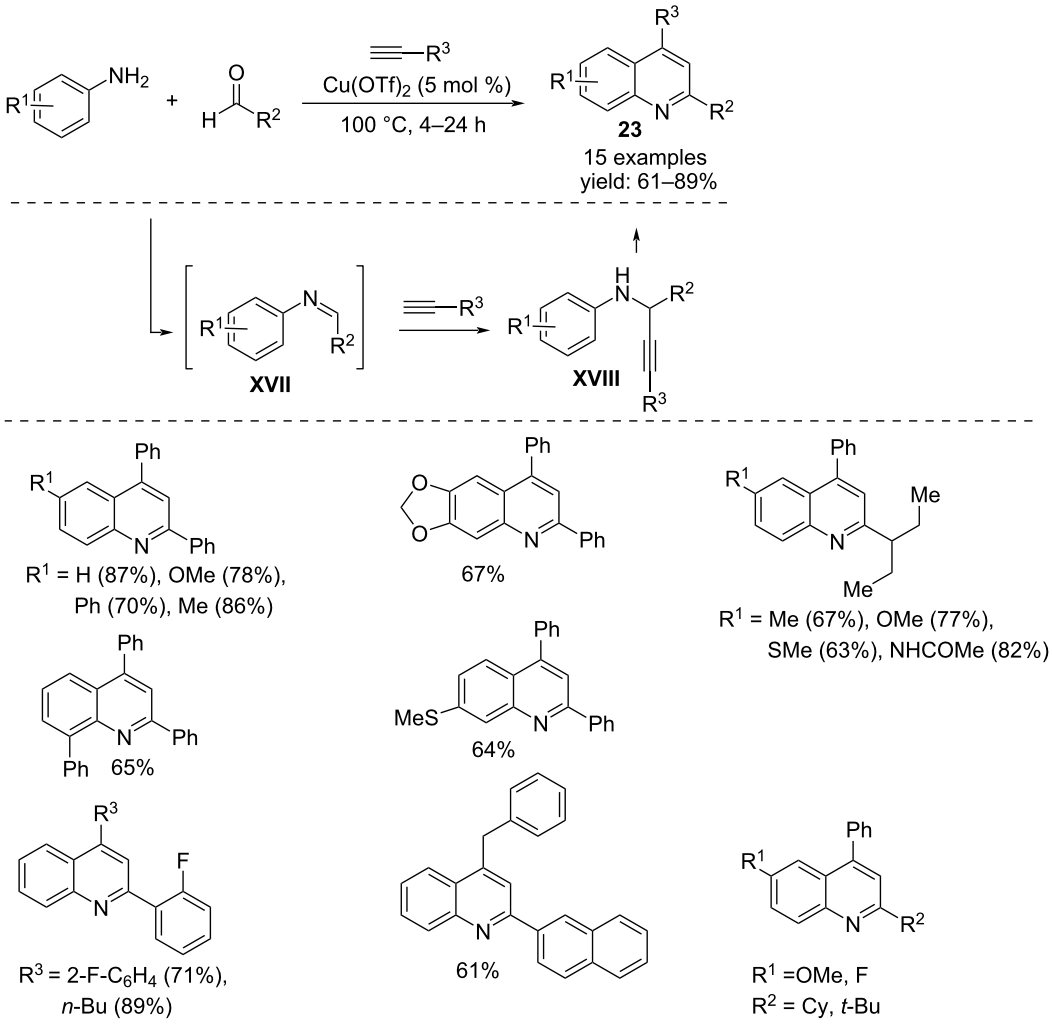

Scheme 17: Synthesis of 2,4-substituted quinolines **23**.

mation of α-ketocarbene **XXVI** from α-diazoketone, able to react with the amine affording imine **XXV** after copper-catalyzed oxidative dehydrogenation. The subsequent [3 + 2] cycloaddition reaction with the nitroalkene produces the pyrrolidine **XXVII**, which then aromatizes by extrusion of HNO_2 (Scheme 21) [38].

Substituted pyrrolidines **30** were achieved in an enantioselective form starting from amino acid esters, electron-poor olefins and 4-substituted-2-picolinaldehydes or 4-methylthiazole-2-carboxaldehyde as chelating agent, in the presence of copper triflate and the chiral diamine ligand **28**. The stereoselectivity was directed by the formation of a proposed catalyst complex **29** involving two molecules of Schiff base (Scheme 22) [39].

The three-component annulation of aldehydes, hydrazines and alkenes with $Cu(OTf)_2$ (20 mol %) in CH_2Cl_2 at reflux is a useful tool to access substituted 4,5-dihydropyrazoles **31** (Scheme 23) [40]. The products reasonably result from a Mannich/cyclization/oxidative transformation of the substrates in which $Cu(OTf)_2$ is involved in more steps. The reaction begins with a nucleophilic attack of hydrazine on the aldehyde, activated by the copper salt, to give the corresponding hydrazone **XXVIII**. Subsequently, the formation of a Mannich-type intermediate **XXIX** was hypothesized by interaction between the hydrazone and the alkene mediated by $Cu(OTf)_2$ coordination, which favors the approach of the reaction centers. It is again a metal coordination that activates the C–C double bond towards an intramolecular reaction to give the tetrahydropyrazole **XXX** via formation of a C–N bond. The final oxidation in air gives the 4,5-dihydropyrazole **31**.

$Cu(OTf)_2$ is also capable of promoting the three-component cascade cyclization of 2-formylbenzonitriles, alkyl aryl ketones,

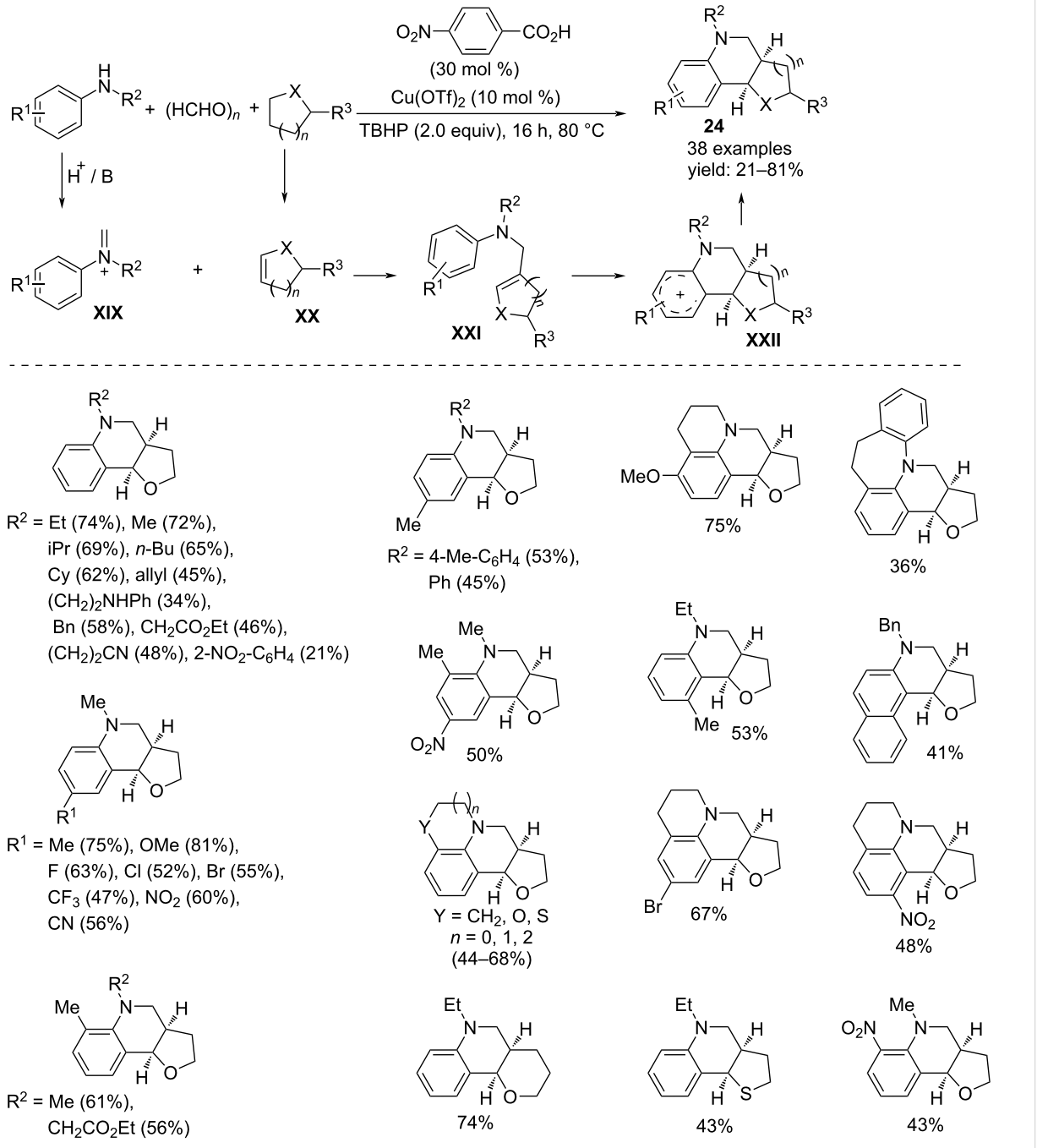

Scheme 18: Synthesis of cyclic ether-fused tetrahydroquinolines **24**.

and diaryliodonium salts to afford 2-arylisoindolinones **32** (Scheme 24) [41]. It is conceivable that the reaction starts with the formation of an *N*-arylnitrilium cation **XXXI** that, after hydrolysis, reacts with an enol species activated by the copper catalyst, affording the final product. The same research group reported an extension of this study by starting from arylacetylenes instead of arylketones [42].

Imidazo[1,2-*a*]pyridine derivatives **33** can be achieved by $Cu(OTf)_2$-catalyzed multicomponent reactions starting from different reagents. In a first approach proposed by Meshram and co-workers, pyridin-2-one, *O*-tosylhydroxylamine and acetophenone treated in an ionic liquid assembled through the cascade formation of three C–N bonds to give the imidazo[1,2-*a*]pyridine scaffold **33** (Scheme 25) [43]. The reaction is facili-

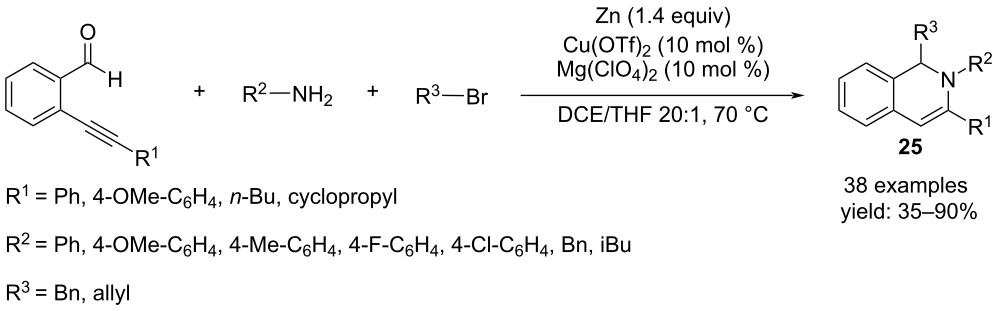

Scheme 19: Practical route for 1,2-dihydroisoquinolines **25**.

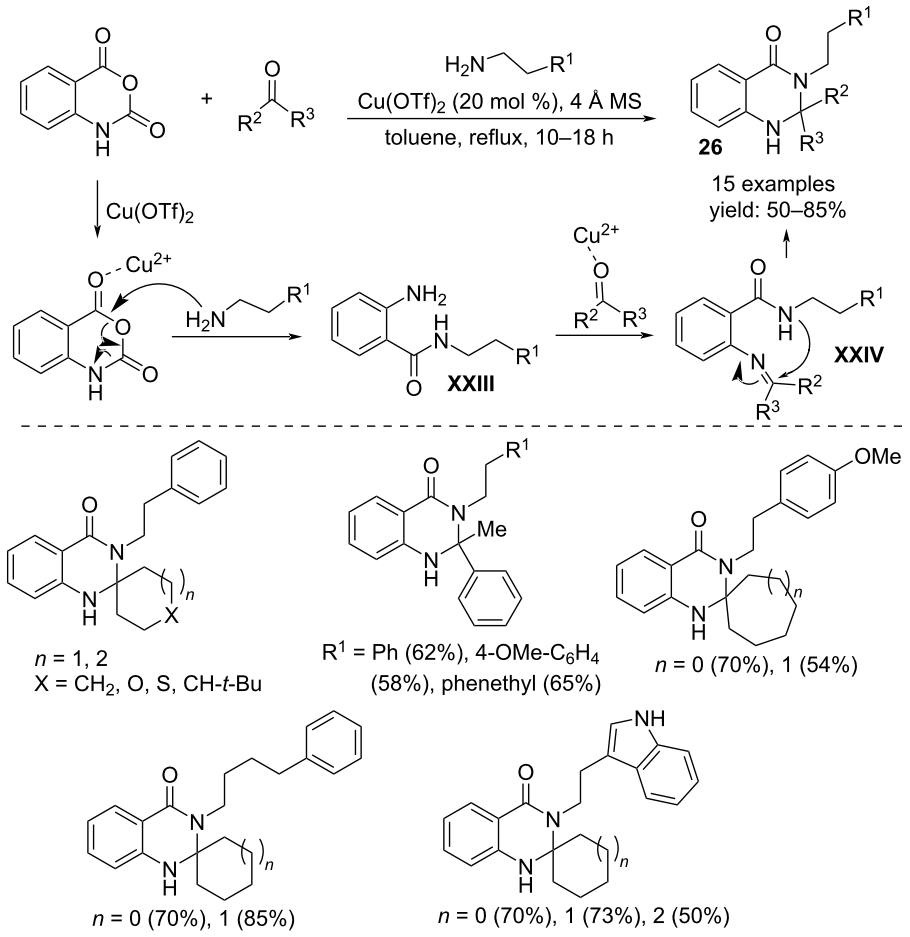

Scheme 20: Synthesis of 2,3-dihydroquinazolin-4(1*H*)-one derivatives **26**.

tated under microwave irradiation and can be extended to the preparation of an imidazo-fused (benzo)thiazole skeleton **34** starting from (benzo)thiazol-2-ones instead of pyridin-2-ones. Moreover, the $Cu(OTf)_2$ in $[bmim]BF_4$ can be recovered and reused for multiple processes. The key step of the mechanism is the attack of the protonated pyridin-2-one to the copper-complex of the enamine **XXXII** resulting from the reaction between acetophenone and *O*-tosylhydroxylamine, which occurs with elimination of TsOH. The so-obtained imino–copper complex **XXXIII** gives rise to an intramolecular C–N bond formation releasing $Cu(OTf)_2$. The final bicyclic product **33** arises from isomerization and water elimination.

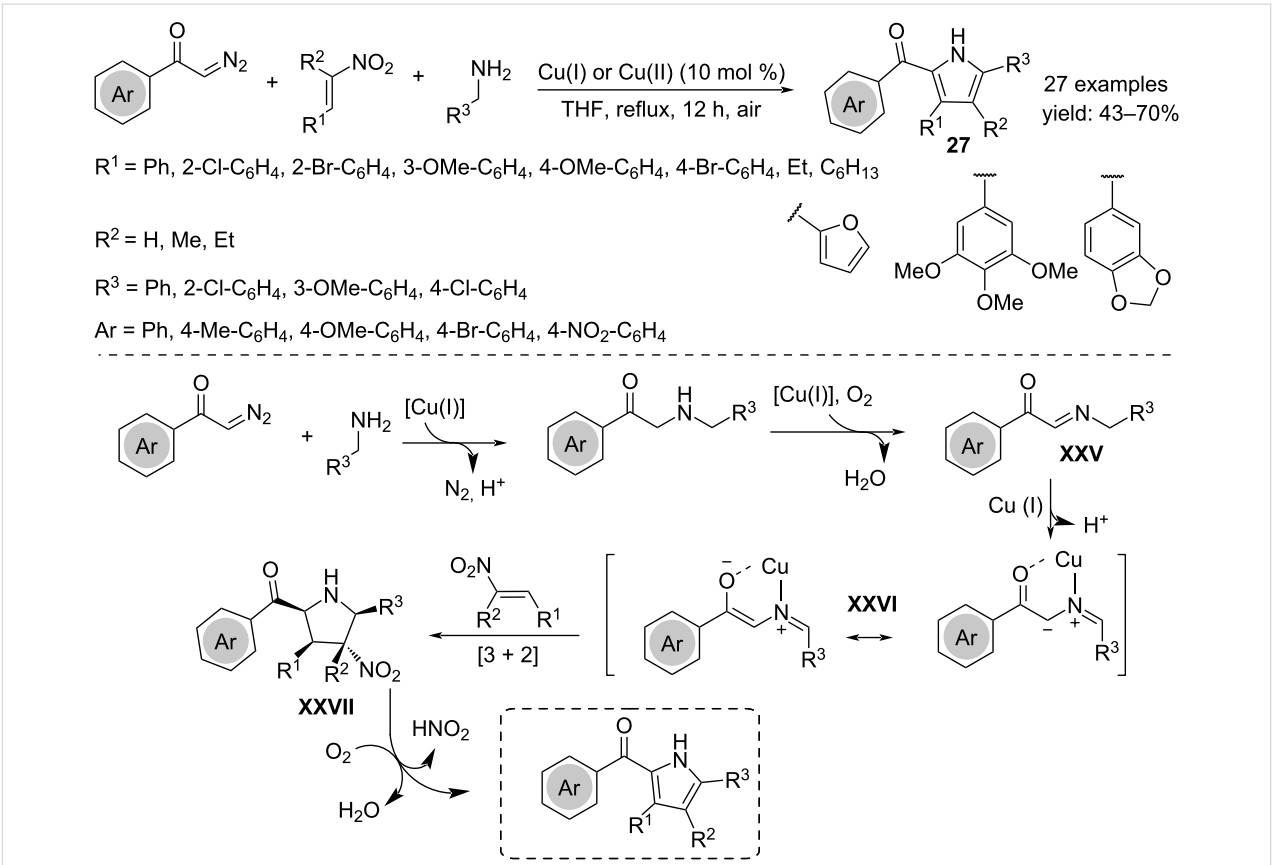

Scheme 21: Synthesis of polysubstituted pyrroles **27**.

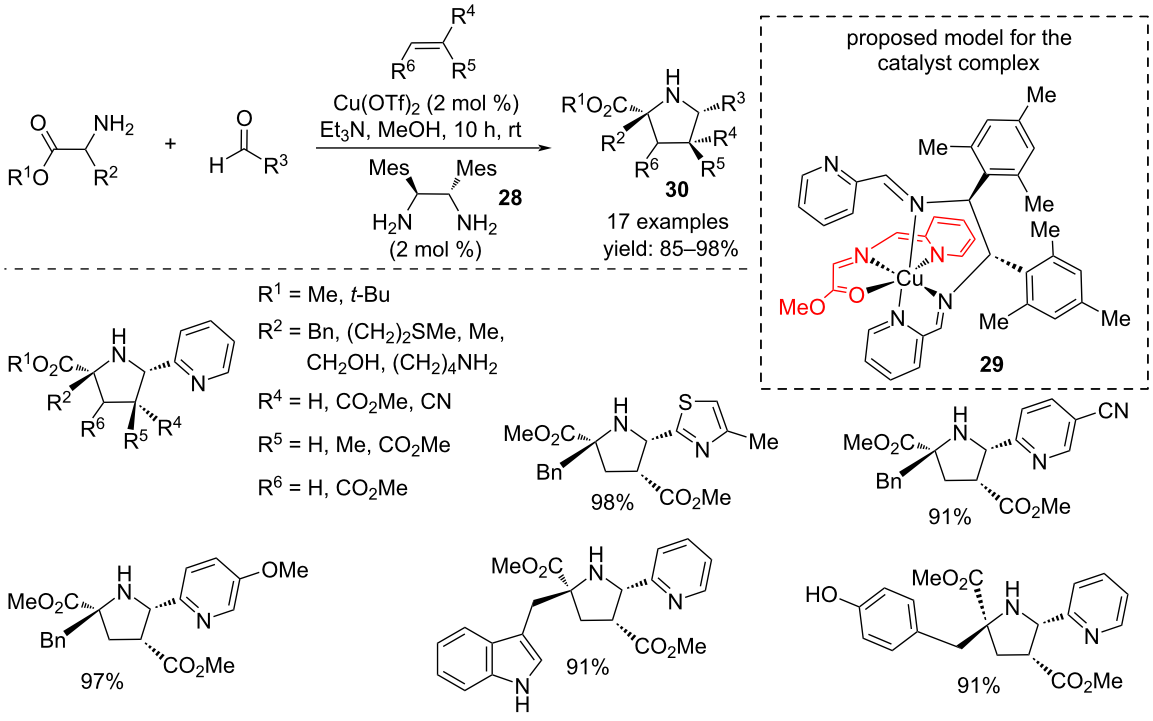

Scheme 22: Enantioselective synthesis of polysubstituted pyrrolidines **30** directed by the copper complex **29**.

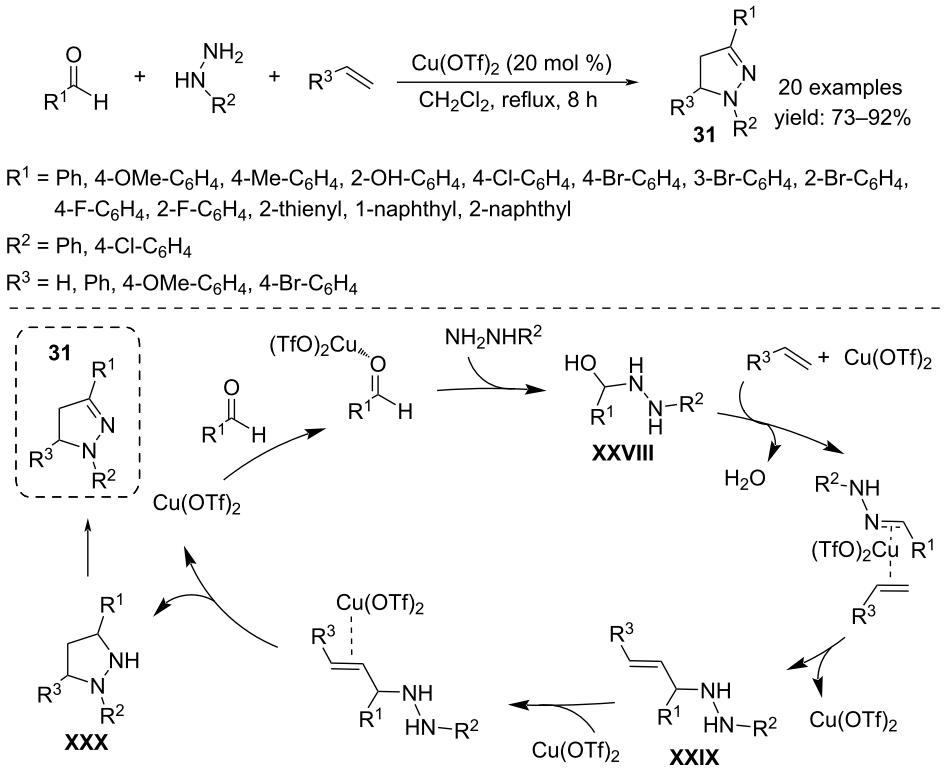

Scheme 23: Synthesis of 4,5-dihydropyrazoles **31**.

Recently, Singh's research group developed a cascade process to access imidazo[1,2-*a*]pyridines-linked isoxazoles **35**. Isoxazole carbaldehydes treated with 2-aminopyridines and isonitriles in the presence of catalytic amounts of $Cu(OTf)_2$ lead to the formation of the products through formation of one C–C bond and three C–N bonds (Scheme 26) [44]. The same procedure allows a more general scope, giving access to imidazo[1,2-*a*]pyrimidine, imidazo[1,2-*a*]pyrazine and imidazo[2,1-*b*]thiazole derivatives. From the mechanistic point of view, it is expected that the reaction proceeds via formation of an imine **XXXIV** between isoxazole carbaldehyde, activated by the copper salt, and 2-aminoazine, which in turn undergoes a non-concerted [4 + 1] cycloaddition involving isonitrile to give the imidazole ring of intermediate **XXXV**. Finally, the final product **35** is yielded via a 1,3-hydride shift.

The reaction between diazo derivatives, nitriles, and azodicarboxylates catalyzed by $Cu(OTf)_2$ is an efficient synthetic method to obtain 2,3-dihydro-1,2,4-triazole derivatives **36** (Scheme 27) [45]. The reaction proceeds via a [3 + 2] cycloaddition reaction between azodicarboxylates and nitrile ylides **XXXVI** as 1,3-dipoles. The latter are generated from diazoalkanes under the coordination of the copper catalyst to form a carbenoid species that undergoes nucleophilic attack of the nitriles. This transformation has demonstrated high tolerance to functional groups and runs, under mild conditions, with electron-poor diazo derivatives such as 2-diazoacetate, 2-diazoacetonitrile, 2-diazo-1,1,1-trifluoromethane, diazoamide, and diazophosphonate.

Condensation of 2-naphthol, aromatic aldehydes and acyclic 1,3-dicarbonyl compounds catalyzed by copper triflate under ultrasound irradiation allowed the one-pot formation of 1*H*-benzo[*f*]chromen-2-yl(phenyl)methanones (naphthopyranes) **37**. The comparison with conventional method showed better yields and shorter reaction times. The suggested reaction mechanism showed the formation of an *ortho*-quinone methide intermediate **XXXVII** formed through nucleophilic attack of the 2-naphthol to the aldehyde followed by reaction with 1,3-dicarbonyl compound coordinated by the copper. The subsequent intramolecular nucleophilic attack of the oxygen to the enol and water elimination resulted in the final product **37** (Scheme 28) [46].

Analogously, benzo[*g*]chromene derivatives **38** were achieved starting from 2-hydroxynaphthalene-1,4-dione, aromatic aldehydes and malononitrile with copper triflate as catalyst and ultrasonic irradiation (Scheme 29) [47].

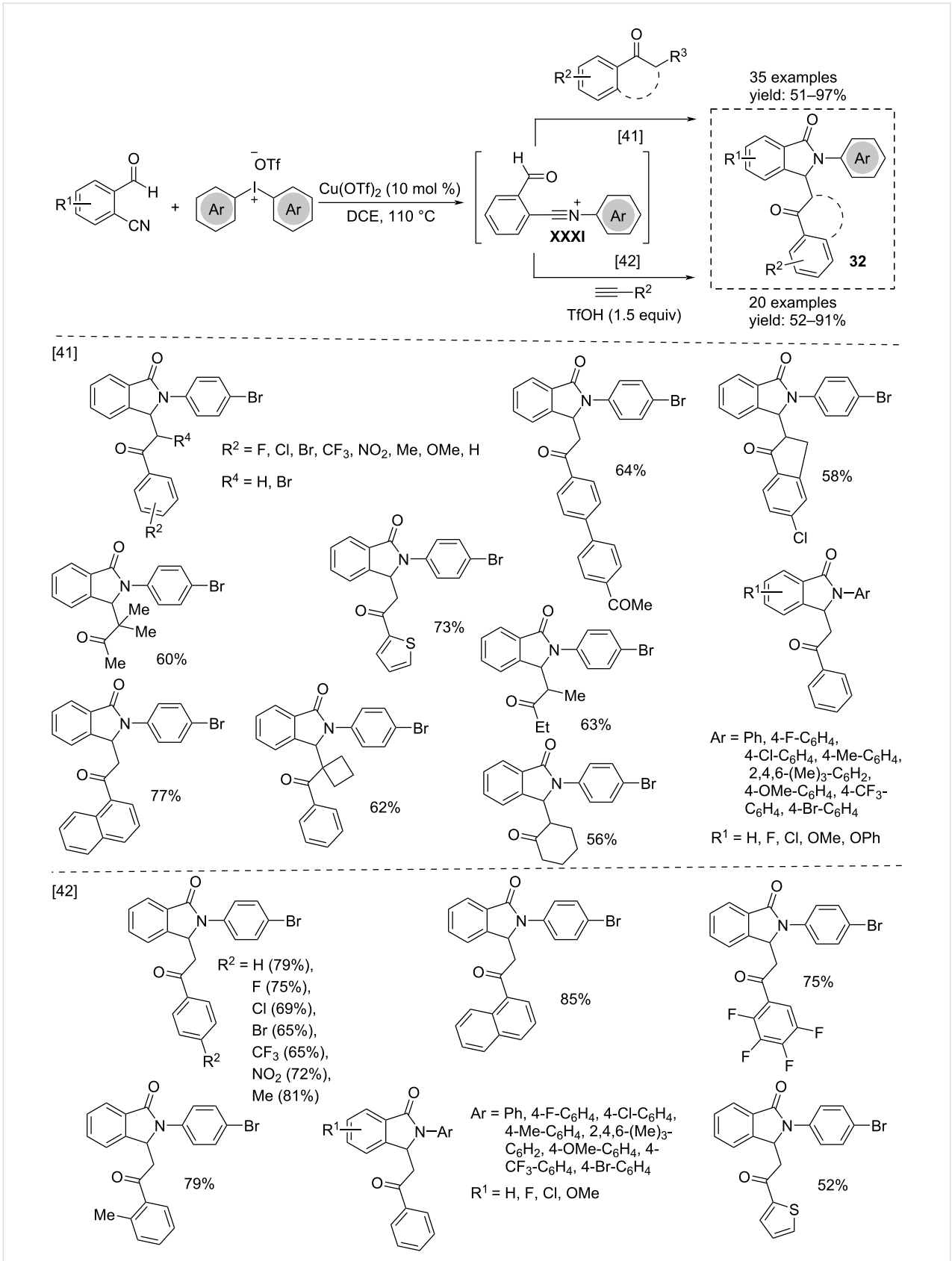

Scheme 24: Synthesis of 2 arylisoindolinones **32**.

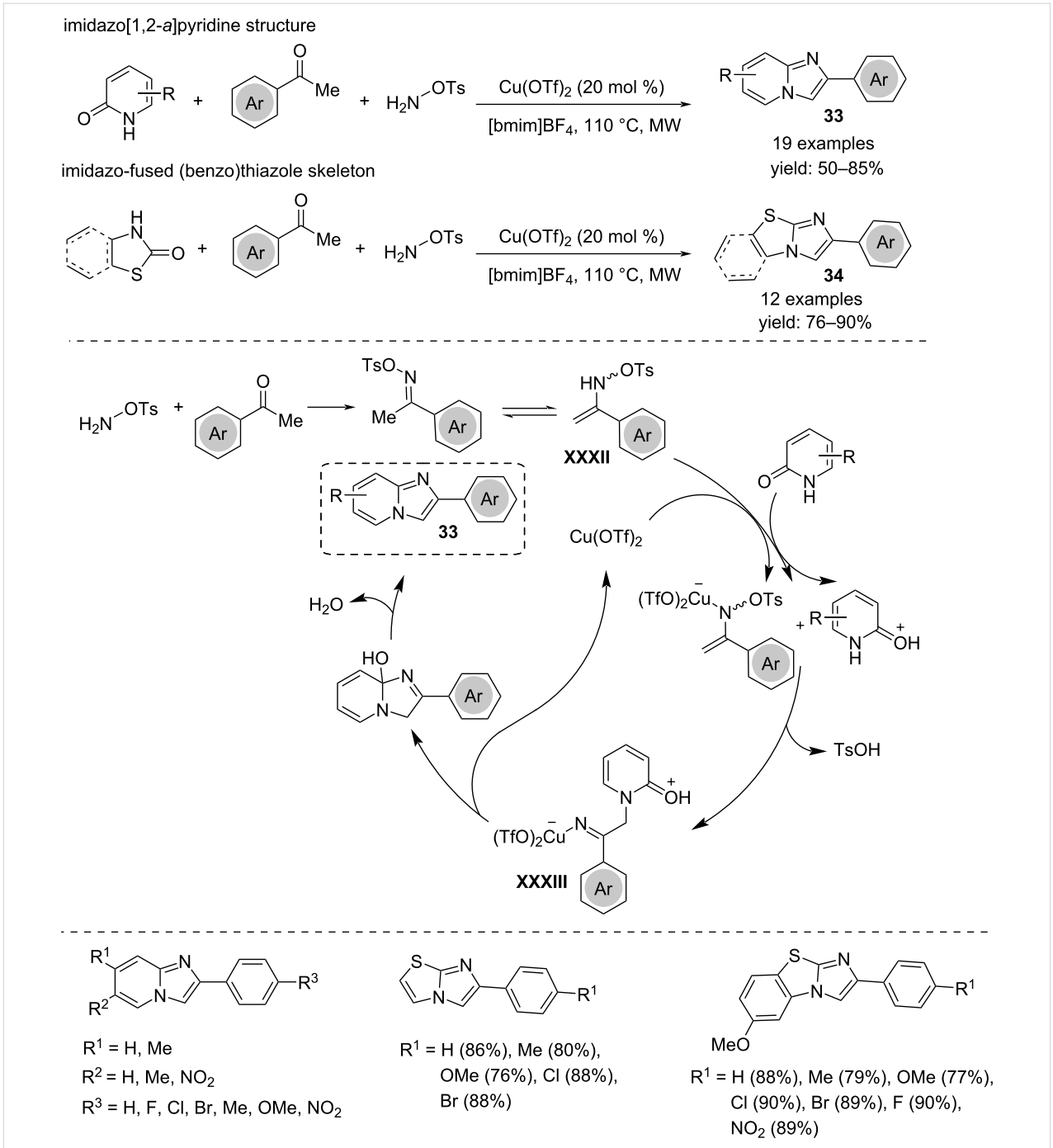

Scheme 25: Synthesis of imidazo[1,2-*a*]pyridines **33**.

Naphthalene-annulated 2-aminothiazoles **39** were prepared exploiting the multicomponent reaction by using aminonaphthalenes, CS_2 and secondary amines. The mechanism involved the Ullmann-type coupling of the bromo(amino)naphthalene with the dithiocarbamate salt followed by intramolecular nucleophilic attack of the naphthalene amino group to the C=S bond. The subsequent elimination of H_2S afforded the final product (Scheme 30) [48].

Analogously, piperazinylthiazoloquinolines **40** and thiazolocoumarins **41** were obtained using piperazine or piperidine, CS_2 and substituted quinolines or coumarins [49].

The synthesis of furo[3,4-*b*]pyrazolo[4,3-*f*]quinolinones **42** was achieved via the one-pot reaction of tetronic acid, 5-aminoindazole and arylaldehydes under copper catalysis and ultrasonic irradiation, in acetonitrile as solvent. The mechanism involves a

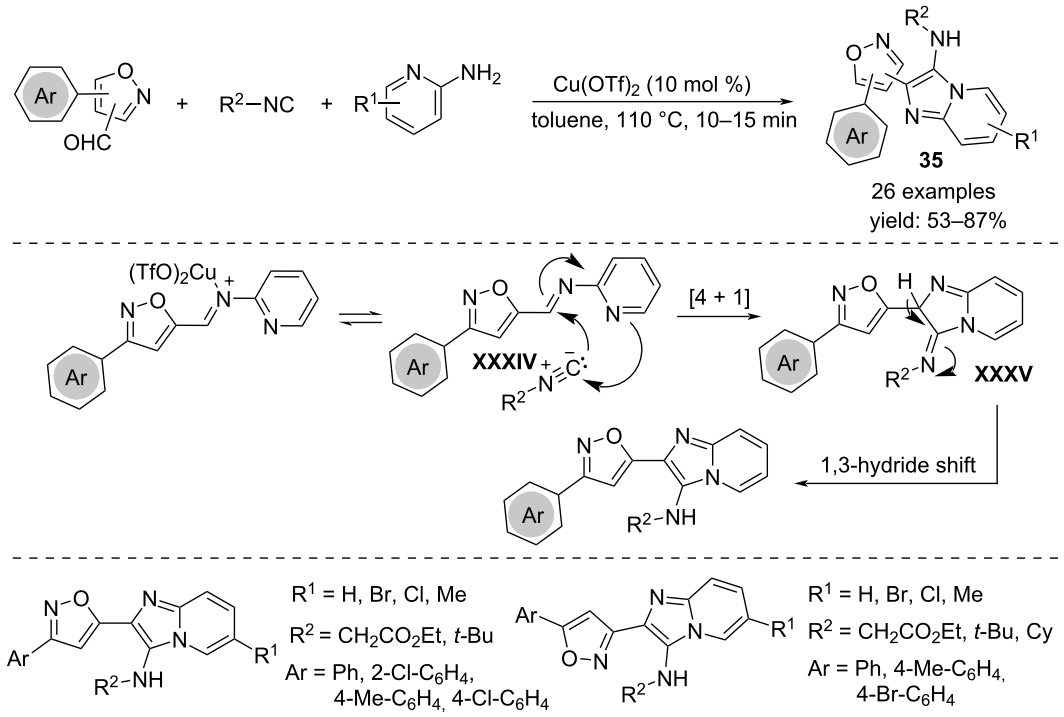

Scheme 26: Synthesis of isoxazole-linked imidazo[1,2-*a*]azines **35**.

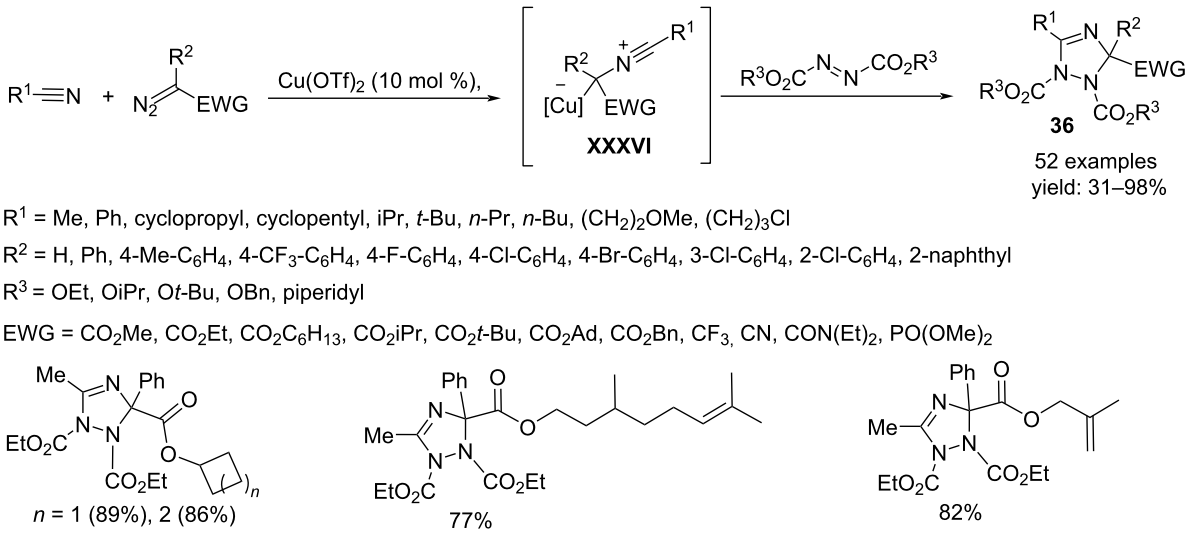

Scheme 27: Synthesis of 2,3-dihydro-1,2,4-triazoles **36**.

Knoevenagel condensation between the tetronic acid and the arylaldehyde as first step, followed by a Michael-type addition of 5-aminoindazole to afford the first coupling product **XXXVIII**. The subsequent intramolecular amination and dehydration then leads to the final product (Scheme 31) [50].

Polycyclic spiroindoline-3,4'-pyrano[3,2-*b*]pyran-4-ones **43** were synthesized exploiting the three-component reaction of isatin, 5-hydroxy-2-(hydroxymethyl)-4*H*-pyran-4-one (i.e. kojic acid) and malononitriles or cyanoacetates (Scheme 32) [51]. Compared to other Lewis acids, $Cu(OTf)_2$ proved to be the best.

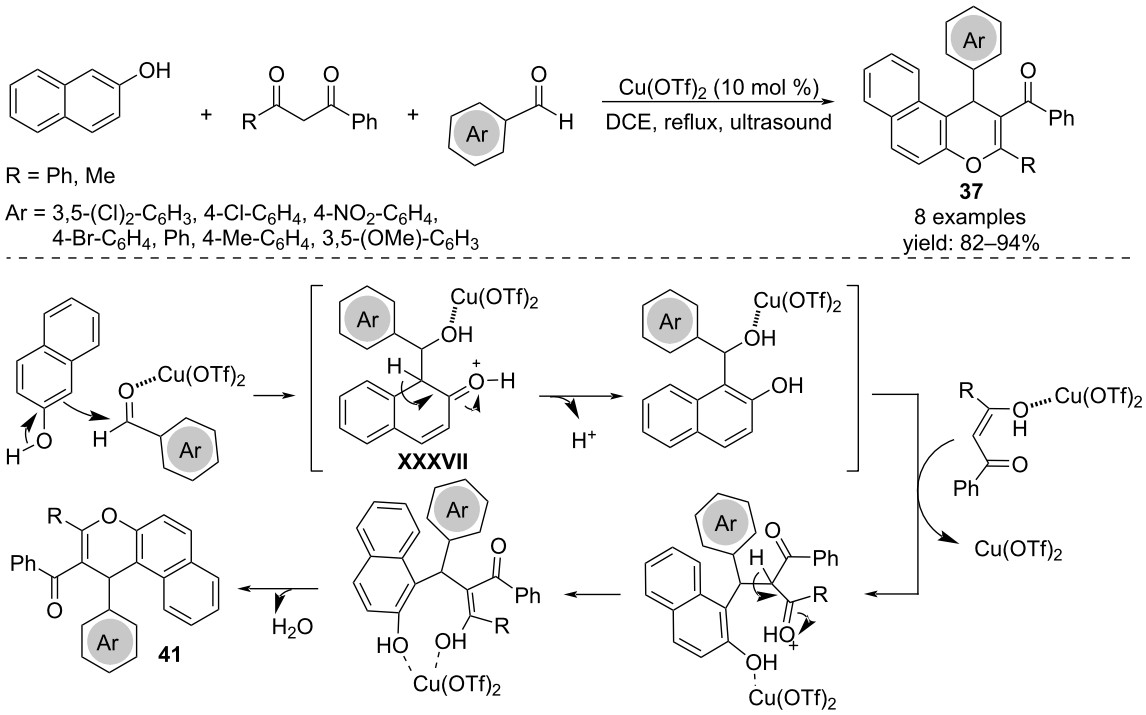

Scheme 28: Synthesis of naphthopyrans **37**.

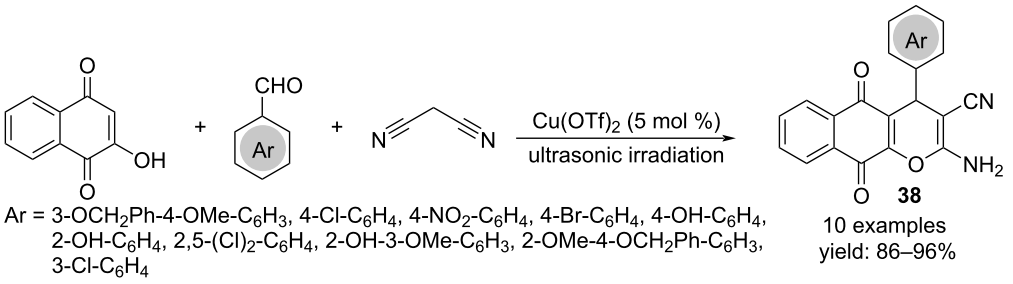

Scheme 29: Synthesis of benzo[*g*]chromene derivatives **38**.

Mechanistically, the process begins with a Knoevenagel-type condensation between isatin and the cyano derivative, yielding a 3-alkylidene-substituted oxindole **XXXIX** that, after coordination with $Cu(OTf)_2$, is able to react with the enolic form of kojic acid to generate the C-alkylated intermediate **XL**. Subsequent intramolecular nucleophilic attack of the enolic hydroxy group to the copper-activated cyano group, results in a spirocyclized intermediate **XLI** that affords the final product by deprotonation and loss of the copper species.

Four-component reactions

Two different four-component procedures catalyzed by $Cu(OTf)_2$ are reported in the literature, both to access 1,2,3-triazole derivatives. The first one is a cascade reaction for the preparation of α-alkoxy-*N*-alkyltriazoles **44** that was developed starting from aliphatic aldehydes, alcohols, $TMSN_3$ as azide source and alkynes (Scheme 33) [52]. The reaction occurs under mild conditions in acetonitrile at room temperature but is inhibited when using aromatic aldehydes and phenols. The mechanism involves the reaction of the azide with the hemiacetal **XLII** generated in situ from the aldehydes and alcohols, followed by coupling with the alkynes to form the triazole ring. Both, copper triflate and copper metal are essential for the success of the reaction.

On the other hand, 4-(α-tetrasubstituted)alkyl-1,2,3-triazoles **45** can be obtained by a two-step reaction of cyclohexanone, amines, silylacetylene, and aryl or alkyl azides in the presence

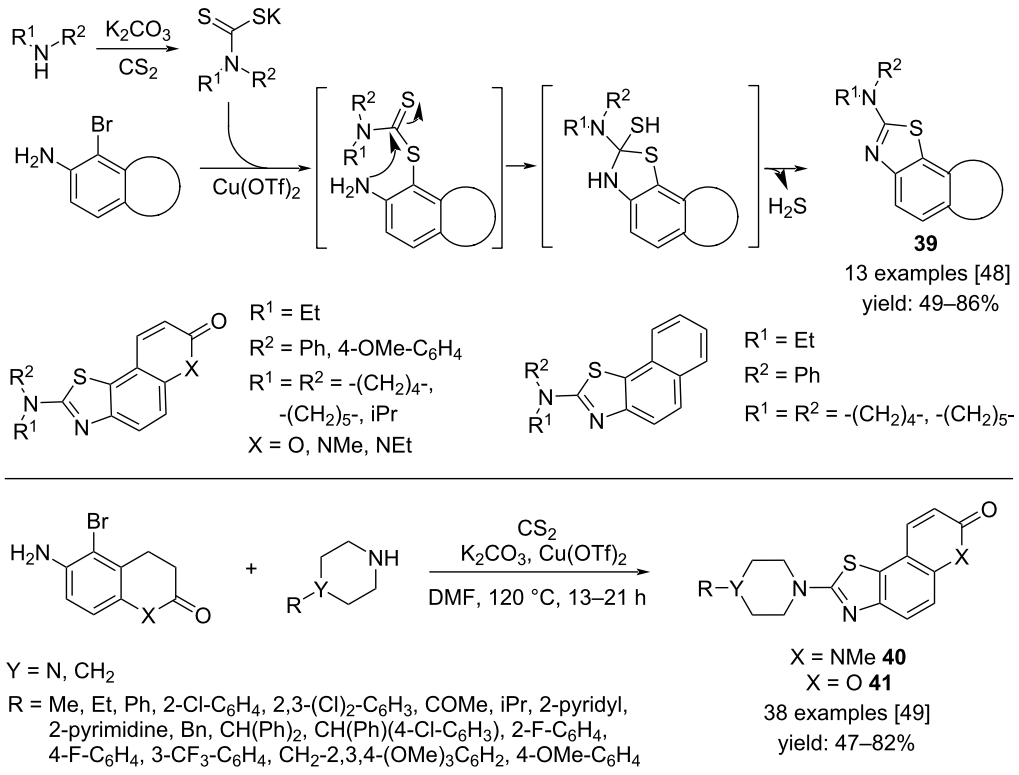

Scheme 30: Synthesis of naphthalene annulated 2-aminothiazoles **39**, piperazinyl-thiazoloquinolines **40** and thiazolocoumarins **41**.

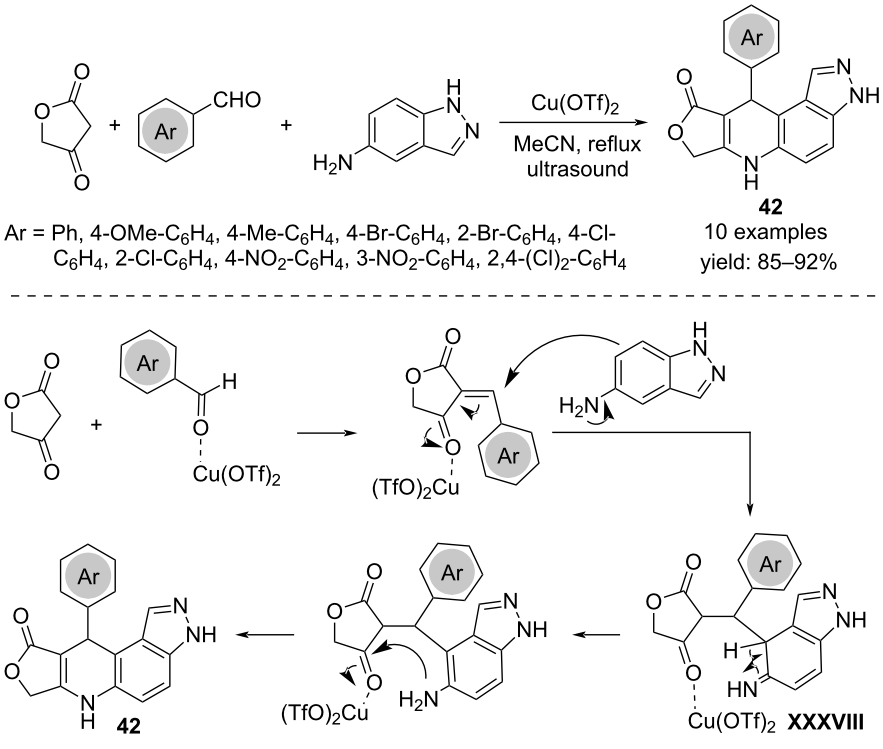

Scheme 31: Synthesis of furo[3,4-*b*]pyrazolo[4,3-*f*]quinolinones **42**.

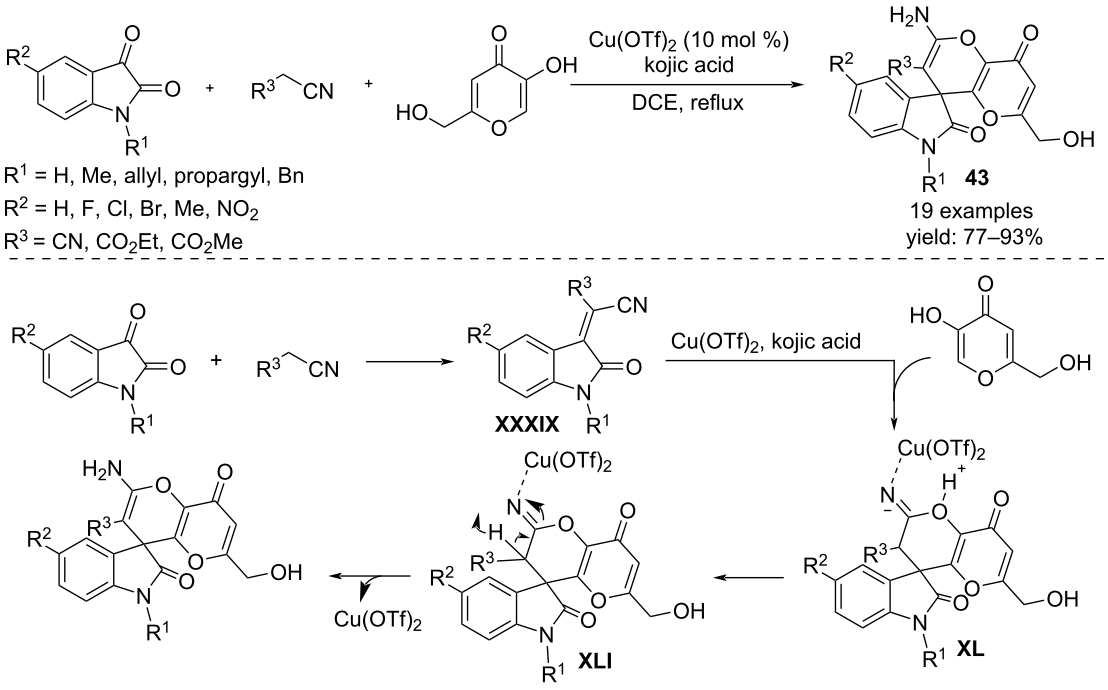

Scheme 32: Synthesis of spiroindoline-3,4'-pyrano[3,2-*b*]pyran-4-ones **43**.

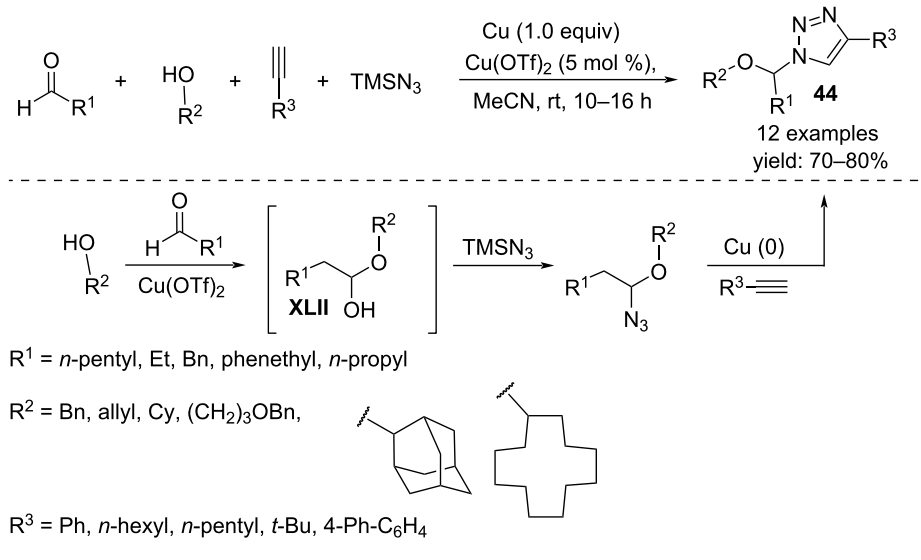

Scheme 33: Synthesis of *N*-(α-alkoxy)alkyl-1,2,3-triazoles **44**.

of copper(II) catalysts (Scheme 34) [53]. In a first step, there is the formation of a propargylamine derivative **XLIII**, followed by silyl deprotection and azide cycloaddition resulting in the triazole product. The presence of $Cu(OTf)_2$ as the catalyst, sodium ascorbate as a mild reductant and TBAF to deprotect the alkyne moiety are crucial in the cycloaddition step.

Conclusion

In this review the developments on the multicomponent synthesis of acyclic and heteropolycyclic systems under copper(II) triflate catalysis are reported. Using alkenes and alkynes as substrates, various types of reactions were considered, including hydroamination, condensation, cross-coupling, C–H functionalization, cycloaddition, aza-Diels–Alder, also in regio- and

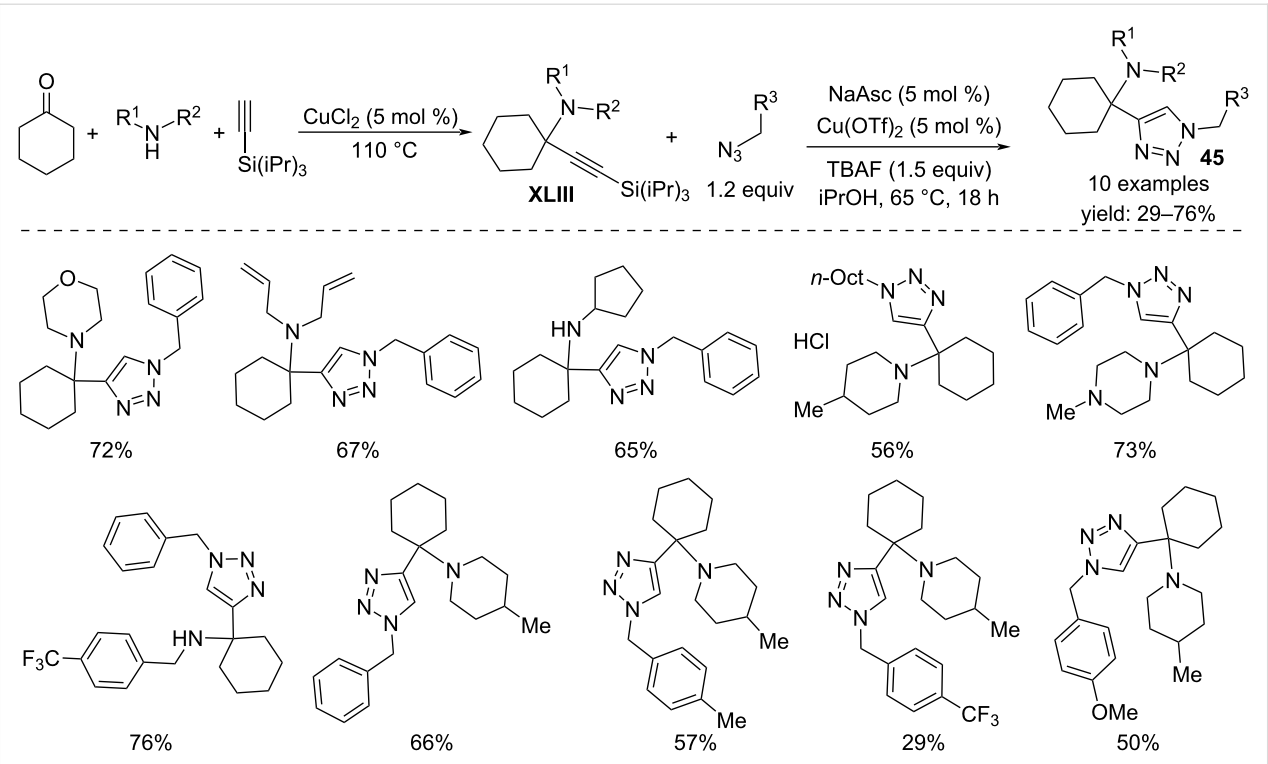

Scheme 34: Synthesis of 4-(α-tetrasubstituted)alkyl-1,2,3-triazoles **45**.

stereoselective processes. The interest for these strategies arises from the cost-effectiveness as one-pot processes, the ease of application and the great efficiency when directed to the synthesis of biologically active compounds.

Funding

This work has been supported by Università degli Studi dell'Insubria and Università degli Studi di Milano.

Author Contributions

Sara Colombo: writing – original draft. Camilla Loro: writing – original draft. Egle M. Beccalli: writing – review & editing. Gianluigi Broggini: writing – review & editing. Marta Papis: conceptualization; writing – original draft; writing – review & editing.

ORCID® iDs

Sara Colombo - https://orcid.org/0009-0002-6128-7394
Camilla Loro - https://orcid.org/0000-0001-9616-2335
Egle M. Beccalli - https://orcid.org/0000-0002-1189-2572
Gianluigi Broggini - https://orcid.org/0000-0003-2492-5078
Marta Papis - https://orcid.org/0000-0003-3730-9936

Data Availability Statement

Data sharing is not applicable as no new data was generated or analyzed in this study.

References

1. Aneeja, T.; Neetha, M.; Afsina, C. M. A.; Anilkumar, G. *RSC Adv.* **2020,** *10,* 34429–34458. doi:10.1039/d0ra06518h
2. Chemler, S. R. *Beilstein J. Org. Chem.* **2015,** *11,* 2252–2253. doi:10.3762/bjoc.11.244
3. Tschan, M. J.-L.; Thomas, C. M.; Strub, H.; Carpentier, J.-F. *Adv. Synth. Catal.* **2009,** *351,* 2496–2504. doi:10.1002/adsc.200800750
4. Rosenfeld, D. C.; Shekhar, S.; Takemiya, A.; Utsunomiya, M.; Hartwig, J. F. *Org. Lett.* **2006,** *8,* 4179–4182. doi:10.1021/ol061174+
5. Loro, C.; Papis, M.; Foschi, F.; Broggini, G.; Poli, G.; Oble, J. *J. Org. Chem.* **2023,** *88,* 13995–14003. doi:10.1021/acs.joc.3c01536
6. Loro, C.; Oble, J.; Foschi, F.; Papis, M.; Beccalli, E. M.; Giofrè, S.; Poli, G.; Broggini, G. *Org. Chem. Front.* **2022,** *9,* 1711–1718. doi:10.1039/d2qo00114d
7. Taylor, J. G.; Whittall, N.; Hii, K. K. (Mimi). *Chem. Commun.* **2005,** 5103–5105. doi:10.1039/b509933a
8. Hertweck, C. *J. Prakt. Chem.* **2000,** *342,* 316–321. doi:10.1002/(sici)1521-3897(200003)342:3<316::aid-prac316>3.3.co;2-j
9. Chemler, S. R. *J. Organomet. Chem.* **2011,** *696,* 150–158. doi:10.1016/j.jorganchem.2010.08.041
10. Rao, W.; Kothandaraman, P.; Koh, C. B.; Chan, P. W. H. *Adv. Synth. Catal.* **2010,** *352,* 2521–2530. doi:10.1002/adsc.201000450
11. Ton, T. M. U.; Himawan, F.; Chang, J. W. W.; Chan, P. W. H. *Chem. – Eur. J.* **2012,** *18,* 12020–12027. doi:10.1002/chem.201201219
12. Ghorai, M. K.; Ghosh, K.; Das, K. *Tetrahedron Lett.* **2006,** *47,* 5399–5403. doi:10.1016/j.tetlet.2006.05.059

13. Asao, N.; Kasahara, T.; Yamamoto, Y. *Angew. Chem., Int. Ed.* **2003,** *42,* 3504–3506. doi:10.1002/anie.200351390
14. Motornov, V. A.; Tabolin, A. A.; Nelyubina, Y. V.; Nenajdenko, V. G.; Ioffe, S. L. *Org. Biomol. Chem.* **2021,** *19,* 3413–3427. doi:10.1039/d1ob00146a
15. Paraskar, A. S.; Sudalai, A. *Tetrahedron Lett.* **2006,** *47,* 5759–5762. doi:10.1016/j.tetlet.2006.06.008
16. Muraki, T.; Fujita, K.-i.; Terakado, D. *Synlett* **2006,** 2646–2648. doi:10.1055/s-2006-951479
17. Dindulkar, S. D.; Puranik, V. G.; Jeong, Y. T. *Tetrahedron Lett.* **2012,** *53,* 4376–4380. doi:10.1016/j.tetlet.2012.06.022
18. Cavaca, L. A. S.; Gomes, R. F. A.; Afonso, C. A. M. *Molecules* **2022,** *27,* 1673. doi:10.3390/molecules27051673
19. Cheng, C.; Chen, D.; Li, Y.; Xiang, J.-N.; Li, J.-H. *Org. Chem. Front.* **2023,** *10,* 943–950. doi:10.1039/d2qo01580c
20. Meyet, C. E.; Pierce, C. J.; Larsen, C. H. *Org. Lett.* **2012,** *14,* 964–967. doi:10.1021/ol2029492
21. Dou, X.-Y.; Shuai, Q.; He, L.-N.; Li, C.-J. *Adv. Synth. Catal.* **2010,** *352,* 2437–2440. doi:10.1002/adsc.201000379
22. Liu, T.; Ding, Y.; Fan, X.; Wu, J. *Org. Chem. Front.* **2018,** *5,* 3153–3157. doi:10.1039/c8qo00965a
23. Mindner, J.; Rombach, S.; Werz, D. B. *Org. Lett.* **2024,** *26,* 2124–2128. doi:10.1021/acs.orglett.4c00498
24. Paraskar, A. S.; Sudalai, A. *ARKIVOC* **2006,** No. x, 183–189. doi:10.3998/ark.5550190.0007.a21
25. Brown, M. K.; Degrado, S. J.; Hoveyda, A. H. *Angew. Chem., Int. Ed.* **2005,** *44,* 5306–5310. doi:10.1002/anie.200501251
26. Biginelli, P. *Gazz. Chim. Ital.* **1893,** *23,* 360.
27. Tron, G. C.; Minassi, A.; Appendino, G. *Eur. J. Org. Chem.* **2011,** 5541–5550. doi:10.1002/ejoc.201100661
28. Paraskar, A. S.; Dewkar, G. K.; Sudalai, A. *Tetrahedron Lett.* **2003,** *44,* 3305–3308. doi:10.1016/s0040-4039(03)00619-1
29. Pasunooti, K. K.; Chai, H.; Jensen, C. N.; Gorityala, B. K.; Wang, S.; Liu, X.-W. *Tetrahedron Lett.* **2011,** *52,* 80–84. doi:10.1016/j.tetlet.2010.10.150
30. Huseynzada, A. E.; Jelch, C.; Akhundzada, H. V. N.; Soudani, S.; Ben Nasr, C.; Israyilova, A.; Doria, F.; Hasanova, U. A.; Khankishiyeva, R. F.; Freccero, M. *RSC Adv.* **2021,** *11,* 6312–6329. doi:10.1039/d0ra10255e
31. Li, S.; Yang, Q.; Wang, J. *Tetrahedron Lett.* **2016,** *57,* 4500–4504. doi:10.1016/j.tetlet.2016.08.085
32. Patil, K. N.; Mane, R. A.; Jadhav, S. B.; Mane, M. M.; Helavi, V. B. *Chem. Data Collect.* **2019,** *21,* 100233. doi:10.1016/j.cdc.2019.100233
33. Naresh, G.; Kant, R.; Narender, T. *Org. Lett.* **2014,** *16,* 4528–4531. doi:10.1021/ol502072k
34. Meyet, C. E.; Larsen, C. H. *J. Org. Chem.* **2014,** *79,* 9835–9841. doi:10.1021/jo5015883
35. Duan, P.; Sun, J.; Zhu, Z.; Zhang, M. *Org. Biomol. Chem.* **2023,** *21,* 397–401. doi:10.1039/d2ob02066a
36. Gao, K.; Wu, J. *J. Org. Chem.* **2007,** *72,* 8611–8613. doi:10.1021/jo7016839
37. Zhu, X.; Kang, S. R.; Xia, L.; Lee, J.; Basavegowda, N.; Lee, Y. R. *Mol. Diversity* **2015,** *19,* 67–75. doi:10.1007/s11030-014-9557-z
38. Hong, D.; Zhu, Y.; Li, Y.; Lin, X.; Lu, P.; Wang, Y. *Org. Lett.* **2011,** *13,* 4668–4671. doi:10.1021/ol201891r
39. Chaulagain, M. R.; Felten, A. E.; Gilbert, K.; Aron, Z. D. *J. Org. Chem.* **2013,** *78,* 9471–9476. doi:10.1021/jo401015y
40. Wu, Q.; Liu, P.; Pan, Y.-m.; Xu, Y.-l.; Wang, H.-s. *RSC Adv.* **2012,** *2,* 10167–10170. doi:10.1039/c2ra21106h
41. Liu, L.; Bai, S.-H.; Li, Y.; Ding, X.-D.; Liu, Q.; Li, J. *Adv. Synth. Catal.* **2018,** *360,* 1617–1621. doi:10.1002/adsc.201701580
42. Li, Y.; Li, Y.; Fei, H.; Kong, R.; Yu, Z.; He, L. *J. Chem. Res.* **2022,** *46,* 1–8. doi:10.1177/17475198211063799
43. Kumar, G. S.; Ragini, S. P.; Kumar, A. S.; Meshram, H. M. *RSC Adv.* **2015,** *5,* 51576–51580. doi:10.1039/c5ra09025c
44. Singh, D.; Sharma, S.; Thakur, R. K.; Vaishali; Nain, S.; Jyoti; Malakar, C. C.; Singh, V. *Tetrahedron* **2024,** *152,* 133809. doi:10.1016/j.tet.2023.133809
45. Cai, B.-G.; Li, Q.; Xuan, J. *Green Synth. Catal.* **2024,** *5,* 191–194. doi:10.1016/j.gresc.2023.01.007
46. Zeleke, T. Y.; Turhan, K.; Turgut, Z. *Am. Chem. Sci. J.* **2016,** *13,* 1–8. doi:10.9734/acsj/2016/24655
47. Perumal, M.; Sengodu, P.; Venkatesan, S.; Srinivasan, R.; Paramsivam, M. *ChemistrySelect* **2017,** *2,* 5068–5072. doi:10.1002/slct.201700170
48. Majumdar, K. C.; Nirupam, D.; Ghosh, D.; Ponra, S.; Roy, B. *Synthesis* **2012,** *44,* 87–92. doi:10.1055/s-0031-1289608
49. Patel, R. V.; Patel, J. K.; Nile, S. H.; Park, S. W. *Arch. Pharm. (Weinheim, Ger.)* **2013,** *346,* 221–231. doi:10.1002/ardp.201200383
50. Damavandi, S.; Sandaroos, R.; Mohammadi, A. *Heterocycl. Commun.* **2013,** *19,* 105–108. doi:10.1515/hc-2011-0086
51. Parthasarathy, K.; Praveen, C.; Balachandran, C.; Senthil kumar, P.; Ignacimuthu, S.; Perumal, P. T. *Bioorg. Med. Chem. Lett.* **2013,** *23,* 2708–2713. doi:10.1016/j.bmcl.2013.02.086
52. Yadav, J. S.; Subba Reddy, B. V.; Madhusudhan Reddy, G.; Rehana Anjum, S. *Tetrahedron Lett.* **2009,** *50,* 6029–6031. doi:10.1016/j.tetlet.2009.08.027
53. Palchak, Z. L.; Nguyen, P. T.; Larsen, C. H. *Beilstein J. Org. Chem.* **2015,** *11,* 1425–1433. doi:10.3762/bjoc.11.154

License and Terms

BEILSTEIN JOURNAL OF ORGANIC CHEMISTRY

Recent advances in electrochemical copper catalysis for modern organic synthesis

Yemin Kim and Won Jun Jang*

Review

Open Access

Address:
Department of Chemistry and Nanoscience, Ewha Womans University, Seoul, 03760, Korea

Email:
Won Jun Jang* - wonjunjang@ewha.ac.kr

* Corresponding author

Keywords:
copper; electrochemistry; radical chemistry; single-electron transfer; sustainable catalysis

Beilstein J. Org. Chem. **2025,** *21,* 155–178.
https://doi.org/10.3762/bjoc.21.9

Received: 23 October 2024
Accepted: 23 December 2024
Published: 16 January 2025

This article is part of the thematic issue "Copper catalysis: a constantly evolving field".

Guest Editor: J. Yun

Abstract

In recent decades, organic electrosynthesis has emerged as a practical, sustainable, and efficient approach that facilitates valuable transformations in synthetic chemistry. Combining electrochemistry with transition-metal catalysis is a promising and rapidly growing methodology for effectively forming challenging C–C and C–heteroatom bonds in complex molecules in a sustainable manner. In this review, we summarize the recent advances in the combination of electrochemistry and copper catalysis for various organic transformations.

Introduction

Transition-metal-catalyzed cross-coupling has emerged as an effective method for forming carbon–carbon (C–C) and carbon–heteroatom (C–X, where X = N, O, or halogens) bonds in organic synthesis. Copper was one of the first transition metals employed in cross-coupling to form C–C and C–X bonds [1,2]. In 1901, Ullmann reported the first cross-coupling reaction for the formation of biaryl compounds in the presence of stoichiometric quantities of a copper reagent [3]. This pioneering work, known as the "classical Ullmann reaction", was extended by Ullmann and Goldberg to enable the C–N and C–O bond formation [4-6]. Subsequently, key developments in Cu-catalyzed cross-coupling reactions were achieved, including the Rosenmund–von Braun reaction [7], Hurtley's coupling [8], and the Cadiot–Chodkiewicz reaction [9]. However, these classical reactions often restrict the substrate scope and functional group compatibility due to the harsh conditions required, such as strong bases, high temperatures, and stoichiometric amounts of copper reagents. Consequently, investigation into more practical and sustainable reactions remains an area of ongoing research [10].

Conventional cross-coupling reactions typically require C(sp^2)-based electrophiles and nucleophiles as coupling partners. Generally, the reaction is initiated through oxidative addition, fol-

lowed by transmetalation and reductive elimination, to obtain the desired product. Throughout the catalytic cycle, the catalyst undergoes conversion between $[M]^n$ and $[M]^{n+2}$ (Figure 1) [11]. However, using alkyl electrophiles as coupling partners in cross-coupling reactions remains a significant challenge owing to the high energy barrier required for oxidative addition and facile β-hydride elimination [12]. The development of radical approaches facilitated by transition-metal catalysis has provided a promising solution to overcome the limitations of conventional coupling reactions, particularly in controlling the high reactivity and selectivity of radical intermediates [13,14]. Early studies on copper-mediated radical reactions, such as Julia's work on radical cyclization reaction [15], along with advancements in dimerization [16,17], oxidative cleavage [18,19], and olefin addition reactions [20] conducted by various research groups, contributed to this area of research. Recently, the coupling reactions of $C(sp^3)$-based electrophiles were explored using dual photoredox and copper catalysis, achieving selective radical coupling reactions involving alkyl halides [21-24]. Moreover, copper-catalyzed asymmetric radical cross-coupling has advanced significantly over the past decade [25-27], with notable examples including Liu and Stahl's enantioselective cyanation of benzylic C–H bonds using a Cu/chiral bisoxazoline catalyst [28], along with the Peters' and Fu's asymmetric C–N bond cross-coupling reactions by merging photoredox catalysis with copper catalysis [29,30].

Building on the success of photoredox catalysis, electrochemistry has emerged as a complementary and attractive strategy for promoting sustainability of organic synthesis. By offering viable alternatives to conventional chemical oxidizing and reducing agents [31], electrochemical reactions not only enable substrates to undergo single-electron transfer at the cathode or anode, either directly or indirectly, generating highly reactive radical intermediates, but also allow direct electron transfer to the metal catalyst without the need for chemical redox agents, thus providing milder and more sustainable reaction conditions (Figure 2) [32]. Electrochemical reactions can be performed at low potentials, thereby suppressing side reactions, and chemoselectivity and reactivity can be achieved by precisely controlling the potential. Additionally, the merging of electrochemistry and transition-metal catalysis offers advantages in controlling substrate activation, intermediate reactivity, and bond formation, as well as facilitating asymmetric transformations. As a result, electrochemical reactions have become valuable tools in modern synthetic chemistry. Over the past 15 years (since ca. 2010), synthetic organic electrochemistry has undergone remarkable growth, enabling the development of new types of reactions [33].

Numerous review articles have been published [32-38], however, no comprehensive review focusing on Cu-catalyzed electrochemistry has been reported to date. Copper catalysts are potential candidates for pharmaceutical applications owing to their abundance, low cost, and lower toxicity compared with noble transition metals such as palladium [39]. In terms of sustainable chemistry, the combination of copper catalysis and electrochemistry is particularly attractive for overcoming challenges associated with conventional methods, and it has led to extensive research in recent years.

In this review, we highlight the unique contributions of electrochemical copper catalysis to organic synthesis, focusing on recent developments in Cu-catalyzed electrochemical reaction categorized into four types: 1) C–H functionalization, 2) olefin addition, 3) decarboxylative functionalization, and 4) coupling

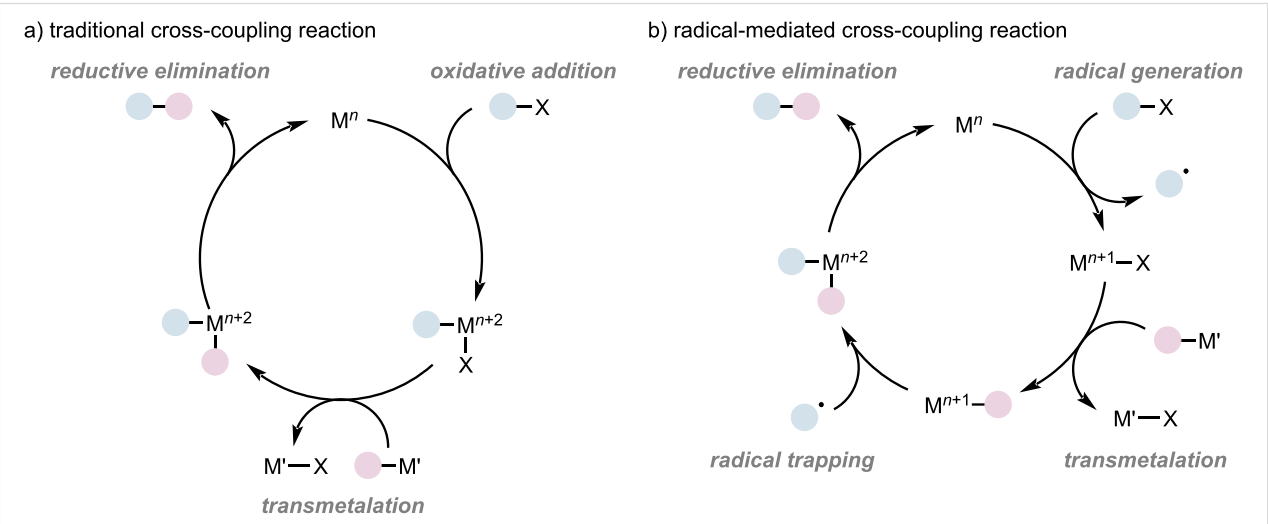

Figure 1: General mechanisms of traditional and radical-mediated cross-coupling reactions.

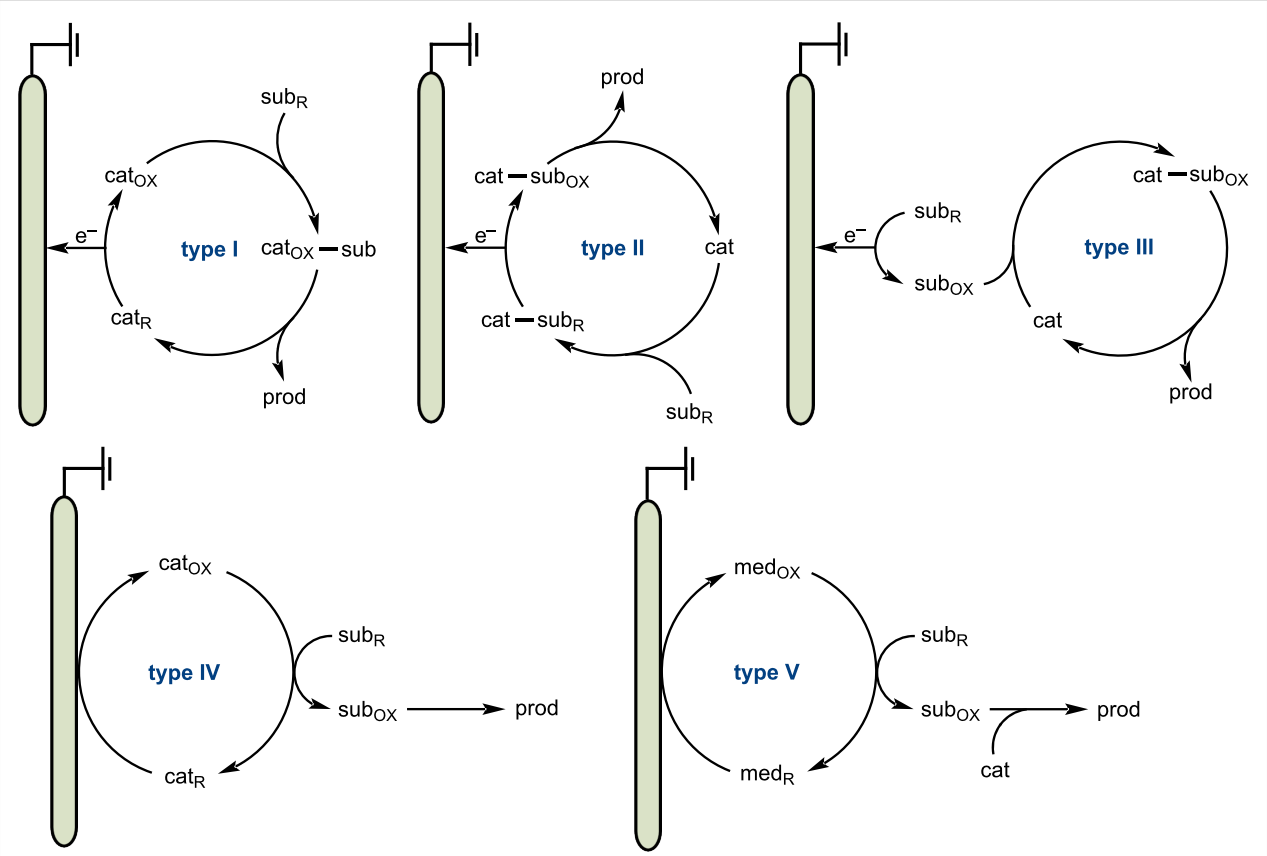

Figure 2: Types of electrocatalysis (using anodic oxidation).

reactions (Figure 3). This review aims to provide insight into the potential of copper-based electrochemical methodologies while also inspiring future research in this rapidly growing field.

Review

C–H Functionalization

Site- and chemoselective C–H functionalization has emerged as a powerful platform for the formation of new C–C and C–heteroatom bonds, offering an efficient and economical approach for molecular synthesis [40]. This strategy has been widely applied in synthetic chemistry, the pharmaceutical industry, and materials science. Over the past few decades, transition-metal-catalyzed C–H activation reactions have been widely developed. Late-stage C–H functionalization of highly complex and diverse molecules, such as those of pharmaceuticals and natural products, has provided new retrosynthetic disconnections for complex compounds, contributing to improved resource efficiency [41-46]. Recently, the merging of C–H activation and electrochemistry has emerged as a potential synthetic tool for the formation of new C–C, and C–heteroatom bonds using electricity to replace the stoichiometric amounts of conventional chemical redox reagents [47].

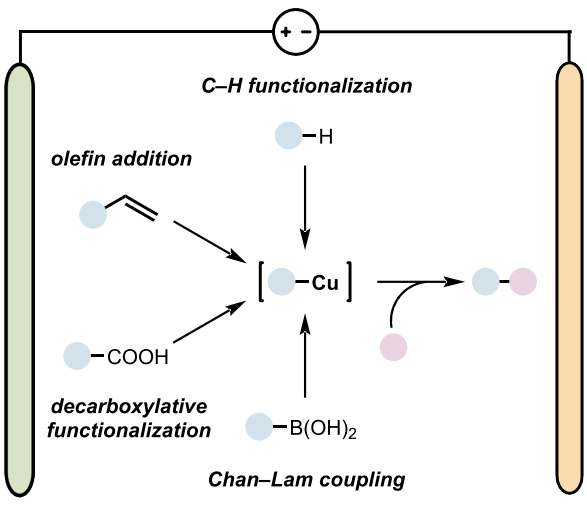

Figure 3: Recent developments and features of electrochemical copper catalysis.

C–C Bond formation

In 2019, the Ackermann group established a synthetic method for isoindolones using a Cu-catalyzed electrochemical C–H activation strategy through C–H alkynylation of arylamides followed by electrooxidative cascade annulation (Figure 4) [48]. This reaction enables sustainable C–H functionalization by utilizing electricity as the terminal oxidant instead of stoichiometric amounts of toxic chemical oxidants and releasing hydrogen gas as the sole byproduct. Various benzamides **1** and terminal arylalkynes **2** bearing electron-rich or electron-withdrawing groups provided the desired products **3** with high chemoselectivities. However, terminal alkynes with alkyl substituents did not yield the desired annulation products. Moreover, the same products were generated using alkynyl carboxylic acids instead of terminal alkynes via decarboxylative C–H alkynylation and annulation.

Cyclic voltammetry (CV) studies exhibited an oxidative current at 0.95 V vs SCE in the presence of the Cu(II) salt, base, and benzamide, however, no relevant competitive oxidation peak was observed with only $Cu(OAc)_2$. These results indicate that Cu(II) intermediate **5** was generated. Based on the mechanistic

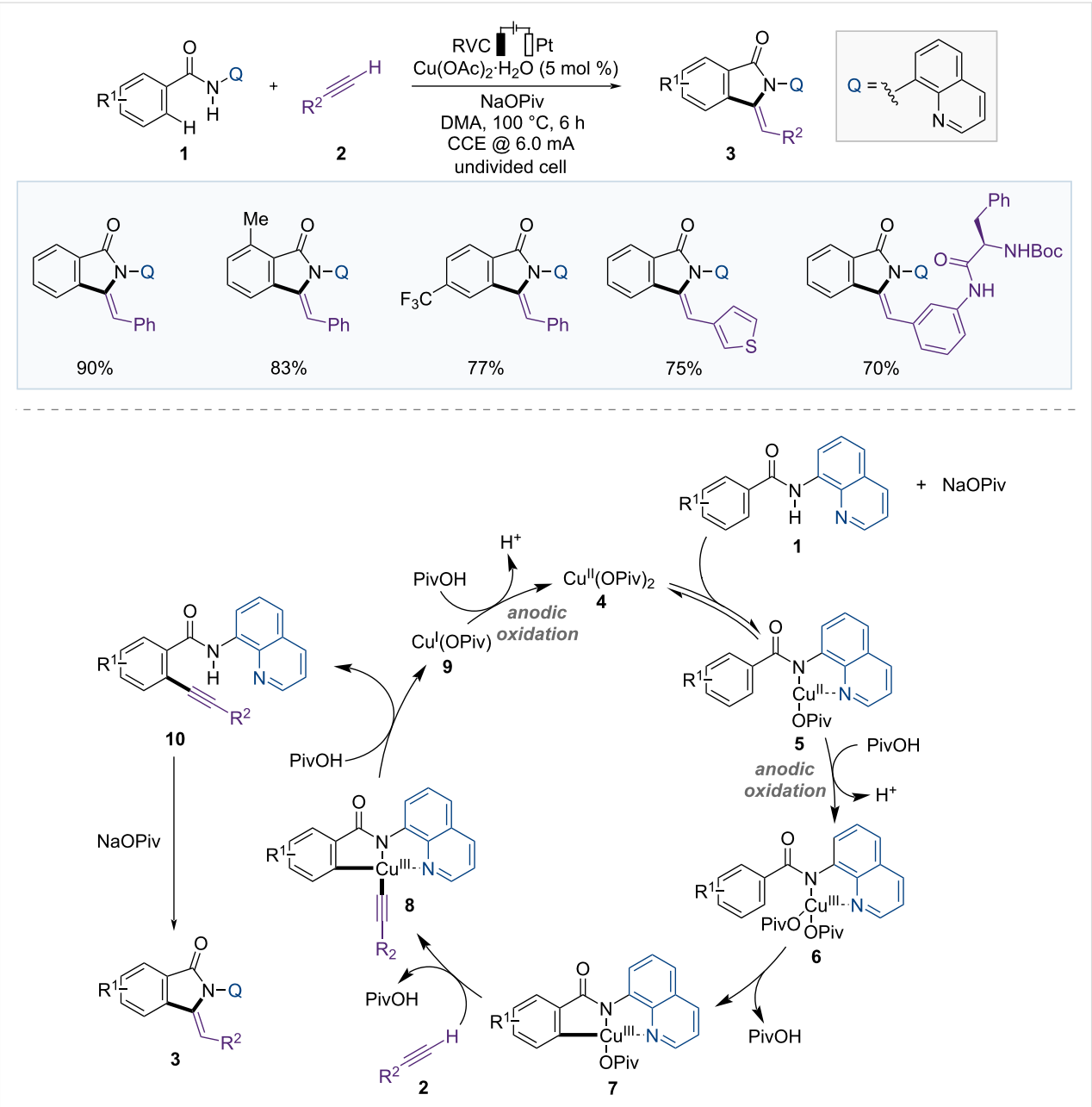

Figure 4: Scheme and proposed mechanism for Cu-catalyzed alkynylation and annulation of benzamide.

studies, the authors suggested plausible reaction mechanisms (Figure 4). First, the Cu(II) catalyst coordinates with substrate **1** in the presence of a base to form Cu(II) complex **5**, which undergoes anodic oxidation to generate Cu(III) intermediate **6**. Carboxylate-assisted C–H activation of the benzamide subsequently leads to the formation of Cu(III) species **7**. Metalation of the terminal alkyne **2**, followed by reductive elimination, produces C–H alkynylated arene **10**, which then forms the final product **3** through intramolecular cyclization. Finally, the Cu(I) complex **9** produced via reductive elimination is reoxidized at the anode to regenerate the Cu(II) complex **4**, completing the catalytic cycle.

Yao and Shi developed the enantioselective C–H alkynylation of ferrocene carboxamides with terminal alkynes by using Cu/BINOL and an electrocatalytic system (Figure 5) [49]. 8-Aminoquinoline-assisted C–H functionalization provided planar chiral ferrocenes with high yield and enantioselectivity. This reaction can be applied to a wide range of substrates, including arylacetylenes with electron-donating and electron-withdrawing groups, and ferrocenyl amides with alkyl and acyl substituents on the other Cp ring. Additionally, the reaction showed similar reactivity and enantioselectivity on a 1 mmol scale.

In 2020, Mei et al. reported the asymmetric C(sp^3)–H alkynylation of tertiary cyclic amines by merging Cu(II)/TEMPO catalysis with electrochemistry to yield chiral C1-alkynylated tetrahydroisoquinolines (THIQs) (Figure 5) [50]. As a co-catalytic redox mediator, TEMPO plays an essential role in the formation of iminium intermediate **15** and in decreasing the oxidation potential. A range of functional groups, such as halides, ethers, and heterocycles, were tolerated well, yielding the corresponding enantioenriched products **14** with high enantioselectivity in the presence of chiral bisoxazoline ligand **L2**.

A possible mechanism is depicted in Figure 5. First, TEMPO is converted to $TEMPO^+$ through anodic oxidation, and iminium intermediate **15** is created through hydride transfer from THIQ (**13**) to $TEMPO^+$. TEMPO–H, generated during the hydrogen transfer step, then returns to $TEMPO^+$ through anodic oxidation. Chiral acetylide species **17** is produced from the terminal alkyne **2** in the presence of a chiral copper catalyst and base, which reacts with the electrophilic iminium intermediate **15** to yield the desired chiral product **14**. Active Cu(I) is regenerated either through cathodic reduction or by reaction with TEMPO–H.

A year after the Mei group's report, the Xu group developed the electrocatalytic racemic C(sp^3)–H alkynylation of THIQs with terminal alkynes in a continuous-flow microreactor using copper/TEMPO relay catalysis [51]. The electrocatalytic reaction in continuous flow facilitates straightforward scale-up and demonstrating a broad substrate scope.

In 2023, the Mei group reported the C(sp^3)–H alkenylation of THIQs with acrolein by a combination of Cu/TEMPO and electrooxidation (Figure 6) [52]. CV experiments demonstrated that TEMPO was a suitable redox mediator, and on/off experiments confirmed that the reaction continued even without electrolysis. THIQ (**13**) was rapidly oxidized to an iminium intermediate under the action of electricity and oxygen. However, when the iminium intermediate was converted to the desired product **19**, electrolysis had no effect, and this step proceeded more gradually than the initial oxidation step. Therefore, the optimized conditions allowed the reaction to proceed under a constant current electrolysis at 1.5 mA for 6 hours, followed by stirring for additional 24 hours with the electricity turned off. These reaction conditions were applicable to various *N*-aryl-THIQ derivatives with various functional groups. Using quinine as a chiral ligand under standard conditions, the chiral product was obtained with a high yield and 79% ee.

Enantioselective C(sp^3)–H functionalization is an attractive strategy for synthesizing chiral molecules. Significant progress has been achieved in transition-metal-catalyzed asymmetric C–H functionalization with directing groups, however, achieving similar results without the assistance of a directing group continues to be a significant challenge [53,54]. Radical-based approaches can facilitate C(sp^3)–H functionalization without directing groups, however, controlling the selectivity is difficult. In 2022, Xu and co-workers established a site- and enantioselective cyanation of benzylic C(sp^3)–H bonds using an electro-photochemical strategy (Figure 7) [55]. The reaction conditions show a broad substrate tolerance, and the late-stage functionalization of complex molecules derived from natural products and drugs has proven to be useful in these reactions.

As shown in Figure 7, the photocatalyst sodium anthraquinone-2,7-disulfonate (**AQDS**) is excited by 395 nm light to form **AQDS*** and undergoes electron transfer with arylalkanes **20** to generate an ion-radical pair (**AQDS**$^{\bullet-}$, **20**$^{\bullet+}$). This ion radical pair (**AQDS**$^{\bullet-}$, **20**$^{\bullet+}$) then generate a benzylic radical **23** and a semiquinone radical (**[AQDS–H]**$^{\bullet}$) through proton transfer. The benzylic radical intermediate **23** subsequently reacts with the chiral copper catalyst **L3**Cu(II)$(CN)_2$ (**25**) to form a Cu(III) complex **26**, which undergoes reductive elimination to produce a chiral product **22**. The reduced copper catalyst **24** and **[AQDS–H]**$^{\bullet}$ are reoxidized to **L3**Cu(II)$(CN)_2$ (**25**) and **AQDS** at the anode, respectively, completing the catalytic cycle.

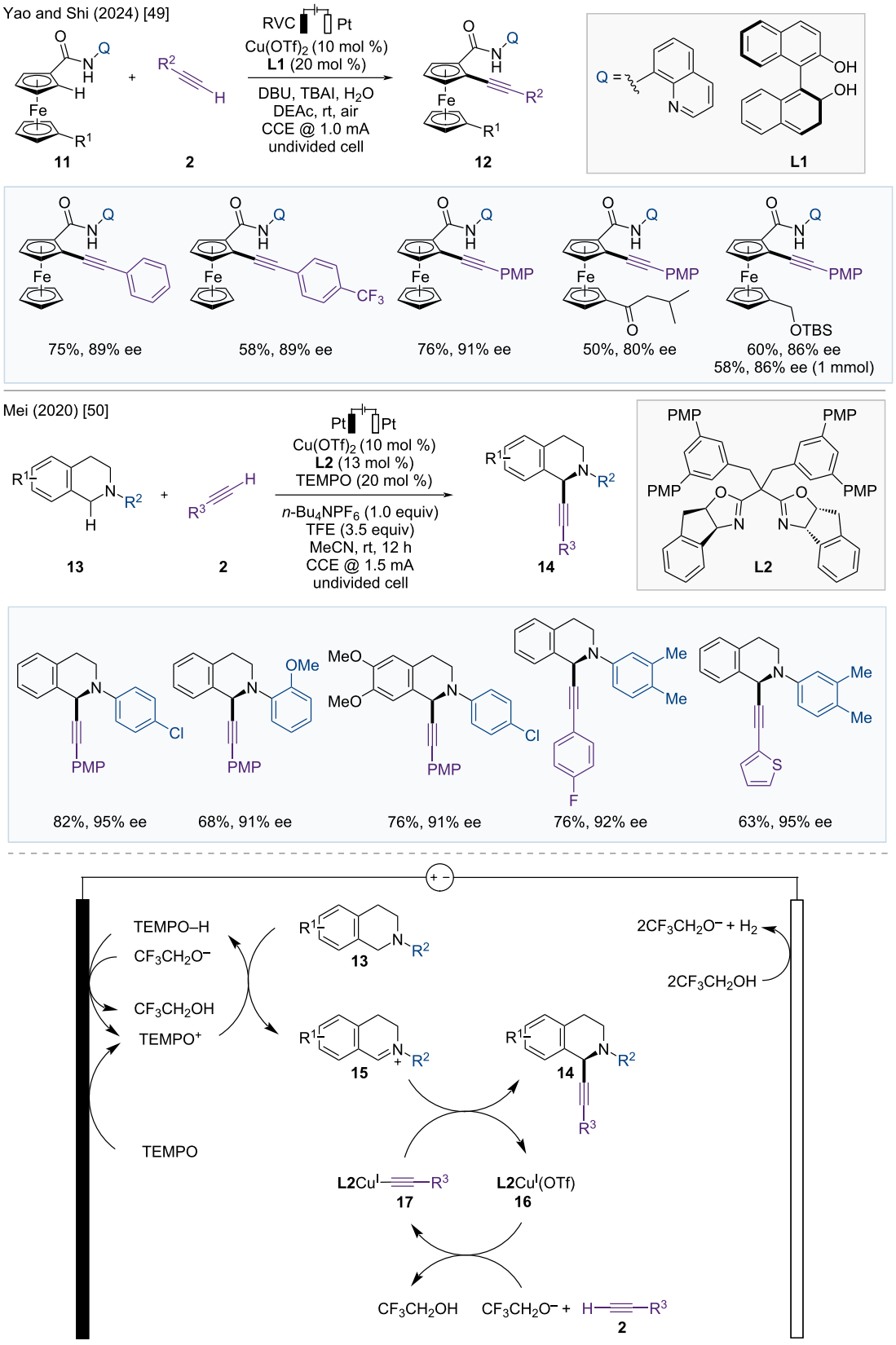

Figure 5: Scheme and proposed mechanism for Cu-catalyzed asymmetric C–H alkynylation.

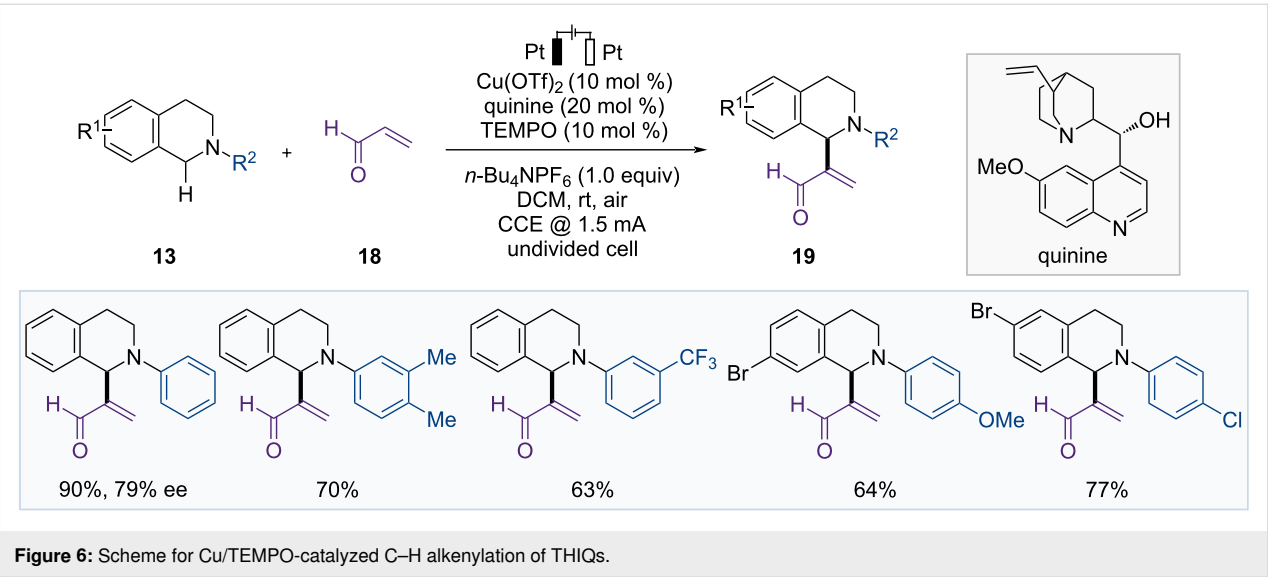

Figure 6: Scheme for Cu/TEMPO-catalyzed C–H alkenylation of THIQs.

In the same year, following a similar approach, the Liu group explored a Cu-catalyzed photoelectrochemical enantioselective cyanation of benzylic C(sp^3)–H bonds (Figure 7) [56]. A wide range of electron-poor and electron-rich alkylarenes **20** are suitable substrates for this electrophotocatalytic radical relay strategy. Additionally, late-stage functionalization of bioactive molecules provides the corresponding chiral cyanation products with high enantioselectivity.

The catalytic cycle is depicted in Figure 7. The photoexcited photocatalyst anthraquinone (**AQ***) acts as a hydrogen-atom transfer (HAT) acceptor and transforms the alkylarene **20** into benzylic radical intermediate **23** together with reduced **[AQ–H]•**. The benzylic radical intermediate **23** is captured by the **L2**Cu(II)$(CN)_2$ complex **25** and then undergoes reductive elimination to provide the chiral nitrile product **22**. Finally, the reduced **[AQ–H]•** and **L2**Cu(I)CN (**24**) are reoxidized at the anode to complete the catalytic cycle.

In 2023, Xu and Lai developed a three-component system for the enantioselective dicarbofunctionalization of olefins, using photoelectrocatalysis with asymmetric copper catalysis (Figure 8) [57]. This asymmetric heteroarylcyanation of arylalkenes **27** via C–H functionalization has a broad substrate scope, including various arylalkenes and heteroarenes, yielding enantioenriched nitrile products **29**.

The proposed mechanism is illustrated in Figure 8. **[Mes-Acr-Ph]$^+$*** is generated through the photoexcitation of the photocatalyst **[Mes-Acr-Ph]$^+$**, which undergoes electron transfer to the heteroarene **28**, resulting in the formation of the **[Mes-Acr-Ph]•** and heteroarene radical cation **30**. The **[Mes-Acr-Ph]•** is regenerated to the ground-state acridinium **[Mes-Acr-Ph]$^+$** through a single oxidation step on the anode, and the heteroarene radical cation **30** then reacts with the arylalkene **27** to form a benzylic radical intermediate **31**. The benzylic radical intermediate **31** is subsequently captured by a chiral Cu(II) complex **25** to generate the Cu(III) complex **32**. Subsequent reductive elimination provides the chiral product **29** and the Cu(I) complex **24**. The catalytic cycle is completed when the Cu(I) complex **24** is reoxidized to the Cu(II) complex **25** through anodic oxidation.

In 2023, Guo and co-workers reported Cu-catalyzed asymmetric electrochemical regiodivergent cross-dehydrogenative coupling of Schiff bases and hydroquinones (Figure 9) [58]. In this approach, a chiral copper complex was used as a Lewis acid catalyst, yielding various synthetic routes for synthesizing chiral amino esters containing a quaternary stereocenter, and the control of regioselectivity depended on the bulkiness of the substrates. Additionally, the electrochemical system served as an internal syringe pump, generating quinone from hydroquinone in situ through anodic oxidation, which enhanced the enantioselectivity. First, the reaction of ketimine ester **33** and 2,3-dimethylhydroquinone at 10 °C provided the chiral 1,4-addition product **35** via dynamic kinetic asymmetric transformation (DyKAT). Conversely, when the reaction was performed at −10 °C, the reaction pathway switched from DyKAT to kinetic resolution (KR) of the racemic ketimine ester, providing the same chiral product **35** with recovered enantioenriched starting material. Additionally, when a 1-naphthyl ester was used instead of a methyl ester at −10 °C, 1,4-addition followed by intramolecular tandem annulation generated the corresponding chiral product **36**. Finally, using 1-naphthyl ester and relatively bulkier 2,6-dimethylhydroqunone as starting materials produced chiral 1,6-addition products **37**.

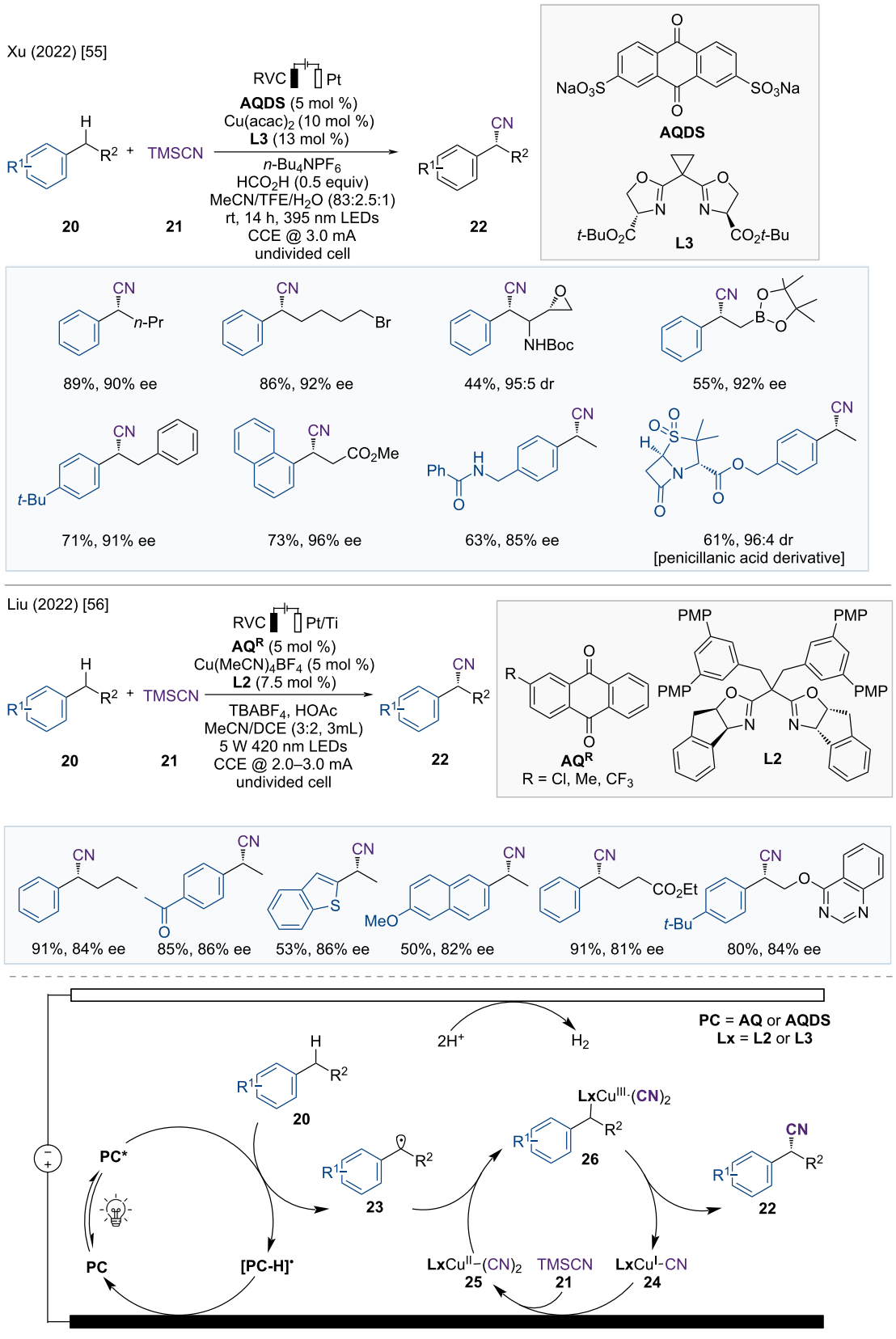

Figure 7: Scheme and proposed mechanism for Cu-catalyzed electrophotochemical enantioselective cyanation of benzylic C(sp^3)–H bonds.

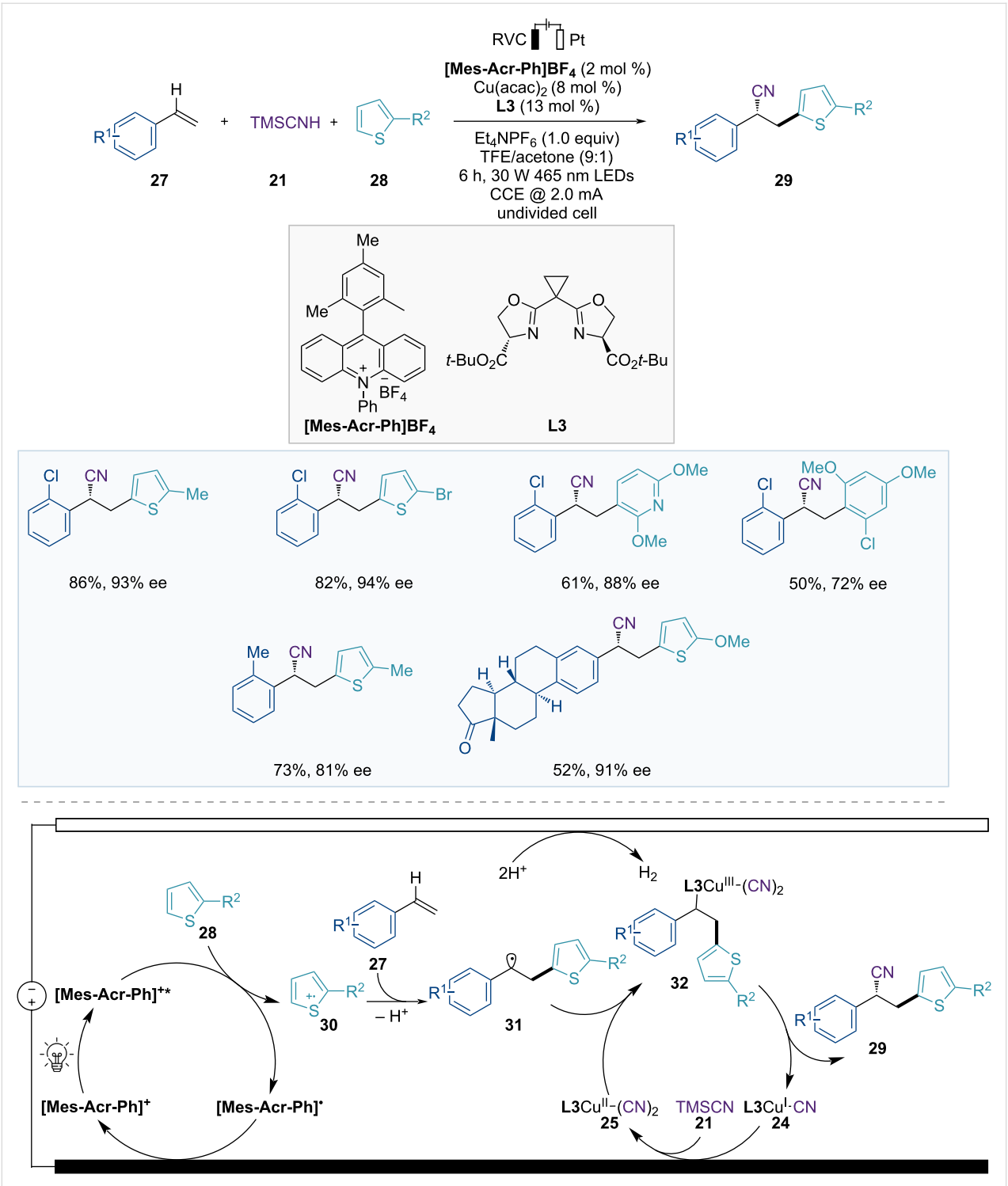

Figure 8: Scheme and proposed mechanism for Cu-catalyzed electrophotochemical asymmetric heteroarylcyanation of alkenes.

In mechanistic studies, using quinone **38** instead of hydroquinone **34** in the electrochemical-free process produced the desired product **36**, with a similar yield but a significantly lower ee (48%) than that obtained under standard electrochemical conditions. By contrast, when quinone was added gradually over 4.5 h using a syringe pump, the desired product **36** was obtained with a similar yield and enantioselectivity. This result corresponded to that of a standard Cu-catalyzed electrochemical protocol. Based on mechanistic studies, the proposed mechanism is shown in Figure 9. First, hydroquinone **34** is oxidized

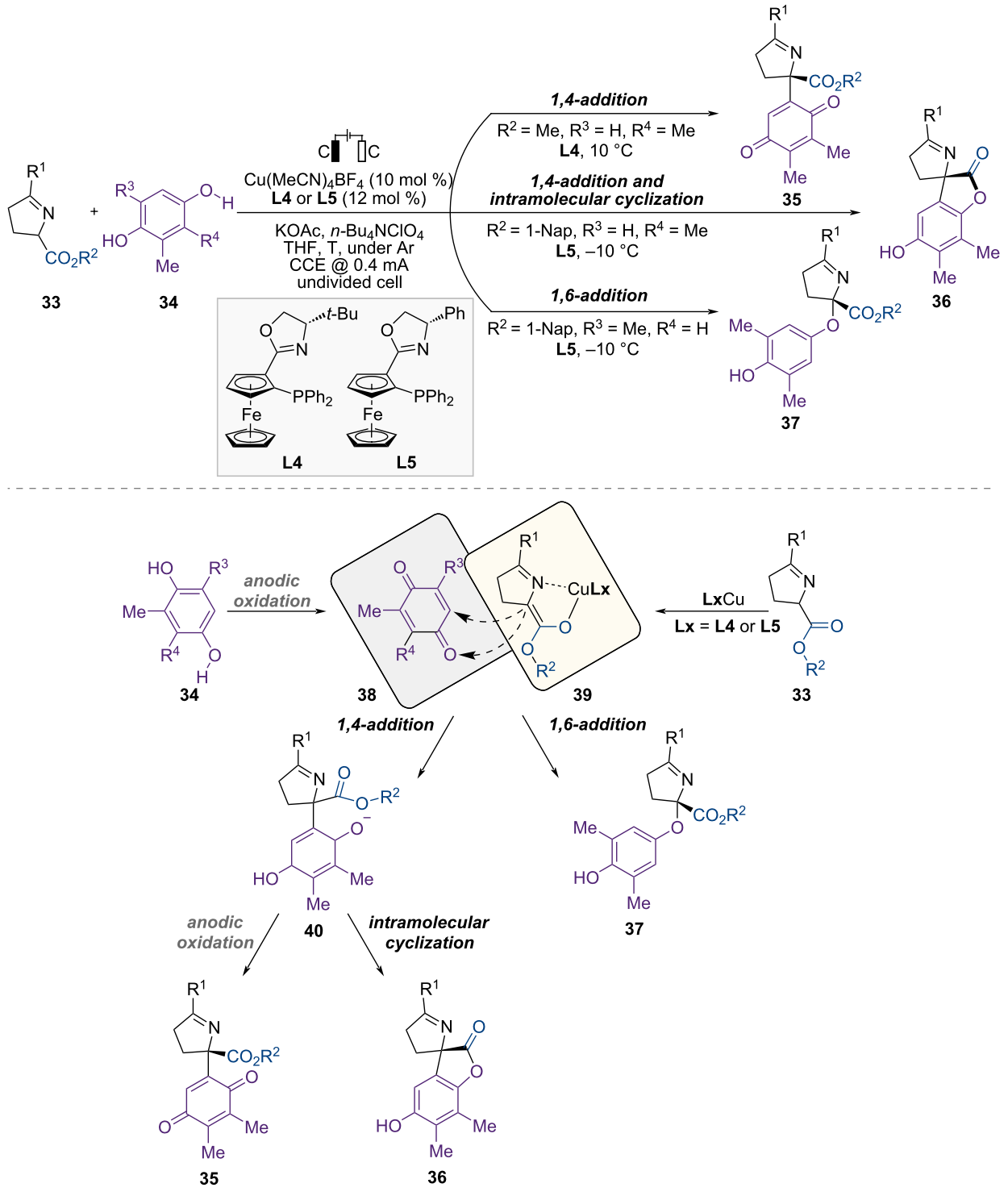

Figure 9: Scheme and proposed mechanism for Cu-catalyzed enantioselective regiodivergent cross-dehydrogenative coupling of Schiff bases with hydroquinones.

at the anode to generate a quinone intermediate **38**. Meanwhile, the chiral copper catalyst reacts with the Schiff base **33**, generating a nucleophilic copper-coordinated azomethine ylide **39**. Subsequently, the chiral products **35**–**37** are produced through the reaction between the metalated azomethine ylide **39** and the quinone intermediate **38**. The reaction pathway, either 1,4-addi-

tion or 1,6-addition, depends on the structure of the hydroquinone **34**. The less sterically hindered hydroquinone promotes 1,4-addition, resulting in the formation of an α-arylated intermediate **40**, and different products are generated depending on the substituents on the Schiff base. For example, a methyl-substituted Schiff base provided a chiral quinone **35** after 1,4-addition and electrochemical oxidation. In contrast, the naphthyl-substituted Schiff base generated the corresponding enantioenriched product **36** through 1,4-addition followed by intramolecular annulation. When 2,6-disubstituted hydroquinone was used as the starting material, 1,6-addition occurred due to steric hindrance, yielding an α-aryloxylation product **37**.

After their investigation of Cu-catalyzed electrochemical reactions, the same group further developed synergistic Cu/Ni catalysis for the stereodivergent electrooxidation of benzoxazolyl acetate (Figure 10) [59].

In this catalytic system, copper and nickel activate identical racemic carbonyl nucleophiles to generate Cu-enolate **44** and Ni-enolate **43** simultaneously (Figure 10). The Ni-enolate **43** undergoes anodic oxidation through single-electron transfer, releasing nickel-bound α-carbonyl radical **45**, whereas the copper complex **44** remains electrochemically inert under standard conditions. Subsequently, radical-polar coupling between electrophilic Ni-bound α-carbonyl radical intermediate **45** and remaining nucleophilic Cu-enolate **44** provides a chiral product **42** containing vicinal quaternary stereocenters with high stereoselectivity, and all three possible stereoisomers of the product are accessible by adjusting the two distinct chiral catalysts.

C–N Bond formation

In 2018, Mei et al. developed the electrochemical C–H amination of arenes with amine electrophiles using copper catalysis, which provided a step-economical approach for the synthesis of aromatic amines by employing electricity as an oxidant (Figure 11) [60].

Mechanistic studies have indicated that *n*-Bu_4NI acts as a redox mediator at the anode, and the electron transfer between the copper complex and the iodine radical is the rate-determining step. The author proposed a catalytic cycle, as illustrated in Figure 11. Initially, the Cu(II) catalyst **50** coordinates with substrate **47** and amine electrophile **48** to generate Cu(II) intermediate **51**, which is then oxidized by the iodine radical to form Cu(III) complex **52**. Cu(III) complex **52** undergoes electron transfer to produce radical cation intermediate **53**. Subsequent intramolecular amine transfer to the radical cation intermediate **53**, followed by ligand exchange, yields amination product **49** and Cu(I) species **55**. Cu(II) catalyst **50** is regenerated by anodic oxidation, thereby completing the catalytic cycle.

In 2019, Nicholls et al. reported a Cu-catalyzed directed C–H amination of benzamides with secondary amine electrophiles independently (Figure 11) [61].

In 2023, De Sarkar and Baidya reported the Cu-catalyzed electrocatalytic azidation of N-arylenamines, followed by denitrogenative annulation for quinoxaline synthesis (Figure 12) [62]. Only 0.5 mol % $CuCl_2$ catalyst was required, and anodic oxidation was employed instead of stoichiometric chemical oxidants. This cascade strategy is compatible with various substituted *N*-arylenamines **57** that bear electron-withdrawing and electron-donating groups, facilitating the production of quinoxaline scaffolds **59**.

According to the reaction mechanism outlined in Figure 12, the copper catalyst reacts with an azide ion to generate a Cu(II)–N_3 complex **60**, which is then anodically oxidized to the Cu(III)–N_3 complex **61**. The Cu(III)–N_3 complex **61** releases the azidyl radical **62** from the azide ion **58**, returning it to the Cu(II)–N_3 complex **60**. The azidyl radical **62** then reacts with *N*-arylenamine **57** via radical addition. Thereafter, it undergoes oxidation to form a kinetically labile vinyl azide intermediate **64**. This vinyl azide intermediate **64** dissociates, yielding Cu(II) iminyl complex **65** via denitrogenation. Accordingly, the formation of the Cu(II) iminyl complex **65** promotes the electrochemical oxidation of Cu(III) iminyl complex **66**, which then dissociates to generate the iminyl radical **67**. Finally, the iminyl radical delivers the quinoxaline product **59** via radical annulation, followed by rearomatization through oxidation.

C–X Bond formation

Cu-catalyzed electrochemical reactions have been developed for the formation of C–C, C–N, and C–X bonds. For instance, in 2013, the Kakiuchi group reported Cu-catalyzed electrochemical chlorination of 1,3-dicarbonyl compounds (Figure 13) [63]. Typical chlorination reactions are performed using electrophilic chlorinating reagents or stable and readily available chloride sources with stoichiometric amounts of chemical oxidants. However, in this catalytic system, chloride (Cl^-) from HCl was used as the chlorinating agent, and electrophilic chlorine (Cl^+) was generated in situ by the anodic oxidation of chloride ions, thus replacing stoichiometric chemical oxidants. This catalytic electrochemical chlorination method is suitable for β-ketoesters **68** with electron-withdrawing or electron-donating groups on aryl substituents, as well as for β-diketone, and β-ketoamides.

In 2020, Fang, Huang, and Mei et al. explored Cu-catalyzed electrochemical C(sp^2)–H bromination of 8-aminoquinoline amide at the C5 site of quinoline using NH_4Br as a brominating reagent under anoxic oxidation conditions (Figure 13) [64].

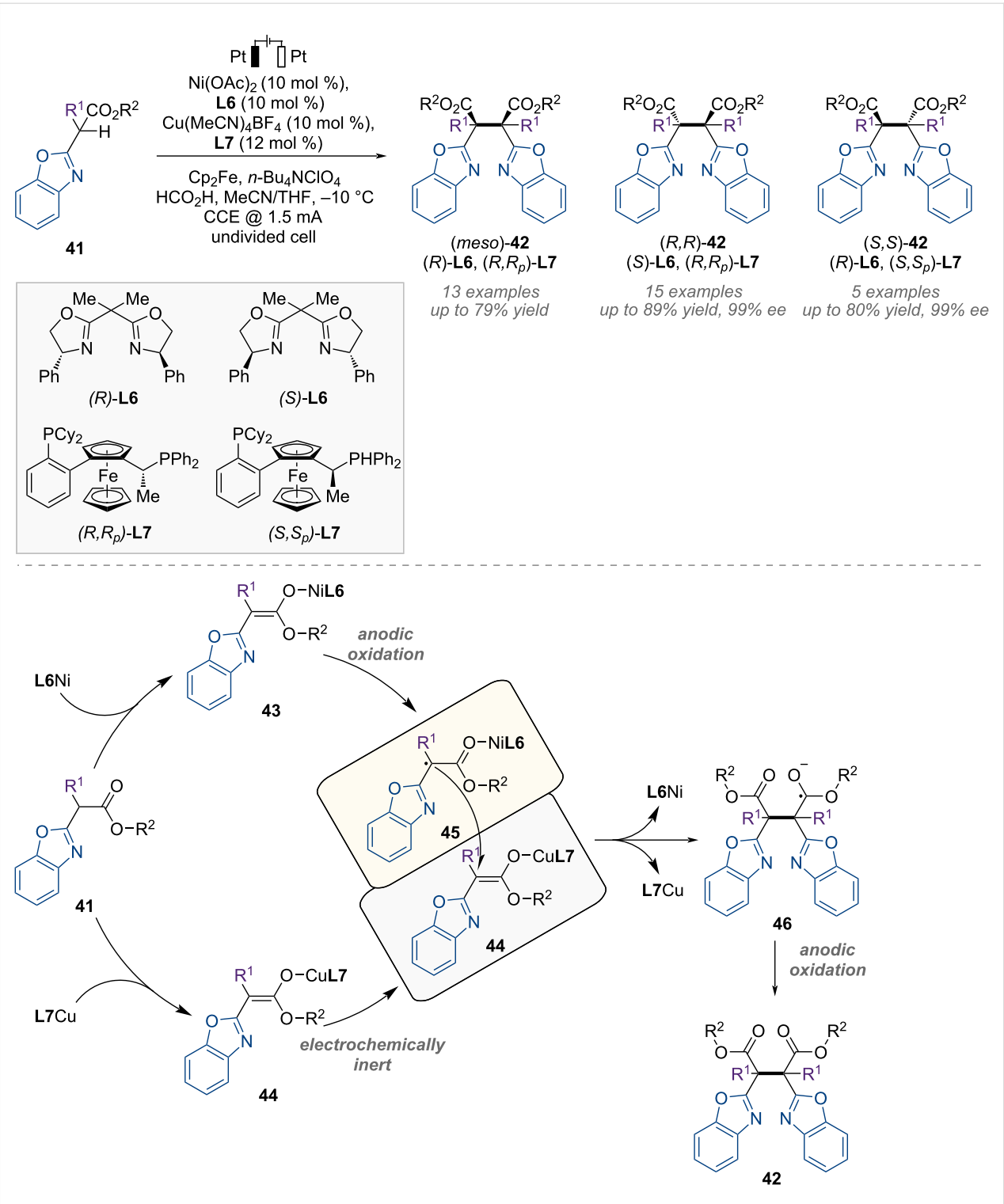

Figure 10: Scheme and proposed mechanism for Cu/Ni-catalyzed stereodivergent homocoupling of benzoxazolyl acetate.

This catalytic reaction has a broad substrate scope, and further investigation of analogous substrates demonstrates that a bidentate nitrogen structure and a free N–H group are essential for this transformation.

The catalytic cycle begins with the coordination of 8-aminoquinoline **71** to Cu(II) catalyst **74**, providing an arylcopper complex **76** (Figure 13). This is followed by a bromine radical attack that leads to the formation of a cationic brominated

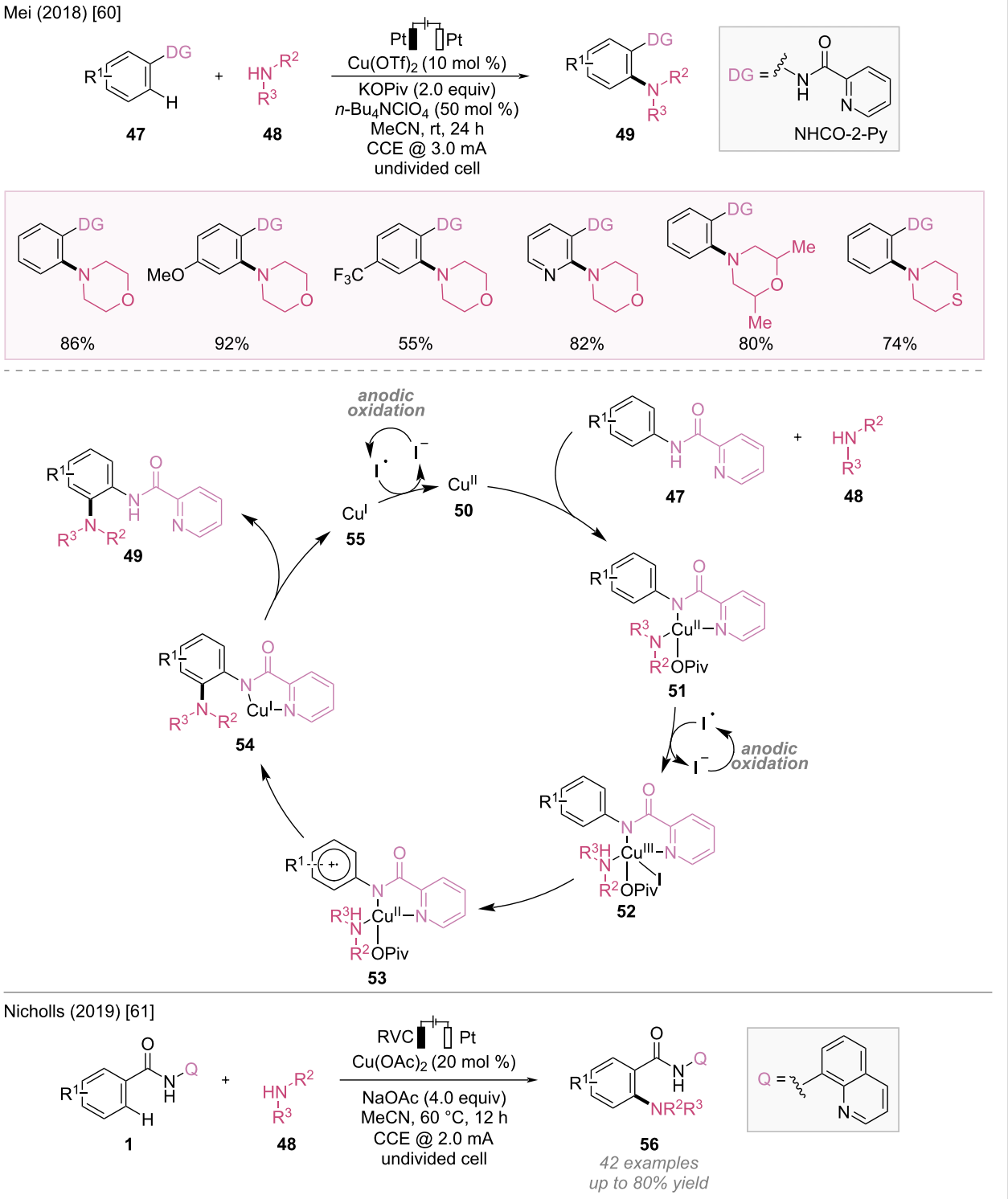

Figure 11: Scheme and proposed mechanism for Cu-catalyzed electrochemical amination.

copper complex **77**. Anodic oxidation and subsequent proton transfer provide the desired product **73** and regenerate the copper catalyst.

Olefin addition

Hydrofunctionalization and difunctionalization of alkenes are valuable methods for synthesizing complex molecules from

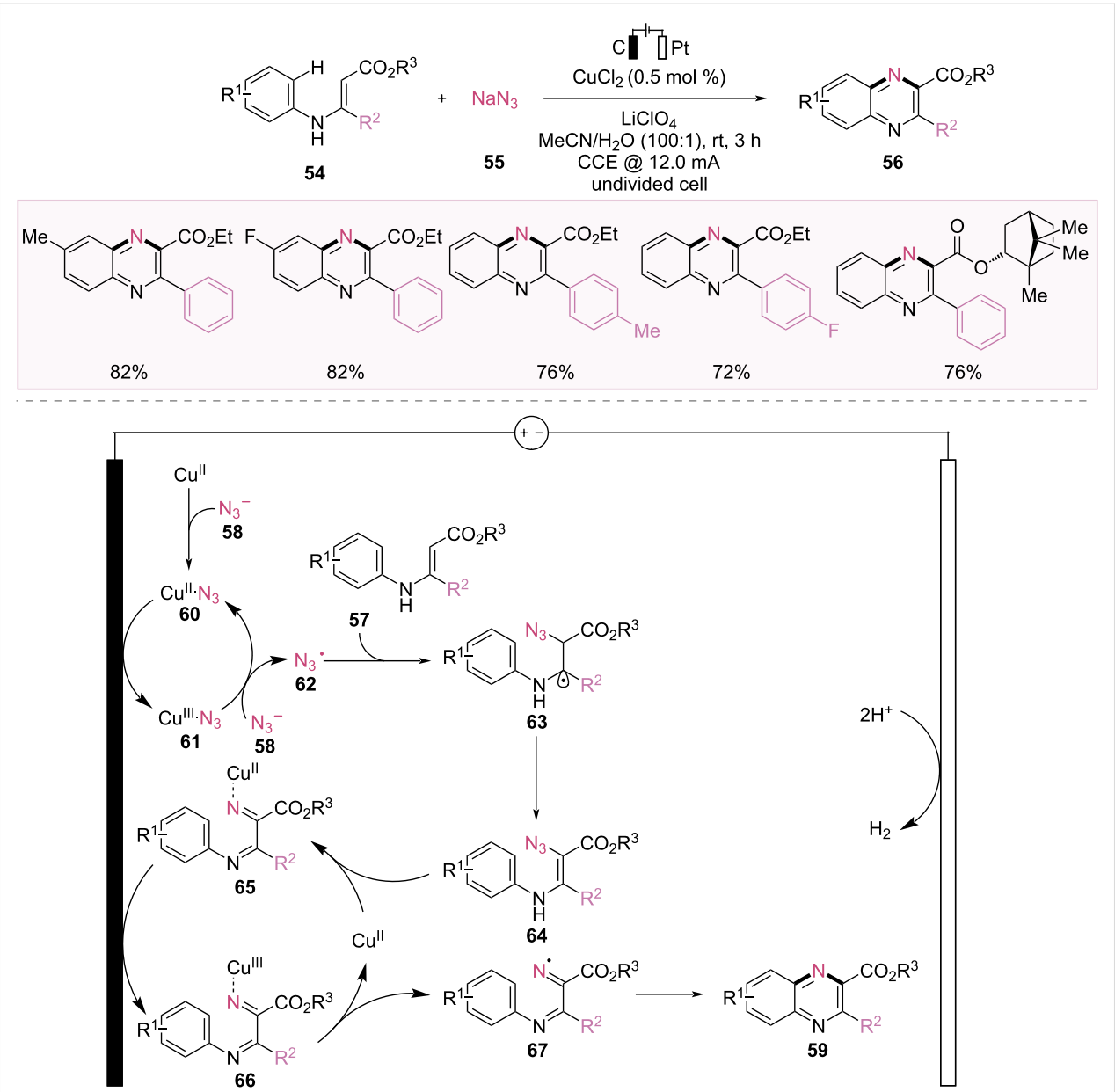

Figure 12: Scheme and proposed mechanism for Cu-catalyzed electrochemical azidation of *N*-arylenamines and annulation.

alkenes, a readily available feedstock [65]. Particularly, transition-metal-catalyzed difunctionalization has recently been extensively investigated, and asymmetric reactions have been developed [66]. Many approaches rely on the addition of a radical species to an alkene to generate a radical intermediate, followed by oxidation, which enables radical-polar crossover (RPC) and the subsequent nucleophilic attack of the cationic intermediate [67]. Alternatively, the initial radical intermediate can be trapped by a transition-metal catalyst, followed by a cross-coupling approach to generate difunctionalization products through reductive elimination. Recently, electrocatalytic difunctionalization has been developed, and dual catalytic systems combining transition-metal catalysis with electrocatalysis have emerged [68].

In 2019, Lin et al. reported the Cu-catalyzed asymmetric electrocatalytic cyanophosphinoylation of vinylarenes (Figure 14) [69]. In the presence of a copper catalyst and the chiral ligand sBOX(iPr) (**L8**) in an electrochemical cell, these three component reactions using styrene derivatives **27**, TMSCN (**21**), and diarylphosphine oxide **80** as starting materials yielded the enantioenriched phosphinoylcyanation products **81** in good yields with high enantioselectivities. Additionally, an appropriate electrolyte ($TBABF_4$) and proton source (TFE) were used

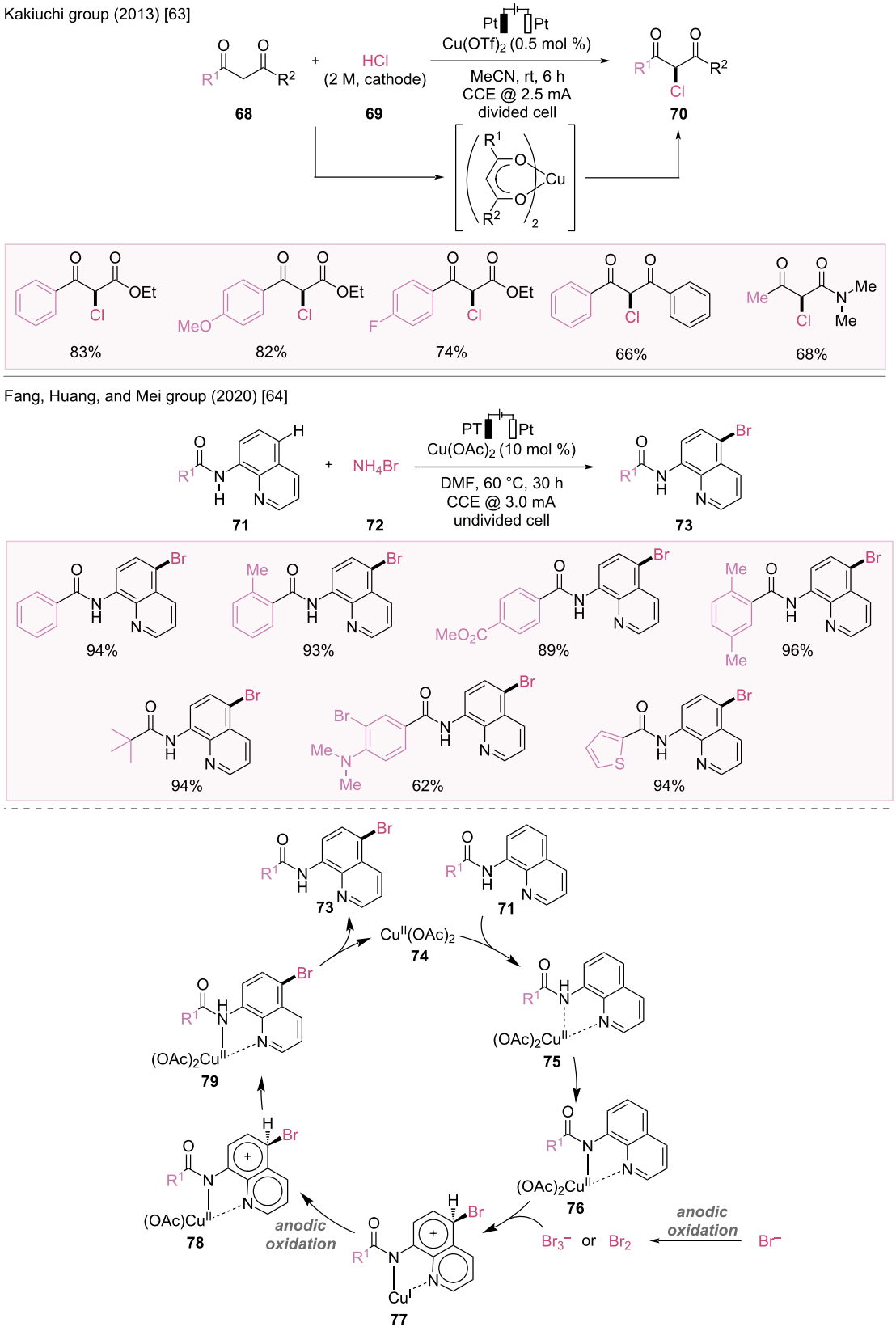

Figure 13: Scheme and proposed mechanism for Cu-catalyzed electrochemical halogenation.

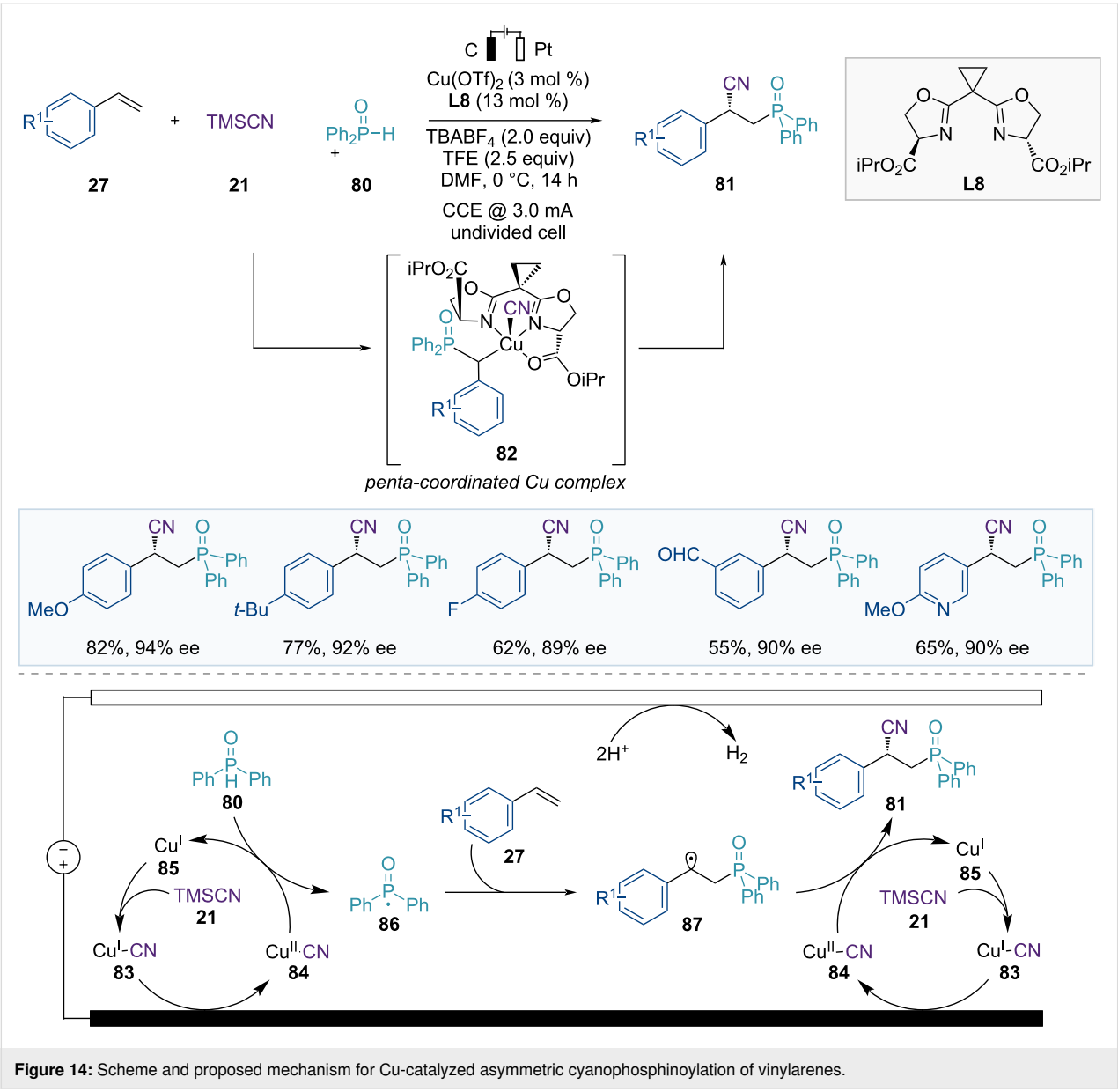

Figure 14: Scheme and proposed mechanism for Cu-catalyzed asymmetric cyanophosphinoylation of vinylarenes.

for this transformation without any conventional chemical oxidants. A key factor in achieving high enantioselectivity is the introduction of serine-derived bisoxazoline ligands **L8** (sBOX). Upon coordination with a copper catalyst, these ligands present second-sphere ester groups, which facilitate the additional stabilization of noncovalent interactions at the penta-coordinated Cu(III) intermediate **82** in the enantio-determining transition states.

Based on the mechanistic studies, a reaction mechanism is proposed in Figure 14. First, the in situ-generated Cu(I)–CN complex **83** is oxidized at the anode to form a Cu(II)–CN complex **84**, which reacts with diarylphosphine oxide **80** to generate a transient P-centered radical **86**. The resulting Cu(I) catalyst **85** is reoxidized at the anode to regenerate the Cu(II)–CN catalyst **84**. The P-centered radical **86** is trapped by the olefin **27** to produce a benzylic radical intermediate **87** that can react with the Cu(II)–CN complex **84** to form an alkyl–Cu(III)–CN intermediate **82**. This intermediate **82** undergoes enantiodetermining reductive elimination to deliver the chiral phosphinoylcyanation products **81** and regenerate the Cu(I) species.

The Lin group developed an electrochemical approach for the asymmetric hydrocyanation of olefins, facilitated by a Cu/Co dual electrocatalytic system (Figure 15) [70]. In this catalytic system, catalytic amounts of Cu(sBOX) (**L3**) and Co(salen) complexes promote the formation of chiral nitriles **89** in the presence of $PhSiH_3$ (**88**) as the hydride source and TMSCN

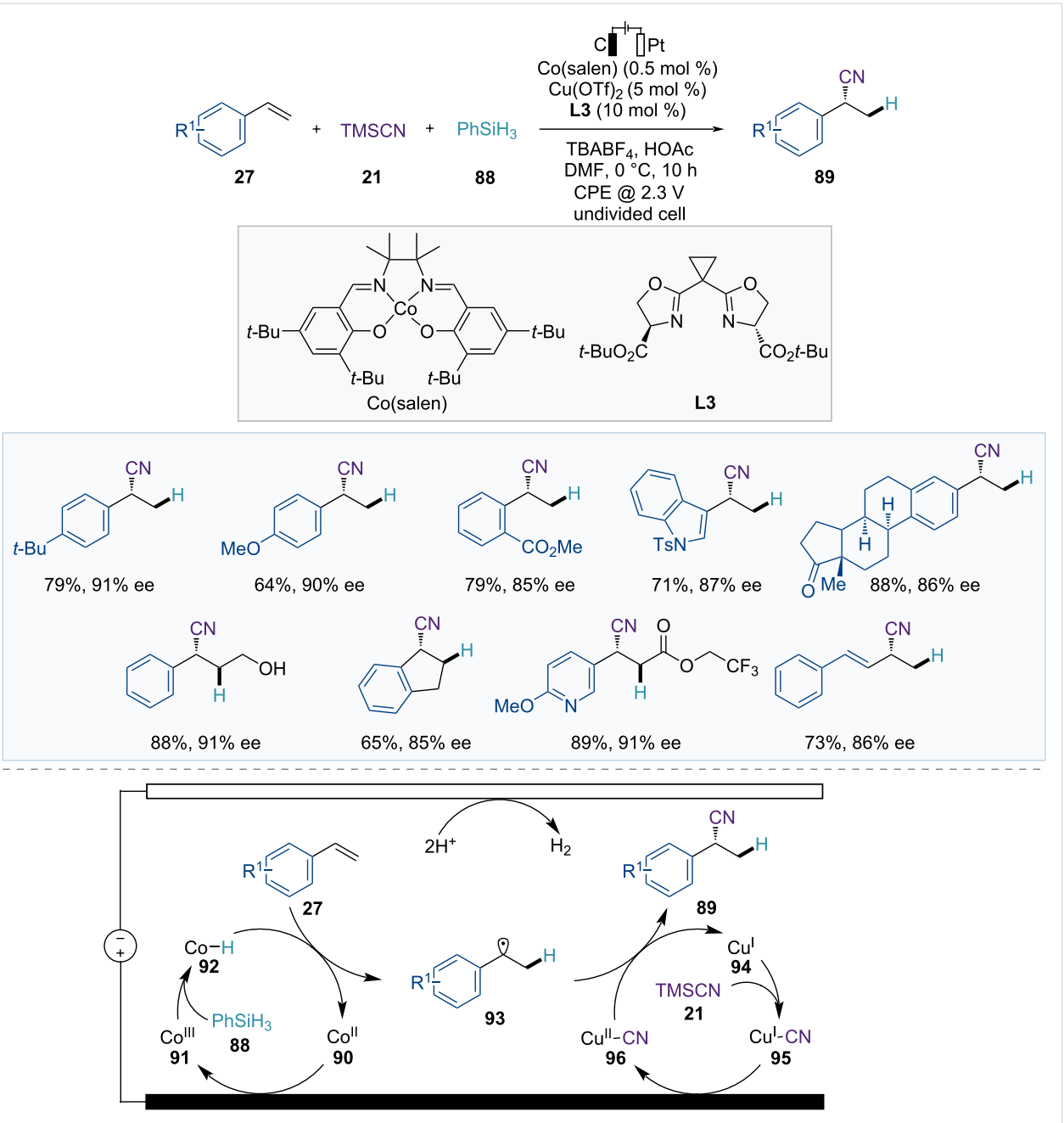

Figure 15: Scheme and proposed mechanism for Cu/Co dual-catalyzed asymmetric hydrocyanation of alkenes.

(**21**) as the cyanide source via the effective sequential addition of a hydrogen atom and a CN group across alkenes **27**. This reaction is applicable not only to a wide range of terminal styrenes but also to internal alkenylarenes, enynes, and allenes, providing enantioenriched products in good yields with high enantioselectivities.

This reaction involves Co-catalyzed HAT and Cu-catalyzed enantioselective radical cyanation. In the proposed catalytic cycle, Co(III)–H species **92** are initially formed from the anodically oxidized Co(III) complex **91** and hydrosilane **88** (Figure 15). Subsequently, the HAT between the Co(III)–H catalyst **92** and the alkene **27** generates a carbon-centered radical species **93** with a newly formed C–H bond. These radical species then enter the second catalytic cycle, facilitating the asymmetric cyanide transfer. The radical species **93** undergo a single oxidative addition to the Cu(II)–CN catalyst **96**, forming a Cu(III) complex. Finally, reductive elimination delivers the enantioenriched nitrile products **89** and a reduced Cu(I) complex **94**, which is reoxidized through anodic oxidation.

The 1,2-diamine moiety is present in numerous natural products and bioactive compounds. In 2022, Xu et al. reported the Cu-catalyzed electrocatalytic diazidation of olefins with ppm-level catalyst loading, providing an alternative strategy for 1,2-diamine synthesis (Figure 16) [71]. This reaction successfully expanded the substrate scope from electron-rich to electron-deficient alkenes, which were considered challenging substrates in previous diazidation reactions.

A possible mechanism is proposed in Figure 16. $Cu(II)(N_3)_2$ (**102**) is generated from $TMSN_3$ (**98**) and $Cu(acac)_2$ in the presence of K_3PO_4; this is followed by anodic oxidation to form a $Cu(III)(N_3)_3$ complex **101**. The resulting $Cu(III)(N_3)_3$ complex **101** releases an azide radical (**103**), and $Cu(II)(N_3)_2$ (**102**). The azide radical (**103**) then reacts with the alkene **97** to produce an alkyl radical **104**, which undergoes ligand transfer from $Cu(II)(N_3)_2$ (**102**) to yield the diazidation product **99** and $Cu(I)(N_3)$ (**100**). The $Cu(I)(N_3)$ (**100**) is reoxidized to $Cu(III)(N_3)_3$ (**101**) on the anode in the presence of N_3^- to complete the catalytic cycle.

In 2024, the Xu group developed a Cu-catalyzed electrochemical azidocyanation of alkenes (Figure 17) [72]. This alkene difunctionalization, using TMSCN (**21**) and $TMSN_3$ (**98**) as starting materials, features oxidant-free conditions, compatibility with both aryl- and alkylalkenes, and a wide functional group tolerance. Moreover, asymmetric transformations are possible when arylalkenes are used as starting materials in the presence of copper and chiral ligand **L3**, yielding the corresponding chiral products.

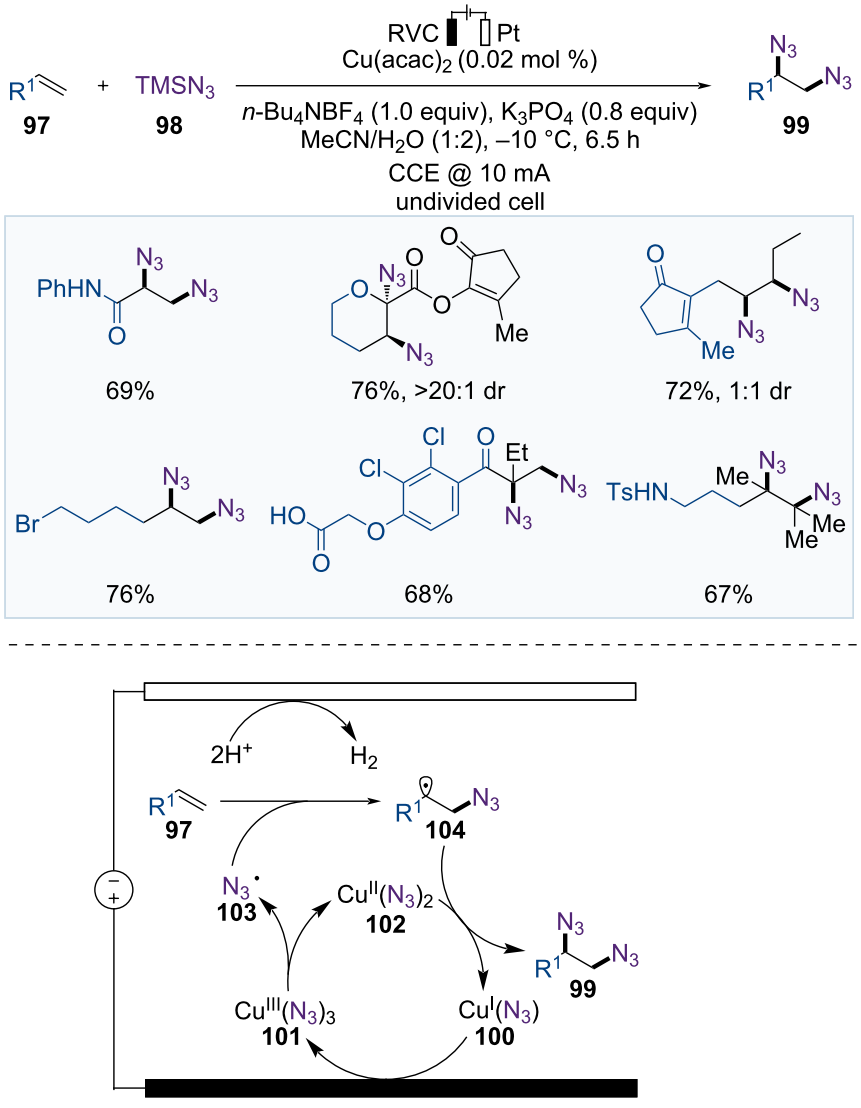

Figure 16: Scheme and proposed mechanism for Cu-catalyzed electrochemical diazidation of olefins.

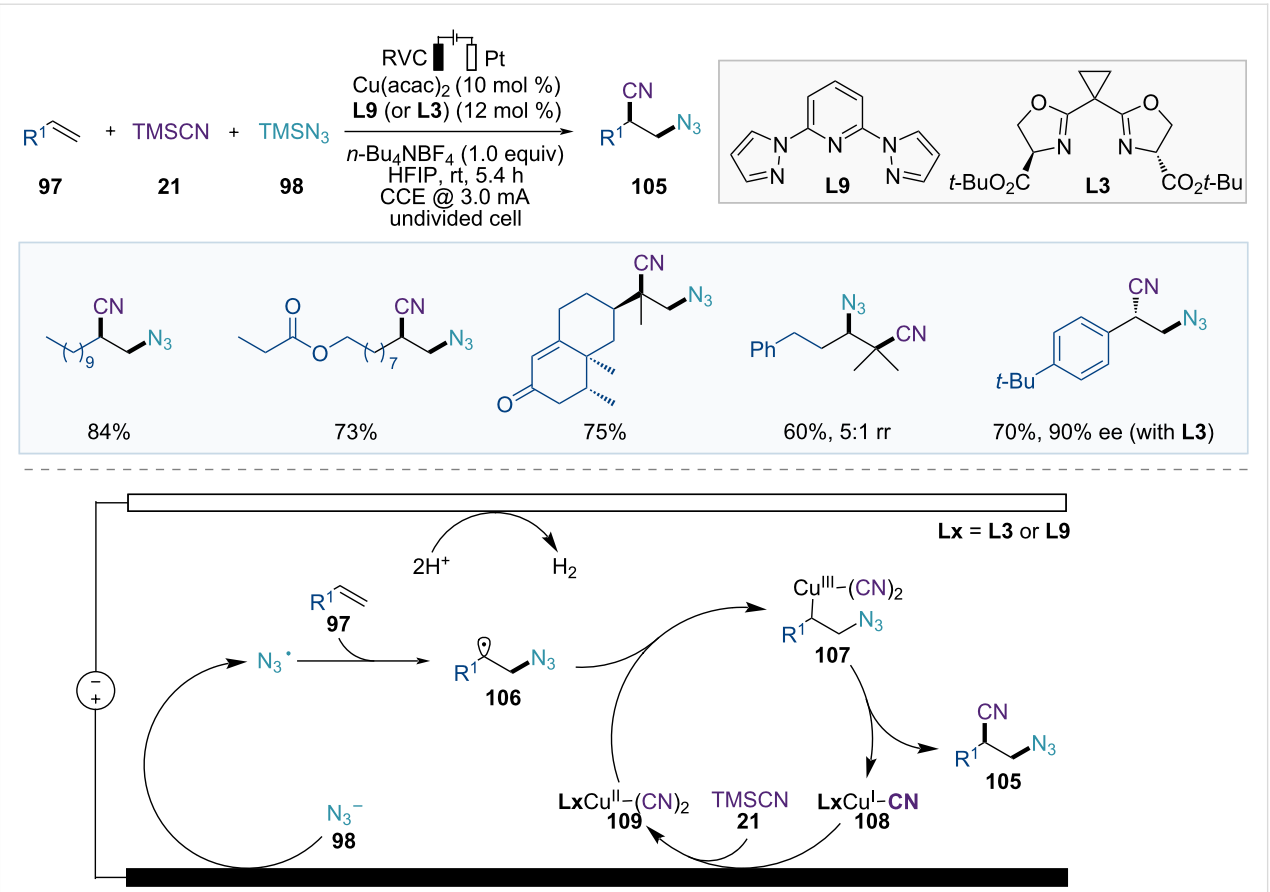

Figure 17: Scheme and proposed mechanism for Cu-catalyzed electrochemical azidocyanation of alkenes.

Based on mechanistic studies, the catalytic cycle begins with anodic oxidation of N_3^- to generate an azide radical, which adds to the alkene **97** to form carbon-centered radical intermediate **106** (Figure 17). The resulting alkyl radical intermediate **106** then reacts with the Cu(II)$(CN)_2$ catalyst **109** to produce a Cu(III) species **107**, which undergoes reductive elimination to deliver the desired product **105** and the Cu(I)CN catalyst **108**. The Cu(II)CN catalyst **109** is regenerated via anodic oxidation to complete its catalytic cycle.

Decarboxylative functionalization

Carboxylic acids are inexpensive, readily available, structurally diverse from both natural and synthetic sources, and easy to handle. Recently, various catalytic transformations of carboxylic acids have been developed, enabling chemists to access a variety of valuable products via diverse reaction pathways [73]. Particularly, decarboxylative cross-coupling of carboxylic acids using radical strategies has emerged as a robust method for the construction of C–C and C–X bonds [74]. Recently, photoelectrochemical asymmetric decarboxylative cyanation was independently established by the groups of Xu, Zhang, and Fu (Figure 18) [75-77]. Each group employed the same Ce/Cu relay catalysis strategy to produce chiral nitrile compounds in high yields and enantioselectivities. Notably, this method does not require prefunctionalization of carboxylic acids or stoichiometric chemical oxidants.

According to their research, Ce(III) salt **112**, which serves as a photocatalyst, is oxidized to a Ce(IV) complex **113** on the anode (Figure 18). The resulting Ce(IV) species **113** coordinates with carboxylic acid and undergoes photoinduced ligand-to-metal charge transfer (LMCT) and regeneration of the Ce(III) species to produce a benzylic radical **115**. The chiral Cu(II) catalyst **117** reacts with benzylic radical **115** to yield Cu(III) intermediate **118**, which then undergoes reductive elimination to provide the desired enantioenriched nitrile product **111** and Cu(I) catalyst **116**. The resulting Cu(I) catalyst **116** is reoxidized to Cu(II) **117** at the anode, completing the catalytic cycle.

Coupling reaction (Chan–Lam coupling)

Transition metal-catalyzed C–N bond formation reactions are essential synthetic methodologies. The discovery of Chan–Lam coupling reactions, which use arylboronic acids and *N*-nucleophiles, provided a C–N bond-forming protocol using copper

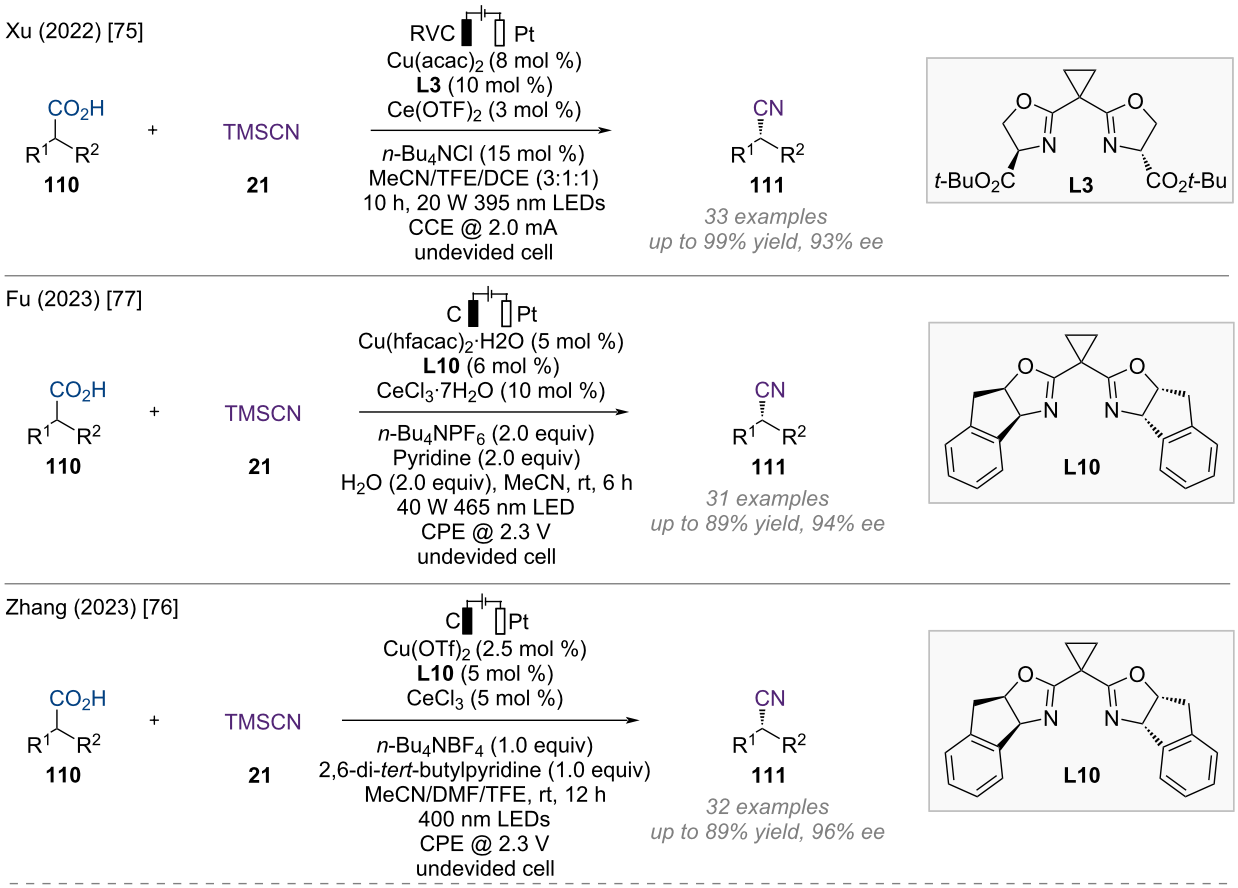

Figure 18: Scheme and proposed mechanism for Cu-catalyzed electrophotochemical asymmetric decarboxylative cyanation.

catalysis, offering a complementary method to noble transition-metal catalysis [78]. Recently, dual-catalytic systems combining copper catalysis with electrocatalysis have been developed to avoid the use of chemical oxidants. Thus, the substrate scope was expanded to include electron-deficient arylboronic acids.

In 2019, Gale-Day et al. developed electrocatalytic Chan–Lam couplings of arylboronic acids with primary anilines using a copper catalyst and dual Cu-electrode system to form C–N bonds (Figure 19) [79]. This catalytic system demonstrates a broad substrate scope, including electron-deficient boronic acids, which are typically regarded as challenging substrates because of their low reactivity in Chan–Lam coupling.

The reaction mechanism is illustrated in Figure 19. During the reaction, the unstable Cu(I) species **121** is reduced to Cu(0) at the cathode and is plated to suppress side reactions. After 10 minutes, when the current is inverted, the copper that previously precipitated as an impure film is reoxidized to Cu(I) **121** at the new anode. The Cu(I) species **121** is either oxidized to the Cu(II) complex by oxygen or plated again on the cathode. The

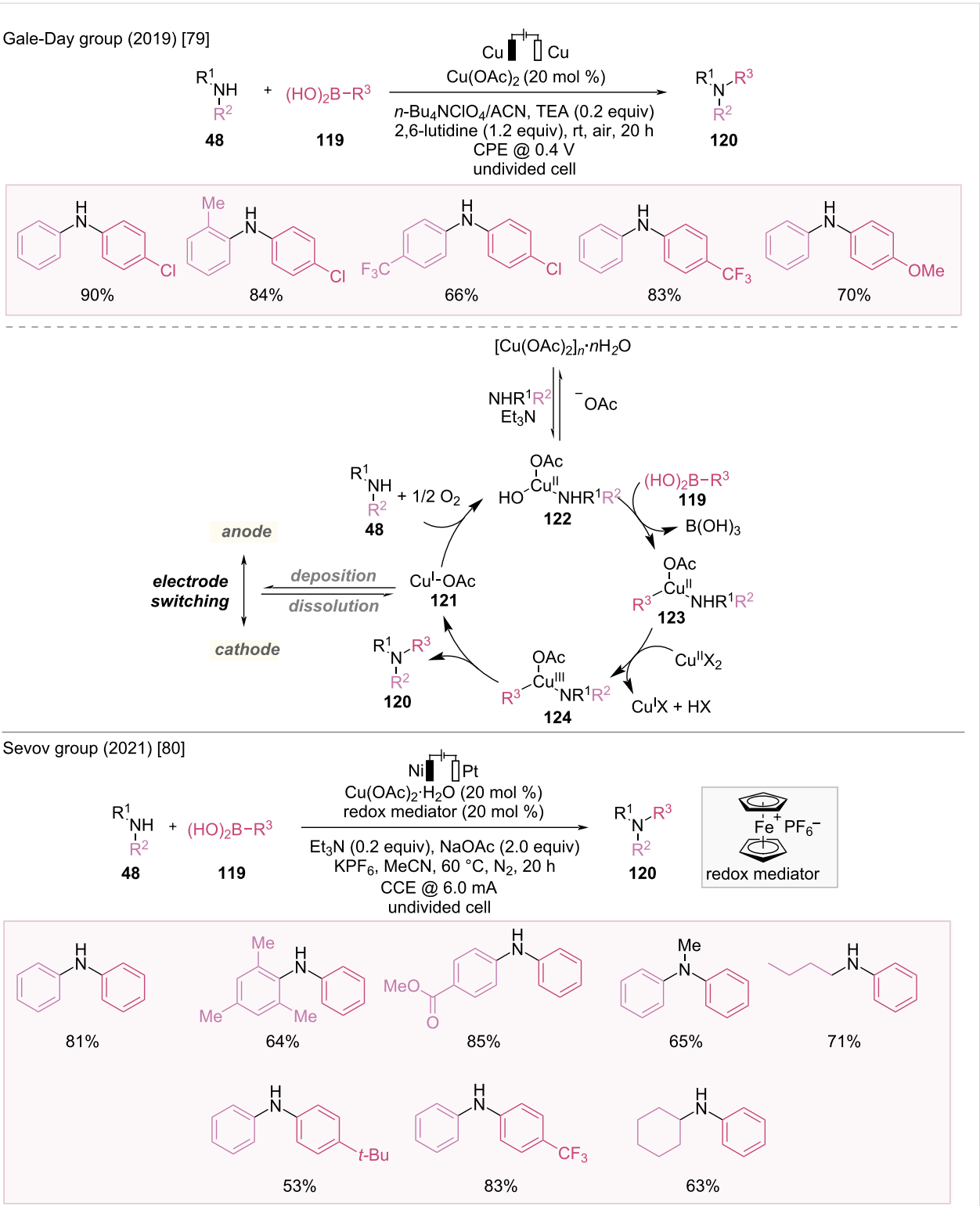

Figure 19: Scheme and proposed mechanism for electrocatalytic Chan–Lam coupling.

Cu(II) catalyst reacts with aniline to produce a Cu(II) intermediate **122**, which then generates a Cu(III) complex **124** through transmetalation of boronic acid and disproportionation. Subsequently, the coupling product **120** is released through reductive elimination, and the resulting Cu(I) species **121** is either reoxidized or plated on the cathode.

Despite the success of electrochemical Chan–Lam coupling for C–N bond formation, the electrooxidative reactions of copper catalysts without ligands face limitations owing to slow electron transfer kinetics, irreversible copper plating, and competing substrate oxidation. To overcome these challenges, Sevov et al. developed a ligand-free, Cu-catalyzed electrochemical Chan–Lam coupling using a ferrocenium salt as a redox mediator with non-copper electrodes (Figure 19) [80]. In the absence of chemical oxidants, this Chan–Lam coupling method resulted in shorter reaction times than those of traditional methods and offered alternative substrate reactivity. This reaction was successfully applied to aryl- and alkylamines with arylboronic acids, achieving high yields. Mechanistic studies revealed that the mediator plays multiple roles, including rapidly oxidizing low-valent Cu intermediates to maintain high Cu(II) concentrations, removing Cu metal from the cathode to regenerate the active Cu catalyst, revealing the Pt surface for proton reduction, and offering anodic overcharge protection to avoid undesirable substrate oxidation.

Conclusion

Over the past two decades, significant progress has been made in electrochemical organic reactions, supported by the development of more sustainable and versatile methodologies for carbon–carbon and carbon–heteroatom bond formation. These advances have been accomplished by recognizing electrochemistry as an effective and sustainable approach for electron transfer processes to enable the generation of highly reactive intermediates. Additionally, the rapid growth of dual catalytic systems (merging electrochemistry with transition-metal catalysis) has led to the development of new, efficient, and chemo- and stereoselective synthetic transformations.

This review highlighted the recent developments in dual catalytic reactions involving copper and electrocatalysis, including C–H activation, olefin addition, decarboxylative coupling, and Chan–Lam coupling. Although remarkable achievements have been made in this field, significant gaps that require attention remain, and further investigation into new and efficient transformations is necessary. The substrate scope is often limited, which can restrict both reactivity and selectivity. Significant progress has been achieved in C–H activation reactions, with the use of directing groups, which play a crucial role in selectivity and reactivity. However, the use of directing groups requires additional synthetic steps for their installation and removal and present challenges with limited substrate compatibility. Future research could focus on designing catalytic systems that reduce dependence on directing groups, such as utilizing transient directing groups to simplify the synthetic process. Moreover, the development of asymmetric transformations remains challenging due to the difficulty in controlling the stereo- and chemoselectivity of highly reactive radical intermediates. Future efforts should focus on designing new ligand frameworks to broaden substrate scopes and enhance selectivity control. The use of greener solvents is also important for more sustainable reactions. Furthermore, the application of electrochemical copper catalysis to complex molecules, such as for the late-stage functionalization of pharmaceuticals or materials and bioorthogonal functionalization of biomacromolecules, is necessary. Further advances in Cu-catalyzed electrochemical reactions are expected in the near future, developing powerful tools for sustainable and efficient organic syntheses.

Funding

This work was supported by the Ewha Womans University Research Grant of 2023, the National Research Foundation of Korea (NRF) grant funded by the Korea government (MSIT) (RS-2024-00350505), and by the Basic Science Research Program through the National Research Foundation of Korea (NRF) funded by the Ministry of Education (2021R1A6A1A10039823).

ORCID® iDs

Yemin Kim - https://orcid.org/0009-0000-2602-0366
Won Jun Jang - https://orcid.org/0000-0002-0673-7607

Data Availability Statement

Data sharing is not applicable as no new data was generated or analyzed in this study.

References

1. Hassan, J.; Sévignon, M.; Gozzi, C.; Schulz, E.; Lemaire, M. *Chem. Rev.* **2002,** *102,* 1359–1470. doi:10.1021/cr000664r
2. Altman, R. A.; Buchwald, S. L. *Nat. Protoc.* **2007,** *2,* 2474–2479. doi:10.1038/nprot.2007.364
3. Ullmann, F.; Bielecki, J. *Ber. Dtsch. Chem. Ges.* **1901,** *34,* 2174–2185. doi:10.1002/cber.190103402141
4. Ullmann, F. *Ber. Dtsch. Chem. Ges.* **1903,** *36,* 2382–2384. doi:10.1002/cber.190303602174
5. Ullmann, F.; Sponagel, P. *Ber. Dtsch. Chem. Ges.* **1905,** *38,* 2211–2212. doi:10.1002/cber.190503802176
6. Goldberg, I. *Ber. Dtsch. Chem. Ges.* **1906,** *39,* 1691–1692. doi:10.1002/cber.19060390298
7. Rosenmund, K. W.; Struck, E. *Ber. Dtsch. Chem. Ges.* **1919,** *52,* 1749–1756. doi:10.1002/cber.19190520840
8. Robert, W.; Hurtley, H. *J. Chem. Soc.* **1929,** 1870–1873. doi:10.1039/jr9290001870
9. Chodkiewicz, W. *Ann. Chim. (Cachan, Fr.)* **1957,** *2,* 819–869. doi:10.1136/bmj.2.5048.819
10. Beletskaya, I. P.; Cheprakov, A. V. *Coord. Chem. Rev.* **2004,** *248,* 2337–2364. doi:10.1016/j.ccr.2004.09.014
11. Biffis, A.; Centomo, P.; Del Zotto, A.; Zecca, M. *Chem. Rev.* **2018,** *118,* 2249–2295. doi:10.1021/acs.chemrev.7b00443
12. Ariafard, A.; Lin, Z. *Organometallics* **2006,** *25,* 4030–4033. doi:10.1021/om060236x

13. Kaga, A.; Chiba, S. *ACS Catal.* **2017,** *7,* 4697–4706. doi:10.1021/acscatal.7b01405
14. Iqbal, J.; Bhatia, B.; Nayyar, N. K. *Chem. Rev.* **1994,** *94,* 519–564. doi:10.1021/cr00026a008
15. Julia, M. *Acc. Chem. Res.* **1971,** *4,* 386–392. doi:10.1021/ar50047a005
16. Rathke, M. W.; Lindert, A. *J. Am. Chem. Soc.* **1971,** *93,* 4605–4606. doi:10.1021/ja00747a051
17. Kozlowski, M. C.; DiVirgilio, E. S.; Malolanarasimhan, K.; Mulrooney, C. A. *Tetrahedron: Asymmetry* **2005,** *16,* 3599–3605. doi:10.1016/j.tetasy.2005.10.008
18. Kaneda, K.; Itoh, T.; Kii, N.; Jitsukawa, K.; Teranishi, S. *J. Mol. Catal.* **1982,** *15,* 349–365. doi:10.1016/0304-5102(82)80027-8
19. Tokunaga, M.; Shirogane, Y.; Aoyama, H.; Obora, Y.; Tsuji, Y. *J. Organomet. Chem.* **2005,** *690,* 5378–5382. doi:10.1016/j.jorganchem.2005.05.018
20. Li, Z.-L.; Fang, G.-C.; Gu, Q.-S.; Liu, X.-Y. *Chem. Soc. Rev.* **2020,** *49,* 32–48. doi:10.1039/c9cs00681h
21. Hossain, A.; Bhattacharyya, A.; Reiser, O. *Science* **2019,** *364,* eaav9713. doi:10.1126/science.aav9713
22. Bissember, A. C.; Lundgren, R. J.; Creutz, S. E.; Peters, J. C.; Fu, G. C. *Angew. Chem., Int. Ed.* **2013,** *52,* 5129–5133. doi:10.1002/anie.201301202
23. Do, H.-Q.; Bachman, S.; Bissember, A. C.; Peters, J. C.; Fu, G. C. *J. Am. Chem. Soc.* **2014,** *136,* 2162–2167. doi:10.1021/ja4126609
24. Matier, C. D.; Schwaben, J.; Peters, J. C.; Fu, G. C. *J. Am. Chem. Soc.* **2017,** *139,* 17707–17710. doi:10.1021/jacs.7b09582
25. Zhou, H.; Li, Z.-L.; Gu, Q.-S.; Liu, X.-Y. *ACS Catal.* **2021,** *11,* 7978–7986. doi:10.1021/acscatal.1c01970
26. Zhang, Z.; Chen, P.; Liu, G. *Chem. Soc. Rev.* **2022,** *51,* 1640–1658. doi:10.1039/d1cs00727k
27. Gu, Q.-S.; Li, Z.-L.; Liu, X.-Y. *Acc. Chem. Res.* **2020,** *53,* 170–181. doi:10.1021/acs.accounts.9b00381
28. Zhang, W.; Wang, F.; McCann, S. D.; Wang, D.; Chen, P.; Stahl, S. S.; Liu, G. *Science* **2016,** *353,* 1014–1018. doi:10.1126/science.aaf7783
29. Kainz, Q. M.; Matier, C. D.; Bartoszewicz, A.; Zultanski, S. L.; Peters, J. C.; Fu, G. C. *Science* **2016,** *351,* 681–684. doi:10.1126/science.aad8313
30. Chen, C.; Peters, J. C.; Fu, G. C. *Nature* **2021,** *596,* 250–256. doi:10.1038/s41586-021-03730-w
31. Liu, J.; Lu, L.; Wood, D.; Lin, S. *ACS Cent. Sci.* **2020,** *6,* 1317–1340. doi:10.1021/acscentsci.0c00549
32. Yan, M.; Kawamata, Y.; Baran, P. S. *Chem. Rev.* **2017,** *117,* 13230–13319. doi:10.1021/acs.chemrev.7b00397
33. Novaes, L. F. T.; Liu, J.; Shen, Y.; Lu, L.; Meinhardt, J. M.; Lin, S. *Chem. Soc. Rev.* **2021,** *50,* 7941–8002. doi:10.1039/d1cs00223f
34. Ackermann, L. *Acc. Chem. Res.* **2020,** *53,* 84–104. doi:10.1021/acs.accounts.9b00510
35. Jiao, K.-J.; Xing, Y.-K.; Yang, Q.-L.; Qiu, H.; Mei, T.-S. *Acc. Chem. Res.* **2020,** *53,* 300–310. doi:10.1021/acs.accounts.9b00603
36. Wang, F.; Stahl, S. S. *Acc. Chem. Res.* **2020,** *53,* 561–574. doi:10.1021/acs.accounts.9b00544
37. Chang, X.; Zhang, Q.; Guo, C. *Angew. Chem., Int. Ed.* **2020,** *59,* 12612–12622. doi:10.1002/anie.202000016
38. Malapit, C. A.; Prater, M. B.; Cabrera-Pardo, J. R.; Li, M.; Pham, T. D.; McFadden, T. P.; Blank, S.; Minteer, S. D. *Chem. Rev.* **2022,** *122,* 3180–3218. doi:10.1021/acs.chemrev.1c00614
39. Gandeepan, P.; Müller, T.; Zell, D.; Cera, G.; Warratz, S.; Ackermann, L. *Chem. Rev.* **2019,** *119,* 2192–2452. doi:10.1021/acs.chemrev.8b00507
40. Docherty, J. H.; Lister, T. M.; Mcarthur, G.; Findlay, M. T.; Domingo-Legarda, P.; Kenyon, J.; Choudhary, S.; Larrosa, I. *Chem. Rev.* **2023,** *123,* 7692–7760. doi:10.1021/acs.chemrev.2c00888
41. Wang, W.; Lorion, M. M.; Shah, J.; Kapdi, A. R.; Ackermann, L. *Angew. Chem., Int. Ed.* **2018,** *57,* 14700–14717. doi:10.1002/anie.201806250
42. Guillemard, L.; Kaplaneris, N.; Ackermann, L.; Johansson, M. J. *Nat. Rev. Chem.* **2021,** *5,* 522–545. doi:10.1038/s41570-021-00300-6
43. Son, J. *Beilstein J. Org. Chem.* **2021,** *17,* 1733–1751. doi:10.3762/bjoc.17.122
44. Zhang, L.; Ritter, T. *J. Am. Chem. Soc.* **2022,** *144,* 2399–2414. doi:10.1021/jacs.1c10783
45. Wang, Y.; Dana, S.; Long, H.; Xu, Y.; Li, Y.; Kaplaneris, N.; Ackermann, L. *Chem. Rev.* **2023,** *123,* 11269–11335. doi:10.1021/acs.chemrev.3c00158
46. Bellotti, P.; Huang, H.-M.; Faber, T.; Glorius, F. *Chem. Rev.* **2023,** *123,* 4237–4352. doi:10.1021/acs.chemrev.2c00478
47. Sauermann, N.; Meyer, T. H.; Qiu, Y.; Ackermann, L. *ACS Catal.* **2018,** *8,* 7086–7103. doi:10.1021/acscatal.8b01682
48. Tian, C.; Dhawa, U.; Scheremetjew, A.; Ackermann, L. *ACS Catal.* **2019,** *9,* 7690–7696. doi:10.1021/acscatal.9b02348
49. Zhang, Z.-Z.; Zhou, G.; Yue, Q.; Yao, Q.-J.; Shi, B.-F. *ACS Catal.* **2024,** *14,* 4030–4039. doi:10.1021/acscatal.3c05955
50. Gao, P.-S.; Weng, X.-J.; Wang, Z.-H.; Zheng, C.; Sun, B.; Chen, Z.-H.; You, S.-L.; Mei, T.-S. *Angew. Chem., Int. Ed.* **2020,** *59,* 15254–15259. doi:10.1002/anie.202005099
51. Guo, B.; Xu, H.-C. *Beilstein J. Org. Chem.* **2021,** *17,* 2650–2656. doi:10.3762/bjoc.17.178
52. He, Z.; Liu, H.-L.; Wang, Z.-H.; Jiao, K.-J.; Li, Z.-M.; Li, Z.-J.; Fang, P.; Mei, T.-S. *J. Org. Chem.* **2023,** *88,* 6203–6208. doi:10.1021/acs.joc.3c00223
53. Lu, Q.; Glorius, F. *Angew. Chem., Int. Ed.* **2017,** *56,* 49–51. doi:10.1002/anie.201609105
54. Zhang, C.; Li, Z.-L.; Gu, Q.-S.; Liu, X.-Y. *Nat. Commun.* **2021,** *12,* 475. doi:10.1038/s41467-020-20770-4
55. Cai, C.-Y.; Lai, X.-L.; Wang, Y.; Hu, H.-H.; Song, J.; Yang, Y.; Wang, C.; Xu, H.-C. *Nat. Catal.* **2022,** *5,* 943–951. doi:10.1038/s41929-022-00855-7
56. Fan, W.; Zhao, X.; Deng, Y.; Chen, P.; Wang, F.; Liu, G. *J. Am. Chem. Soc.* **2022,** *144,* 21674–21682. doi:10.1021/jacs.2c09366
57. Lai, X.-L.; Xu, H.-C. *J. Am. Chem. Soc.* **2023,** *145,* 18753–18759. doi:10.1021/jacs.3c07146
58. Xie, T.; Huang, J.; Li, J.; Peng, L.; Song, J.; Guo, C. *Nat. Commun.* **2023,** *14,* 6749. doi:10.1038/s41467-023-42603-w
59. Zhang, J.; Zhu, W.; Chen, Z.; Zhang, Q.; Guo, C. *J. Am. Chem. Soc.* **2024,** *146,* 1522–1531. doi:10.1021/jacs.3c11429
60. Yang, Q.-L.; Wang, X.-Y.; Lu, J.-Y.; Zhang, L.-P.; Fang, P.; Mei, T.-S. *J. Am. Chem. Soc.* **2018,** *140,* 11487–11494. doi:10.1021/jacs.8b07380
61. Kathiravan, S.; Suriyanarayanan, S.; Nicholls, I. A. *Org. Lett.* **2019,** *21,* 1968–1972. doi:10.1021/acs.orglett.9b00003
62. Baidya, M.; De Sarkar, S. *Org. Lett.* **2023,** *25,* 5896–5901. doi:10.1021/acs.orglett.3c02186
63. Tsuchida, K.; Kochi, T.; Kakiuchi, F. *Asian J. Org. Chem.* **2013,** *2,* 935–937. doi:10.1002/ajoc.201300168
64. Yang, X.; Yang, Q.-L.; Wang, X.-Y.; Xu, H.-H.; Mei, T.-S.; Huang, Y.; Fang, P. *J. Org. Chem.* **2020,** *85,* 3497–3507. doi:10.1021/acs.joc.9b03223

65. Chen, J.; Lu, Z. *Org. Chem. Front.* **2018,** *5,* 260–272. doi:10.1039/c7qo00613f
66. Dhungana, R. K.; KC, S.; Basnet, P.; Giri, R. *Chem. Rec.* **2018,** *18,* 1314–1340. doi:10.1002/tcr.201700098
67. Pitzer, L.; Schwarz, J. L.; Glorius, F. *Chem. Sci.* **2019,** *10,* 8285–8291. doi:10.1039/c9sc03359a
68. Sauer, G. S.; Lin, S. *ACS Catal.* **2018,** *8,* 5175–5187. doi:10.1021/acscatal.8b01069
69. Fu, N.; Song, L.; Liu, J.; Shen, Y.; Siu, J. C.; Lin, S. *J. Am. Chem. Soc.* **2019,** *141,* 14480–14485. doi:10.1021/jacs.9b03296
70. Song, L.; Fu, N.; Ernst, B. G.; Lee, W. H.; Frederick, M. O.; DiStasio, R. A., Jr.; Lin, S. *Nat. Chem.* **2020,** *12,* 747–754. doi:10.1038/s41557-020-0469-5
71. Cai, C.-Y.; Zheng, Y.-T.; Li, J.-F.; Xu, H.-C. *J. Am. Chem. Soc.* **2022,** *144,* 11980–11985. doi:10.1021/jacs.2c05126
72. Zheng, Y.-T.; Xu, H.-C. *Angew. Chem., Int. Ed.* **2024,** *63,* e202313273. doi:10.1002/anie.202313273
73. Rodríguez, N.; Goossen, L. J. *Chem. Soc. Rev.* **2011,** *40,* 5030–5048. doi:10.1039/c1cs15093f
74. Laudadio, G.; Palkowitz, M. D.; El-Hayek Ewing, T.; Baran, P. S. *ACS Med. Chem. Lett.* **2022,** *13,* 1413–1420. doi:10.1021/acsmedchemlett.2c00286
75. Lai, X.-L.; Chen, M.; Wang, Y.; Song, J.; Xu, H.-C. *J. Am. Chem. Soc.* **2022,** *144,* 20201–20206. doi:10.1021/jacs.2c09050
76. Yuan, Y.; Yang, J.; Zhang, J. *Chem. Sci.* **2023,** *14,* 705–710. doi:10.1039/d2sc05428k
77. Yang, K.; Wang, Y.; Luo, S.; Fu, N. *Chem. – Eur. J.* **2023,** *29,* e202203962. doi:10.1002/chem.202203962
78. West, M. J.; Fyfe, J. W. B.; Vantourout, J. C.; Watson, A. J. B. *Chem. Rev.* **2019,** *119,* 12491–12523. doi:10.1021/acs.chemrev.9b00491
79. Wexler, R. P.; Nuhant, P.; Senter, T. J.; Gale-Day, Z. J. *Org. Lett.* **2019,** *21,* 4540–4543. doi:10.1021/acs.orglett.9b01434
80. Walker, B. R.; Manabe, S.; Brusoe, A. T.; Sevov, C. S. *J. Am. Chem. Soc.* **2021,** *143,* 6257–6265. doi:10.1021/jacs.1c02103

License and Terms

BEILSTEIN JOURNAL OF ORGANIC CHEMISTRY

Dioxazolones as electrophilic amide sources in copper-catalyzed and -mediated transformations

Seungmin Lee[‡1], Minsuk Kim[‡2], Hyewon Han[1] and Jongwoo Son[*1,2]

Review

Open Access

Address:
[1]Department of Chemistry, Dong-A University, Busan 49315, South Korea and [2]Department of Chemical Engineering (BK21 FOUR Graduate Program), Dong-A University, Busan 49315, South Korea

Email:
Jongwoo Son[*] - sonorganic@dau.ac.kr

* Corresponding author ‡ Equal contributors

Keywords:
amidation; copper salts; dioxazolones; electrophilic nitrogen; *N*-acyl nitrene

Beilstein J. Org. Chem. **2025,** *21,* 200–216.
https://doi.org/10.3762/bjoc.21.12

Received: 26 September 2024
Accepted: 07 January 2025
Published: 22 January 2025

This article is part of the thematic issue "Copper catalysis: a constantly evolving field".

Guest Editor: J. Yun

Abstract

Over the past decade, dioxazolones have been widely used as *N*-acylamide sources in amidation processes of challenging substrates, typically employing precious transition metals. However, these catalytic systems often present several challenges associated with cost, toxicity, stability, and recyclability. Among the 3d transition metals, copper catalysts have been gaining increasing attention owing to their abundance, cost-effectiveness, and sustainability. Recently, these catalytic systems have been applied to the chemical transformation of dioxazolones, conferring a convenient protocol towards amidated products. This review highlights recent advancements in the synthetic transformations of dioxazolones, with particular examples of copper salts.

Introduction

Dioxazolones, first synthesized and reported by Beck and co-workers [1], have been employed as electrophiles in various nucleophilic transformations due to their susceptibility to rapid decomposition into the corresponding isocyanates (Scheme 1a) [2,3]. They have attracted increasing interest as electrophilic amide sources in amidation using transition-metal catalysts such as ruthenium, rhodium, and iridium (Scheme 1b) [4-19]. Notably, dioxazolones have primarily been studied in directed carbon–hydrogen amidation processes, which can circumvent the need for tedious prefunctionalizations.

Copper catalysts have gained recognition and attracted increasing interest as affordable, versatile, and sustainable catalytic systems. These catalysts are extensively employed in organic synthesis owing to their cost-effectiveness, reduced toxicity, and natural abundance [20-28]. The use of copper salts has enabled a variety of conventionally challenging functionalizations, such as *N*- or *O*-arylations using aryl halides [29-38] or arylboronic acids [39-42], hydrofunctionalizations of unsaturated motifs [25,43-56], the oxidation of alcohols [57-61], and photoinduced alkylations of various nucleophiles [22,62-68].

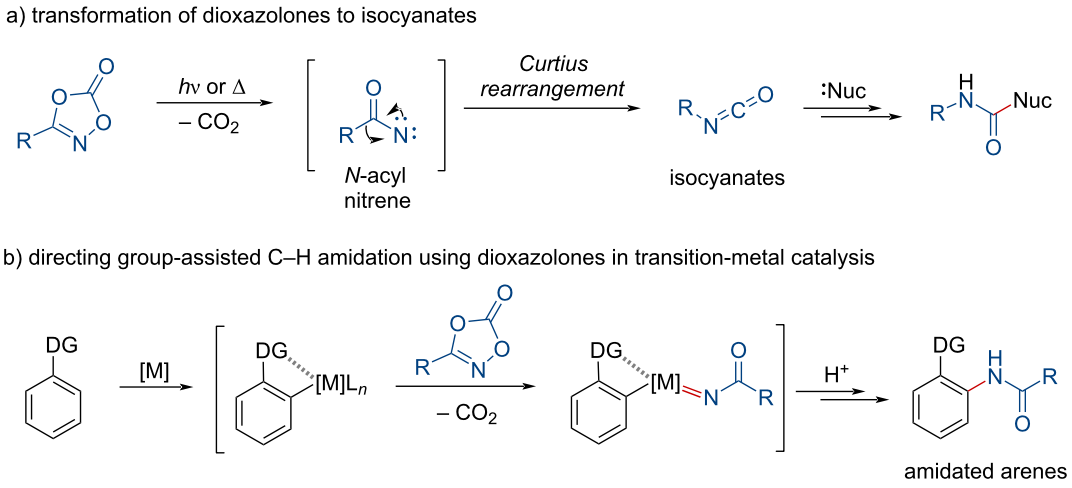

Scheme 1: Formation of isocyanates and amidated arenes from dioxazolones.

Recently, these sustainable catalytic systems have gradually been applied to amidations employing dioxazolones as amide sources.

To the best of our knowledge, no review article has yet covered the recent progress in the chemical transformation of dioxazolones using copper salts. This review provides an overview of the recent achievements in the use of copper salts as sustainable metal systems for the transformation of dioxazolones. This review also discusses several related proposed mechanisms.

Review

1 Transformations via the formation of copper nitrenoids

1.1 C(sp^3)–H amidation

Lactams are recognized as one of the most significant nitrogen-containing heterocycles in drug discovery [69,70]. Among these, six-membered lactams, known as 2-piperidinones, have been extensively studied due to their potential bioactivity [70-73]. Despite the development of synthetic approaches for six-membered lactams, including transition-metal-catalyzed transformations, several limitations remain, particularly with regard to regioselectivity and asymmetric C–N bond formation, which are still limited. In 2023, the Chang group elegantly unveiled a protocol for an enantioselective C–N bond formation, introducing δ-lactams from dioxazolones using a copper(I) catalyst and a chiral BOX ligand [74].

As shown in Scheme 2, dioxazolones containing aryl and heteroaryl groups were converted into the corresponding lactams in high yields and excellent enantioselectivities (**2a**, **2b**, and **2d**). It was observed that the steric environment affected both reactivity and enantioselectivity (**2c**). Six-membered lactams featuring propargylic (**2e**) and alkenyl (**2f**) motifs were also obtained with excellent regioselectivity and enantioselectivity. Furthermore, a lactam containing a quaternary carbon center (**2g**) was prepared. However, a lower enantioselectivity was observed for product **2h** due to the similar steric environment of the two alkyl substituents.

As shown in Figure 1, a catalytic cycle was proposed for the intramolecular C–H amidation process of dioxazolones. Dioxazolone **1** binds to the chiral copper complex **3**, generating the adduct **INT-1**. Decarboxylation then occurs, forming the copper nitrenoid intermediate **INT-2**, subsequently undergoing hydrogen atom transfer in a regioselective manner to afford **INT-3**. The related acyl nitrenoid intermediate was characterized by the same group [75]. Further radical rebound from **INT-4** induces the enantioselective C–N bond formation. Finally, the desired product **2** is released from **INT-4**, regenerating the active chiral copper species to participate in the catalytic cycle.

1.2 C(sp^2)–H amidation

Recently, Cao and co-workers reported the copper-catalyzed synthesis of 1,2,4-triazole derivatives via an *N*-acyl nitrene intermediate [76].

As illustrated in Scheme 3, dioxazolones **4** and *N*-iminoquinolinium ylides **5** served as reactive substrates, leading to the formation of various polycyclic 1,2,4-triazole analogues **6**. Both dioxazolones **4** and *N*-iminoquinolinium ylides **5** demonstrated excellent tolerance in this transformation. Notably, electron-rich dioxazolones exhibited slightly higher reactivity.

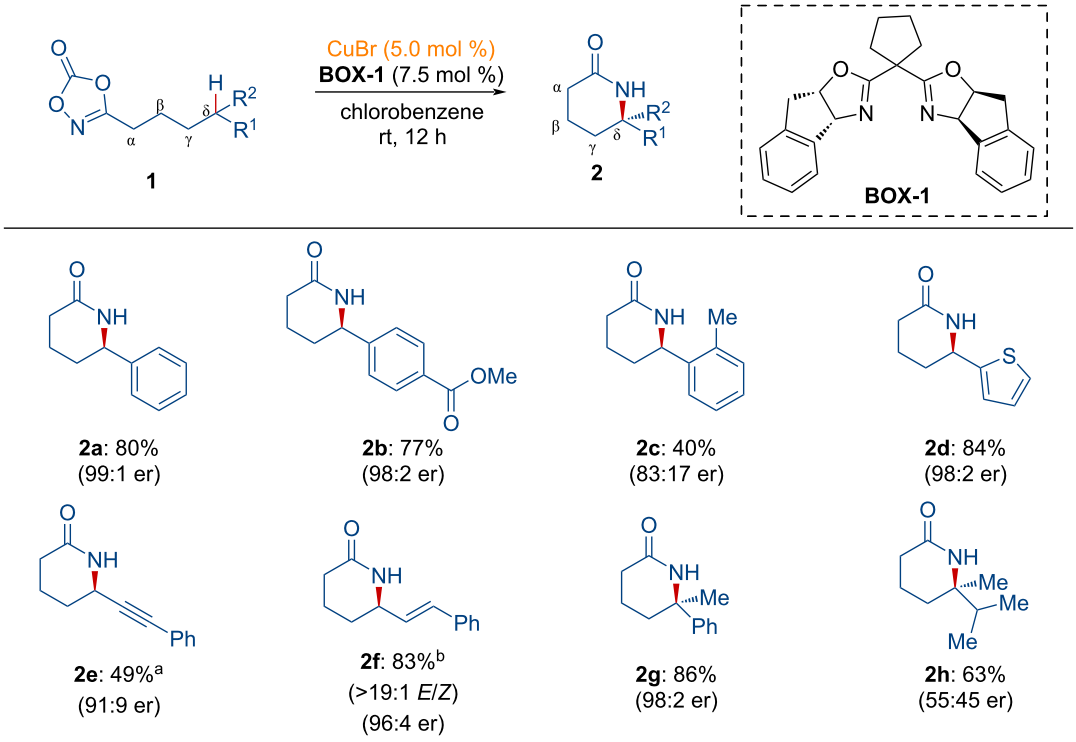

Scheme 2: Copper-catalyzed synthesis of δ-lactams via open-shell copper nitrenoid transfer. [a]CuBr (10 mol %) and **BOX-1** (15 mol %) were used. [b]A stereoisomeric mixture (*E*/*Z* = 1.4:1) of dioxazolones was used.

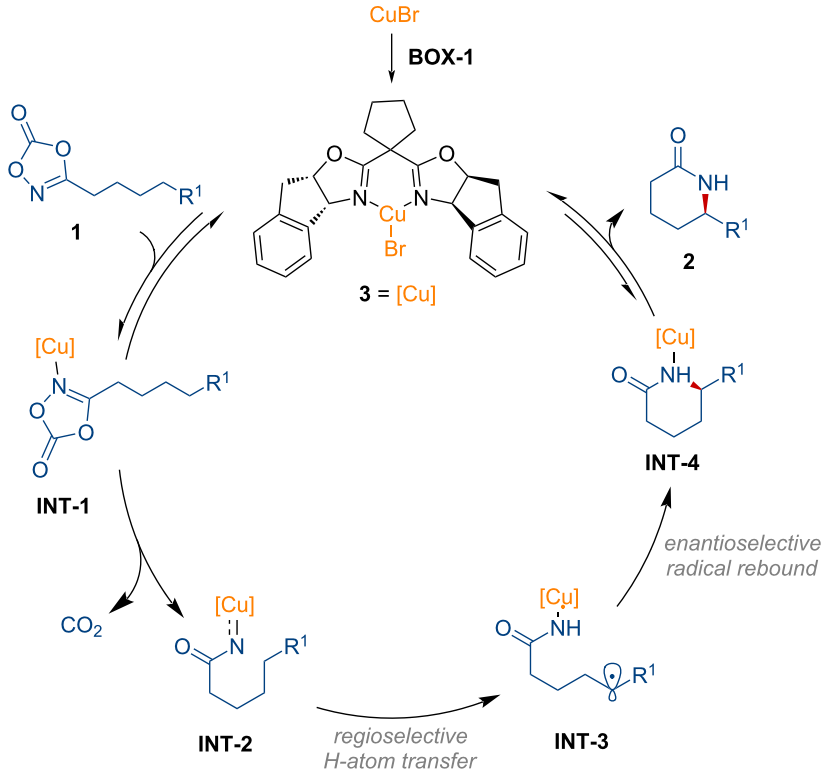

Figure 1: Proposed reaction pathway for the copper-catalyzed synthesis of δ-lactams from dioxazolones.

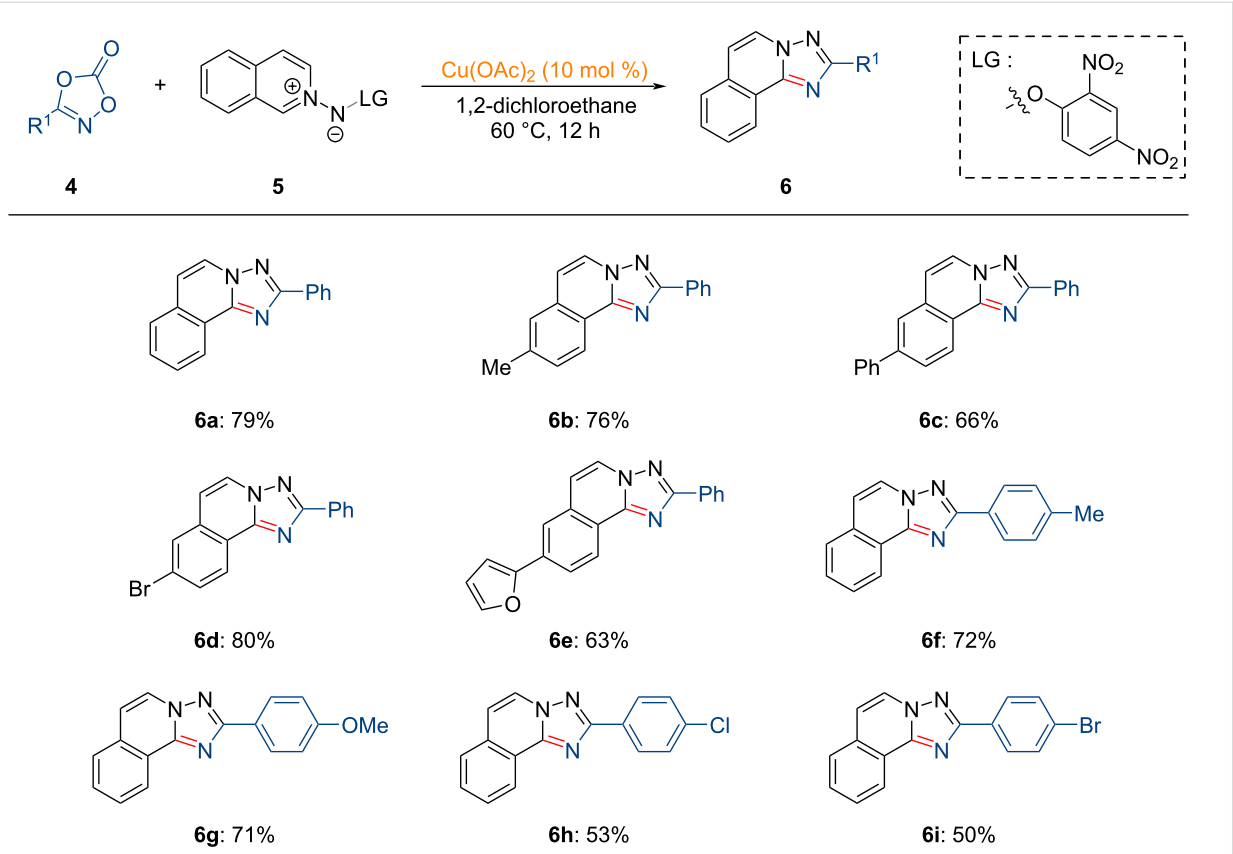

Scheme 3: Copper(II)-catalyzed synthesis of 1,2,4-triazole derivatives.

The proposed catalytic cycle for the copper-catalyzed synthesis of 1,2,4-triazole derivatives is depicted in Figure 2. The reaction is initiated by formation of the five-membered copper-containing intermediate **INT-5** through coordination of $Cu(OAc)_2$ with the *N*-iminoquinolinium ylide species **5**. This process is followed by decarboxylative N–O bond insertion into **4**, yielding the *N*-acyl copper(III) nitrenoid intermediate **INT-7**. Subsequent nitrene insertion, protodemetalation, and intramolecular cyclization furnish the desired 1,2,4-triazole.

1.3 Three-component formation of *N*-acyl amidines

In 2019, *N*-acyl amidines were prepared from dioxazolones using a copper catalyst with terminal alkynes and secondary amines via an *N*-acyl nitrene intermediate [77]. Amidines, found in biologically active compounds, have been widely investigated in medicinal chemistry due to their potent antiviral, antibacterial, anticancer, and other therapeutic properties [78-81].

As shown in Scheme 4, dioxazolones bearing linear alkyl groups were transformed into *N*-acyl amidines **10a–c** by copper catalysis. Moreover, good functional group tolerance was observed with a terminal alkene motif (**10d**). The cyclohexyl-substituted dioxazolone successfully provided the corresponding *N*-acyl amidine **10e**. However, the dioxazolone bearing a phenyl group showed no reactivity toward benzoyl amidine under the optimized reaction conditions. Instead, the authors employed a less bulky copper iodide catalyst in the absence of phosphine, successfully affording aryloyl amidine **10f**. Furthermore, the electron-rich ethynylanisole afforded the product **10g** in good yield. Acetylenes containing tolyl and trifluorophenyl substituents also exhibited improved reactivity (**10h** and **10i**). Heteroaromatic acetylenes were effective in this transformation, forming *N*-acyl amidines **10j** and **10k**, respectively. On the other hand, the use of linear terminal alkynes did not result in the desired *N*-acyl amidine **10l**. Based on the substrate scope of acetylenes, the authors noted that the lower acidity of terminal acetylenes led to a diminished formation of the copper acetylide intermediate. Based on several mechanistic experiments and density functional theory (DFT) calculations, a proposed reaction mechanism is suggested as shown in Figure 3.

Initially, copper acetylide **INT-11** is formed by the reaction of acetylene with a copper precatalyst, leading to the formation of an *N*-acyl nitrene acetylide intermediate **INT-12** after the incorporation of dioxazolone **7**. Subsequently, nitrene insertion of

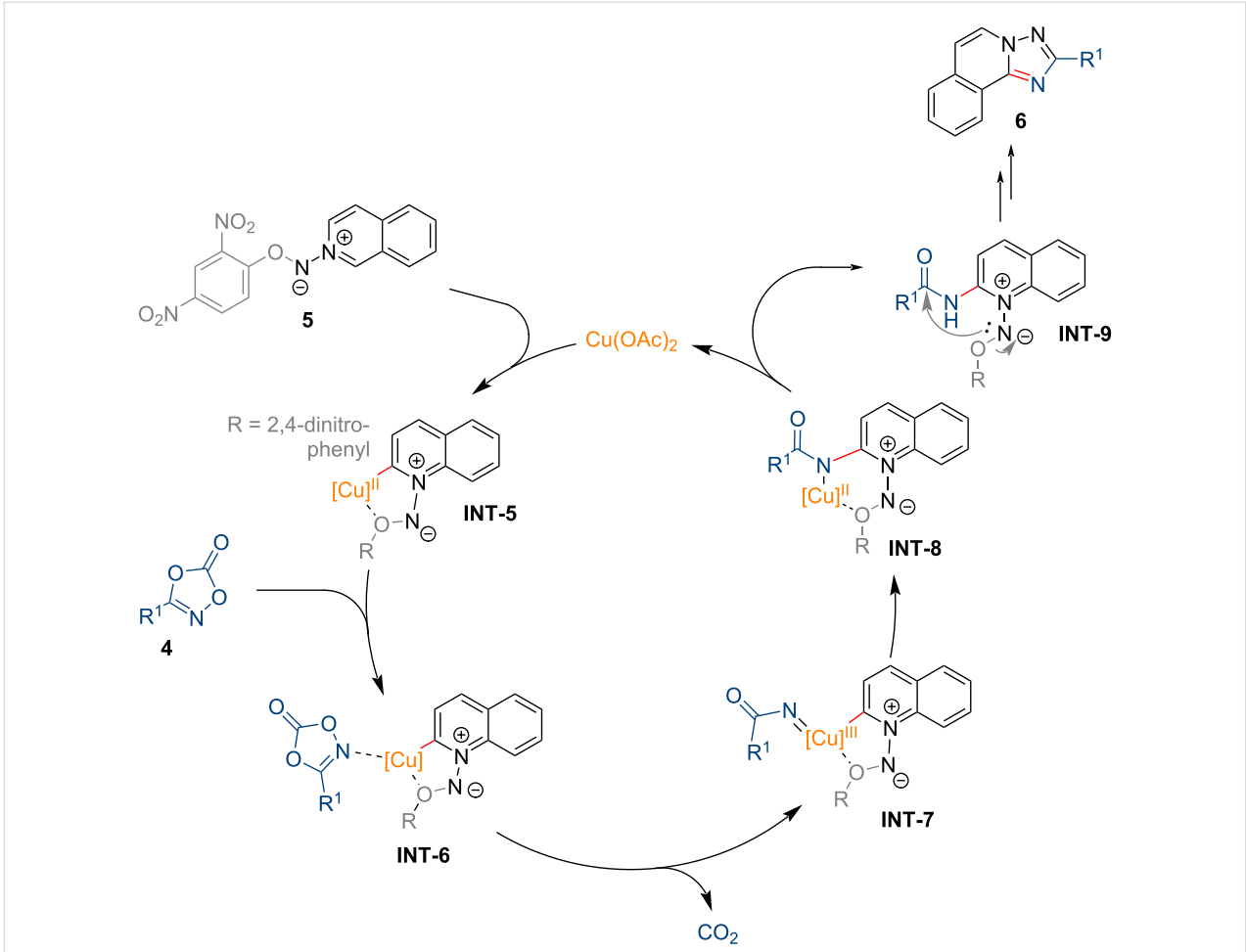

Figure 2: Proposed reaction mechanism for the copper-catalyzed synthesis of 1,2,4-triazole analogues from dioxazolones and *N*-iminoquinolinium ylides.

INT-12 into the Cu–C bond, forms **INT-13**, which then undergoes isomerization and protodemetalation, followed by catalyst regeneration, as suggested by the DFT calculations. Finally, the nucleophilic addition of the amine to the electrophilic intermediate **INT-15** leads to the formation of the *N*-acyl amidine product **10**.

1.4 *N*-Arylation of dioxazolones

Amides bearing *N*-substituents are key structural motifs in a wide range of polymers [82], natural products [83], and pharmaceuticals [84,85]. Conventional synthetic routes for *N*-arylamides typically involve the condensation of carboxylic acids with anilines, often promoted by activating agents such as thionyl chloride or peptide coupling agents [86-89]. However, these protocols rely on environmentally harmful reagents and produce unwanted byproduct wastes. Recently, the research group of Son showcased a synthetic methodology for *N*-arylamides **13** from dioxazolones **11** and boronic acids **12** using copper salts (Scheme 5) [90].

As illustrated, dioxazolones with both electron-rich and electron-poor substituents, including alkyl substituents, were well-tolerated, providing the desired products **13a**–**h**. However, the substrate scope of boronic acids was limited in this transformation. To elucidate the reaction process, kinetic and control experiments were conducted, which led to the proposed reaction pathway for the copper-mediated synthesis of *N*-arylamides from dioxazolones as shown in Figure 4.

Initially, copper(I) chloride reacts with boronic acids, forming the copper aryl complex **INT-16**, which then undergoes decarboxylative N–O bond insertion to generate the copper nitrenoid intermediate **INT-17**. Thereafter, nitrene insertion into the copper–carbon bond occurs, forming a new C(sp^2)–N bond (**INT-18**). Finally, the desired *N*-arylamide **13** is yielded through protodemetalation. In this process, copper does not undergo further catalytic turnover, presumably due to the formation of inactive copper fluoride or copper hydroxide species.

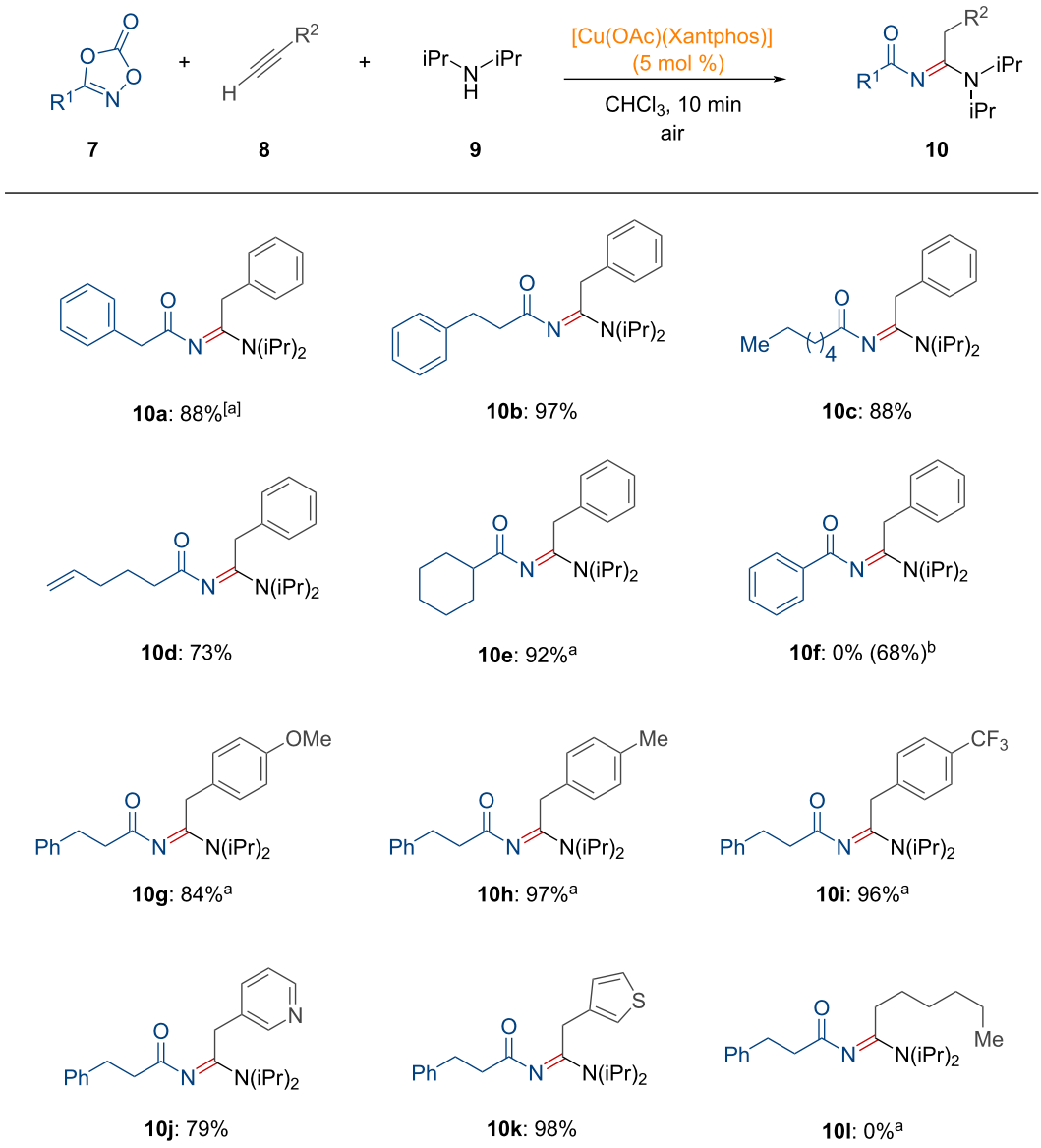

Scheme 4: Copper(I)-catalyzed synthesis of *N*-acyl amidines from dioxazolones, acetylenes, and amines. [a]Performed under N_2 atmosphere. [b]10 mol % of CuI was used instead of [Cu(OAc)(Xantphos)], with a reaction time of 30 min.

1.5 *N*-Phosphorylation of dioxazolones

Recently, Son and Kuniyil reported the *N*-phosphorylation of dioxazolones using organic phosphines and copper catalysts [91]. As shown in Scheme 6, a variety of dioxazolones **14** were explored for the synthesis of *N*-acyl iminophosphoranes **16**. Dioxazolones containing aryl and heteroaryl groups were successfully transformed into the desired products in high yields (**16a**–**c**).

Moreover, alkyl groups were tolerated during the formation of *N*-acyl iminophosphoranes (**16d**, **16f**). It is noteworthy that dioxazolones derived from bioactive motifs, such as peptides, natural products, and commercially available drugs were also compatible with this transformation, providing the corresponding products (**16g**–**k**).

Mechanistically, the reaction begins with the generation of the active copper species **17**, successively forming **INT-19** and **INT-20** (Figure 5). The penta-coordinated copper nitrenoid species **INT-20**, as suggested by DFT calculations, undergoes reductive elimination to yield the stable intermediate **INT-21**. This intermediate releases the *N*-acyl iminophosphorane **16** through the incorporation of another organic phosphine, thereby regenerating the active copper species **17**.

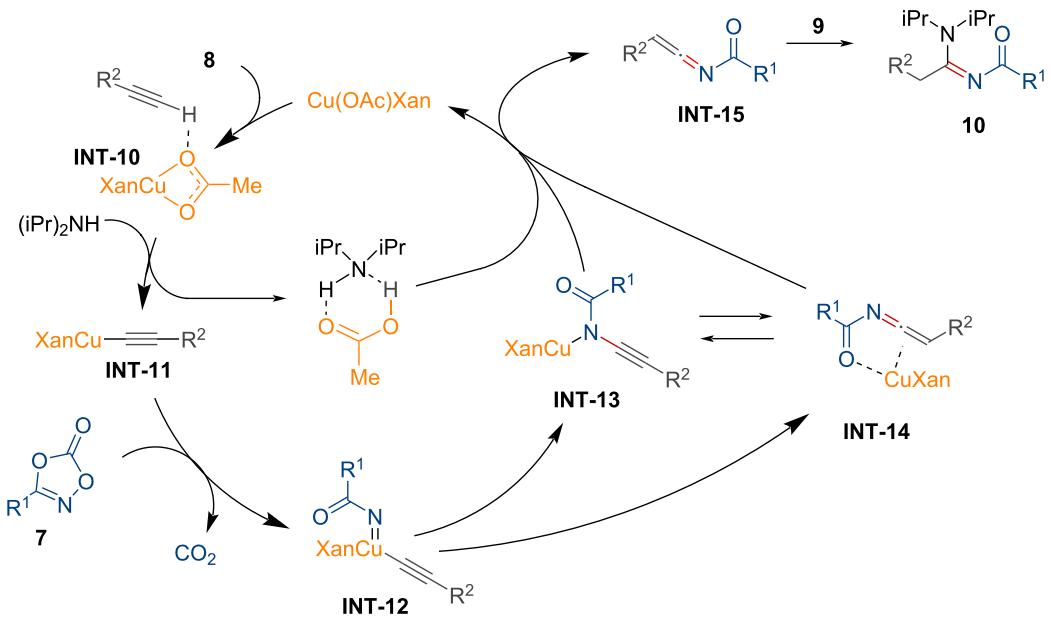

Figure 3: Proposed reaction mechanism for the copper(I)-catalyzed synthesis of *N*-acyl amidines.

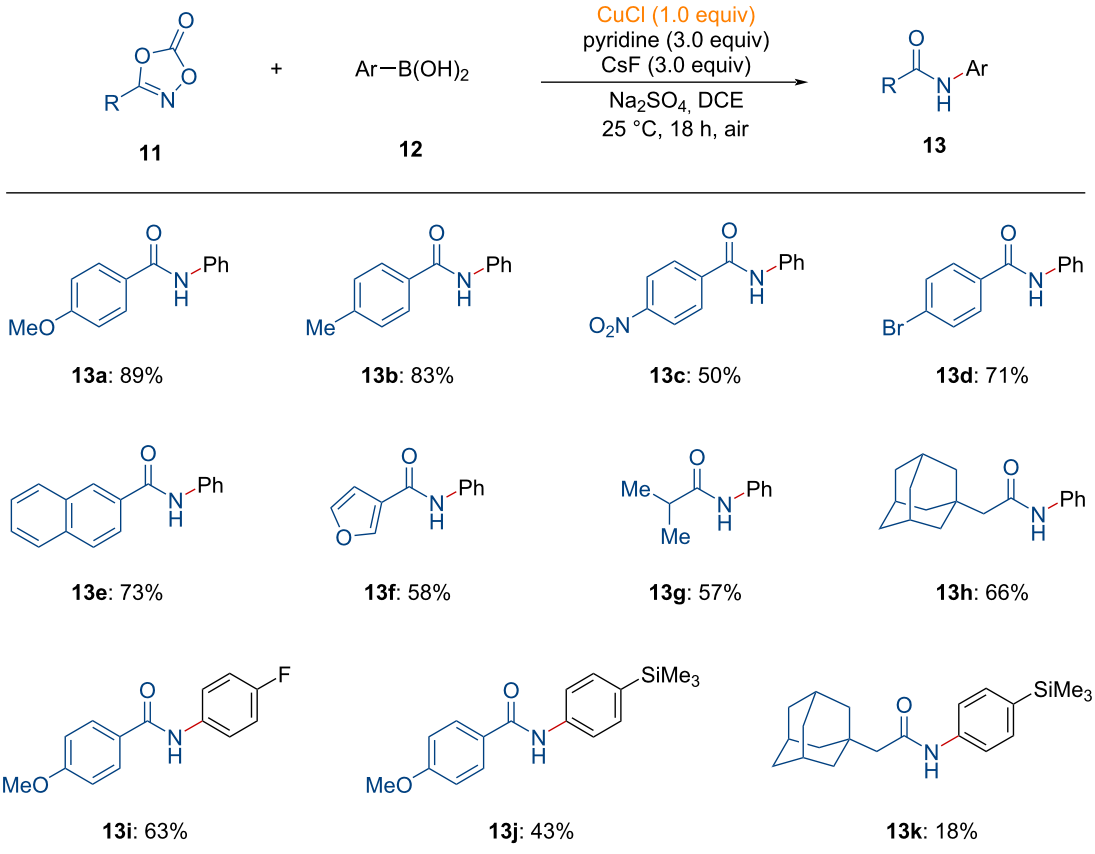

Scheme 5: Preparation of *N*-arylamides from dioxazolones and boronic acids using a copper salt.

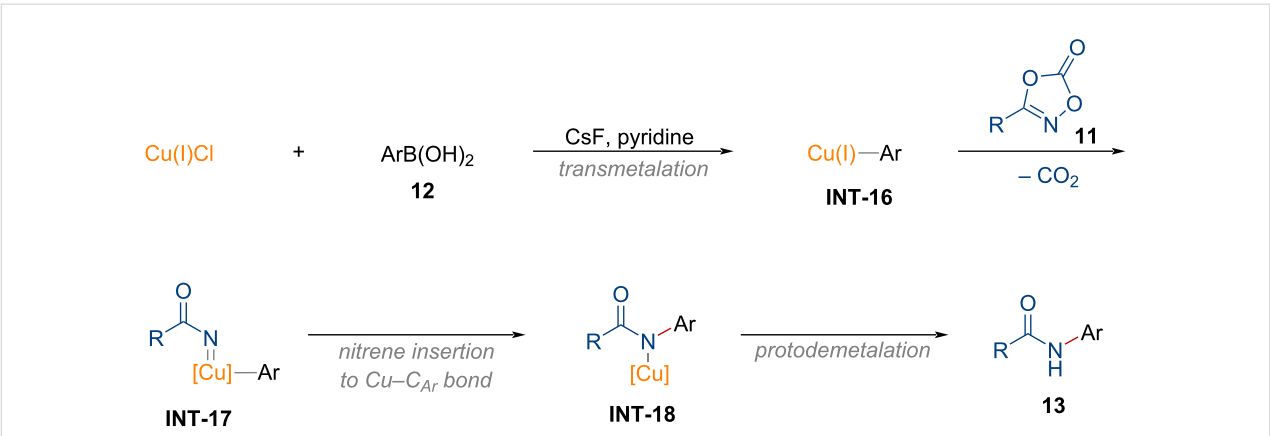

Figure 4: Proposed reaction pathway for the copper-mediated synthesis of *N*-arylamides from dioxazolones.

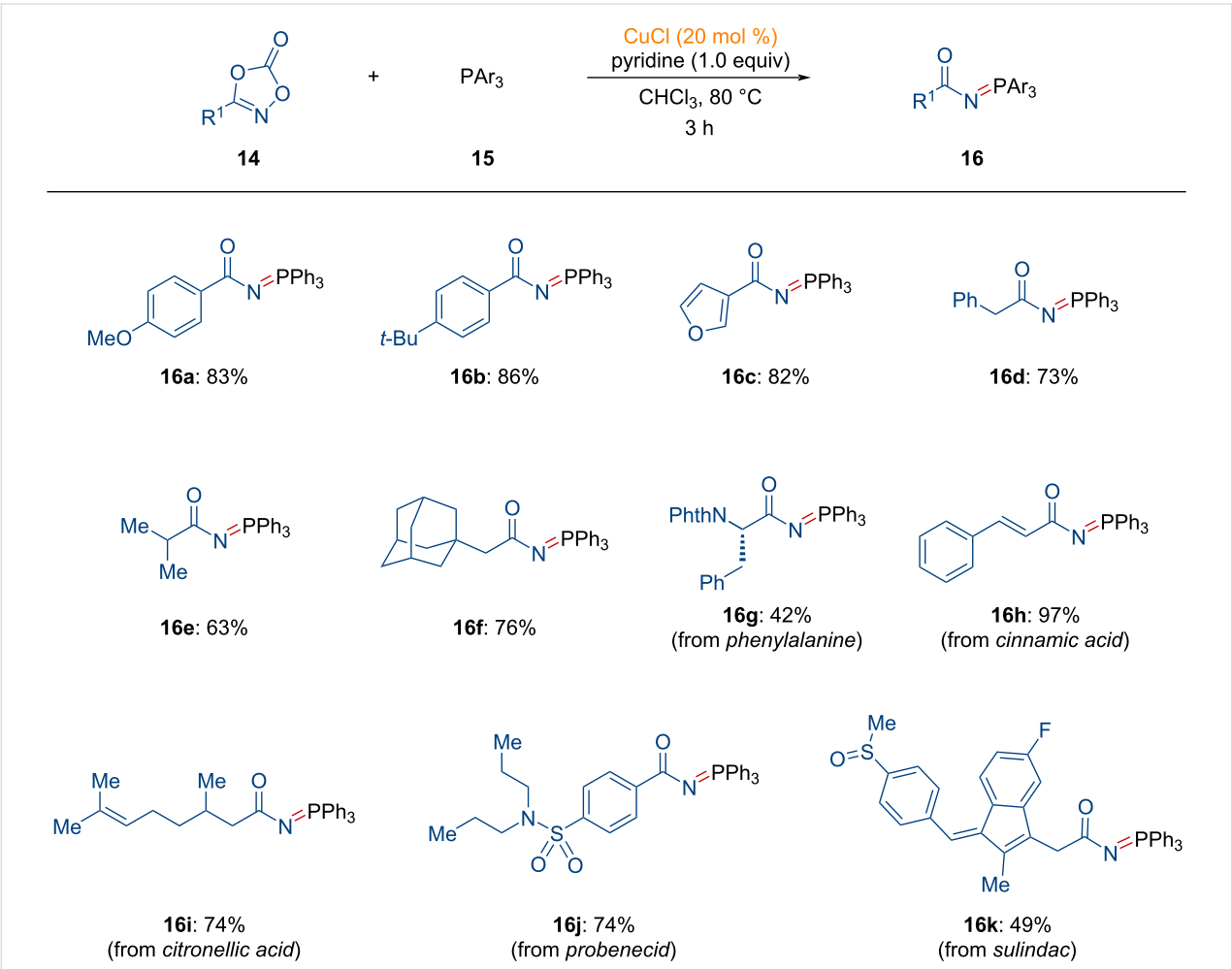

Scheme 6: Copper-catalyzed preparation of *N*-acyl iminophosphoranes from dioxazolones.

1.6 Synthesis of *N*-sulfenamides

In 2022, the research groups of Wang and Chen introduced a modular copper-catalyzed method for the synthesis of *N*-acyl sulfenamides **20** from dioxazolones **18** using thiols **19** via nitrogen–sulfur bond formation (Scheme 7) [92]. Secondary and tertiary thiols were highly effective in affording the correspond-

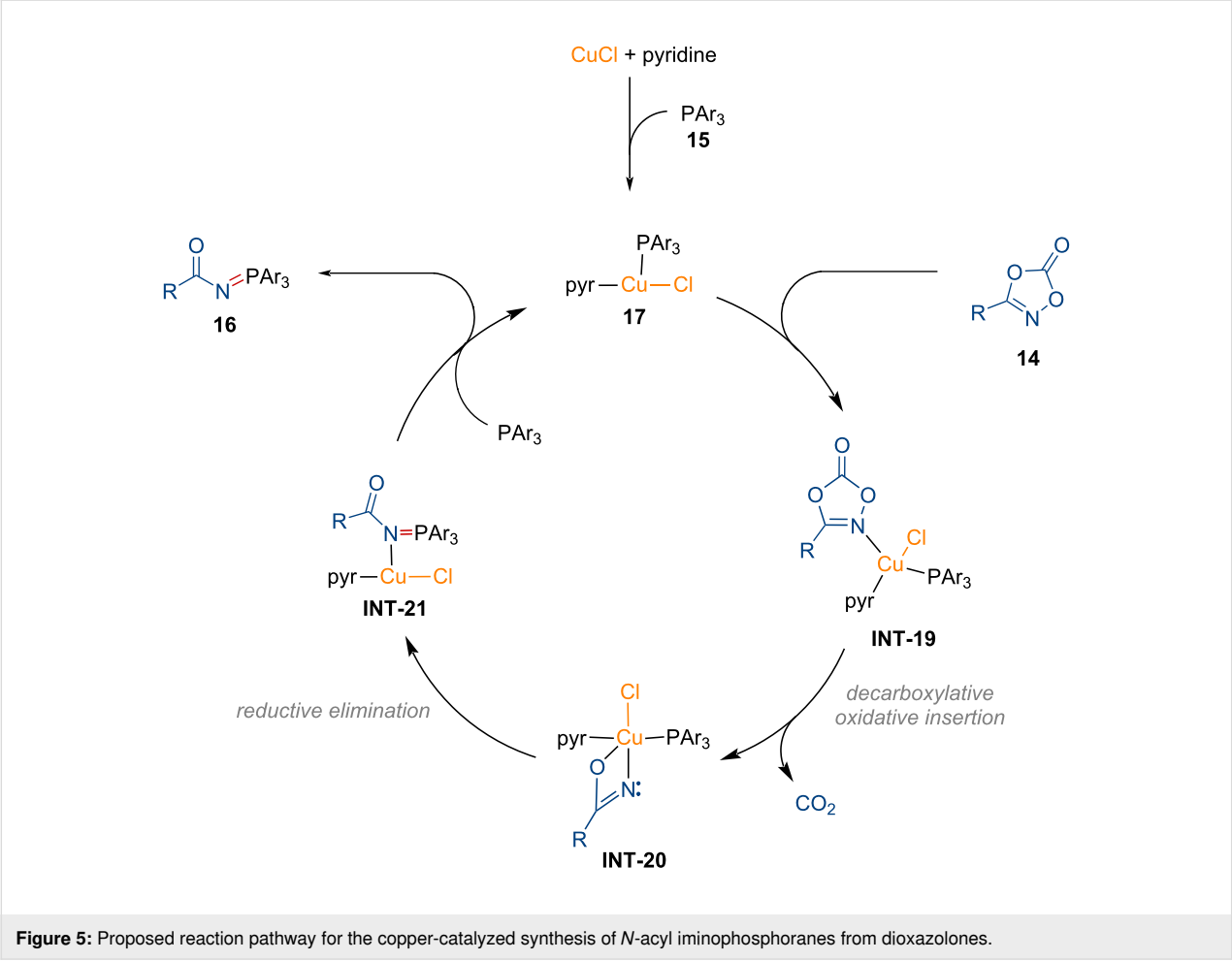

Figure 5: Proposed reaction pathway for the copper-catalyzed synthesis of *N*-acyl iminophosphoranes from dioxazolones.

ing *N*-acyl sulfenamides **20a**–**d**. Moreover, the bioactive motifs on both thiols and dioxazolones were well tolerated in late-stage functionalizations, representing excellent chemoselectivity (**20e**–**g**). This copper-catalyzed conjugative strategy allows for the modular preparation of biologically relevant *N*-acyl sulfenamides.

Based on several mechanistic experiments, a plausible reaction pathway is described in Figure 6. Decarboxylation of dioxazolone in **INT-22** forms the copper nitrene intermediate **INT-23**. The thiol then attacks the electrophilic nitrogen center of **INT-23**, which further leads to the formation of intermediate **INT-24**. Finally, the desired product **20** is afforded through protonolysis, regenerating the active copper species to complete the catalytic cycle.

2 Amidation via oxidative insertion to N–O bonds and reductive elimination

2.1 Hydroamidation of vinylarenes

Amines bearing stereogenic centers have been widely investigated in the research area of medicinal chemistry [93-97]. In 2018, Buchwald and co-workers unveiled the enantioselective synthesis of benzylic amines through the asymmetric Markovnikov hydroamidation of alkenes utilizing diphenylsilane in copper catalysis under mild reaction conditions [98]. Dioxazolones, as amide sources, were employed in this transformation.

As shown in Scheme 8, several dioxazolones containing electron-rich substituents were transformed into the desired products with excellent enantioselectivity (**23a** and **23b**). Otherwise, the electron-poor substituent-containing dioxazolones showed slightly diminished reactivity (**23c** and **23d**). In addition, poor reactivity was observed with dioxazolones bearing thiophene, implying that the undesired coordination of sulfur to copper reduces the reactivity (**23e**). Despite the reduced reactivity, excellent enantioselectivity was still maintained. Moreover, styrene derivatives bearing both electron-rich and electron-poor groups underwent the desired transformation with high yields and enantioselectivities (**23g** and **23h**). However, the styrene scaffold bearing a trifluoromethyl group showed reduced enantioselectivity (**23i**). Styrenes containing heterocyclic motifs

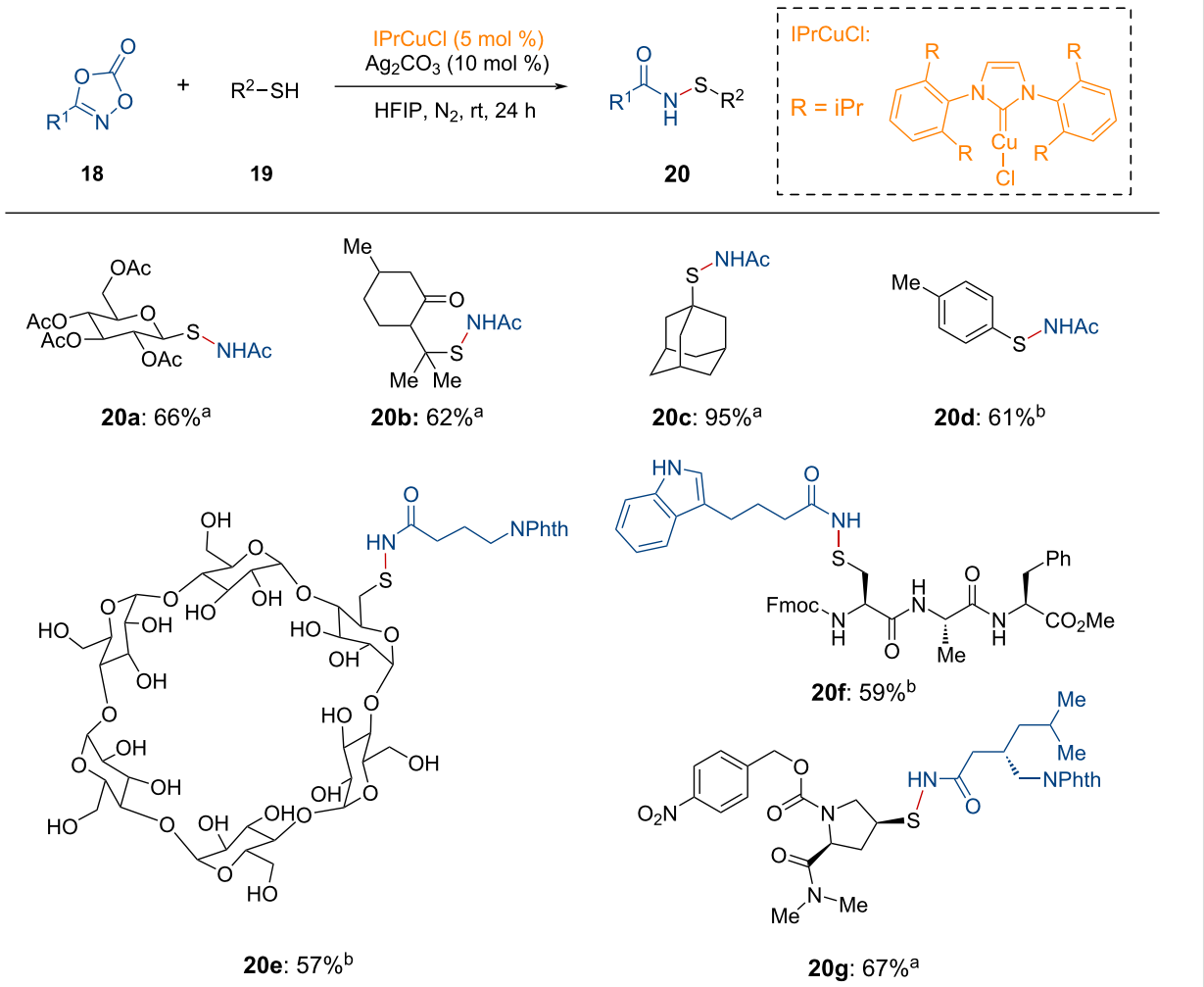

Scheme 7: Copper-catalyzed synthesis of *N*-acyl sulfenamides. [a]1.0 equiv of **18** and 2.0 equiv of **19** were used. [b]2.0 equiv of **18** and 1.0 equiv of **19** were used.

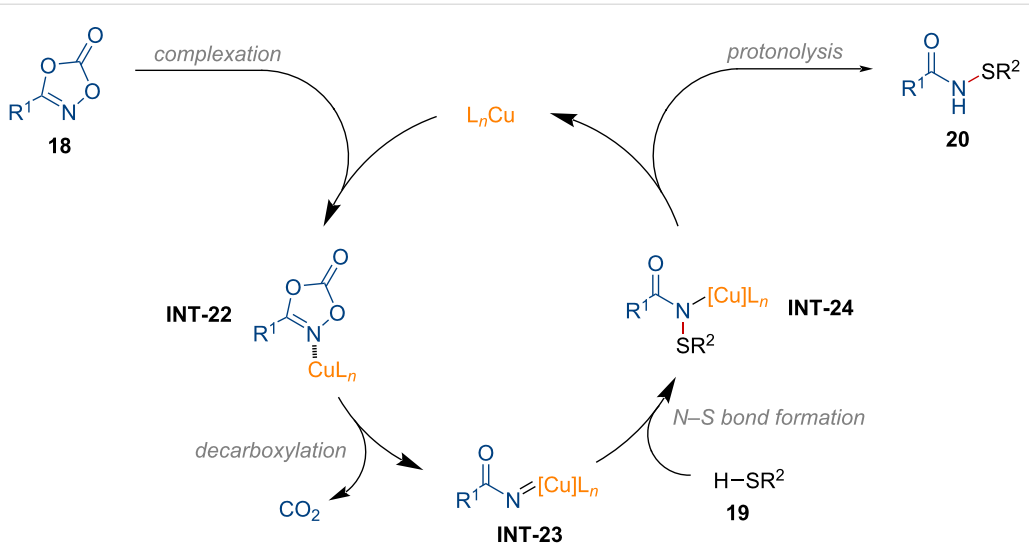

Figure 6: Proposed reaction mechanism for the copper-catalyzed *S*-amidation of thiols.

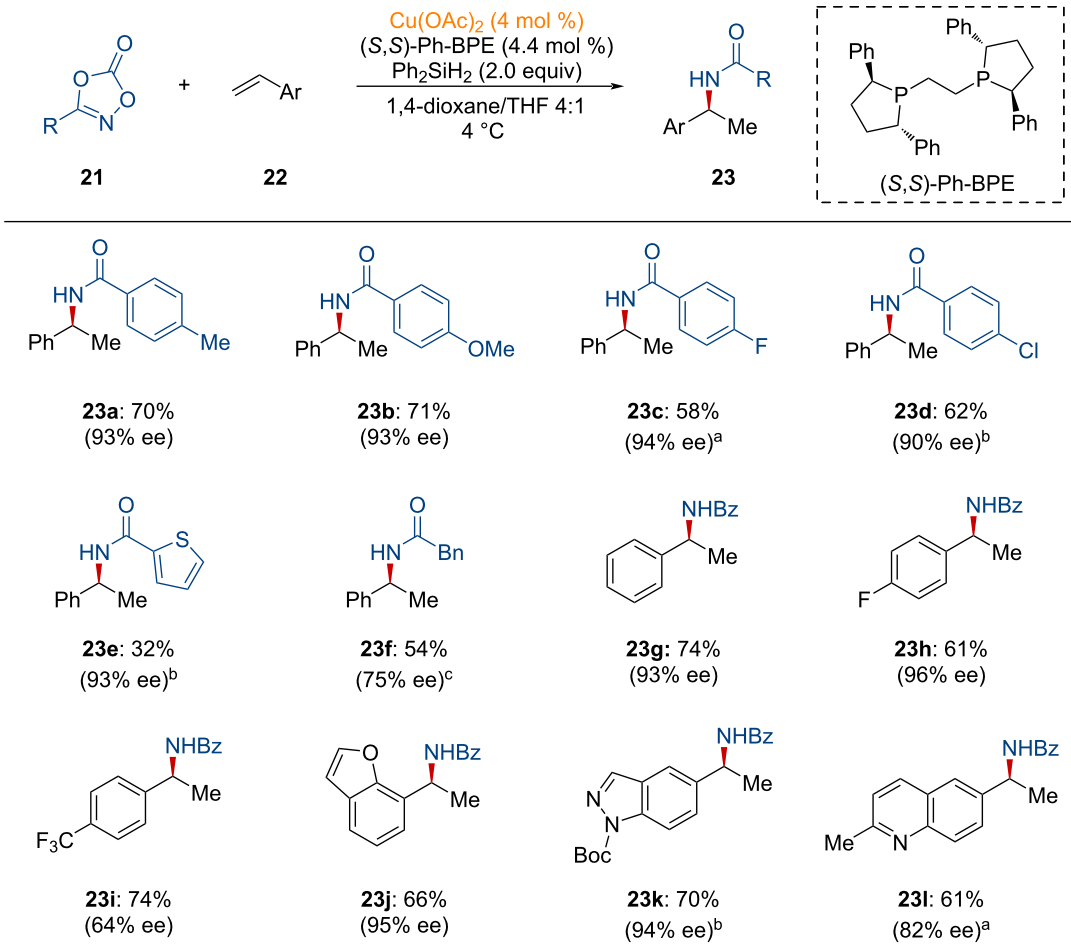

Scheme 8: Copper-catalyzed asymmetric hydroamidation of vinylarenes. [a]4 mol % + 2 mol % catalyst was used. [b]4 mol % + 4 mol % catalyst was used. [c]Slow addition of the amide electrophile solution.

such as a benzofuran, indazole, and quinoline were also shown to undergo the desired Markovnikov amidation with high efficiency (**23j–l**).

Several mechanistic experiments were performed to rationalize the reaction pathways. As shown in Figure 7, copper hydride, generated from a copper precatalyst and silane, undergoes the enantio-determining hydrocupration of the vinylarene, affording **INT-25** [25]. Next, oxidative insertion of **INT-25** into the N–O bond of the dioxazolone, forms **INT-26**, followed by decarboxylative reductive elimination to generate **INT-27**. Further incorporation of silane delivers the targeted amidated product upon protonation, while simultaneously regenerating the active copper hydride species.

2.2 Hydroamidation of alkynes

In 2022, Sato and co-workers introduced a copper-catalyzed hydroamidation of alkynes **25** using dioxazolones **24** as amide sources (Scheme 9) [99].

A dioxazolone bearing a linear alkyl group was efficiently converted to the *N*-vinylamide **26a** in good yield. The observed regioselectivity followed the anti-Markovnikov fashion stemming from the regioselective hydrozirconation of the alkyne using Schwartz's reagent [100]. Aryl substituents on the dioxazolone were tolerated, while a dioxazolone containing bromobenzene displayed lower reactivity (**26c**). The enamide **26d**, derived from lobatamide, was successfully produced without altering the stereochemistry of the oxime ether. Terminal alkynes with linear alkyl group, protected alcohol, and sulfonamide functionalities were well tolerated in this transformation (**26e–g**). Moreover, an olefin-containing terminal alkyne was suitable to afford product **26h**, demonstrating excellent chemoselectivity. However, the formation of **26i** was not observed under the standard reaction conditions. Instead, the decomposition of phenylacetylene was confirmed. Based on previous mechanistic insight from electrophilic amidation studies [101,102], the catalytic amidation of alkynes is proposed as shown in Figure 8.

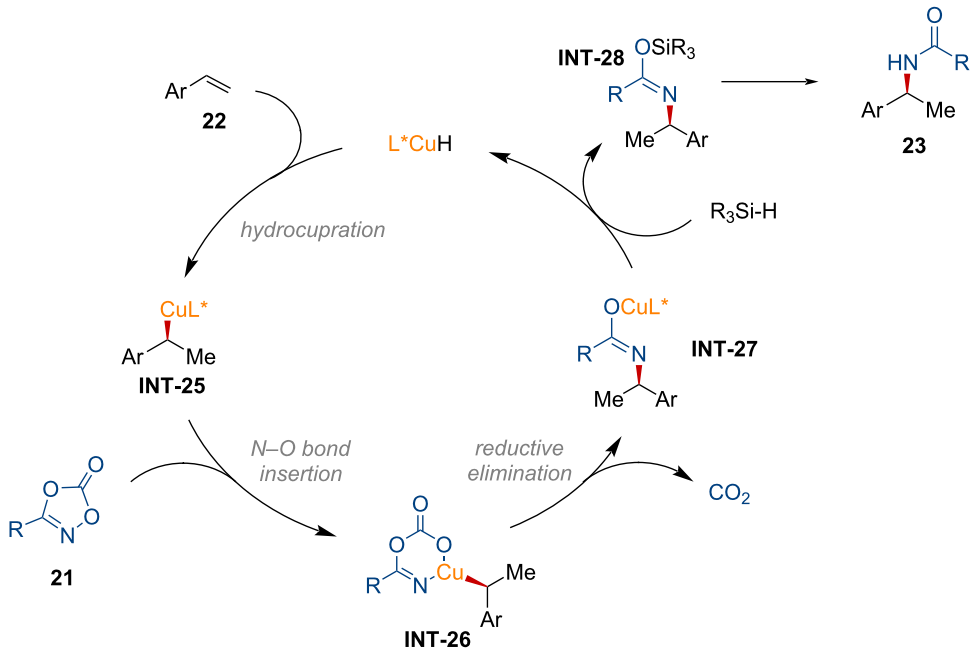

Figure 7: Proposed reaction mechanism for the copper-catalyzed hydroamidation of vinylarenes.

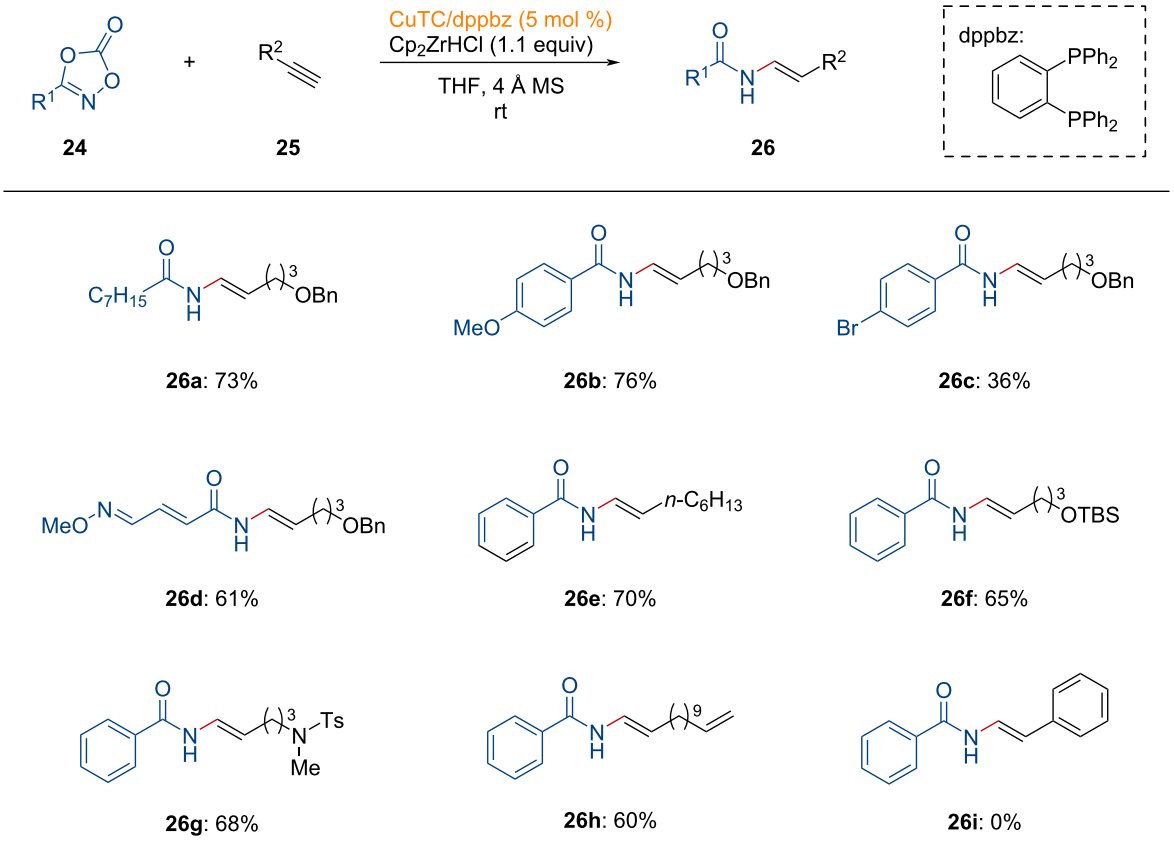

Scheme 9: Copper-catalyzed anti-Markovnikov hydroamidation of alkynes.

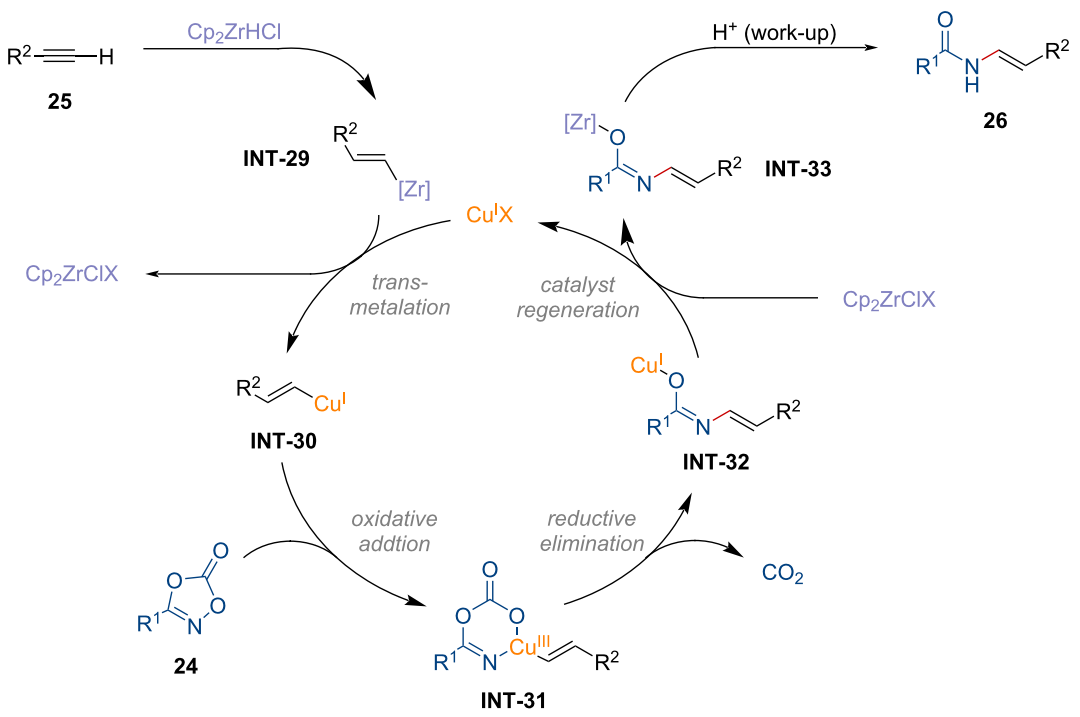

Figure 8: Proposed reaction mechanism for the copper-catalyzed amidation of alkynes.

First, the alkenylzirconium complex **INT-29**, formed through hydrozirconation of alkyne **25**, undergoes transmetalation with the copper catalyst, providing the vinyl copper intermediate **INT-30**. This intermediate then undergoes oxidative addition to the N–O bond of the dioxazolone to generate **INT-31**. Subsequently, decarboxylative reductive elimination occurs, forming the copper imidate **INT-32**. The active copper species is regenerated by the zirconium species, producing the formation of the desired product via the zirconium imidate **INT-33** after aqueous workup. Overall, this copper-catalyzed transformation requires a stoichiometric amount of zirconium species to achieve the anti-Markovnikov amidation.

3 Miscellaneous

3.1 Synthesis of primary amides via the generation of copper–imidate radical intermediates

In a subsequent study, the research group of Son developed a method for the reduction of dioxazolones to synthesize primary amides under mild reducing conditions in copper catalysis (Scheme 10) [103].

The reaction was conducted using a catalytic amount of copper acetate and a phenanthroline ligand, with a stoichiometric amount of silane serving as the reductant. Both aryl- and alkyl-substituted dioxazolones proved to be compatible under the standard reaction conditions, yielding the desired primary amides **28a**–**f**. Notably, dioxazolones containing free -OH groups exhibited excellent functional group tolerance, leading to the formation of primary amides **28g** and **28h**. Moreover, biologically relevant scaffolds on dioxazolones were successfully transformed in this transformation (**28i**–**k**). As illustrated in Figure 9, a catalytic cycle was proposed for the copper-catalyzed synthesis of primary amides.

Dioxazolone first binds to the copper catalyst, forming the dioxazolone-copper complex (**INT-34**). The silane reductant then reduces **INT-34**, forming the copper imidate radical species **INT-35**, furnishing the formation of primary amides **28** via intermediate **INT-36**. The involvement of a radical intermediate was suggested by experiments using TEMPO as a radical scavenger.

Conclusion

This review provides an overview of the recent copper-catalyzed and/or -promoted transformations of dioxazolones, describing examples of C(sp^2)–N, C(sp^3)–N, S–N, P–N, and N–H bond-forming reactions. Several studies have proposed copper nitrenoid intermediates originating from dioxazolones, involving an *N*-acyl nitrene transfer or hydrogen atom transfer process, representing creative synthetic solutions that were previously unachievable using conventional approaches. Despite the synthetic strategies to generate the copper nitrenoid intermediates are gaining more attention [104,105], several limitations still remain. First, multiple steps are required to prepare dioxa-

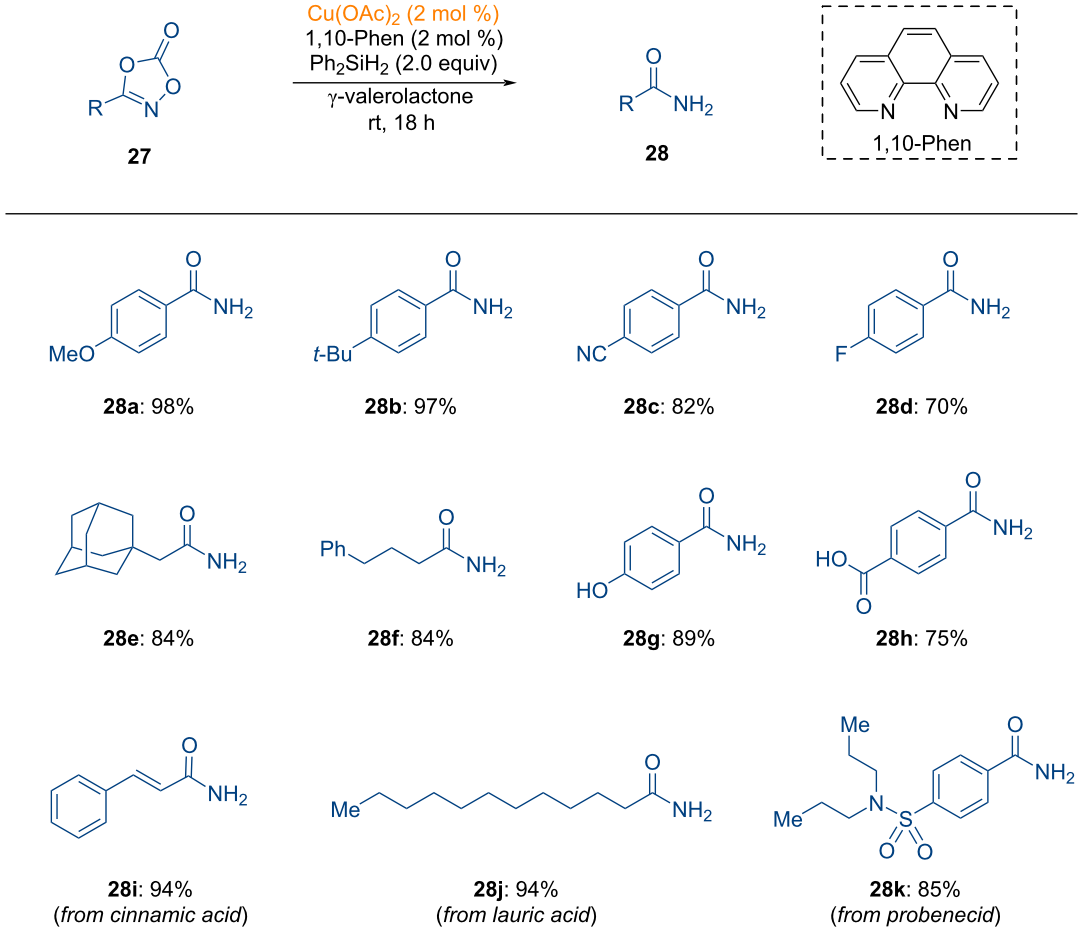

Scheme 10: Copper-catalyzed preparation of primary amides through N–O bond reduction using reducing agent.

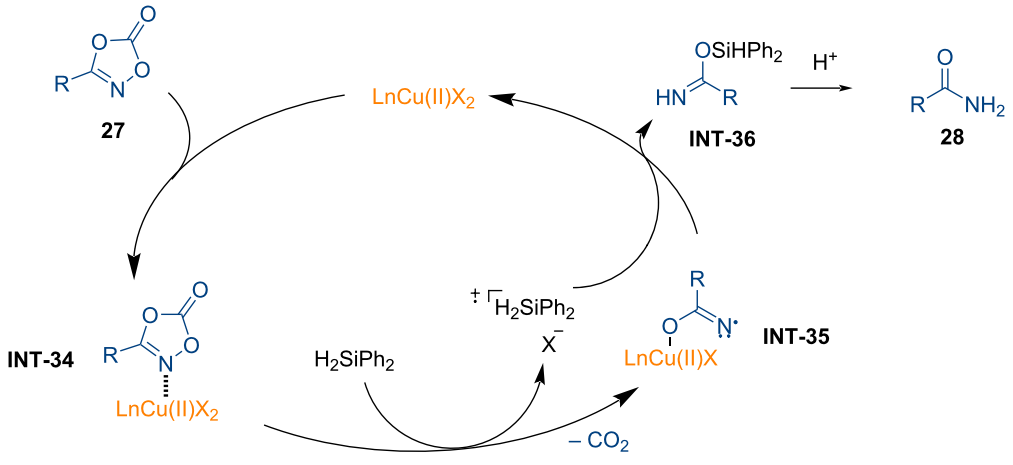

Figure 9: Proposed catalytic cycle for the copper-catalyzed reduction of dioxazolones.

zolones, synthesized conventionally from carboxylic acids or acid chlorides over two steps. Moreover, copper-catalyzed asymmetric C(sp^3)–N bond-forming transformations are still underexplored except for elegant studies by the research groups of Buchwald [98] and Chang [74]. Given the versatility and sustainability of the copper-catalyzed transformation of dioxa-

zolones, further investigations for late-stage functionalizations of complex scaffolds such as peptides, drug molecules, and natural products containing unprotected free OH and NH groups are anticipated.

Funding

This work was supported by the National Research Foundation of Korea grant (RS-2024-00333890) funded by the South Korean Government (MSIT). This work was also supported by the Korea Environment Industry & Technology Institute (KEITI) through the Technology Development Program for Safety Management of Household Chemical Products, funded by the Korea Ministry of Environment (MOE) (2022002980008).

ORCID® iDs

Seungmin Lee - https://orcid.org/0009-0008-5069-0843
Hyewon Han - https://orcid.org/0009-0002-9645-2150
Jongwoo Son - https://orcid.org/0000-0003-0420-5065

Data Availability Statement

Data sharing is not applicable as no new data was generated or analyzed in this study.

References

1. Beck, G. *Chem. Ber.* **1951,** *84,* 688–689. doi:10.1002/cber.19510840807
2. Dubé, P.; Nathel, N. F. F.; Vetelino, M.; Couturier, M.; Aboussafy, C. L.; Pichette, S.; Jorgensen, M. L.; Hardink, M. *Org. Lett.* **2009,** *11,* 5622–5625. doi:10.1021/ol9023387
3. Sauer, J.; Mayer, K. K. *Tetrahedron Lett.* **1968,** *9,* 319–324. doi:10.1016/s0040-4039(01)98753-2
4. Sheng, Y.; Zhou, J.; Gao, Y.; Duan, B.; Wang, Y.; Samorodov, A.; Liang, G.; Zhao, Q.; Song, Z. *J. Org. Chem.* **2021,** *86,* 2827–2839. doi:10.1021/acs.joc.0c02779
5. Devkota, S.; Kim, S.; Yoo, S. Y.; Mohandoss, S.; Baik, M.-H.; Lee, Y. R. *Chem. Sci.* **2021,** *12,* 11427–11437. doi:10.1039/d1sc02138a
6. Zhou, Z.; Chen, S.; Hong, Y.; Winterling, E.; Tan, Y.; Hemming, M.; Harms, K.; Houk, K. N.; Meggers, E. *J. Am. Chem. Soc.* **2019,** *141,* 19048–19057. doi:10.1021/jacs.9b09301
7. Massouh, J.; Petrelli, A.; Bellière-Baca, V.; Hérault, D.; Clavier, H. *Adv. Synth. Catal.* **2022,** *364,* 831–837. doi:10.1002/adsc.202101099
8. Lee, M.; Heo, J.; Kim, D.; Chang, S. *J. Am. Chem. Soc.* **2022,** *144,* 3667–3675. doi:10.1021/jacs.1c12934
9. Lee, S.; Rovis, T. *ACS Catal.* **2021,** *11,* 8585–8590. doi:10.1021/acscatal.1c02406
10. Wang, W.; Wu, J.; Kuniyil, R.; Kopp, A.; Lima, R. N.; Ackermann, L. *Chem* **2020,** *6,* 3428–3439. doi:10.1016/j.chempr.2020.10.026
11. Tang, S.-B.; Fu, X.-P.; Wu, G.-R.; Zhang, L.-L.; Deng, K.-Z.; Yang, J.-Y.; Xia, C.-C.; Ji, Y.-F. *Org. Biomol. Chem.* **2020,** *18,* 7922–7931. doi:10.1039/d0ob01655a
12. Shi, P.; Tu, Y.; Wang, C.; Kong, D.; Ma, D.; Bolm, C. *Org. Lett.* **2020,** *22,* 8842–8845. doi:10.1021/acs.orglett.0c03212
13. Park, Y.; Park, K. T.; Kim, J. G.; Chang, S. *J. Am. Chem. Soc.* **2015,** *137,* 4534–4542. doi:10.1021/jacs.5b01324
14. Park, Y.; Jee, S.; Kim, J. G.; Chang, S. *Org. Process Res. Dev.* **2015,** *19,* 1024–1029. doi:10.1021/acs.oprd.5b00164
15. Antien, K.; Geraci, A.; Parmentier, M.; Baudoin, O. *Angew. Chem., Int. Ed.* **2021,** *60,* 22948–22955. doi:10.1002/anie.202110019
16. Hong, S. Y.; Park, Y.; Hwang, Y.; Kim, Y. B.; Baik, M.-H.; Chang, S. *Science* **2018,** *359,* 1016–1021. doi:10.1126/science.aap7503
17. Hwang, Y.; Park, Y.; Chang, S. *Chem. – Eur. J.* **2017,** *23,* 11147–11152. doi:10.1002/chem.201702397
18. Hong, S. Y.; Hwang, Y.; Lee, M.; Chang, S. *Acc. Chem. Res.* **2021,** *54,* 2683–2700. doi:10.1021/acs.accounts.1c00198
19. van Vliet, K. M.; de Bruin, B. *ACS Catal.* **2020,** *10,* 4751–4769. doi:10.1021/acscatal.0c00961
20. Xiong, Y.; Li, S.; Xiao, H.; Zhang, G. *Synthesis* **2021,** *53,* 4327–4340. doi:10.1055/a-1533-3597
21. Fairoosa, J.; Neetha, M.; Anilkumar, G. *RSC Adv.* **2021,** *11,* 3452–3469. doi:10.1039/d0ra10472h
22. Chen, C.; Peters, J. C.; Fu, G. C. *Nature* **2021,** *596,* 250–256. doi:10.1038/s41586-021-03730-w
23. Afsina, C. M. A.; Aneeja, T.; Neetha, M.; Anilkumar, G. *Eur. J. Org. Chem.* **2021,** 1776–1808. doi:10.1002/ejoc.202001549
24. Sekar, G.; Sangeetha, S.; Nandy, A.; Saha, R. Cu-Catalyzed Reactions for Carbon–Heteroatom Bond Formations. In *Copper Catalysis in Organic Synthesis;* Anilkumar, G.; Saranya, S., Eds.; Wiley-VCH: Weinheim, Germany, 2020; pp 395–422. doi:10.1002/9783527826445.ch18
25. Liu, R. Y.; Buchwald, S. L. *Acc. Chem. Res.* **2020,** *53,* 1229–1243. doi:10.1021/acs.accounts.0c00164
26. Trammell, R.; Rajabimoghadam, K.; Garcia-Bosch, I. *Chem. Rev.* **2019,** *119,* 2954–3031. doi:10.1021/acs.chemrev.8b00368
27. McCann, S. D.; Stahl, S. S. *Acc. Chem. Res.* **2015,** *48,* 1756–1766. doi:10.1021/acs.accounts.5b00060
28. Allen, S. E.; Walvoord, R. R.; Padilla-Salinas, R.; Kozlowski, M. C. *Chem. Rev.* **2013,** *113,* 6234–6458. doi:10.1021/cr300527g
29. Jones, G. O.; Liu, P.; Houk, K. N.; Buchwald, S. L. *J. Am. Chem. Soc.* **2010,** *132,* 6205–6213. doi:10.1021/ja100739h
30. Strieter, E. R.; Bhayana, B.; Buchwald, S. L. *J. Am. Chem. Soc.* **2009,** *131,* 78–88. doi:10.1021/ja0781893
31. Zheng, Z.-G.; Wen, J.; Wang, N.; Wu, B.; Yu, X.-Q. *Beilstein J. Org. Chem.* **2008,** *4,* 40. doi:10.3762/bjoc.4.40
32. Strieter, E. R.; Blackmond, D. G.; Buchwald, S. L. *J. Am. Chem. Soc.* **2005,** *127,* 4120–4121. doi:10.1021/ja050120c
33. Lan, J.-B.; Zhang, G.-L.; Yu, X.-Q.; You, J.-S.; Chen, L.; Yan, M.; Xie, R.-G. *Synlett* **2004,** 1095–1097. doi:10.1055/s-2004-820059
34. Klapars, A.; Huang, X.; Buchwald, S. L. *J. Am. Chem. Soc.* **2002,** *124,* 7421–7428. doi:10.1021/ja0260465
35. Wolter, M.; Klapars, A.; Buchwald, S. L. *Org. Lett.* **2001,** *3,* 3803–3805. doi:10.1021/ol0168216
36. Klapars, A.; Antilla, J. C.; Huang, X.; Buchwald, S. L. *J. Am. Chem. Soc.* **2001,** *123,* 7727–7729. doi:10.1021/ja016226z
37. Altman, R. A.; Shafir, A.; Choi, A.; Lichtor, P. A.; Buchwald, S. L. *J. Org. Chem.* **2008,** *73,* 284–286. doi:10.1021/jo702024p
38. Ma, D.; Cai, Q. *Org. Lett.* **2003,** *5,* 3799–3802. doi:10.1021/ol0350947
39. Lam, P. Y. S.; Vincent, G.; Bonne, D.; Clark, C. G. *Tetrahedron Lett.* **2003,** *44,* 4927–4931. doi:10.1016/s0040-4039(03)01037-2
40. Lam, P. Y. S.; Bonne, D.; Vincent, G.; Clark, C. G.; Combs, A. P. *Tetrahedron Lett.* **2003,** *44,* 1691–1694. doi:10.1016/s0040-4039(02)02882-4

41. Chan, D. M. T.; Monaco, K. L.; Li, R.; Bonne, D.; Clark, C. G.; Lam, P. Y. S. *Tetrahedron Lett.* **2003,** *44,* 3863–3865. doi:10.1016/s0040-4039(03)00739-1
42. Lam, P. Y. S.; Deudon, S.; Hauptman, E.; Clark, C. G. *Tetrahedron Lett.* **2001,** *42,* 2427–2429. doi:10.1016/s0040-4039(01)00203-9
43. Deutsch, C.; Krause, N.; Lipshutz, B. H. *Chem. Rev.* **2008,** *108,* 2916–2927. doi:10.1021/cr0684321
44. Xi, Y.; Hartwig, J. F. *J. Am. Chem. Soc.* **2017,** *139,* 12758–12772. doi:10.1021/jacs.7b07124
45. Zhu, S.; Niljianskul, N.; Buchwald, S. L. *J. Am. Chem. Soc.* **2013,** *135,* 15746–15749. doi:10.1021/ja4092819
46. Lee, J.-E.; Yun, J. *Angew. Chem., Int. Ed.* **2008,** *47,* 145–147. doi:10.1002/anie.200703699
47. Lee, D.-w.; Yun, J. *Tetrahedron Lett.* **2004,** *45,* 5415–5417. doi:10.1016/j.tetlet.2004.05.048
48. Lee, D.; Kim, D.; Yun, J. *Angew. Chem., Int. Ed.* **2006,** *45,* 2785–2787. doi:10.1002/anie.200600184
49. Noh, D.; Chea, H.; Ju, J.; Yun, J. *Angew. Chem., Int. Ed.* **2009,** *48,* 6062–6064. doi:10.1002/anie.200902015
50. Rucker, R. P.; Whittaker, A. M.; Dang, H.; Lalic, G. *J. Am. Chem. Soc.* **2012,** *134,* 6571–6574. doi:10.1021/ja3023829
51. Lalic, G.; Rucker, R. P. *Synlett* **2013,** *24,* 269–275. doi:10.1055/s-0032-1317744
52. Uehling, M. R.; Suess, A. M.; Lalic, G. *J. Am. Chem. Soc.* **2015,** *137,* 1424–1427. doi:10.1021/ja5124368
53. Yang, X.; Tsui, G. C. *Org. Lett.* **2020,** *22,* 4562–4567. doi:10.1021/acs.orglett.0c01646
54. Dong, T.; Tsui, G. C. *Chem. Rec.* **2021,** *21,* 4015–4031. doi:10.1002/tcr.202100231
55. Yang, X.; Tsui, G. C. *Synlett* **2022,** *33,* 713–720. doi:10.1055/a-1709-3098
56. Fu, Z.; Tsui, G. C. *Org. Chem. Front.* **2024,** *11,* 4697–4701. doi:10.1039/d4qo00768a
57. Hoover, J. M.; Stahl, S. S. *J. Am. Chem. Soc.* **2011,** *133,* 16901–16910. doi:10.1021/ja206230h
58. Hill, N. J.; Hoover, J. M.; Stahl, S. S. *J. Chem. Educ.* **2013,** *90,* 102–105. doi:10.1021/ed300368q
59. Ochen, A.; Whitten, R.; Aylott, H. E.; Ruffell, K.; Williams, G. D.; Slater, F.; Roberts, A.; Evans, P.; Steves, J. E.; Sanganee, M. J. *Organometallics* **2019,** *38,* 176–184. doi:10.1021/acs.organomet.8b00546
60. Steves, J. E.; Stahl, S. S. *J. Am. Chem. Soc.* **2013,** *135,* 15742–15745. doi:10.1021/ja409241h
61. Hoover, J. M.; Ryland, B. L.; Stahl, S. S. *J. Am. Chem. Soc.* **2013,** *135,* 2357–2367. doi:10.1021/ja3117203
62. Ratani, T. S.; Bachman, S.; Fu, G. C.; Peters, J. C. *J. Am. Chem. Soc.* **2015,** *137,* 13902–13907. doi:10.1021/jacs.5b08452
63. Kainz, Q. M.; Matier, C. D.; Bartoszewicz, A.; Zultanski, S. L.; Peters, J. C.; Fu, G. C. *Science* **2016,** *351,* 681–684. doi:10.1126/science.aad8313
64. Ahn, J. M.; Ratani, T. S.; Hannoun, K. I.; Fu, G. C.; Peters, J. C. *J. Am. Chem. Soc.* **2017,** *139,* 12716–12723. doi:10.1021/jacs.7b07052
65. Matier, C. D.; Schwaben, J.; Peters, J. C.; Fu, G. C. *J. Am. Chem. Soc.* **2017,** *139,* 17707–17710. doi:10.1021/jacs.7b09582
66. Ahn, J. M.; Peters, J. C.; Fu, G. C. *J. Am. Chem. Soc.* **2017,** *139,* 18101–18106. doi:10.1021/jacs.7b10907
67. Bartoszewicz, A.; Matier, C. D.; Fu, G. C. *J. Am. Chem. Soc.* **2019,** *141,* 14864–14869. doi:10.1021/jacs.9b07875
68. Chen, C.; Fu, G. C. *Nature* **2023,** *618,* 301–307. doi:10.1038/s41586-023-06001-y
69. Caruano, J.; Muccioli, G. G.; Robiette, R. *Org. Biomol. Chem.* **2016,** *14,* 10134–10156. doi:10.1039/c6ob01349j
70. Lepikhina, A.; Bakulina, O.; Dar'in, D.; Krasavin, M. *RSC Adv.* **2016,** *6,* 83808–83813. doi:10.1039/c6ra19196g
71. Seibel, J.; Brown, D.; Amour, A.; Macdonald, S. J.; Oldham, N. J.; Schofield, C. J. *Bioorg. Med. Chem. Lett.* **2003,** *13,* 387–389. doi:10.1016/s0960-894x(02)00995-2
72. Mladentsev, D. Y.; Kuznetsova, E. N.; Skvortsova, M. N.; Dashkin, R. R. *Org. Process Res. Dev.* **2022,** *26,* 2311–2329. doi:10.1021/acs.oprd.2c00188
73. Patel, R.; Evitt, L.; Mariolis, I.; Di Giambenedetto, S.; d'Arminio Monforte, A.; Casado, J.; Cabello Úbeda, A.; Hocqueloux, L.; Allavena, C.; Barber, T.; Jha, D.; Kumar, R.; Kamath, R. D.; Vincent, T.; van Wyk, J.; Koteff, J. *Infect. Dis. Ther.* **2021,** *10,* 2051–2070. doi:10.1007/s40121-021-00522-7
74. Kim, S.; Song, S. L.; Zhang, J.; Kim, D.; Hong, S.; Chang, S. *J. Am. Chem. Soc.* **2023,** *145,* 16238–16248. doi:10.1021/jacs.3c05258
75. Jung, H.; Kweon, J.; Suh, J.-M.; Lim, M. H.; Kim, D.; Chang, S. *Science* **2023,** *381,* 525–532. doi:10.1126/science.adh8753
76. Liu, X.; Li, W.; Jiang, W.; Lu, H.; Liu, J.; Lin, Y.; Cao, H. *Org. Lett.* **2022,** *24,* 613–618. doi:10.1021/acs.orglett.1c04044
77. van Vliet, K. M.; Polak, L. H.; Siegler, M. A.; van der Vlugt, J. I.; Guerra, C. F.; de Bruin, B. *J. Am. Chem. Soc.* **2019,** *141,* 15240–15249. doi:10.1021/jacs.9b07140
78. Sprogøe, K.; Manniche, S.; Larsen, T. O.; Christophersen, C. *Tetrahedron* **2005,** *61,* 8718–8721. doi:10.1016/j.tet.2005.06.086
79. Greenhill, J. V.; Lue, P. Amidines and Guanidines in Medicinal Chemistry. In *Progress in Medicinal Chemistry;* Ellis, G. P.; Luscombe, D. K., Eds.; Elsevier: Amsterdam, Netherlands, 1993; Vol. 30, pp 203–326. doi:10.1016/s0079-6468(08)70378-3
80. Wesseling, C. M. J.; Slingerland, C. J.; Veraar, S.; Lok, S.; Martin, N. I. *ACS Infect. Dis.* **2021,** *7,* 3314–3335. doi:10.1021/acsinfecdis.1c00466
81. Arya, S.; Kumar, N.; Roy, P.; Sondhi, S. M. *Eur. J. Med. Chem.* **2013,** *59,* 7–14. doi:10.1016/j.ejmech.2012.10.046
82. Guo, X.; Facchetti, A.; Marks, T. J. *Chem. Rev.* **2014,** *114,* 8943–9021. doi:10.1021/cr500225d
83. Pitzer, J.; Steiner, K. *J. Biotechnol.* **2016,** *235,* 32–46. doi:10.1016/j.jbiotec.2016.03.023
84. Zhang, D.-W.; Zhao, X.; Hou, J.-L.; Li, Z.-T. *Chem. Rev.* **2012,** *112,* 5271–5316. doi:10.1021/cr300116k
85. Ghose, A. K.; Viswanadhan, V. N.; Wendoloski, J. J. *J. Comb. Chem.* **1999,** *1,* 55–68. doi:10.1021/cc9800071
86. Isidro-Llobet, A.; Kenworthy, M. N.; Mukherjee, S.; Kopach, M. E.; Wegner, K.; Gallou, F.; Smith, A. G.; Roschangar, F. *J. Org. Chem.* **2019,** *84,* 4615–4628. doi:10.1021/acs.joc.8b03001
87. El-Faham, A.; Albericio, F. *Chem. Rev.* **2011,** *111,* 6557–6602. doi:10.1021/cr100048w
88. Valeur, E.; Bradley, M. *Chem. Soc. Rev.* **2009,** *38,* 606–631. doi:10.1039/b701677h
89. Han, S.-Y.; Kim, Y.-A. *Tetrahedron* **2004,** *60,* 2447–2467. doi:10.1016/j.tet.2004.01.020
90. Adegboyega, A. K.; Son, J. *Org. Lett.* **2022,** *24,* 4925–4929. doi:10.1021/acs.orglett.2c01837

91. Park, J.; Krishnapriya, A. U.; Park, Y.; Kim, M.; Reidl, T. W.; Kuniyil, R.; Son, J. *Adv. Synth. Catal.* **2023,** *365,* 4495–4501. doi:10.1002/adsc.202300693
92. Bai, Z.; Zhu, S.; Hu, Y.; Yang, P.; Chu, X.; He, G.; Wang, H.; Chen, G. *Nat. Commun.* **2022,** *13,* 6445. doi:10.1038/s41467-022-34223-7
93. Mikami, S.; Sasaki, S.; Asano, Y.; Ujikawa, O.; Fukumoto, S.; Nakashima, K.; Oki, H.; Kamiguchi, N.; Imada, H.; Iwashita, H.; Taniguchi, T. *J. Med. Chem.* **2017,** *60,* 7658–7676. doi:10.1021/acs.jmedchem.7b00709
94. Branch, S. K.; Agranat, I. *J. Med. Chem.* **2014,** *57,* 8729–8765. doi:10.1021/jm402001w
95. Naito, R.; Yonetoku, Y.; Okamoto, Y.; Toyoshima, A.; Ikeda, K.; Takeuchi, M. *J. Med. Chem.* **2005,** *48,* 6597–6606. doi:10.1021/jm050099q
96. Patchett, A. A. *J. Med. Chem.* **1993,** *36,* 2051–2058. doi:10.1021/jm00067a001
97. Ananthanarayanan, V. S.; Tetreault, S.; Saint-Jean, A. *J. Med. Chem.* **1993,** *36,* 1324–1332. doi:10.1021/jm00062a004
98. Zhou, Y.; Engl, O. D.; Bandar, J. S.; Chant, E. D.; Buchwald, S. L. *Angew. Chem., Int. Ed.* **2018,** *57,* 6672–6675. doi:10.1002/anie.201802797
99. Banjo, S.; Nakata, K.; Nakasuji, E.; Yasui, S.; Chida, N.; Sato, T. *Org. Lett.* **2022,** *24,* 8662–8666. doi:10.1021/acs.orglett.2c03497
100. Hart, D. W.; Schwartz, J. *J. Am. Chem. Soc.* **1974,** *96,* 8115–8116. doi:10.1021/ja00833a048
101. Banjo, S.; Nakasuji, E.; Meguro, T.; Sato, T.; Chida, N. *Chem. – Eur. J.* **2019,** *25,* 7941–7947. doi:10.1002/chem.201901145
102. Katahara, S.; Takahashi, T.; Nomura, K.; Uchiyama, M.; Sato, T.; Chida, N. *Chem. – Asian J.* **2020,** *15,* 1869–1872. doi:10.1002/asia.202000270
103. Bae, H.; Park, J.; Yoon, R.; Lee, S.; Son, J. *RSC Adv.* **2024,** *14,* 9440–9444. doi:10.1039/d4ra00320a
104. Ren, Z.; Feng, T.; Gao, T.; Han, B.; Guo, R.; Ma, H.; Wang, J.-J.; Zhang, Y. *Org. Lett.* **2024,** *26,* 8532–8536. doi:10.1021/acs.orglett.4c03118
105. Wan, Y.; Zhang, H. K.; Qian, J.; Aliyu, M. A.; Norton, J. R. *Chem* **2024,** *10,* 2538–2549. doi:10.1016/j.chempr.2024.04.020

License and Terms

BEILSTEIN JOURNAL OF ORGANIC CHEMISTRY

Recent advances in allylation of chiral secondary alkylcopper species

Minjae Kim[1], Gwanggyun Kim[1], Doyoon Kim[1], Jun Hee Lee[*2] and Seung Hwan Cho[*1]

Review

Open Access

Address:
[1]Department of Chemistry, Pohang University of Science and Technology (POSTECH), Pohang, 37673, Republic of Korea and [2]Department of Advanced Materials Chemistry, Dongguk University WISE, Gyeongju 38066, Republic of Korea

Email:
Jun Hee Lee[*] - leejunhee@dongguk.ac.kr;
Seung Hwan Cho[*] - seunghwan@postech.ac.kr

* Corresponding author

Keywords:
allylic substitution; chiral secondary organocopper; copper-mediated reaction; stereoselectivity

Beilstein J. Org. Chem. **2025,** *21,* 639–658.
https://doi.org/10.3762/bjoc.21.51

Received: 30 December 2024
Accepted: 13 March 2025
Published: 20 March 2025

This article is part of the thematic issue "Copper catalysis: a constantly evolving field".

Guest Editor: J. Yun

Abstract

The transition-metal-catalyzed asymmetric allylic substitution represents a pivotal methodology in organic synthesis, providing remarkable versatility for complex molecule construction. Particularly, the generation and utilization of chiral secondary alkylcopper species have received considerable attention due to their unique properties in stereoselective allylic substitution. This review highlights recent advances in copper-catalyzed asymmetric allylic substitution reactions with chiral secondary alkylcopper species, encompassing several key strategies for their generation: stereospecific transmetalation of organolithium and organoboron compounds, copper hydride catalysis, and enantiotopic-group-selective transformations of 1,1-diborylalkanes. Detailed mechanistic insights into stereochemical control and current challenges in this field are also discussed.

Introduction

The transition-metal-catalyzed regio- and enantioselective allylic substitution represents a pivotal methodology in organic synthesis, providing remarkable versatility for complex molecule construction [1-4]. The significance of this transformation lies in its unique ability to efficiently create a stereogenic center while forming new carbon–carbon or carbon–heteroatom bonds (e.g., C–N, C–O, and C–S) with excellent selectivities.

The field of metal-catalyzed allylic substitution has evolved significantly since its inception (Scheme 1). Early studies were mainly focused on palladium catalysts [5-8], as demonstrated by the independent pioneering works of Tsuji and Trost in the 1960s and 1970s, respectively. While palladium catalysts demonstrated excellent reactivity with soft stabilized nucleophiles in the eponymous Tsuji–Trost reaction, they faced a significant limitation: poor regioselectivity with non-symmetrical allylic substrates **2**. This constraint led to the predominant development of Pd-catalyzed methods using symmetric 1,3-disubstituted allylic substrates **1** that contain a leaving group in the allylic terminus.

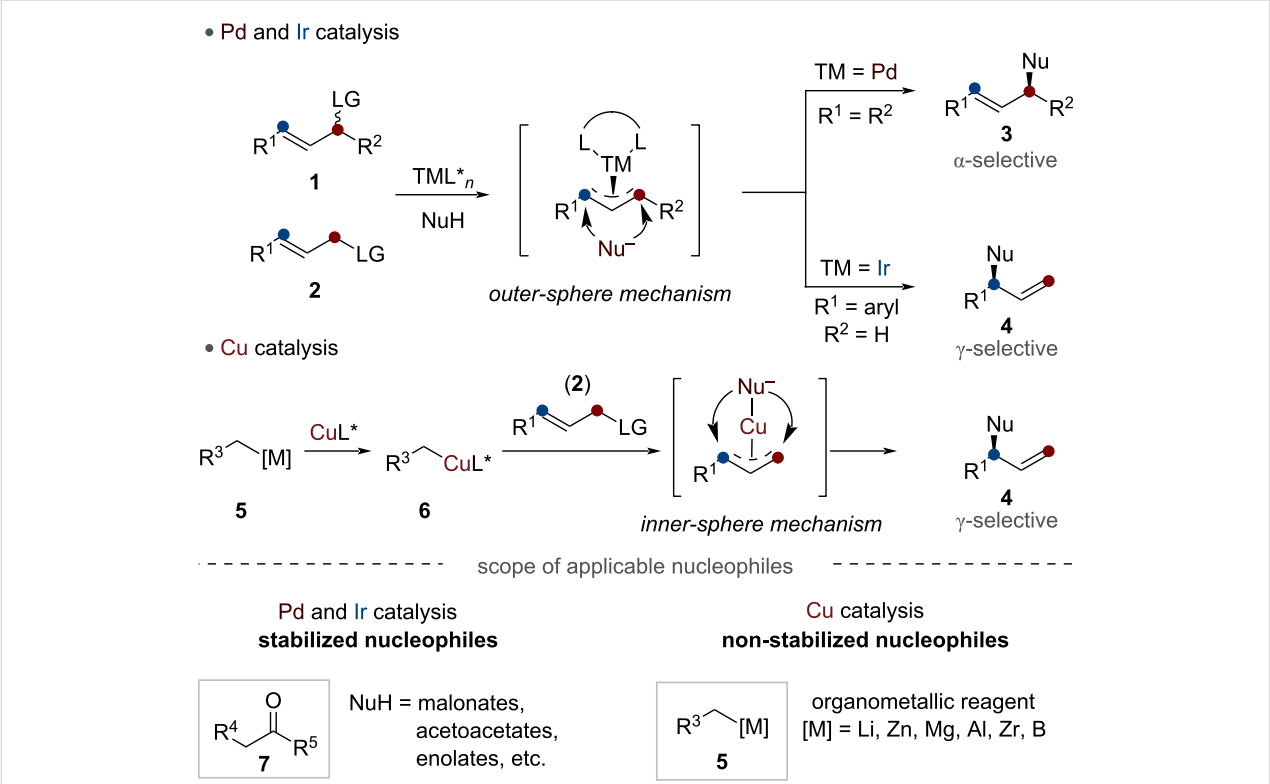

Scheme 1: Representative transition-metal catalysis for allylic substitution.

In search of complementary approaches, other transition metals including W [9], Mo [10], Ru [11,12], Rh [13-15], and Ni [16,17] have been explored. Among these alternatives, Ir catalysis emerged as a particularly powerful complement to Pd catalysis. The field of iridium-catalyzed allylic substitution reactions began to develop with the groundbreaking work of Takeuchi and Kashio, and subsequent research has revealed that iridium catalysts behave quite differently from their palladium counterparts [18]. The most notable distinction lies in their contrasting regioselectivity patterns. Palladium catalysts generally produce straight-chain products lacking chirality when reacting with monosubstituted allylic substrates, whereas iridium catalysts selectively generate branched products with high optical purity and precise control over the reaction site.

Furthermore, the development of chiral phosphoramidite ligands significantly advanced this field, with contributions from numerous research groups including Hartwig, Helmchen, Carreira, Alexakis, and You [19].

In general, soft nucleophiles that typically possess conjugate acids with pK_a values less than 25 have been utilized in most Pd and Ir-catalyzed allylic substitution reactions [20]. To address these limitations, copper-catalyzed processes have emerged as a promising alternative. Copper-catalyzed allylic substitutions are distinguished by their unique inner-sphere mechanistic pathway, which enables the incorporation of hard, non-stabilized nucleophiles **5** that have conjugate acids with pK_a values greater than 25 such as organolithium, organomagnesium, organozinc, and organozirconium reagents. This crucial distinction effectively expanded the scope of allylic substitution reactions beyond traditional boundaries.

The evolution of copper-catalyzed asymmetric allylic alkylation (AAA) has been remarkable since its initial development in 1995, when Bäckvall and van Koten first reported moderate enantioselectivity using Grignard reagents with allylic acetates [21,22]. This discovery triggered extensive research endeavors, significantly expanding the scope and efficiency of these reactions. A notable advancement came from Knochel's introduction of dialkylzinc reagents in 1999, which substantially broadened the range of applicable organometallic compounds [23].

Subsequent significant progress was achieved independently by Feringa and Alexakis through their exploration of phosphoramidite ligands with various organometallic nucleophiles [24,25]. The field was further advanced by the research group of Hoveyda, who made substantial contributions by introducing bidentate N-heterocyclic carbene (NHC)-based chiral ligands, achieving high selectivity with dialkylzinc reagents as nucleo-

philes [26]. They subsequently expanded the methodology by successfully employing triorganoaluminum reagents [27].

Recent developments in transition-metal-catalyzed AAA have increasingly turned to organoboron compounds [28-31]. These reagents offer numerous advantages, including non-toxicity, bench-stability, structural diversity, straightforward preparation, and broad commercial availability. Significant contributions include Sawamura's work with alkyl–9-BBN [32-37] as a nucleophile. These developments have collectively transformed copper-catalyzed AAA into a powerful and versatile tool in asymmetric synthesis, capable of employing a wide array of organometallic reagents that furnish the desired compounds with high efficiency and selectivity.

The regioselective asymmetric construction of stereogenic carbon centers from prochiral allylic substrates largely depends on the choice of the nucleophilic organometallic species (Scheme 2). For example, the asymmetric copper-catalyzed allylic alkylation utilizing organometallic species **5** bearing a primary carbon–metal bond predominantly constructs the stereogenic center derived from electrophiles. The stereoselective allylic substitution reaction with organometallic species **9** bearing a secondary carbon–metal bond has rarely been reported, despite its potential to enable complementary formation of the stereogenic center derived from nucleophiles. These reactions face significant challenges due to the relatively low configurational stability of the chiral secondary organometallic **9** and organocopper species **10** [38]. Therefore, the development of a more broadly applicable catalytic system that could accomplish copper-catalyzed stereoselective allylic alkylation with chiral secondary nucleophiles represents a crucial advancement in this field. In particular, a key objective is developing regio-, diastereo-, and enantioselective allylic substitution reactions that can effectively construct enantioenriched stereogenic centers from either allylic electrophiles or organometallic nucleophiles [39,40]. This advancement requires establishing catalytic systems that effectively utilize chiral secondary organocopper species, making the understanding of their nature and behavior crucial for expanding the synthetic utility of this transformation.

The purpose of this review is to present recent procedures for generating configurationally unstable organocopper species with secondary carbon–metal bonds, their unique properties, and related mechanistic insights. This review also aims to outline future research directions and prospects, contributing to the development of more efficient and selective copper-catalyzed AAA methodologies.

Review

Copper-catalyzed stereospecific coupling of chiral organometallic species with allylic electrophiles

The asymmetric construction of carbon–carbon bonds through copper-catalyzed AAA has emerged as a powerful synthetic tool in organic chemistry [41-45]. The generation of chiral sec-

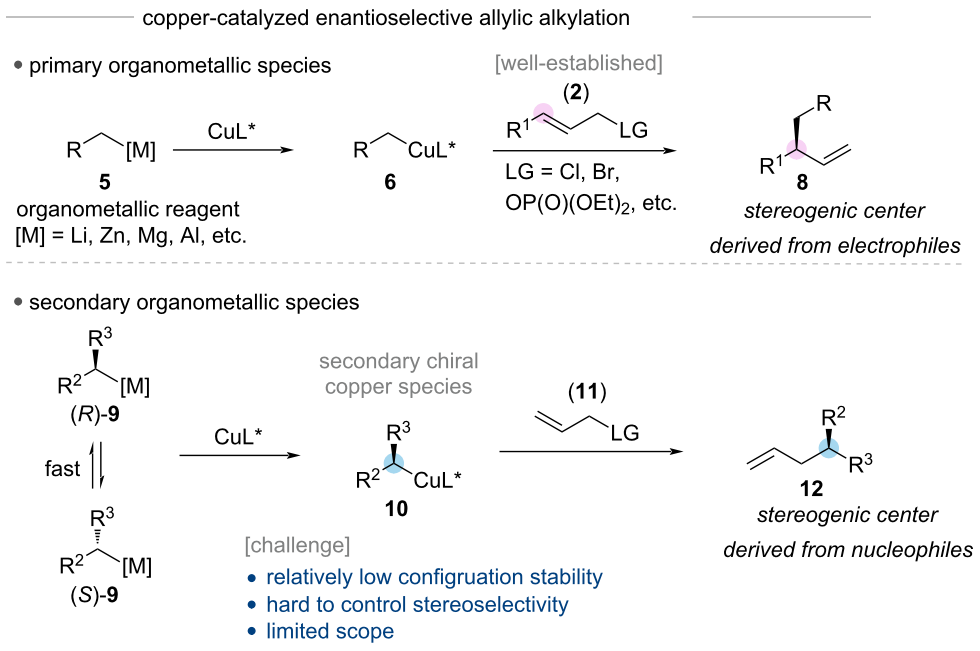

Scheme 2: Formation of stereogenic centers in copper-catalyzed allylic alkylation reactions.

ondary alkylcopper species has been a significant challenge in organic synthesis, primarily due to their inherent instability and tendency to racemization [38]. For generating the key chiral organocopper intermediates, two distinct approaches have been developed: one utilizing chiral organolithium species and the other employing chiral organoboron compounds.

Copper-mediated stereospecific coupling of chiral organolithium species with allylic electrophiles

In the organolithium approach, a breakthrough was achieved by Knochel and co-workers through carefully controlled reaction conditions (Scheme 3) [46]. Their methodology involves a stereoretentive I/Li exchange at −100 °C, followed by transmetalation with $CuBr{\cdot}P(OEt)_3$ to generate the secondary alkylcopper species **14**.

These organocopper species demonstrated remarkable reactivity in S_N2-type additions to allylic bromides with exceptional regioselectivity (S_N2/S_N2' = >99:1). The reaction with 3-methylbut-2-en-1-yl bromide (**15**) was particularly noteworthy, as it exhibited superior selectivity compared to the corresponding phosphates. The high efficiency of this protocol was demonstrated through the synthesis of various functionalized alkenes with complete stereocontrol. For example, the reaction of *syn*-alkylcopper species **14** with 3-methylbut-2-en-1-yl bromide (**15**) provided the corresponding S_N2 product **16** in excellent yield and stereoselectivity (S_N2/S_N2' = >99:1, dr = 97:3).

Remarkably, the regioselectivity of these reactions could be completely reversed by adding zinc halides (Scheme 4). When treated with allylic phosphates **17** in the presence of $ZnCl_2$, these copper reagents **14** showed a dramatic shift in selectivity, favoring S_N2' substitution. This exceptional reversed regioselectivity likely occurs through the in situ formation of copper–zinc mixed species $[RCu{\cdot}ZnX_2{\cdot}L]$ {X = Br, Cl; L = $P(OEt)_3$}. Under these modified conditions, the reaction with allylic phosphates **17** proceeded with excellent S_N2' selectivity (S_N2/S_N2' = 5:95) while maintaining high stereochemical fidelity. The versatility of this approach was further demonstrated through reactions with various chiral cycloallylic phosphates **17**, which consistently yielded the corresponding S_N2' products **18** with high stereoselectivity.

The synthetic utility and broad applicability of this methodology was prominently demonstrated through the total synthesis of biologically important natural products. The high stereochemical selectivity of both S_N2 and S_N2' pathways enabled the efficient construction of complex molecular frameworks. Notably, this approach facilitated the enantioselective synthesis of three ant pheromones: (+)-lasiol, (+)-13-norfaranal, and (+)-faranal.

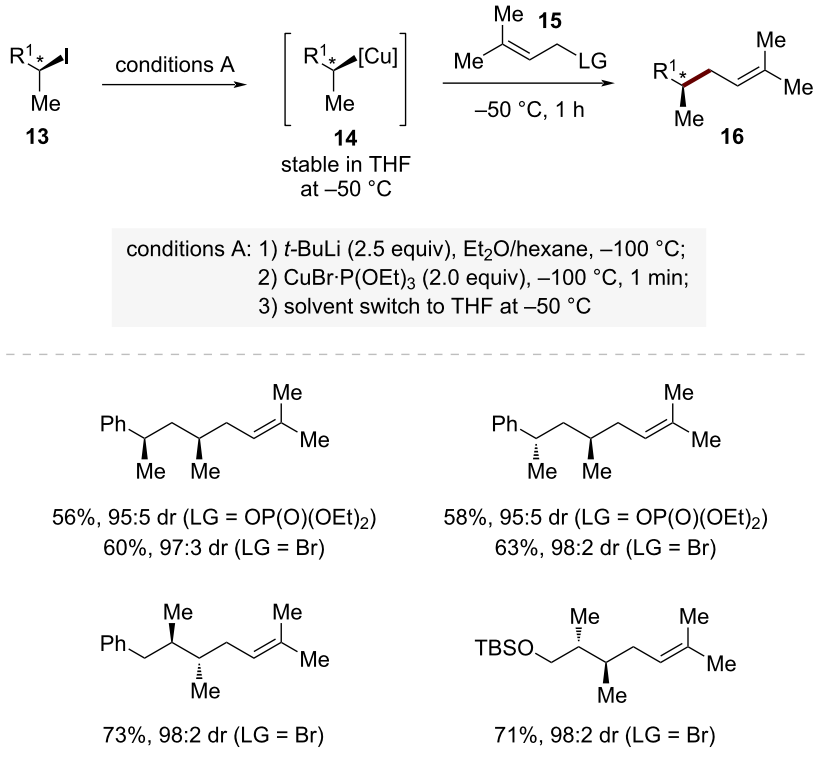

Scheme 3: Copper-mediated, stereospecific S_N2-selective allylic substitution through retentive transmetalation sequence.

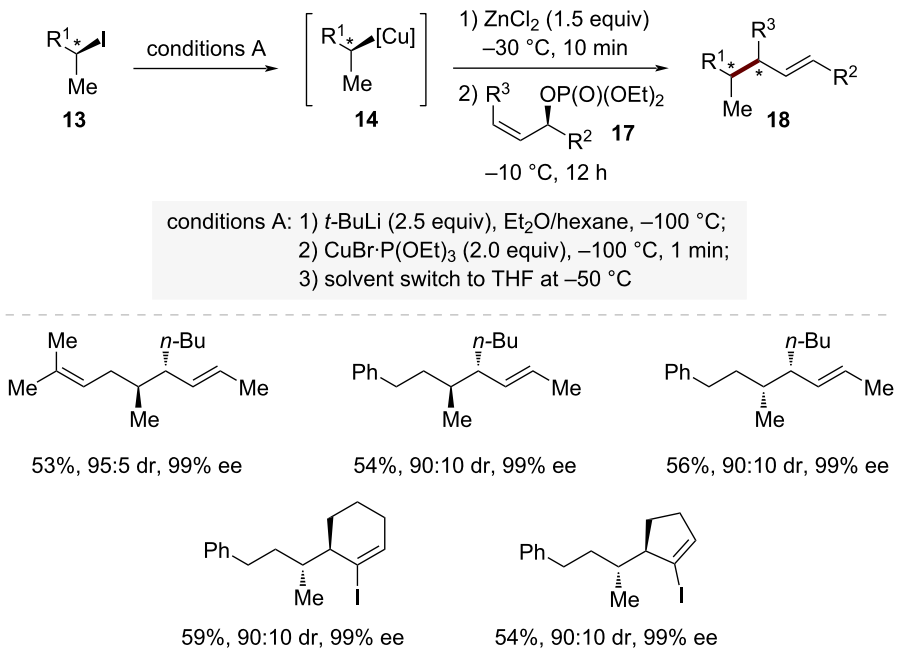

Scheme 4: $ZnCl_2$-promoted stereospecific S_N2' allylic substitution of secondary alkylcopper species via sequential iodide–lithium–copper transmetalation.

The synthesis of (+)-lasiol was achieved through a highly selective S_N2 substitution (S_N2/S_N2' = >99:1, dr = 98:2, 99% ee), while the preparation of (+)-13-norfaranal and (+)-faranal showcased the versatility of the methodology in constructing more complex terpene frameworks. These successful applications in natural product synthesis underscore the robustness and reliability of this copper-mediated transformation in creating stereochemically complex molecules.

Mechanistic investigations revealed several key factors controlling the stereochemical outcome of these transformations. The extremely low temperature (−100 °C) during the Li/I exchange is essential for preventing racemization of the configurationally labile organolithium intermediate. The subsequent transmetalation with $CuBr{\cdot}P(OEt)_3$ introduces $P(OEt)_3$ as a supporting ligand, which plays a vital role in stabilizing the resulting chiral organocopper species **14**. A key breakthrough in this process was the discovery of a solvent effect: switching from Et_2O/hexane to THF at −50 °C after organocopper species formation dramatically enhances configurational stability.

Further investigations into the stability of the secondary organocopper species **14a** revealed the critical importance of reaction conditions after $ZnCl_2$ addition (Scheme 5). When the reaction mixture was stirred at −30 °C for 1 hour (entry 1 in Scheme 5), the product **19** maintained a high diastereomeric ratio (dr), indicating minimal racemization. However, extending the stirring time or increasing the reaction temperature led to a significant decrease in dr values, suggesting partial racemization. This observation highlights the importance of careful experimental handling of $[RCu{\cdot}ZnX_2{\cdot}L]$ species {X = Br, Cl; L = $P(OEt)_3$}, where both temperature control and reaction time must be precisely managed to maintain stereochemical integrity. Through these careful experimental controls, Knochel and co-workers effectively addressed the long-standing challenge of handling these traditionally unstable chiral organometallic intermediates.

Copper-catalyzed stereospecific coupling of chiral organoboron species with allylic electrophiles

While the direct formation of chiral copper species from organolithium compounds provides an efficient route to stereospecific allylic alkylation products, the requirement of stoichiometric amounts of the copper reagent limits its practical application [46]. An alternative approach utilizing more configurationally stable organoboron compounds was recently developed by Morken and co-workers, which employs only catalytic amounts of copper [47,48]. Their strategy uses chiral secondary organoboron compounds **20** as precursors to generate chiral alkylcopper species through a carefully controlled activation and transmetalation sequence (Scheme 6).

For secondary boronic esters, Morken and co-workers conducted a systematic investigation to develop an efficient activation strategy [47]. Computational studies using DFT revealed an important relationship between the length of the boron–carbon

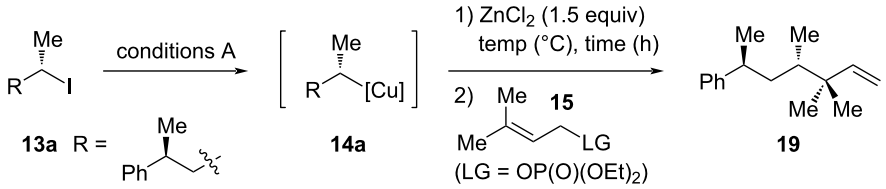

conditions A: 1) *t*-BuLi (2.5 equiv), Et_2O/hexane, –100 °C;
2) $CuBr{\cdot}P(OEt)_3$ (2.0 equiv), –100 °C, 1 min;
3) solvent switch to THF at –50 °C

entry	temp (°C)	time (h)	yield (%)	dr
1	–30	1	66	92:8
2	–20	1	73	92:8
3	–10	1	73	89:11
4	0	1	65	88:12
5	–10	10	62	81:19
6	rt	10	69	82:18

Scheme 5: Temperature and time-dependent configurational stability of chiral secondary organocopper species.

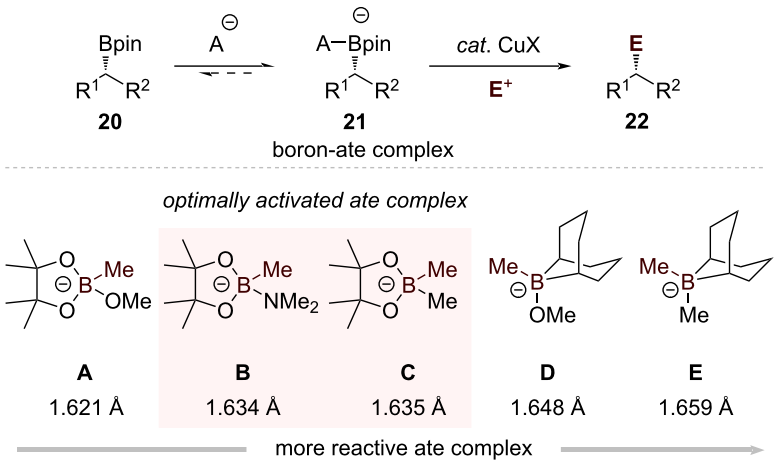

Scheme 6: DFT analysis of B–C bond lengths in various boronate complexes and correlation with reactivity.

bonds and the corresponding complex's chemical behavior (Scheme 6). Among the analyzed four-coordinate boron species, the unreactive trialkoxyborate complex **A** exhibited the most compact B–C bond at 1.621 Å. Following a clear trend, the B–C bond distance progressively lengthened as oxygen atoms were substituted with elements of lower electronegativity, reaching 1.648 Å in the reactive alkoxytrialkyl complex **D** and 1.659 Å in the tetraalkyl "ate" complex **E**. The B–C bond lengths in amido- and alkyl-substituted boronic ester complexes **B** and **C** fell between these extremes, suggesting an intermediate level of activation. These findings prompted investigation into whether such moderate activation strategies could facilitate copper-mediated coupling reactions of sterically demanding alkylboronic esters under mild conditions. After thorough reaction optimization, *t*-BuLi emerged as the superior activating agent, outperforming other organolithium compounds including *s*-BuLi, *n*-BuLi, and PhLi. The optimized protocol, employing CuCN as a catalyst, enabled efficient coupling between *t*-BuLi-activated complexes **10** and allylic halides **11**, furnishing products **12** with complete retention of

stereochemistry and high yields (Scheme 7). The method's versatility and consistent stereochemical outcome highlight its practical utility.

Their subsequent work with chiral tertiary boronic esters **25** revealed an effective strategy for constructing quaternary stereogenic centers through allylic substitution reactions (Scheme 8) [48]. By employing in situ-generated adamantyllithium as an activator, they found that tertiary alkyl groups underwent selective transmetalation over the adamantyl group. Under optimized conditions, the activated chiral tertiary boronic esters **26** underwent efficient copper-catalyzed coupling with allylic electrophiles **23** to provide products **27** bearing quaternary stereogenic centers with high stereospecificity. This methodology represents a significant advancement in the construction of challenging all-carbon quaternary stereogenic centers through stereospecific allylic substitution reactions.

To elucidate the origin of the selective boron group transfer, X-ray crystallographic analysis of the (*tert*-butyl)(adamantyl)Bpin·Li(THF)$_2$ complex revealed that the B–(adamantyl) bond is shorter than the B–(*tert*-butyl) bond (1.673 vs 1.692 Å). DFT calculations further illuminated the underlying mechanism by comparing two distinct transition states: **TS1** involving adamantyl transfer and **TS2** involving *tert*-butyl transfer (Scheme 9). Analysis of these transition states revealed that both require significant pyramidalization of the transferring carbon center, with the barrier for adamantyl transfer (**TS1**) being 2.3 kcal/mol higher than that for *tert*-butyl transfer (**TS2**). The structural features of the *tert*-butyl group allow more efficient pyramidalization compared to the rigid adamantyl framework, suggesting that the flexibility of the transferring group plays a crucial role in facilitating transmetalation.

Copper hydride chemistry for enantioselective allylic substitution reactions

Among the various approaches in copper-catalyzed asymmetric allylic substitution, copper hydride (CuH) catalysis has received significant attention due to its unique ability to generate config-

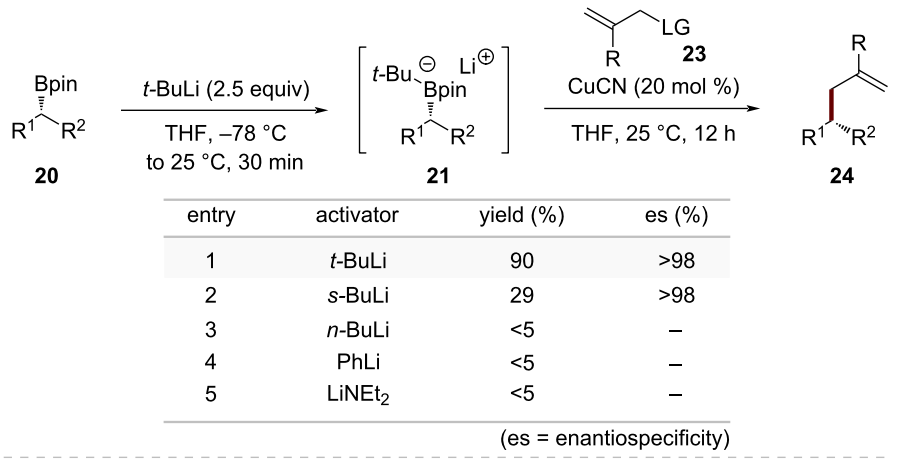

entry	activator	yield (%)	es (%)
1	*t*-BuLi	90	>98
2	*s*-BuLi	29	>98
3	*n*-BuLi	<5	–
4	PhLi	<5	–
5	$LiNEt_2$	<5	–

(es = enantiospecificity)

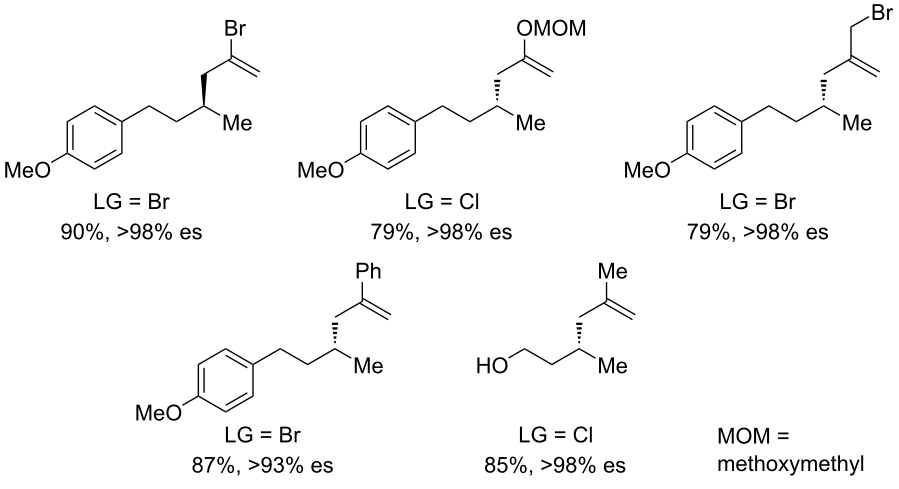

Scheme 7: Copper-catalyzed stereospecific allylic alkylation of secondary alkylboronic esters via *tert*-butyllithium activation.

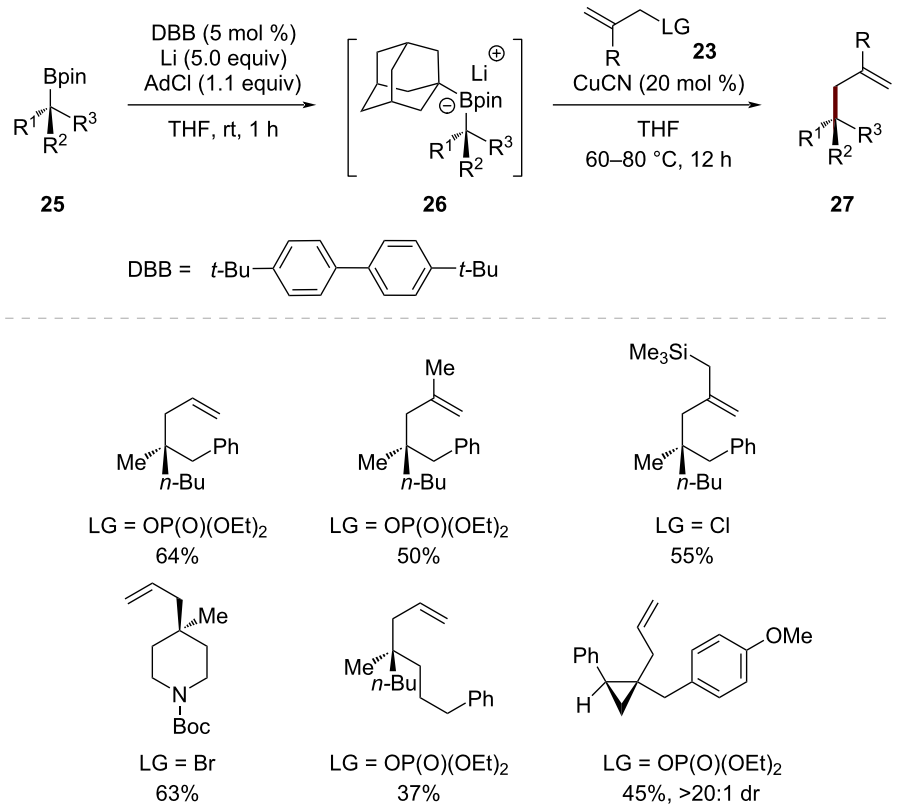

Scheme 8: Copper-catalyzed stereospecific allylic alkylation of chiral tertiary alkylboronic esters via adamantyllithium activation.

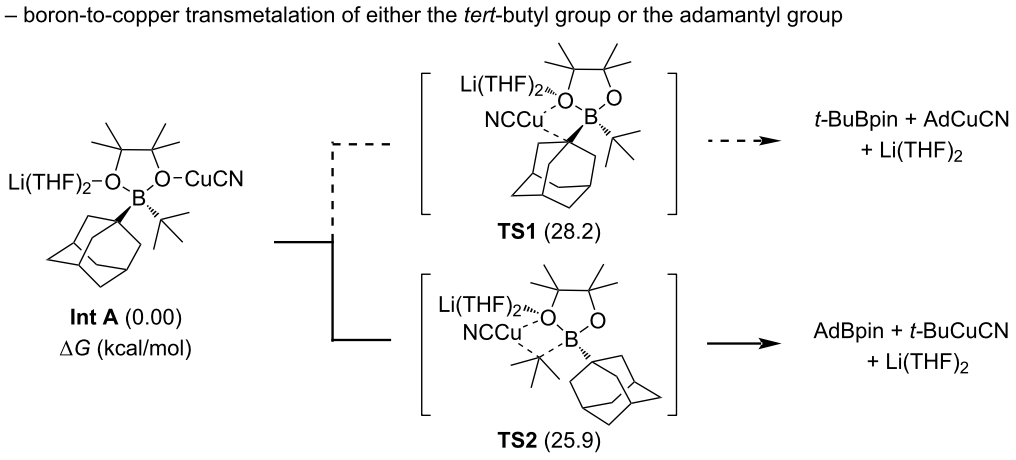

Scheme 9: DFT-calculated energy surface for boron-to-copper transmetalation of either the *tert*-butyl group or the adamantyl group.

urationally well-defined chiral organocopper species **28** under mild conditions without requiring stoichiometric organometallic reagents [49] (Scheme 10). The distinctive reactivity of the CuH species allows for precise control over the stereochemical outcome through the regio- and enantioselective hydrocupration of olefins **27**, followed by stereospecific trapping with allylic electrophiles **11**.

Enantioselective hydroallylation and allylboration of styrenes

A significant advance in the CuH-catalyzed enantioselective allylic substitution was reported by Buchwald and co-workers in 2016, who demonstrated the first successful hydroallylation of vinylarenes **30** using allylic phosphate electrophiles **31** (Scheme 11) [50]. This methodology is distinguished by its

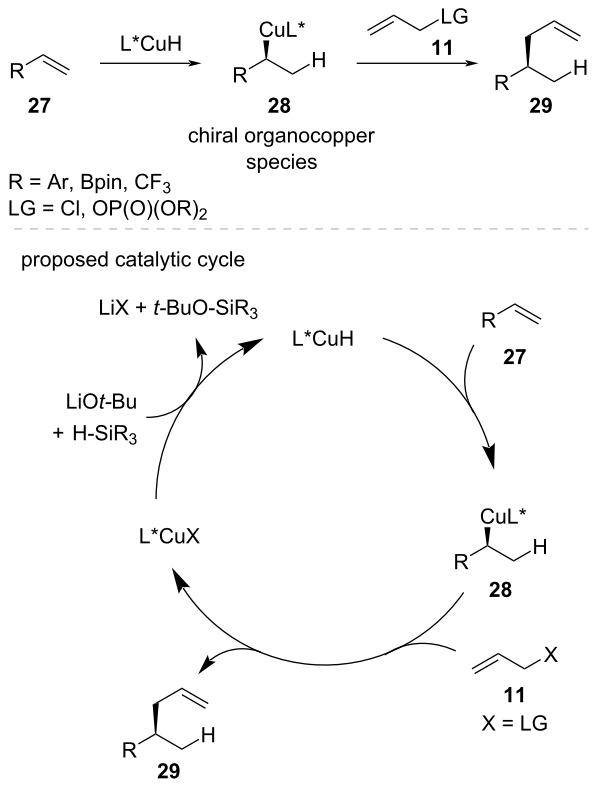

Scheme 10: CuH-catalyzed enantioselective allylic substitution and postulated catalytic cycle.

ability to efficiently construct configurationally well-defined stereogenic centers during C–C-bond formation through the intermediacy of benzylic copper species.

Initial investigations suggested that the reaction outcome was highly dependent on both the leaving group of the allylic electrophile and the choice of the supporting ligand. When (+)-1,2-bis{(2*S*,5*S*)-2,5-diphenylphospholano}ethane {(*S*,*S*)-Ph-BPE} (**L1**) was employed as the supporting chiral ligand, initially allylic chloride was found to provide the desired product **32** with excellent enantioselectivity, although in moderate yield. Notably, the presence of a chloride anion in the reaction mixture proved crucial for high enantioselectivity, leading to the discovery that a 1:1 complex of copper(I) chloride and (*S*,*S*)-Ph-BPE (**L1**) could serve as an optimal catalyst system. Further optimization revealed LiO*t*-Bu and diphenyl phosphate as the optimal metal alkoxide and leaving group, delivering the desired product **32** in high yield and high enantioselectivity at room temperature with only 2 mol % catalyst loading.

The scope of this transformation proved to be remarkably broad. In addition to the parent allyl group, a variety of 2-substituted electrophiles **31** could be applied. These included those bearing alkyl groups of varying steric demand, halides, and both electron-rich and electron-poor aryl substituents. The olefin coupling partner scope was equally impressive, toler-

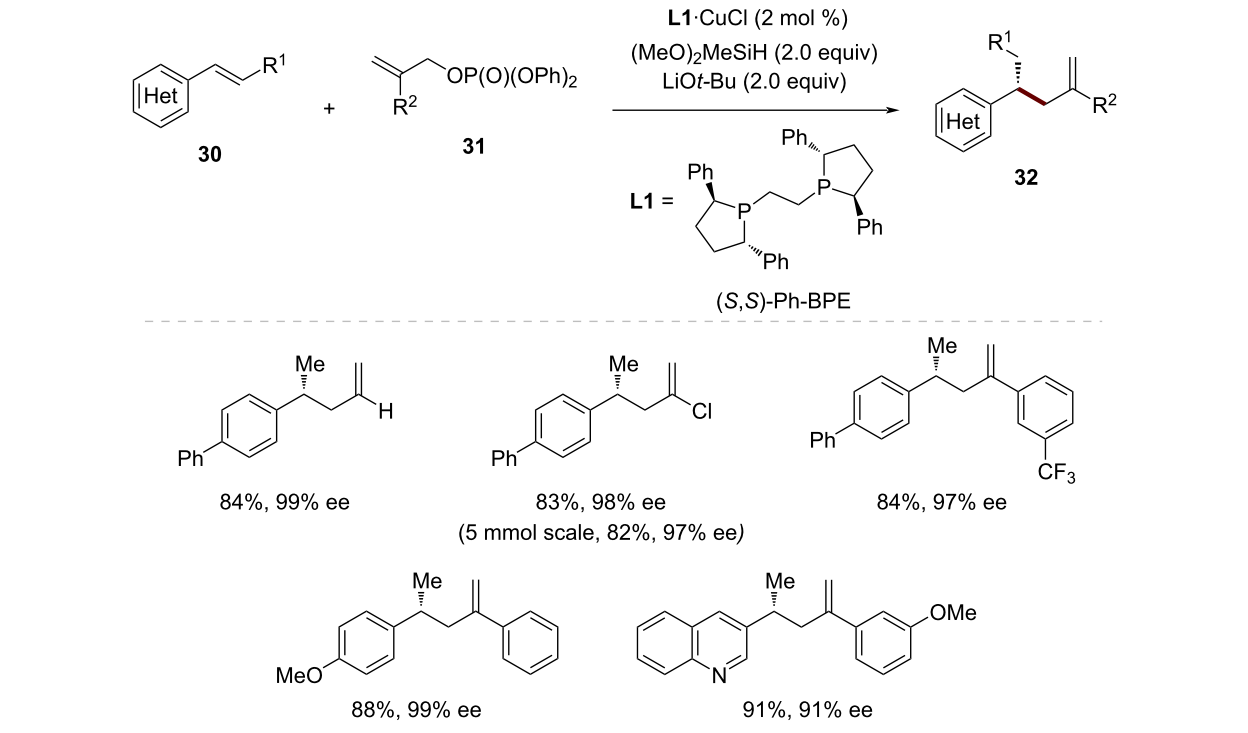

Scheme 11: CuH-catalyzed enantioselective allylic substitution of vinylarenes.

ating styrenes with diverse electronic properties as well as those containing sensitive functional groups such as esters, amides, and vinyl halides, to yield the desired β-chiral olefins in high enantioselectivity. Notably, the methodology could even be applied to vinylferrocene and vinylsilane derivatives, providing rapid access to highly enantioenriched organometallic and organosilicon compounds.

Mechanistic studies using a deuterium-labeled allylic phosphate revealed that the C–C-bond formation occurs through an S_N2'-like process, with attack of the organocopper species at the 3-position of the allylic phosphate. The absolute stereochemistry of the products was found to be consistent with that of previously reported CuH-catalyzed transformations using (*S*,*S*)-Ph-BPE (**L1**) as the supporting ligand, suggesting a common mode of stereoinduction.

In parallel, Hoveyda and co-workers demonstrated the first copper-catalyzed enantioselective allylic substitution of styrenes utilizing Cu–Bpin species [51]. Through implementation of a chiral NHC–Cu complex with $B_2(pin)_2$, they achieved the highly selective formation of homoallylic boronic esters with excellent enantioselectivities (up to 98% ee). This methodology represents a complementary approach to the hydroallylation protocol developed by the research group of Buchwald, enabling a direct construction of versatile organoboron compounds that can be readily elaborated to more complex molecular architectures.

Enantioselective hydroallylation of vinylboronic esters

Following the initial demonstration by Buchwald that styrenes are viable substrates for the CuH-catalyzed hydroallylation, the development of methods applicable to vinylboronic esters presented unique opportunities for the synthesis of versatile chiral organoboron compounds [52]. A breakthrough in this field was achieved in 2016 by Yun and co-workers, who developed a copper-catalyzed regio- and enantioselective hydroallylation of vinylboronic acid pinacol esters (Bpin) and 1,8-diaminonaphthalene boramides (Bdan) **33** (Scheme 12) [53]. Subsequently, Hoveyda and co-workers introduced a complementary approach focused on the diastereoselective formation of homoallylic boronic esters **36** through a carefully controlled sequence of hydrocupration and allylic substitution [39].

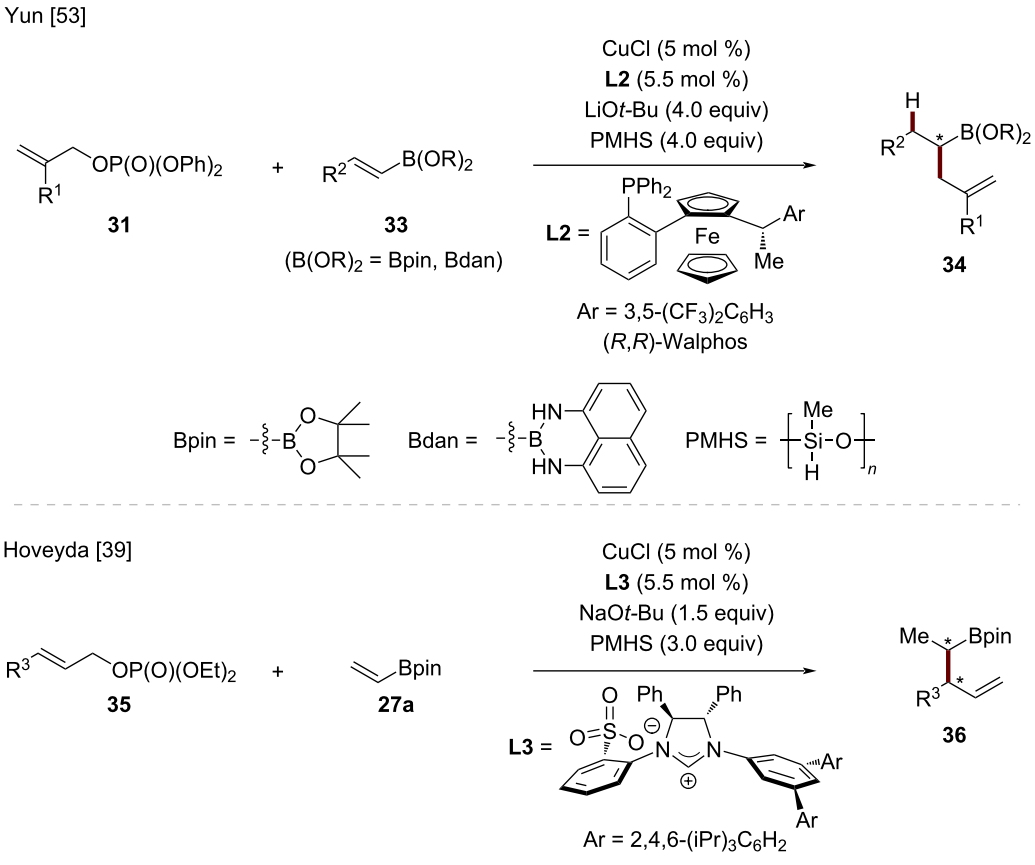

Scheme 12: CuH-catalyzed stereoselective allylic substitution of vinylboronic esters.

Through optimization studies, Yun found that CuCl with the Walphos ligand (**L2**) in Et_2O provided optimal results, delivering the desired products with up to 99% ee. This methodology worked effectively with both pinacol boronic esters (Bpin) and 1,8-diaminonaphthalene boramides (Bdan), showing broad vinylboron substrate scope across alkyl, aryl, and heteroaryl substituents. The practical utility of the enantioenriched alkylboronic esters **34** was demonstrated through the efficient synthesis of (*S*)-massoialactone.

Subsequently, Hoveyda developed a highly selective copper-catalyzed allylic substitution of (*E*)-1,2-disubstituted allylic phosphates **35** with vinylBpin **27a** using polymethylhydrosiloxane (PMHS) as the hydride source [39]. The reaction, catalyzed by a sulfonate-containing chiral NHC–Cu complex, proceeded with excellent chemo-, regio- (S_N2'-), diastereo-, and enantioselectivity to afford homoallylic boronates **36**. The resulting organoboron compounds could be oxidized to secondary homoallylic alcohols, providing an alternative to traditional crotyl addition to acetaldehyde. This methodology represents the first example of highly enantio- and diastereoselective copper-catalyzed allylic substitution that controls vicinal stereogenic centers.

DFT calculations revealed that the high enantioselectivity (98:2 er) originates from a face-selective formation of the chiral organocopper species **37** (Scheme 13a). The 3,5-(2,4,6-triisopropylphenyl) substituent of the NHC ligand **L3** effectively blocks one face of the reactive center, forcing vinylBpin **27a** to approach the CuH complex from the less hindered face. This precise steric control during copper complex formation and subsequent selective olefin insertion results in the high levels of enantioselectivity (98:2 er) observed experimentally.

DFT calculations further elucidated the origin of the high diastereoselectivity (up to 96:4 dr) in the allylic substitution step

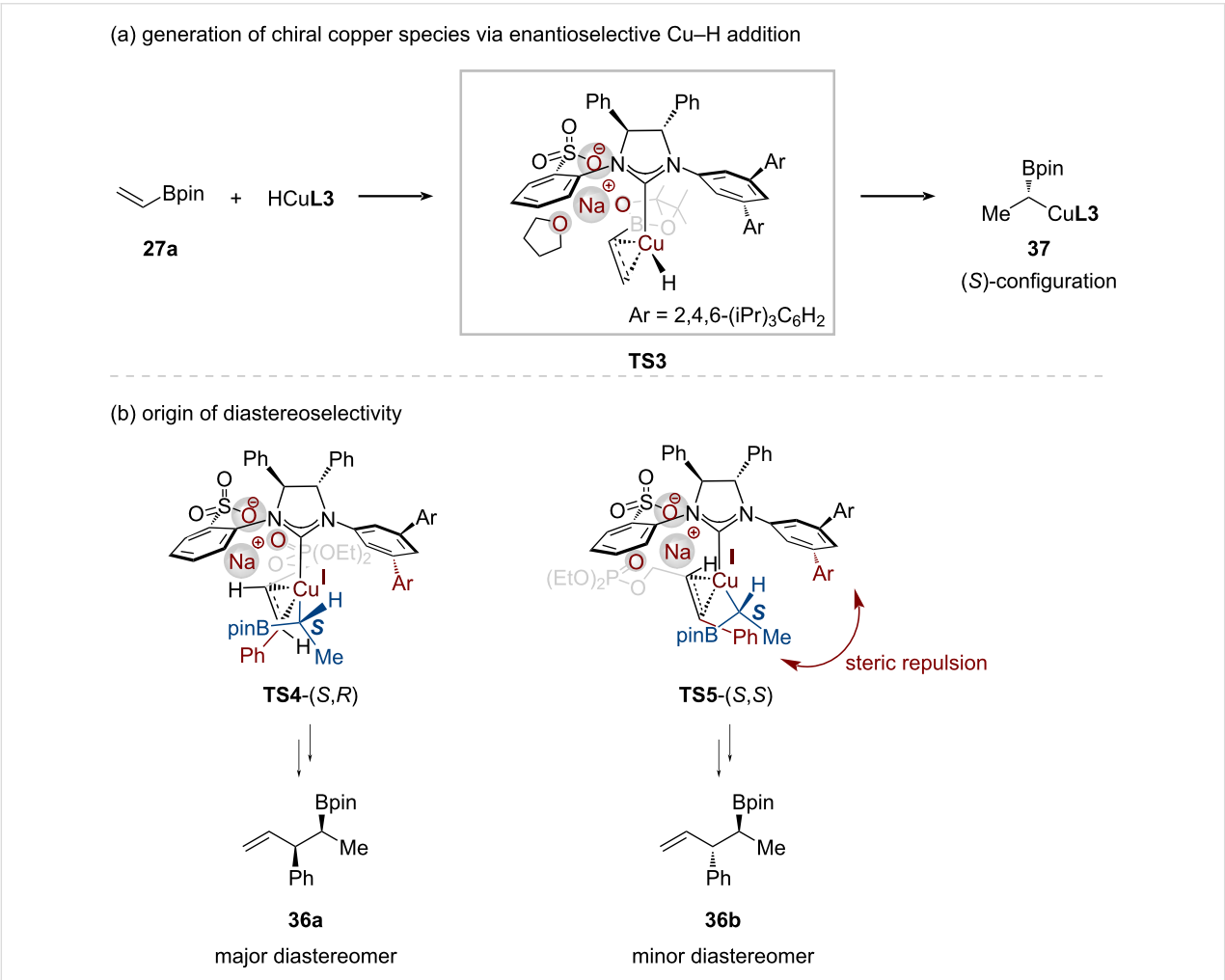

Scheme 13: (a) Generation of chiral copper species via enantioselective CuH addition to vinylBpin. (b) Regarding the origin of diastereoselectivity in CuH-catalyzed enantioselective allylic substitution.

(Scheme 13b). Analysis of the competing transition states showed that the chiral α-borylalkylcopper species **37** could approach the olefinic moiety of allylic electrophile **35** from either the *re*- or *si*-face. The *re*-face approach is energetically favored, minimizing steric interactions between the bulky aryl substituent of NHC ligand **L3** and the allylic electrophile **35**. In contrast, a *si*-face attack leads to a higher-energy transition state due to significant steric repulsion.

Enantioselective hydroallylation of vinyltrifluoromethyl compounds

The direct functionalization of 1-trifluoromethylalkenes **38** through copper catalysis has been challenging due to the tendency of α-CF_3-substituted alkylcopper intermediates **39** to undergo undesired β-F elimination (Scheme 14a) [54]. In 2021, Hirano and co-workers made a significant advance in this area by disclosing a copper-catalyzed regio- and enantioselective hydroallylation of 1-trifluoromethylalkenes **38** with hydrosilanes and allylic chlorides **40** (Scheme 14b) [55]. In their work, a chiral α-CF_3 alkylcopper intermediate **39** was formed through the regio- and enantioselective hydrocupration of electron-deficient alkenes **38** with an in situ-generated CuH species. Subsequent electrophilic trapping of the α-CF_3-alkylcopper species **39** with the allylic electrophile **40** leads to the optically active hydroallylated product **41**. The key to the success of this protocol was the combination of an appropriate chiral bisphosphine ligand, (*R*)-DTBM-Segphos (**L4**), and the use of 18-crown-6 to suppress the otherwise predominant β-F elimination from the α-CF_3-alkylcopper intermediate **39**. Detailed kinetic studies confirmed the effect of the crown ether. When KOPiv was employed alone, the initial rate of defluorination increased by 1.57-fold, whereas the addition of 18-crown-6 reduced this acceleration to 1.22-fold. These observations supported the hypothesis that the crown ether effectively disrupts the interaction between the alkali metal cation and fluorine atom, thereby decreasing the rate of β-F elimination.

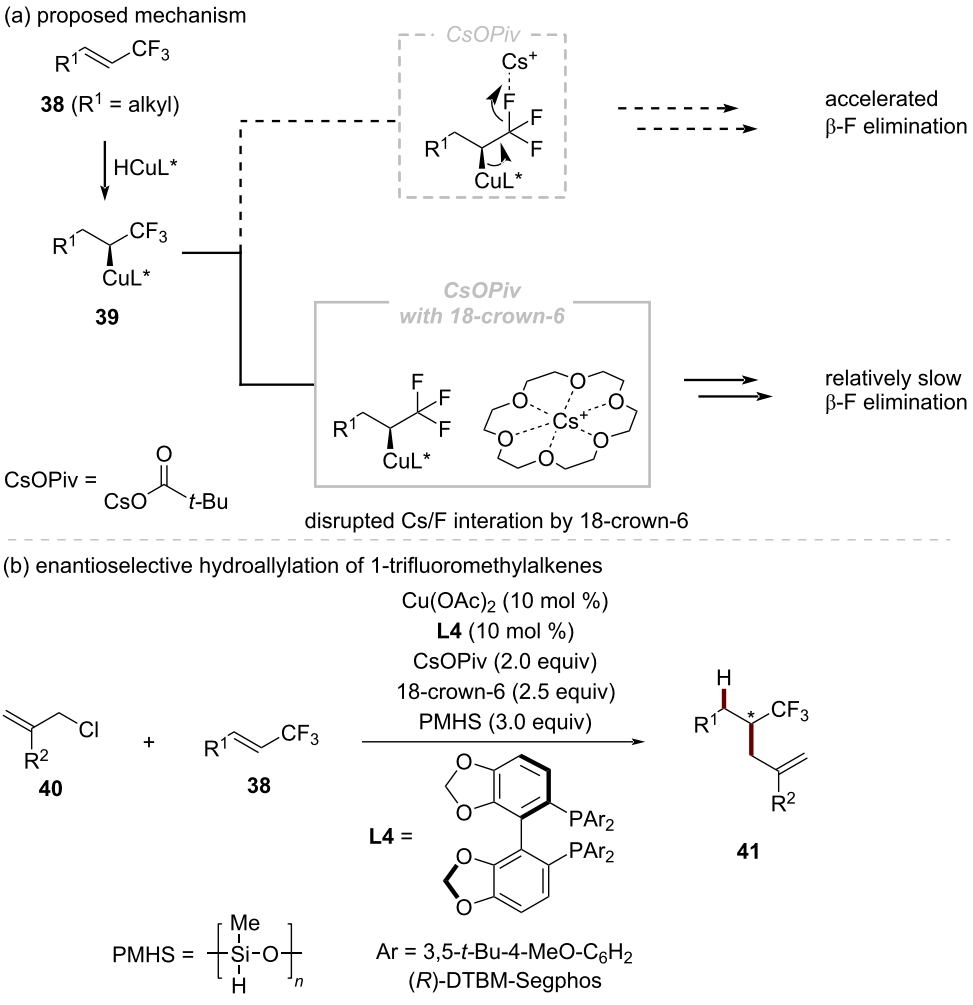

Scheme 14: CuH-catalyzed enantioselective allylic substitution of 1-trifluoromethylalkenes with 18-crown-6.

This asymmetric copper-catalyzed protocol represents one of the rare examples that allows to construct non-benzylic and non-allylic CF_3-substituted C(sp^3) stereogenic centers. The synthetic utility of this allylation process was demonstrated through the facile functionalization of the allylic moiety in the enantioenriched product **41**, providing access to optically active CF_3-containing compounds bearing various functionalities. Notably, no erosion of enantiomeric excess was observed during any of the transformations.

Double CuH insertion into alkynes for regiodivergent allylic substitution

Generating chiral secondary alkylcopper species in situ through sequential hydrocupration of terminal alkynes in a chemo-, regio-, and enantioselective manner represents a recent advance in copper hydride chemistry. Along these lines, in 2024, Su and co-workers developed a strategy for the copper-catalyzed regio- and enantioselective synthesis of secondary homoallylboron compounds by assembling four readily available starting materials: terminal alkynes, HBdan, polymethylhydrosiloxane (PMHS), and allylic phosphates, through a complex cascade hydroboration and hydroallylation sequence [56].

Shortly after this work, Xiong, Zhu, and co-workers reported a ligand-controlled copper-catalyzed regiodivergent asymmetric difunctionalization of terminal alkynes through a cascade process involving initial hydroboration followed by a hydroallylation (Scheme 15) [57]. Employing a catalytic system consisting of (*R*)-DTBM-Segphos (**L4**) and CuBr resulted in the exclusive 1,1-difunctionalization of aryl- and alkyl-substituted terminal alkynes **42**, including the industrially relevant acetylene and propyne. Interestingly, switching to the ligand (*S*,*S*)-Ph-BPE (**L1**) resulted in the asymmetric 1,2-difunctionalization of aryl-substituted terminal alkynes **42**. The high levels of regio- and stereoselectivity achieved under mild conditions render this method attractive for constructing complex chiral molecular architectures.

A plausible mechanistic pathway for this cascade asymmetric hydroboration and hydroallylation of alkynes was proposed

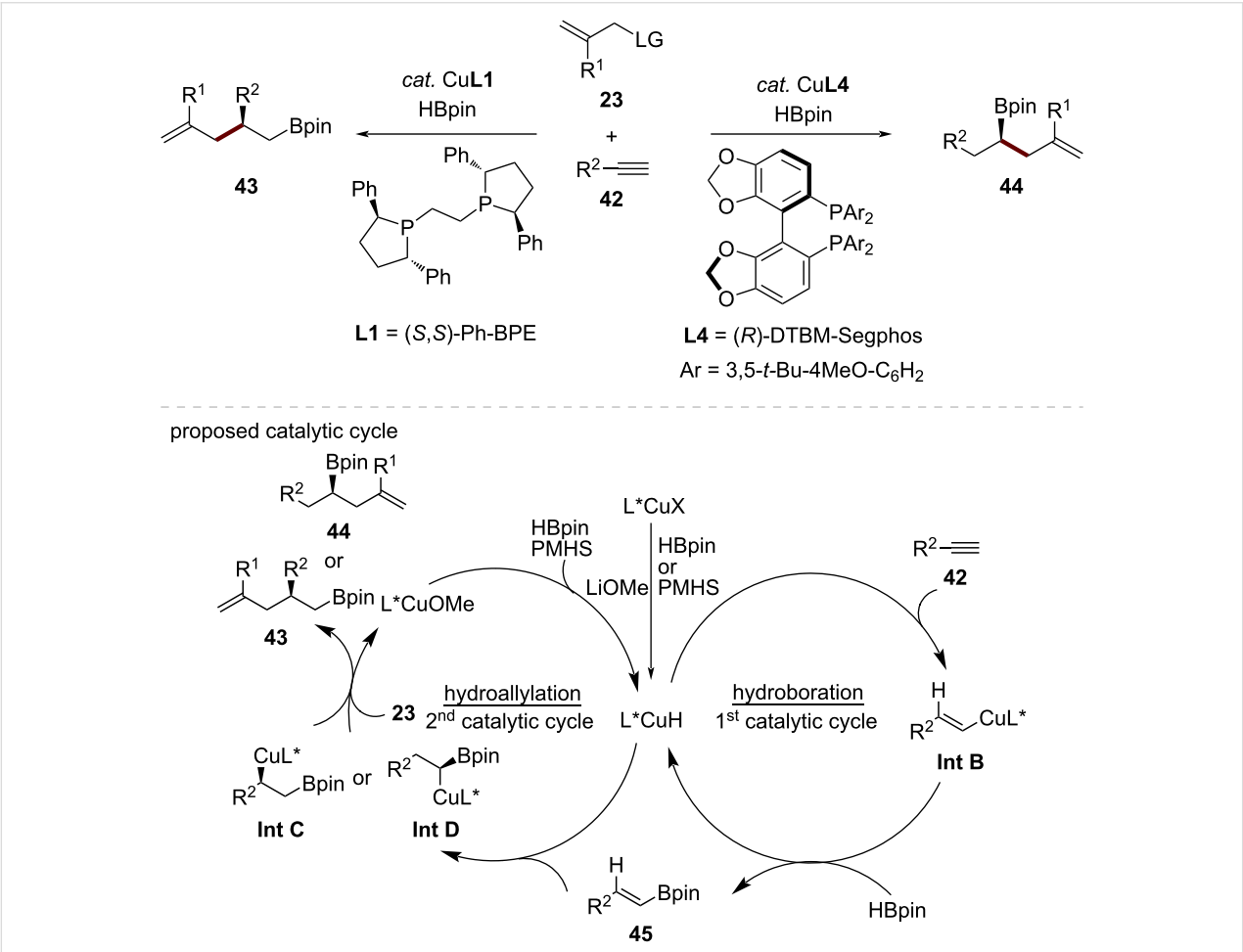

Scheme 15: CuH-catalyzed enantioselective allylic substitution of terminal alkynes.

based on a series of control experiments, including deuterium-labeling experiments and DFT calculations. The first hydroboration catalytic cycle is initiated by L*CuH species (L* = a chiral ligand) formed in situ through the combination of CuBr, LiOMe, and HBpin in the presence of a chiral ligand. Subsequent alkyne migratory insertion provides a vinyl cuprate intermediate **Int B**, followed by σ-bond metathesis with HBpin to afford a vinylboronic ester intermediate **45** alongside the regenerated L*CuH catalyst, completing the first catalytic cycle. Subsequently, a ligand-controlled regioselective migratory insertion of L*CuH into the vinylboronic ester **18** delivers the corresponding chiral alkylcopper species **Int C** or **Int D**, which undergoes an S_N2'-like pathway with allylic phosphates **23** to generate the chiral products **43** or **44** along with the release of L*CuOR species. A σ-bond metathesis of this alkoxycopper species with HBpin and/or PMHS regenerates the L*CuH catalyst, completing the secondary asymmetric regiodivergent hydroallylation cycle.

Copper-catalyzed enantiotopic-group-selective allylation of 1,1-diborylalkanes

The generation of chiral non-racemic organocopper species through enantiotopic-group-selective transmetalation of 1,1-diborylalkanes **47** has recently garnered significant interest [58]. This methodology has emerged as a powerful strategy for constructing stereogenic centers with high levels of stereocontrol, offering important complementarity to established CuH-catalyzed processes. While CuH-catalyzed processes have proven highly effective for numerous substrates, they exhibit inherent limitations with molecules possessing unsaturated functionalities due to competitive hydrocupration pathways. The approach using 1,1-diborylalkanes **47** circumvents these chemoselectivity issues and enables a selective allylic substitution of substrates containing olefins and alkynes with excellent stereoselectivity. Importantly, this orthogonal reactivity complements established CuH-catalyzed procedures, significantly expanding the scope of copper-catalyzed asymmetric allylic substitution reactions.

In 2021, Cho, Baik, and co-workers reported the first enantioselective copper-catalyzed allylation of 1,1-diborylalkanes **47** using an H_8-BINOL-derived phosphoramidite ligand **L5**, achieving exceptional enantiocontrol (Scheme 16) [59]. Their studies revealed the critical role of both the alkali metal cation and boronic ester moiety. While LiO*t*-Bu provided excellent enantioselectivity (er = 95:5), NaO*t*-Bu and KO*t*-Bu per-

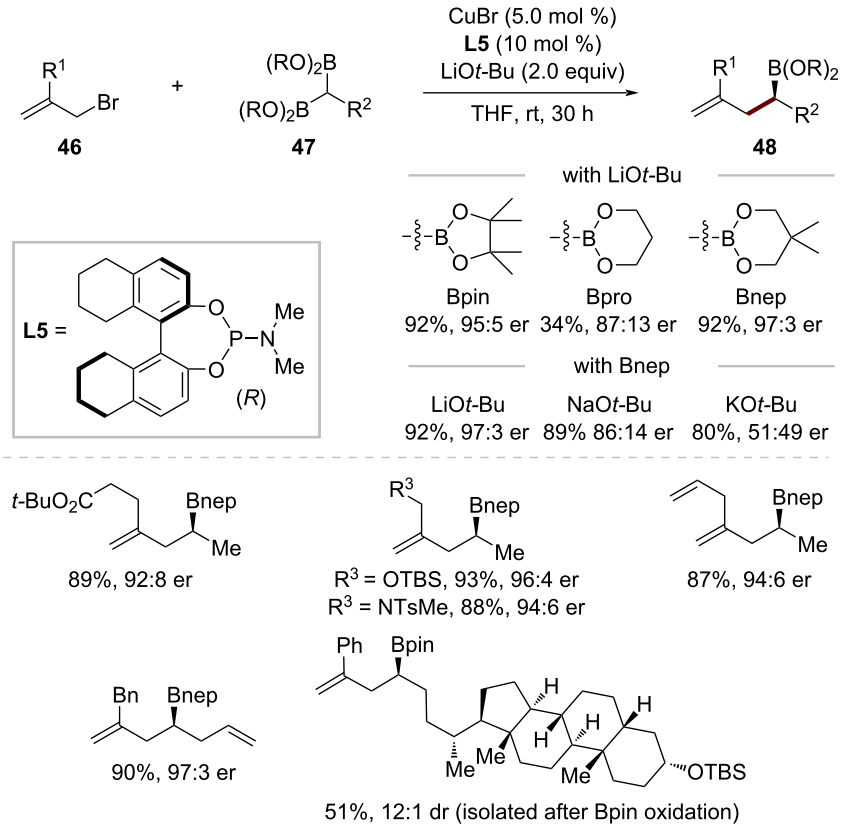

Scheme 16: Copper-catalyzed enantiotopic-group-selective allylic substitution of 1,1-diborylalkanes.

formed poorly due to competitive transition-metal-free processes via α-borylcarbanion formation. The substituent of the boron atom proved equally important: neopentylglycolato groups (Bnep) outperformed pinacolato (Bpin) or propanediolato groups (Bpro) in stereoselectivity. The optimized conditions showed a broad scope, tolerating both 1,1-diborylalkanes with *N*-tosyl-protected amines and TBS-protected alcohols, as well as substrates containing alkenes and alkynes. Various allylic bromides **46** with electron-rich and electron-deficient aryl substituents worked well, giving homoallylic boronic esters **48** that contain a boron-substituted stereogenic center derived from the prochiral 1,1-diborylalkanes **47** in good yields with high stereoselectivity.

DFT calculations of the enantiotopic-group-selective transmetalation between 1,1-diborylalkanes and chiral copper species revealed two possible transition states: an open transition state **TS7** facilitated by LiO*t*-Bu and a closed transition state **TS6** without base assistance (Scheme 17a). The significant energy difference between these pathways ($\Delta\Delta G^{\ddagger}$ =

(a) DFT calculation for the enantiotopic transmetallation

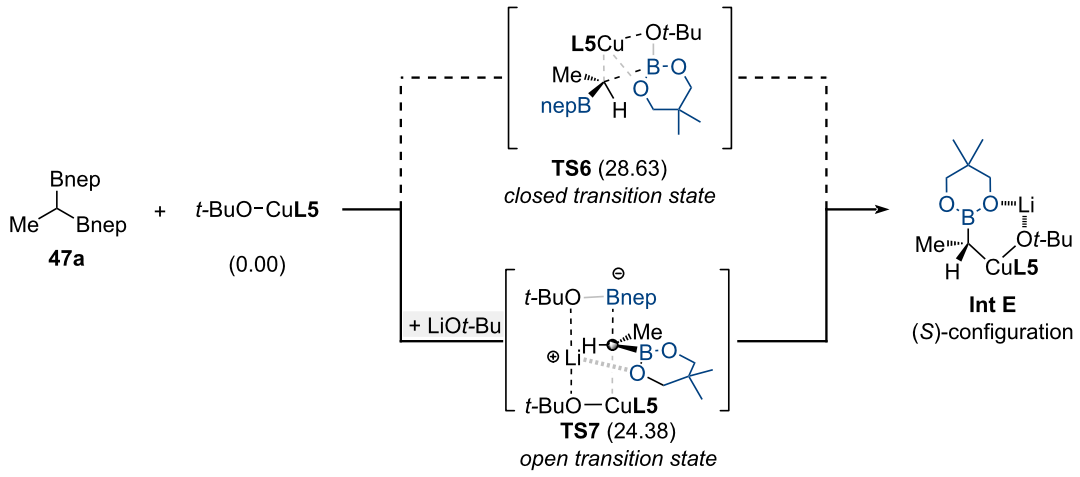

(b) mass spectral analysis of the reaction using isotopic isomer (*S*)-^{10}B-**32**

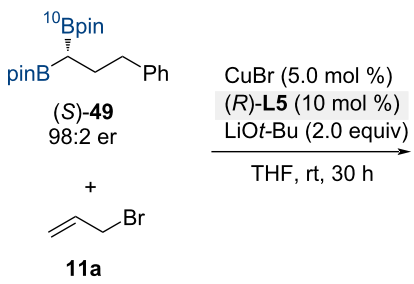

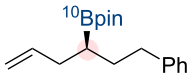

(*S*)-**50**

73% yield, 92:8 er

mass analysis

calcd ^{10}B:^{11}B		found
m/z 285	75.6%	63.9%
m/z 286	21.5%	30.1%
m/z 287	2.8%	5.0%
m/z 288	0.1%	0.6%

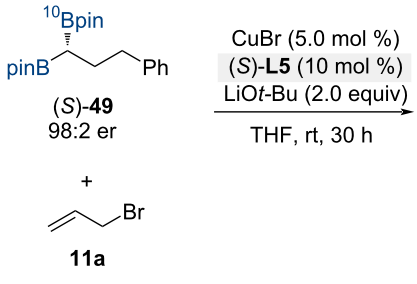

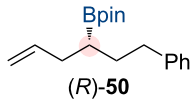

(*R*)-**50**

73% yield, 92:8 er

mass analysis

calcd ^{10}B:^{11}B		found
m/z 285	22.7%	34.7%
m/z 286	63.7%	52.9%
m/z 287	12.3%	11.0%
m/z 288	1.2%	1.3%

Scheme 17: (a) Computational and (b) experimental studies to elucidate the mechanistic details of the enantiotopic-group-selective transmetalation.

4.3 kcal/mol) strongly favors the open transition state **TS7** mechanism, attributed to reduced steric interactions and enhanced electronic stabilization through lithium coordination. This explains the critical role of lithium in achieving a high enantioselectivity. Isotope-labeling experiments using ^{10}B-enriched 1,1-diborylalkanes (*S*)-**49** further supported this mechanism, showing a stereoinvertive transmetalation between the enriched substrate and chiral copper species, consistent with the calculations (Scheme 17b).

In 2024, Cho and co-workers have developed a more stereoselective approach that can significantly broaden the scope of accessible electrophiles using 1,1-diborylalkanes **52** as pronucleophiles (Scheme 18) [40]. The asymmetric copper-catalyzed allylic alkylation enabled the efficient coupling of 1,1-diborylalkanes **52** with various allylic bromides **51**, achieving high levels of regio-, diastereo-, and enantioselectivity (rr = >20:1, dr = >8:1, up to 96:4 er). Under slightly modified conditions, a wide range of 1,1-diborylalkanes bearing an *N*-tosyl-protected amine as well as alkene and alkyne moieties underwent efficient coupling with allylic bromides. A notable advantage of this synthetic approach is that it provides a distinct alternative to traditional CuH-catalyzed allylic alkylation reactions. The method shows exceptional compatibility with 1,1-diborylalkanes bearing unsaturated functional groups such as alkenes or alkynes.

The copper-catalyzed asymmetric allylic substitution occurs via two possible pathways: *anti*-S_N2' and *syn*-S_N2' oxidative addition. To determine which pathway is operative, deuterium-

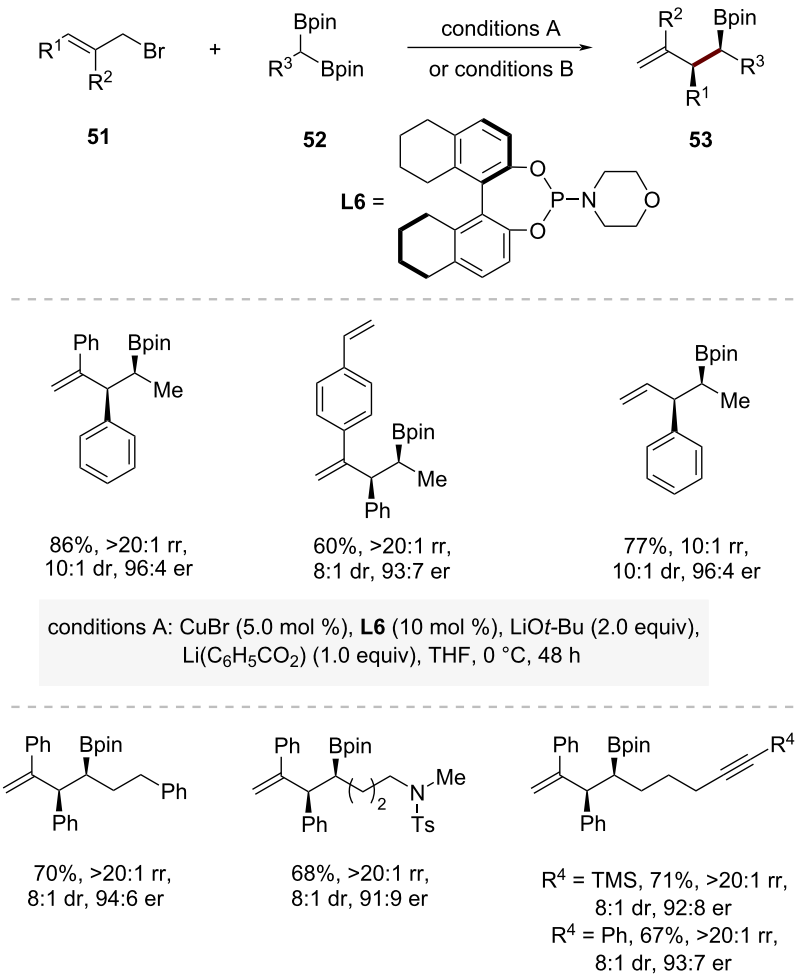

Scheme 18: Copper-catalyzed regio-, diastereo- and enantioselective allylic substitution of 1,1-diborylalkanes.

labeling studies were conducted using an enantioenriched, isotopically labeled allylic bromide (*S*)-**54** (61:39 er) and 1,1-diborylethane **52a** under optimized reaction conditions (Scheme 19a). The resulting product **55** formed with 39:61 *E*/*Z* selectivity, indicating an *anti*-S_N2' oxidative addition mechanism. In this pathway, the chiral α-borylalkylcopper intermediate approaches from the face opposite to the leaving group, consistent with the observed stereochemical outcome.

To explore the stereochemical origins and examine the mechanistic influence of the lithium benzoate additive, computational density functional theory calculations were performed focusing on the oxidative addition transition states (*S*,*R*)-**TS8** and (*S*,*S*)-**TS9** (Scheme 19b). The theoretical analysis revealed a notable energy difference between these diastereomeric transition states, with (*S*,*R*)-**TS8** being 4.11 kcal/mol lower in energy compared to (*S*,*S*)-**TS9**. Both transition states demonstrated a lithium center's coordination involving bromide, benzoate, and ligand oxygen atoms. The (*S*,*R*)-**TS8** transition state exhibited a significantly shorter Li–Br interaction distance (2.81 Å compared to 3.74 Å in (*S*,*S*)-**TS9**), offering mechanistic insight into the observed stereochemical outcome.

Conclusion

This review highlights the evolution of strategies for generating and utilizing chiral nonracemic organocopper species with secondary carbon–metal bonds in asymmetric allylic substitution reactions. Early approaches relied on the stereospecific transmetalation of configurationally stable organometallic reagents, initially employing stoichiometric copper salts with chiral secondary organolithium species. The field then advanced through the development of more practical systems using configuration-

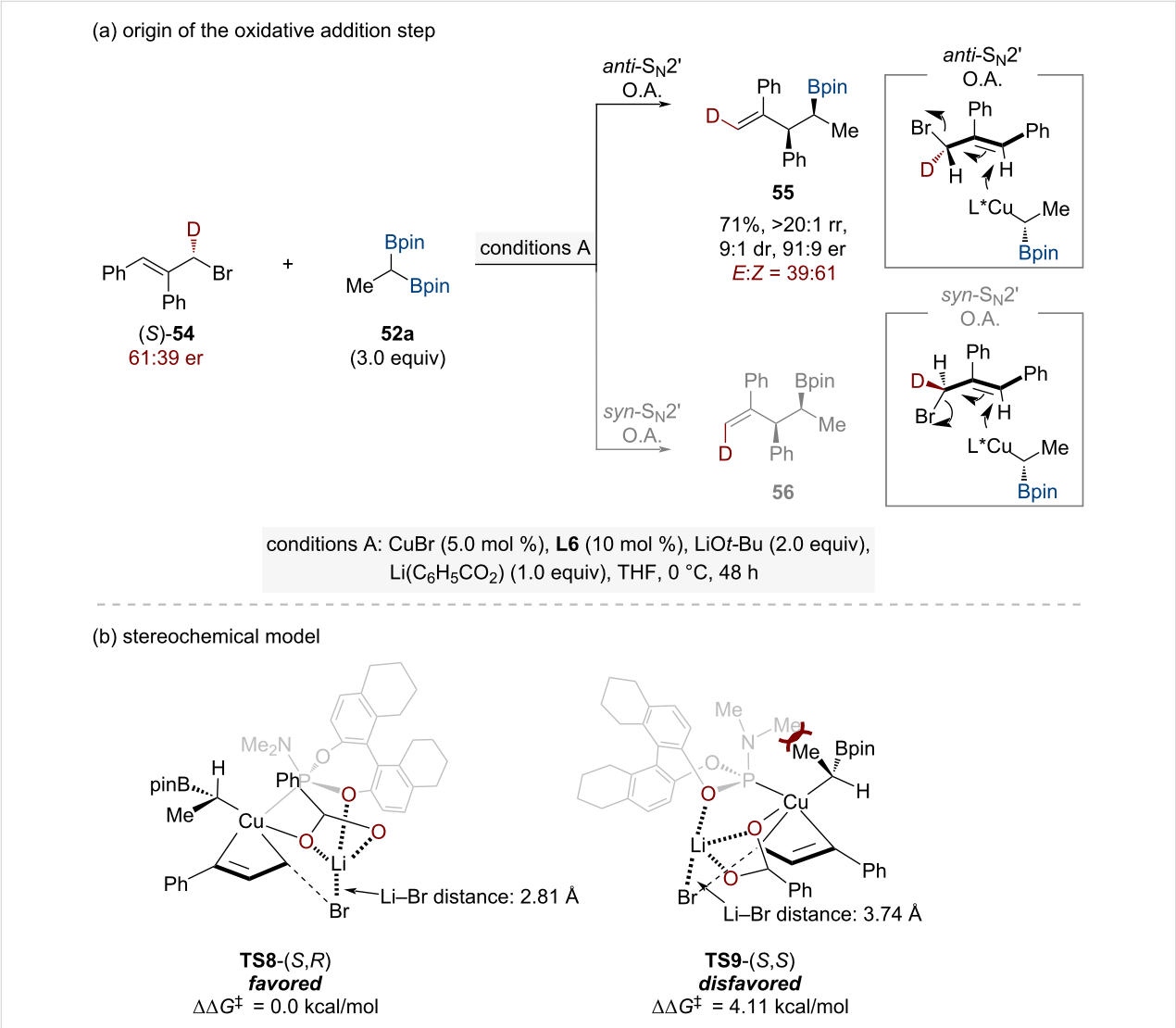

Scheme 19: (a) Experimental and (b) computational studies to understand the stereoselectivities in oxidative addition step.

ally stable chiral organoboron compounds, which enabled catalytic copper processes through carefully controlled activation.

Despite significant progress in copper hydride (CuH) catalysis eliminating the need for stoichiometric organometallic reagents, the scope of viable substrates remains restricted. While this methodology works effectively with olefins bearing electronic directing groups (such as aryl, boryl, or trifluoromethyl substituents) that guide regioselective hydrocupration, unactivated alkyl-substituted alkenes pose a persistent challenge. The recent breakthrough in CuH-catalyzed enantioselective and diastereoselective allylic alkylation of vinylboronic esters underscores both the current limitations and the potential for expanding substrate compatibility in this field.

Most recently, a complementary approach utilizing enantiotopic-group-selective transmetalation of 1,1-diborylalkanes has emerged. This method enables efficient coupling with various allylic electrophiles while achieving high levels of regio-, diastereo-, and enantioselectivity. Significantly, this strategy offers unique compatibility with substrates containing unsaturated functional groups such as alkenes or alkynes, overcoming a key limitation of conventional CuH catalysis.

Looking forward, several opportunities exist for further development in this field. The configurational stability of secondary alkylcopper species suggests broader applications in stereoselective transformations, particularly in the strategic construction of vicinal stereogenic centers through copper-catalyzed asymmetric allylic substitution reactions. While current methodologies have predominantly focused on generating single stereogenic centers, the rational design of compatible allylic electrophiles would provide an intriguing opportunity for accessing diverse stereochemical arrangements. The ability to precisely control multiple contiguous stereogenic centers would significantly expand the synthetic utility of such transformations, particularly in the synthesis of complex molecules such as natural products and pharmaceuticals [60]. Furthermore, future efforts could also focus on developing new catalyst systems for the copper-catalyzed stereoselective C–C-bond formation, as the mechanistic understanding gained from related studies may inform ligand design and expand the scope of nucleophiles and allylic electrophiles in this field. The continued development of these methodologies will be crucial for advancing the field of asymmetric synthesis.

Funding

This work was supported by National Research Foundation of Korea (NRF) grants funded by the Korea government (MSIT) [S. H. Cho: NRF-2022R1A2C3004731 and RS-2023-00219859; J. H. Lee: NRF-2022R1A2C1012021]. This research was also supported by the Bio&Medical Technology Development Program of the National Research Foundation (NRF) funded by the Korean government (MSIT) [RS-2023-00274113]. S. H. Cho thanks Korea Toray Science Foundation for the financial support.

Author Contributions

Minjae Kim: conceptualization; data curation; formal analysis; writing – original draft. Gwanggyun Kim: data curation; writing – review & editing. Doyoon Kim: data curation; writing – review & editing. Jun Hee Lee: conceptualization; funding acquisition; supervision; writing – original draft; writing – review & editing. Seung Hwan Cho: conceptualization; funding acquisition; supervision; writing – original draft; writing – review & editing.

ORCID® iDs

Minjae Kim - https://orcid.org/0009-0002-0346-0662
Gwanggyun Kim - https://orcid.org/0009-0009-4717-4247
Doyoon Kim - https://orcid.org/0009-0007-0651-2970
Jun Hee Lee - https://orcid.org/0000-0003-4108-5074
Seung Hwan Cho - https://orcid.org/0000-0001-5803-4922

Data Availability Statement

Data sharing is not applicable as no new data was generated or analyzed in this study

References

1. Hartwig, J. F.; Stanley, L. M. *Acc. Chem. Res.* **2010,** *43,* 1461–1475. doi:10.1021/ar100047x
2. Hartwig, J. F.; Pouy, M. J. *Top. Organomet. Chem.* **2011,** *34,* 169–208. doi:10.1007/978-3-642-15334-1_7
3. Tosatti, P.; Nelson, A.; Marsden, S. P. *Org. Biomol. Chem.* **2012,** *10,* 3147–3163. doi:10.1039/c2ob07086c
4. Hoveyda, A. H.; Zhou, Y.; Shi, Y.; Brown, M. K.; Wu, H.; Torker, S. *Angew. Chem., Int. Ed.* **2020,** *59,* 21304–21359. doi:10.1002/anie.202003755
5. Trost, B. M.; Van Vranken, D. L. *Chem. Rev.* **1996,** *96,* 395–422. doi:10.1021/cr9409804
6. Trost, B. M. *Chem. Pharm. Bull.* **2002,** *50,* 1–14. doi:10.1248/cpb.50.1
7. Trost, B. M.; Crawley, M. L. *Chem. Rev.* **2003,** *103,* 2921–2944. doi:10.1021/cr020027w
8. Milhau, L.; Guiry, P. J. *Top. Organomet. Chem.* **2011,** *38,* 95–153. doi:10.1007/3418_2011_9
9. Lloyd-Jones, G. C.; Pfaltz, A. *Angew. Chem., Int. Ed. Engl.* **1995,** *34,* 462–464. doi:10.1002/anie.199504621
10. Belda, O.; Moberg, C. *Acc. Chem. Res.* **2004,** *37,* 159–167. doi:10.1021/ar030239v
11. Matsushima, Y.; Onitsuka, K.; Kondo, T.; Mitsudo, T.-a.; Takahashi, S. *J. Am. Chem. Soc.* **2001,** *123,* 10405–10406. doi:10.1021/ja016334l
12. Trost, B. M.; Rao, M.; Dieskau, A. P. *J. Am. Chem. Soc.* **2013,** *135,* 18697–18704. doi:10.1021/ja411310w
13. Evans, P. A.; Nelson, J. D. *J. Am. Chem. Soc.* **1998,** *120,* 5581–5582. doi:10.1021/ja980030q

14. Kazmaier, U.; Stolz, D. *Angew. Chem., Int. Ed.* **2006,** *45,* 3072–3075. doi:10.1002/anie.200600100
15. Sidera, M.; Fletcher, S. P. *Nat. Chem.* **2015,** *7,* 935–939. doi:10.1038/nchem.2360
16. Didiuk, M. T.; Morken, J. P.; Hoveyda, A. H. *J. Am. Chem. Soc.* **1995,** *117,* 7273–7274. doi:10.1021/ja00132a039
17. Kita, Y.; Kavthe, R. D.; Oda, H.; Mashima, K. *Angew. Chem., Int. Ed.* **2016,** *55,* 1098–1101. doi:10.1002/anie.201508757
18. Takeuchi, R.; Kashio, M. *Angew. Chem., Int. Ed. Engl.* **1997,** *36,* 263–265. doi:10.1002/anie.199702631
19. Cheng, Q.; Tu, H.-F.; Zheng, C.; Qu, J.-P.; Helmchen, G.; You, S.-L. *Chem. Rev.* **2019,** *119,* 1855–1969. doi:10.1021/acs.chemrev.8b00506
20. Trost, B. M. *J. Org. Chem.* **2004,** *69,* 5813–5837. doi:10.1021/jo0491004
21. van Klaveren, M.; Persson, E. S. M.; del Villar, A.; Grove, D. M.; Bäckvall, J.-E.; van Koten, G. *Tetrahedron Lett.* **1995,** *36,* 3059–3062. doi:10.1016/0040-4039(95)00426-d
22. Karlström, A. S. E.; Huerta, F. F.; Meuzelaar, G. J.; Bäckvall, J.-E. *Synlett* **2001,** 0923–0926. doi:10.1055/s-2001-14667
23. Dübner, F.; Knochel, P. *Angew. Chem., Int. Ed.* **1999,** *38,* 379–381. doi:10.1002/(sici)1521-3773(19990201)38:3<379::aid-anie379>3.0.co;2-y
24. Alexakis, A.; Malan, C.; Lea, L.; Benhaim, C.; Fournioux, X. *Synlett* **2001,** 0927–0930. doi:10.1055/s-2001-14626
25. Malda, H.; van Zijl, A. W.; Arnold, L. A.; Feringa, B. L. *Org. Lett.* **2001,** *3,* 1169–1171. doi:10.1021/ol0156289
26. Luchaco-Cullis, C. A.; Mizutani, H.; Murphy, K. E.; Hoveyda, A. H. *Angew. Chem., Int. Ed.* **2001,** *40,* 1456–1460. doi:10.1002/1521-3773(20010417)40:8<1456::aid-anie1456>3.0.co;2-t
27. Lee, Y.; Akiyama, K.; Gillingham, D. G.; Brown, M. K.; Hoveyda, A. H. *J. Am. Chem. Soc.* **2008,** *130,* 446–447. doi:10.1021/ja0782192
28. Gao, F.; Carr, J. L.; Hoveyda, A. H. *Angew. Chem., Int. Ed.* **2012,** *51,* 6613–6617. doi:10.1002/anie.201202856
29. Jung, B.; Hoveyda, A. H. *J. Am. Chem. Soc.* **2012,** *134,* 1490–1493. doi:10.1021/ja211269w
30. Takeda, M.; Takatsu, K.; Shintani, R.; Hayashi, T. *J. Org. Chem.* **2014,** *79,* 2354–2367. doi:10.1021/jo500068p
31. Shi, Y.; Jung, B.; Torker, S.; Hoveyda, A. H. *J. Am. Chem. Soc.* **2015,** *137,* 8948–8964. doi:10.1021/jacs.5b05805
32. Ohmiya, H.; Yokobori, U.; Makida, Y.; Sawamura, M. *J. Am. Chem. Soc.* **2010,** *132,* 2895–2897. doi:10.1021/ja9109105
33. Nagao, K.; Yokobori, U.; Makida, Y.; Ohmiya, H.; Sawamura, M. *J. Am. Chem. Soc.* **2012,** *134,* 8982–8987. doi:10.1021/ja302520h
34. Shido, Y.; Yoshida, M.; Tanabe, M.; Ohmiya, H.; Sawamura, M. *J. Am. Chem. Soc.* **2012,** *134,* 18573–18576. doi:10.1021/ja3093955
35. Hojoh, K.; Shido, Y.; Ohmiya, H.; Sawamura, M. *Angew. Chem., Int. Ed.* **2014,** *53,* 4954–4958. doi:10.1002/anie.201402386
36. Shi, Y.; Hoveyda, A. H. *Angew. Chem., Int. Ed.* **2016,** *55,* 3455–3458. doi:10.1002/anie.201600309
37. Zhang, Z.-Q.; Zhang, B.; Lu, X.; Liu, J.-H.; Lu, X.-Y.; Xiao, B.; Fu, Y. *Org. Lett.* **2016,** *18,* 952–955. doi:10.1021/acs.orglett.5b03692
38. Skotnitzki, J.; Morozova, V.; Knochel, P. *Org. Lett.* **2018,** *20,* 2365–2368. doi:10.1021/acs.orglett.8b00699
39. Lee, J.; Torker, S.; Hoveyda, A. H. *Angew. Chem., Int. Ed.* **2017,** *56,* 821–826. doi:10.1002/anie.201611444
40. Kim, M.; Kim, G.; Kim, D.; Cho, S. H. *J. Am. Chem. Soc.* **2024,** *146,* 34861–34869. doi:10.1021/jacs.4c14150
41. Yorimitsu, H.; Oshima, K. *Angew. Chem., Int. Ed.* **2005,** *44,* 4435–4439. doi:10.1002/anie.200500653
42. Alexakis, A.; Bäckvall, J. E.; Krause, N.; Pàmies, O.; Diéguez, M. *Chem. Rev.* **2008,** *108,* 2796–2823. doi:10.1021/cr0683515
43. Falciola, C. A.; Alexakis, A. *Eur. J. Org. Chem.* **2008,** 3765–3780. doi:10.1002/ejoc.200800025
44. Geurts, K.; Fletcher, S. P.; van Zijl, A. W.; Minnaard, A. J.; Feringa, B. L. *Pure Appl. Chem.* **2008,** *80,* 1025–1037. doi:10.1351/pac200880051025
45. Harutyunyan, S. R.; den Hartog, T.; Geurts, K.; Minnaard, A. J.; Feringa, B. L. *Chem. Rev.* **2008,** *108,* 2824–2852. doi:10.1021/cr068424k
46. Skotnitzki, J.; Spessert, L.; Knochel, P. *Angew. Chem., Int. Ed.* **2019,** *58,* 1509–1514. doi:10.1002/anie.201811330
47. Xu, N.; Liang, H.; Morken, J. P. *J. Am. Chem. Soc.* **2022,** *144,* 11546–11552. doi:10.1021/jacs.2c04037
48. Liang, H.; Morken, J. P. *J. Am. Chem. Soc.* **2023,** *145,* 20755–20760. doi:10.1021/jacs.3c07129
49. Liu, R. Y.; Buchwald, S. L. *Acc. Chem. Res.* **2020,** *53,* 1229–1243. doi:10.1021/acs.accounts.0c00164
50. Wang, Y.-M.; Buchwald, S. L. *J. Am. Chem. Soc.* **2016,** *138,* 5024–5027. doi:10.1021/jacs.6b02527
51. Lee, J.; Radomkit, S.; Torker, S.; del Pozo, J.; Hoveyda, A. H. *Nat. Chem.* **2018,** *10,* 99–108. doi:10.1038/nchem.2861
52. Leonori, D.; Aggarwal, V. K. *Acc. Chem. Res.* **2014,** *47,* 3174–3183. doi:10.1021/ar5002473
53. Han, J. T.; Jang, W. J.; Kim, N.; Yun, J. *J. Am. Chem. Soc.* **2016,** *138,* 15146–15149. doi:10.1021/jacs.6b11229
54. Kojima, R.; Akiyama, S.; Ito, H. *Angew. Chem., Int. Ed.* **2018,** *57,* 7196–7199. doi:10.1002/anie.201803663
55. Kojima, Y.; Miura, M.; Hirano, K. *ACS Catal.* **2021,** *11,* 11663–11670. doi:10.1021/acscatal.1c02947
56. Liu, S.; Ding, K.; Su, B. *ACS Catal.* **2024,** *14,* 12102–12109. doi:10.1021/acscatal.4c03735
57. Wang, S.; Chen, K.; Niu, J.; Guo, X.; Yuan, X.; Yin, J.; Zhu, B.; Shi, D.; Guan, W.; Xiong, T.; Zhang, Q. *Angew. Chem., Int. Ed.* **2024,** *63,* e202410833. doi:10.1002/anie.202410833
58. Lee, Y.; Han, S.; Cho, S. H. *Acc. Chem. Res.* **2021,** *54,* 3917–3929. doi:10.1021/acs.accounts.1c00455
59. Kim, M.; Park, B.; Shin, M.; Kim, S.; Kim, J.; Baik, M.-H.; Cho, S. H. *J. Am. Chem. Soc.* **2021,** *143,* 1069–1077. doi:10.1021/jacs.0c11750
60. Yang, K.; Chen, L.; Su, B. *Synthesis* **2024,** *56,* 3365–3376. doi:10.1055/s-0040-1720115

License and Terms

BEILSTEIN JOURNAL OF ORGANIC CHEMISTRY

Regioselective formal hydrocyanation of allenes: synthesis of β,γ-unsaturated nitriles with α-all-carbon quaternary centers

Seeun Lim, Teresa Kim and Yunmi Lee*

Full Research Paper

Open Access

Address:
Department of Chemistry, Kwangwoon University, Seoul 01897, Republic of Korea

Email:
Yunmi Lee* - ymlee@kw.ac.kr

* Corresponding author

Keywords:
α-quaternary nitrile; Cu catalysis; hydrocyanation; regioselectivity; tosyl cyanide

Beilstein J. Org. Chem. **2025,** *21,* 800–806.
https://doi.org/10.3762/bjoc.21.63

Received: 31 December 2024
Accepted: 01 April 2025
Published: 17 April 2025

This article is part of the thematic issue "Copper catalysis: a constantly evolving field".

Guest Editor: J. Yun

Abstract

This study introduces a highly selective hydrocyanation method based on copper-catalyzed hydroalumination of allenes with diisobutylaluminum hydride, followed by the regio- and stereoselective allylation with *p*-toluenesulfonyl cyanide. The proposed methodology is efficient for accessing acyclic β,γ-unsaturated nitriles with α-all-carbon quaternary centers and achieves yields up to 99% and excellent regio- and *E*-selectivity. The reaction proceeds under mild conditions and shows broad applicability to di- and trisubstituted allenes. Its practicality is demonstrated through the gram-scale synthesis and functional group transformations of amines, amides, and lactams, emphasizing its versatility and synthetic significance.

Introduction

Acyclic nitriles that incorporate α-all-carbon quaternary centers are highly valuable structural motifs typically found in natural products, biologically active compounds, and synthetic pharmaceuticals [1-5]. These compounds are important intermediates in organic syntheses because of the versatility of the cyano group, which can be readily transformed into a wide range of functional groups, including amides, carboxylic acids, amines, aldehydes, ketones, and *N*-heterocycles [6-8]. However, the synthesis of all-carbon quaternary centers that contain functional groups is challenging mainly because of their sterically demanding property [9-11]. In this context, the incorporation of cyano groups at the quaternary carbon centers is promising for the development of versatile acyclic all-carbon quaternary stereocenters with diverse functional groups [12-14]. Consequently, the development of selective and predictable strategies for the introduction of cyano groups into quaternary carbon frameworks has become necessary in organic synthesis.

The transition-metal-catalyzed hydrocyanation of carbon–carbon double bonds is one of the most efficient and atom-economical approaches for synthesizing alkyl nitriles [15,16]. Among the potential substrates, allenes have attracted signifi-

cant attention because of their unique structural features, which consist of two orthogonal and contiguous C=C bonds. This dual π-system configuration promotes selective functionalization, enabling the synthesis of various complex products through a single transformation [17-19]. Therefore, allenes have become versatile intermediates in numerous transition-metal-catalyzed reactions [20,21]. Despite extensive studies on the catalytic hydrocyanation of alkenes [22], including the industrially relevant DuPont adiponitrile process from 1,3-butadiene using nickel catalysts [23], the hydrocyanation of allenes to produce functionalized β,γ-unsaturated nitriles with quaternary carbon centers has not been investigated extensively [24]. The limited investigation of allene hydrocyanation can be attributed to the significant challenges posed by the two orthogonal π-systems in allenes. These challenges include achieving high regioselectivity and controlling (*E*)/(*Z*)-stereoselectivity, as 1,2-addition processes to allenes can generate up to four possible regioisomeric products.

Recent research has addressed some of these challenges. Arai [25,26], Fang [27] and Breit [28] investigated the nickel-catalyzed regio- and enantioselective hydrocyanation of 1,1-disubstituted allenes using acetone cyanohydrin or TMSCN/MeOH as the precursor for the in situ generation of hydrogen cyanide (Scheme 1a). This method achieved high regioselectivity and enantioselectivity, highlighting the potential of allene hydrocyanation for the synthesis of complex nitrile-containing products. In another approach, the Minakata group used electrophilic cyanating reagents, such as *p*-toluenesulfonyl cyanide (TsCN) and *N*-cyano-*N*-phenyl-*p*-toluenesulfonamide [29]. The hydroboration of allenes with 9-BBN (9-borabicyclo[3.3.1]nonane) as the hydride source, followed by regioselective cyanation with allylic boranes, provided nitrile-substituted quaternary carbon centers (Scheme 1b). Although both methodologies achieved high regioselectivity, their substrate scopes were limited, and most studies focused on the hydrocyanation of terminal allenes.

Given the synthetic importance of nitriles that bear all-carbon quaternary centers and the distinctive reactivity of allenes, the development of hydrocyanation methodologies with a broadened substrate scope and improved regio- and stereoselectivity is of significant interest. Inspired by our study on the construction of all-carbon quaternary centers via functionalized allylaluminum reagents obtained from the copper-catalyzed regioselective hydroalumination of allenes using diisobutylaluminum hydride (DIBAL-H), we envisioned that the nucleophilic attack of allylaluminum reagents on electrophilic cyanating reagents could provide a regioselective pathway for the synthesis of alkyl nitriles bearing quaternary carbon centers [30-33]. Herein, we report a mild and efficient method for the regio- and (*E*)-stereoselective formal hydrocyanation of di- and trisubstituted allenes. Using DIBAL-H as the hydride source and TsCN as a readily available and bench-stable cyanating agent in the presence of a copper catalyst, we synthesized new and versatile functionalized acyclic nitriles that include all-carbon quaternary centers with high selectivity (Scheme 1c). Compared to previous methodologies, our approach enables the efficient generation of tertiary nitrile products with a broader substrate scope, highlighting its synthetic utility and potential applicability in complex molecule synthesis.

Results and Discussion

We began by optimizing the hydrocyanation of allene **1a** using DIBAL-H as the hydride source and *p*-toluenesulfonyl cyanide

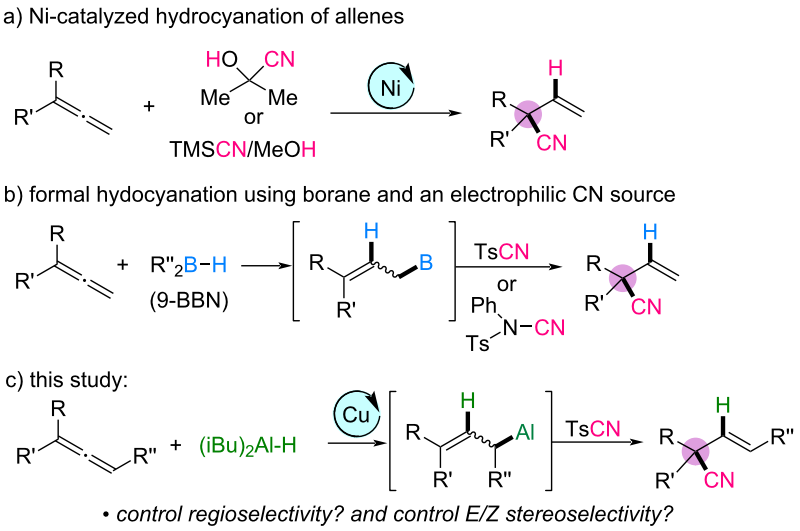

Scheme 1: Synthesis of acyclic nitrile-substituted quaternary carbon centers from allenes.

as the cyanating reagent (Scheme 2). Under previously established conditions, the hydride addition of DIBAL-H to allene **1a** catalyzed by 5 mol % IPrCuCl as the optimal catalyst selectively generated the allylaluminum intermediate **2a** with >98% conversion [30]. Subsequent addition of one equivalent of TsCN to **2a** in a single vessel at room temperature proceeded regioselectively, achieving complete conversion within 30 min and yielding the desired α-quaternary nitrile **3a** in 95% yield. Moreover, no byproducts, such as regioisomeric nitriles or derivatives from over-addition of allylaluminum, were observed.

After having established the optimized reaction conditions, the substrate scope for the formal hydrocyanation with 1,1-disubstituted and 1,1,3-trisubstituted allenes was examined (Scheme 3). All reactions were performed in the presence of 5 mol % IPrCuCl to generate the allylaluminum reagents in situ, followed by cyanation at room temperature for 30 min. This method efficiently constructed α-all-carbon quaternary centers on β,γ-unsaturated nitriles with excellent >98% regioselectivity and >98% (*E*)-selectivity. 1,1-Disubstituted allenes bearing silyl ether- and benzyl ether-tethered propyl groups were successfully converted into the desired nitriles **3a–c** in yields ranging from 88% to 99%. Similarly, chloro-substituted allene **1d** exhibited good tolerance under these conditions, affording the corresponding nitrile **3d** in an 88% yield, whereas phenethyl-substituted allene **1e** provided **3e** in a 95% yield. Allenes **1f–i** featuring phenyl and alkyl substituents, including methyl, ethyl, phenethyl, and allyl groups, also underwent smooth cyanation, resulting in α-quaternary nitriles **3f–i** in yields of 85–94%. Furthermore, aryl-substituted allenes **1j–o**, incorporating electron-donating or electron-withdrawing substituents such as methyl, fluoro, chloro, bromo, trifluoromethyl, or methoxy groups on the phenyl ring, were compatible with the reaction, producing nitriles **3j–o** in 88–93% yields. In particular, thienyl-substituted allene **1p** was efficiently transformed into the desired nitrile **3p**.

We further demonstrated the versatility of this protocol using 1,1,3-trisubstituted allenes. Trisubstituted allenes **1q–s** bearing phenyl and dialkyl groups, including a cyclohexyl moiety, underwent selective cyanation to deliver the (*E*)-isomers of the corresponding nitriles **3q–s** in yields of 90–95%. In addition, aryl- and dialkyl-substituted allenes **1t–x** containing substituents, such as fluoro, chloro, bromo, trifluoromethyl, or methoxy groups on the phenyl ring, were smoothly converted into β,γ-unsaturated nitriles **3t–x** with high efficiency. Particularly, allenes **1y** and **1z** containing benzodioxane or naphthalene moieties were well-tolerated under these reaction conditions, affording nitriles **3y** and **3z** in 85% and 93% yield, respectively. Unfortunately, the 1,1,3-trialkyl-substituted allene **1aa** was not suitable for Cu-catalyzed hydroalumination under the established conditions, resulting in less than 2% conversion to allylaluminum reagents.

In a previous study on the electrophilic cyanation of allylic boranes conducted by the Minakata group (Scheme 1b), only two examples of β,γ-unsaturated nitrile products bearing α-tertiary carbon centers were established, and the yields were moderate [29]. To broaden the applicability of the system, we extended it to the synthesis of nitriles containing both quaternary and tertiary carbon centers. The scope of monosubstituted allenes is illustrated in Scheme 4. Allenes **4a–c** substituted with alkyl groups, including phenethyl, decyl, and cyclohexyl groups, smoothly underwent hydrocyanation, yielding the corresponding nitriles **5a–c** in 79–90% yield with excellent regioselectivity (>98%). Functional groups such as silyl ether, benzyl

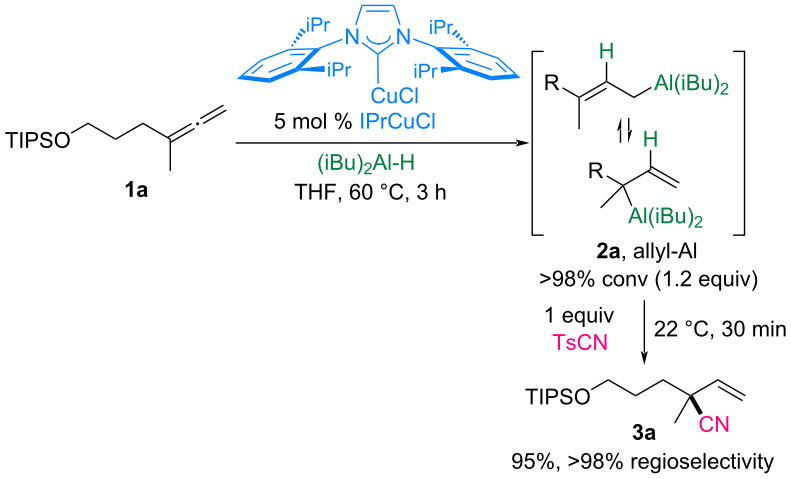

Scheme 2: Hydrocyanation of allene **1a** with tosyl cyanide.

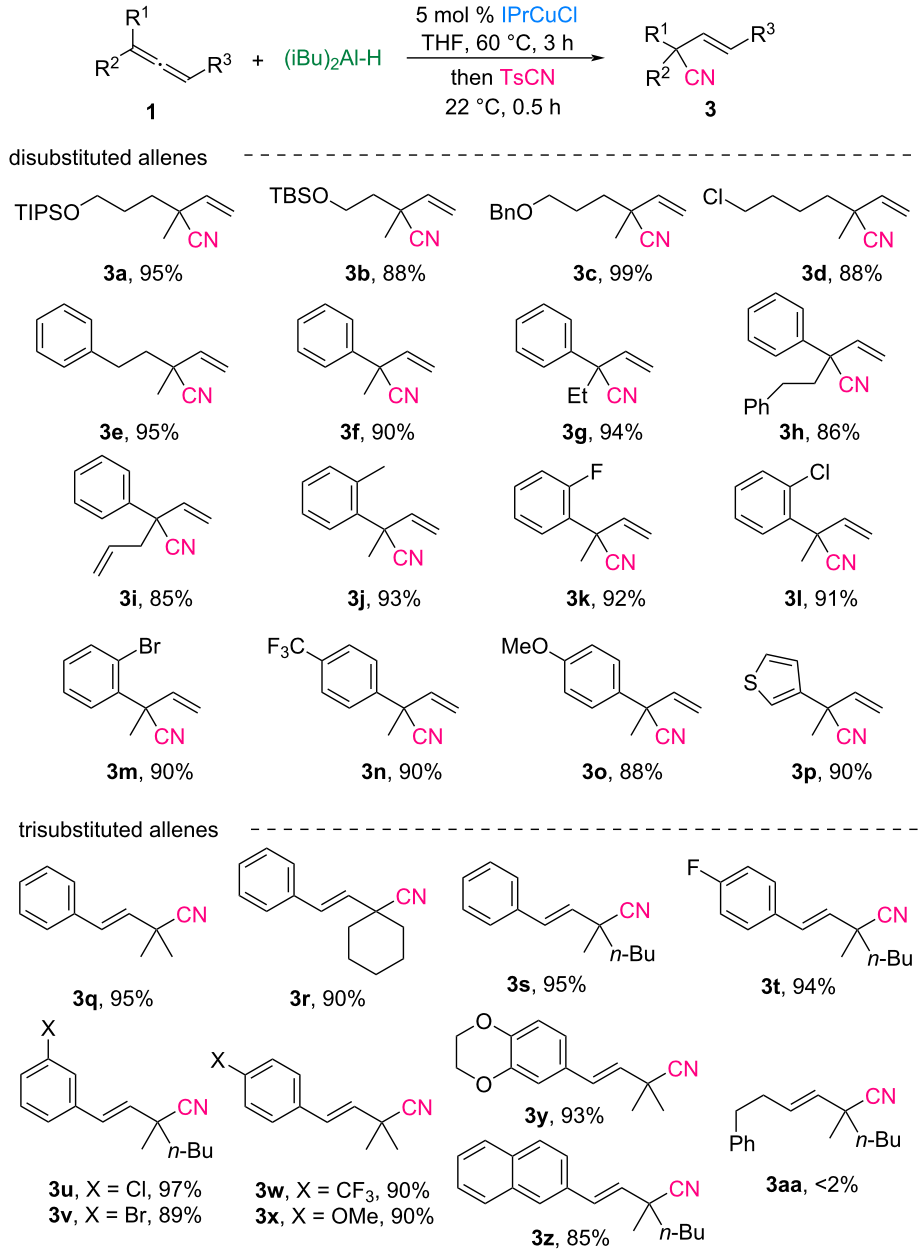

Scheme 3: Hydrocyanation with various di- or trisubstituted allenes. Reaction conditions: allene **1** (0.3 mmol), $(iBu)_2Al$-H (0.3 mmol), IPrCuCl (5 mol %), TsCN (0.25 mmol), THF (0.2 M), under N_2. The yields of the isolated products are given.

ether, and chloro moieties on allenes **4d–f** were well tolerated under the reaction conditions, producing nitrile-substituted tertiary carbon products **5d–f** in yields ranging from 73% to 85%. Moreover, aryl-substituted allene **4g** was efficiently converted to the desired nitrile **5g** in high yield.

Gram-scale reactions were conducted using allenes to demonstrate the practical applicability of this hydrocyanation method (Scheme 5). Allene **1q** (1.04 g, 7.2 mmol) and allene **4b** (1.08 g, 6.0 mmol) were effectively transformed into nitrile products **3q** and **5b**, achieving yields of 93% and 87%, respectively. When the catalyst loading was reduced to 3 mol % for the reaction of allene **4b**, the hydroalumination did not reach full conversion even with an extended reaction time (6 h vs 3 h). As a result, the incomplete hydroalumination led to a side reaction between the remaining DIBAL-H and TsCN, ultimately yielding the cyanation product **5b** in only 54%.

The synthetic potential of the obtained β,γ-unsaturated nitriles featuring α-quaternary carbon centers was further illustrated

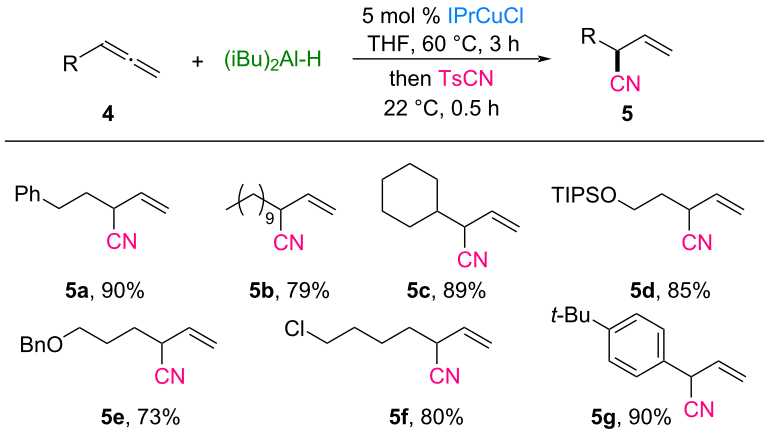

Scheme 4: Hydrocyanation with various monosubstituted allenes. Reaction conditions: allene **4** (0.3 mmol), $(iBu)_2Al$-H (0.3 mmol), IPrCuCl (5 mol %), TsCN (0.25 mmol), THF (0.2 M), under N_2. The yields of the isolated products are given.

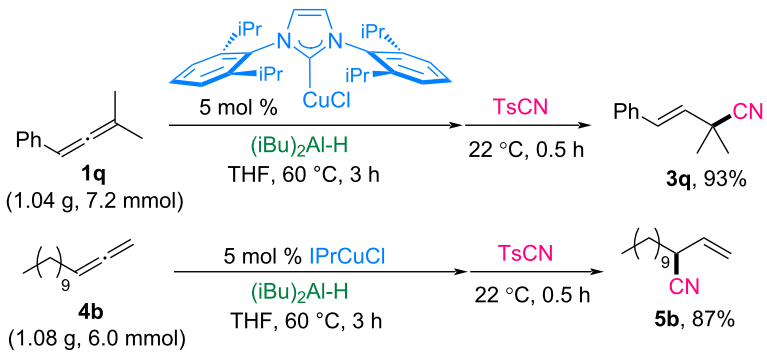

Scheme 5: Gram scale reaction.

using a series of transformations (Scheme 6). Nitrile **3q** was hydrolyzed to amide **6** in a 90% yield under basic conditions using sodium hydroxide and *tert*-butanol. The reduction of nitrile **3q** with lithium aluminum hydride generated amine **7** in an 85% yield, whereas the selective hydrogenation of the alkene moiety of **3q** using a Pd/C catalyst in a H_2 gas environment

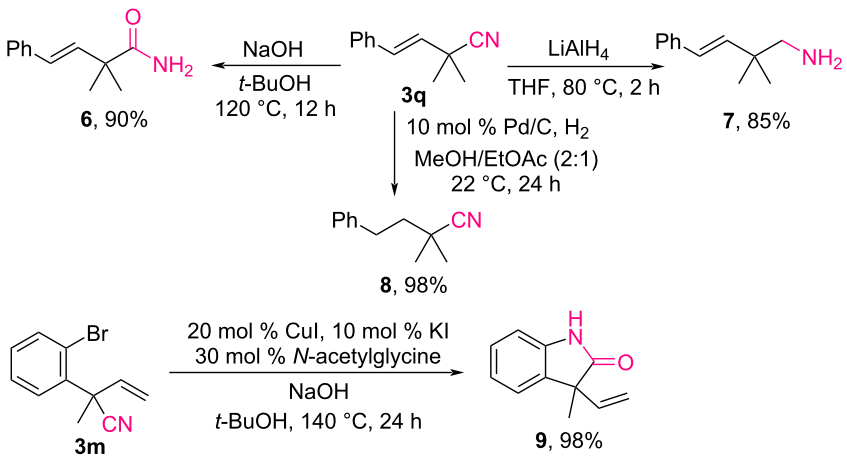

Scheme 6: Synthetic applications.

smoothly produced product **8** in a 98% yield. *Ortho*-bromoaryl-substituted nitrile **3m** also underwent tandem amidation and copper-catalyzed cyclization, efficiently producing lactam **9** in a 98% yield.

Scheme 7 illustrates a plausible reaction mechanism based on previous studies [34]. The process begins with the formation of NHC–copper hydride complex **A** through the reaction of IPrCuCl with DIBAL-H [35]. Copper hydride species **A** reacts regioselectively with allene **1** to form the allylcopper intermediate **B**. Subsequent transmetalation between allyl-Cu **B** and DIBAL-H generates allylaluminum species **C** and regenerates IPrCuH (**A**). The final step involves the regioselective nucleophilic attack of allylaluminum **C** on tosyl cyanide, which proceeds at the γ-position via six-membered ring transition state **D**, leading to the formation of the desired nitrile product. Transition state **D** is responsible for the *E*-selectivity observed in trisubstituted allenes, as it minimizes the allylic strain between the R and R" groups.

Conclusion

In this study, we developed a highly regio- and (*E*)-selective formal hydrocyanation protocol for allenes using a copper-catalyzed hydroalumination/cyanation sequence with DIBAL-H and tosyl cyanide. This approach offers mild reaction conditions, broad functional group compatibility, and high efficiency, enabling the synthesis of new and versatile functionalized β,γ-unsaturated nitriles containing α-all-carbon quaternary centers with exceptional selectivity. The practicality of this approach was validated through gram-scale synthesis and the successful transformation of nitrile products into amines, amides, and lactams. Further studies are underway to broaden the scope and application of the proposed method.

Supporting Information

Supporting Information File 1

General information, experimental procedures, characterization data and copies of spectra.
[https://www.beilstein-journals.org/bjoc/content/supplementary/1860-5397-21-63-S1.pdf]

Funding

This research was supported by the Basic Science Research Program through the National Research Foundation of Korea (NRF) (NRF-2020R1A2C1005817).

Author Contributions

Seeun Lim: investigation; writing – review & editing. Teresa Kim: investigation. Yunmi Lee: conceptualization; data curation; funding acquisition; investigation; methodology; project administration; supervision; writing – original draft.

ORCID® iDs

Seeun Lim - https://orcid.org/0009-0001-9975-0367
Yunmi Lee - https://orcid.org/0000-0003-1315-4001

Data Availability Statement

All data that supports the findings of this study is available in the published article and/or the supporting information of this article.

References

1. Zeng, X.-P.; Sun, J.-C.; Liu, C.; Ji, C.-B.; Peng, Y.-Y. *Adv. Synth. Catal.* **2019,** *361,* 3281–3305. doi:10.1002/adsc.201900015

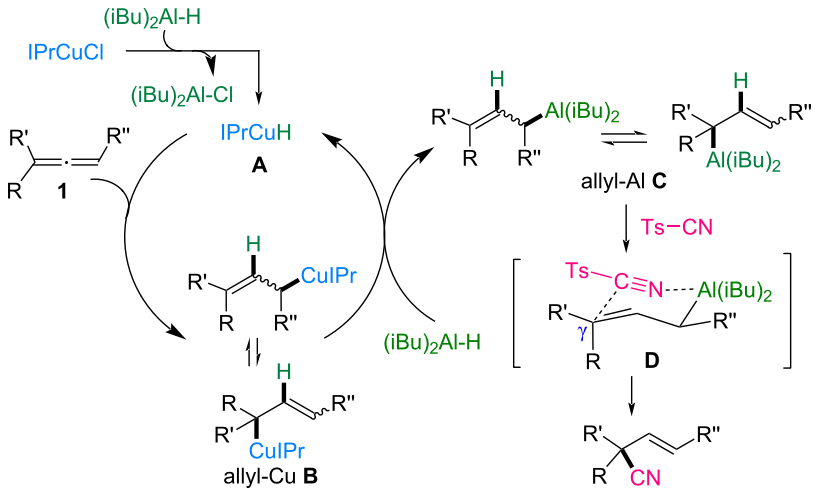

Scheme 7: Proposed mechanism.

2. Fleming, F. F.; Yao, L.; Ravikumar, P. C.; Funk, L.; Shook, B. C. *J. Med. Chem.* **2010,** *53,* 7902–7917. doi:10.1021/jm100762r
3. Fleming, F. F. *Nat. Prod. Rep.* **1999,** *16,* 597–606. doi:10.1039/a804370a
4. Kern, C.; Wolf, C.; Bender, F.; Berger, M.; Noack, S.; Schmalz, S.; Ilg, T. *Insect Mol. Biol.* **2012,** *21,* 456–471. doi:10.1111/j.1365-2583.2012.01151.x
5. Cheng, R. C. K.; Tikhonov, D. B.; Zhorov, B. S. *J. Biol. Chem.* **2009,** *284,* 28332–28342. doi:10.1074/jbc.m109.027326
6. Nakao, Y. *Chem. Rev.* **2021,** *121,* 327–344. doi:10.1021/acs.chemrev.0c00301
7. Kukushkin, V. Y.; Pombeiro, A. J. L. *Chem. Rev.* **2002,** *102,* 1771–1802. doi:10.1021/cr0103266
8. Rappoport, Z., Ed. *The Cyano Group;* PATAI'S Chemistry of Functional Groups; John Wiley & Sons: London, UK, 1970. doi:10.1002/9780470771242
9. Sun, X.; Li, B.-J. *Synthesis* **2022,** *54,* 2103–2118. doi:10.1055/s-0040-1719899
10. Feng, J.; Holmes, M.; Krische, M. J. *Chem. Rev.* **2017,** *117,* 12564–12580. doi:10.1021/acs.chemrev.7b00385
11. Das, J. P.; Marek, I. *Chem. Commun.* **2011,** *47,* 4593–4623. doi:10.1039/c0cc05222a
12. Long, J.; Zhao, R.; Cheng, G.-J.; Fang, X. *Angew. Chem., Int. Ed.* **2023,** *62,* e202304543. doi:10.1002/anie.202304543
13. Chen, L.; Pu, M.; Li, S.; Sang, X.; Liu, X.; Wu, Y.-D.; Feng, X. *J. Am. Chem. Soc.* **2021,** *143,* 19091–19098. doi:10.1021/jacs.1c08382
14. Long, J.; Xia, S.; Wang, T.; Cheng, G.-J.; Fang, X. *ACS Catal.* **2021,** *11,* 13880–13890. doi:10.1021/acscatal.1c03729
15. Zhang, H.; Su, X.; Dong, K. *Org. Biomol. Chem.* **2020,** *18,* 391–399. doi:10.1039/c9ob02374g
16. Wu, W.-B.; Yu, J.-S.; Zhou, J. *ACS Catal.* **2020,** *10,* 7668–7690. doi:10.1021/acscatal.0c01918
17. Li, G.; Huo, X.; Jiang, X.; Zhang, W. *Chem. Soc. Rev.* **2020,** *49,* 2060–2118. doi:10.1039/c9cs00400a
18. Yu, S.; Ma, S. *Angew. Chem., Int. Ed.* **2012,** *51,* 3074–3112. doi:10.1002/anie.201101460
19. Ma, S. *Chem. Rev.* **2005,** *105,* 2829–2872. doi:10.1021/cr020024j
20. Blieck, R.; Taillefer, M.; Monnier, F. *Chem. Rev.* **2020,** *120,* 13545–13598. doi:10.1021/acs.chemrev.0c00803
21. Liu, Y.; Bandini, M. *Chin. J. Chem.* **2019,** *37,* 431–441. doi:10.1002/cjoc.201800568
22. Ahmad, M. S.; Meguellati, K.; Wang, Q. *J. Saudi Chem. Soc.* **2022,** *26,* 101483. doi:10.1016/j.jscs.2022.101483
23. Tolman, C. A. *J. Chem. Educ.* **1986,** *63,* 199–201. doi:10.1021/ed063p199
24. Arai, S. *Chem. Pharm. Bull.* **2019,** *67,* 397–403. doi:10.1248/cpb.c18-00953
25. Arai, S.; Hori, H.; Amako, Y.; Nishida, A. *Chem. Commun.* **2015,** *51,* 7493–7496. doi:10.1039/c5cc01899d
26. Hori, H.; Arai, S.; Nishida, A. *Adv. Synth. Catal.* **2017,** *359,* 1170–1176. doi:10.1002/adsc.201601400
27. Ding, Y.; Long, J.; Fang, X. *Org. Chem. Front.* **2021,** *8,* 5852–5857. doi:10.1039/d1qo01099a
28. Bury, T.; Kullmann, S.; Breit, B. *Adv. Synth. Catal.* **2023,** *365,* 335–341. doi:10.1002/adsc.202201189
29. Kiyokawa, K.; Hata, S.; Kainuma, S.; Minakata, S. *Chem. Commun.* **2019,** *55,* 458–461. doi:10.1039/c8cc09229j
30. Lee, S.; Lee, S.; Lee, Y. *Org. Lett.* **2020,** *22,* 5806–5810. doi:10.1021/acs.orglett.0c01876
31. Yoon, S.; Lee, K.; Kamranifard, T.; Lee, Y. *Bull. Korean Chem. Soc.* **2022,** *43,* 1307–1311. doi:10.1002/bkcs.12629
32. Lee, S.; Lee, Y. *Adv. Synth. Catal.* **2023,** *365,* 4641–4646. doi:10.1002/adsc.202300825
33. Lee, K.; Cho, S.; Lim, S.; Lee, Y. *Org. Chem. Front.* **2024,** *11,* 1366–1371. doi:10.1039/d3qo01855e
34. Nakamura, E.; Mori, S. *Angew. Chem., Int. Ed.* **2000,** *39,* 3750–3771. doi:10.1002/1521-3773(20001103)39:21<3750::aid-anie3750>3.0.co;2-l
35. Jordan, A. J.; Lalic, G.; Sadighi, J. P. *Chem. Rev.* **2016,** *116,* 8318–8372. doi:10.1021/acs.chemrev.6b00366

License and Terms

BEILSTEIN JOURNAL OF ORGANIC CHEMISTRY

Cu–Bpin-mediated dimerization of 4,4-dichloro-2-butenoic acid derivatives enables the synthesis of densely functionalized cyclopropanes

Patricia Gómez-Roibás, Andrea Chaves-Pouso and Martín Fañanás-Mastral*

Letter

Open Access

Address:
Centro Singular de Investigación en Química Biolóxica e Materiais Moleculares (CiQUS), Universidade de Santiago de Compostela, 15782 Santiago de Compostela, Spain

Email:
Martín Fañanás-Mastral* - martin.fananas@usc.es

* Corresponding author

Keywords:
chlorocyclopropanes; copper; cyclization; 4,4-dichloro-2-butenoic acid derivatives; dimerization

Beilstein J. Org. Chem. **2025,** *21,* 877–883.
https://doi.org/10.3762/bjoc.21.71

Received: 30 December 2024
Accepted: 14 April 2025
Published: 05 May 2025

This article is part of the thematic issue "Copper catalysis: a constantly evolving field".

Guest Editor: J. Yun

Abstract

4,4-Dichloro-2-butenoic acid derivatives are shown to undergo a rare dimerization process when reacted with bis(pinacolato)diboron under copper catalysis. The reaction provides densely functionalized products with excellent levels of chemo-, regio-, and diastereoselectivity. This high degree of functionalization makes these products versatile building blocks for the stereoselective synthesis of chlorocyclopropanes.

Introduction

In the last years our group has been focused on the development of catalytic methodologies for the carboboration of unsaturated hydrocarbons [1-7]. In the course of our investigation of the copper-catalyzed borylative coupling of alkynes with allylic *gem*-dichlorides [3], we observed that alkyl 4,4-dichloro-2-butenoates deviated from the general reactivity trend. While allylic *gem*-dichlorides bearing aromatic and aliphatic substituents efficiently provided the allylboration product (Scheme 1a), the use of ester derivative **1** under same reaction conditions led to the formation of an unexpected product arising from the coupling of two dichloride molecules with no alkyne incorporation (Scheme 1b). We have studied this reaction and now report a catalytic methodology for the diastereoselective synthesis of these dimeric structures. The high degree of functionalization present in these molecules, which feature two ester groups, an aliphatic *gem*-dichloride and a dichloroalkene unit, offers ample opportunities for further functionalization. This is illustrated by their chemo- and diastereoselective conversion into densely functionalized cyclopropanes (Scheme 1c).

Results and Discussion

Based on our preliminary result, we started our study by exploring the reaction between ethyl 4,4-dichloro-2-butenoate (**1**) and B_2pin_2 (Table 1). By using NaO*t*-Bu as base and tolu-

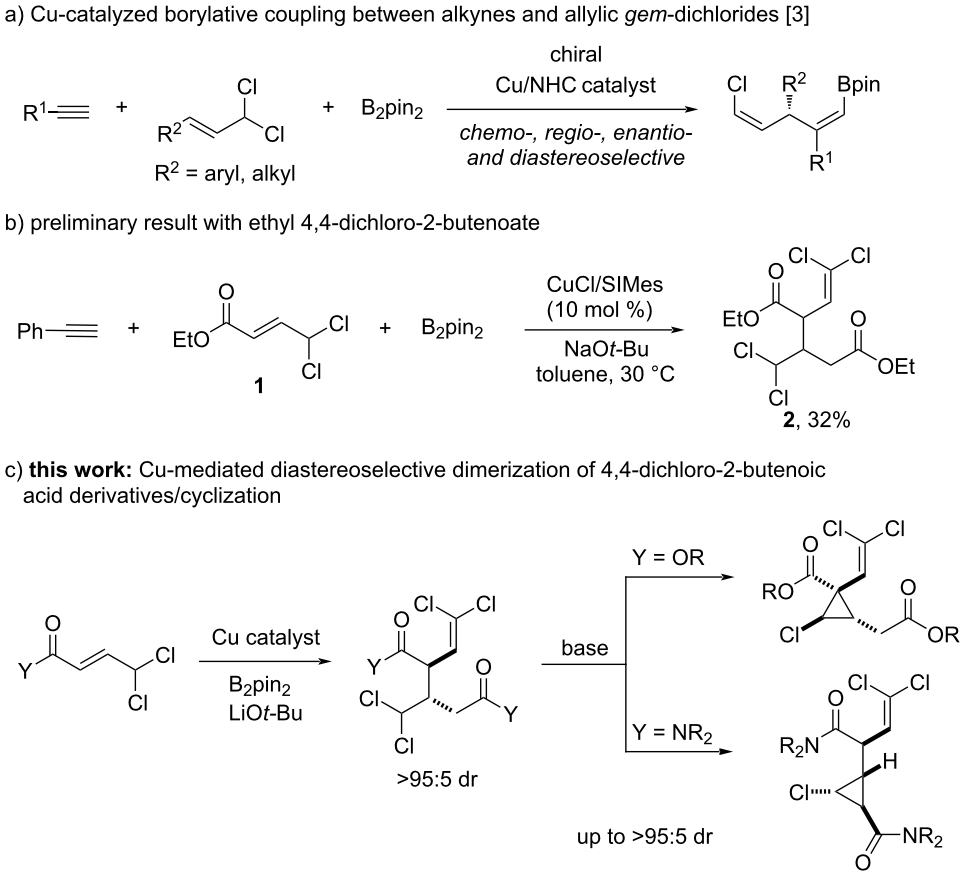

Scheme 1: Chemodivergent reactivity observed in copper-catalyzed borylative couplings of allylic *gem*-dichlorides.

ene as solvent, the Cu/SIMes catalyst provided compound **2** as single reaction product, albeit in low yield and with low diastereoselectivity (Table 1, entry 1). Lowering the amount of B_2pin_2 to 1 equivalent was found to be beneficial (Table 1, entry 2), although the use of sub-stoichiometric amounts led to a significant decrease in reaction yield (Table 1, entry 3). We also tried to reduce the amount of base, but this caused a drop in the reaction efficiency (Table 1, entry 4). Evaluation of different bases demonstrated the important role of the base metal cation. Gratifyingly, we observed that the use of LiO*t*-Bu led to the formation of product **2** as a single diastereomer (Table 1, entry 5). A slightly lower diastereoselectivity was observed when KO*t*-Bu was used, which also gave rise to **2** in diminished yield (Table 1, entry 6). The nature of the solvent also played a role in the reaction outcome. A decrease both in efficiency and diastereoselectivity was observed when THF was used (Table 1, entry 7). The use of dichloromethane eroded the diastereoselectivity and also the chemoselectivity as shown with the additional formation of **3** as a mixture of *Z*:*E* isomers (Table 1, entry 8). Having identified the proper combination of base and solvent, we then screened different copper catalysts. Different NHCs, bisphosphines and phosphines were tested (Table 1, entries 9–14) and excellent chemo- and diastereoselectivity was observed in all cases, with SIPr providing the best result (Table 1, entry 11). Under these optimized conditions, product **2** was isolated in 60% yield as a single diastereomer. The relative configuration of **2** was determined by two-dimensional NMR analysis (see Supporting Information File 1 for details).

This transformation could be efficiently applied to the dimerization of other 4,4-dichloro-2-butenoates and 4,4-dichloro-2-butenamides. The corresponding products **8** and **9** were obtained in good yield and excellent diastereoselectivity (Scheme 2). In sharp contrast, the use of *gem*-dichlorides bearing a ketone group did not result in the formation of the dimerization product and complex mixtures of products were observed in these cases.

To gather insight into the reaction mechanism, several control experiments were performed (Scheme 3).

We first observed that the reaction does not take place in the absence of B_2pin_2 (Scheme 3a). Based on the well accepted

Table 1: Optimization studies.

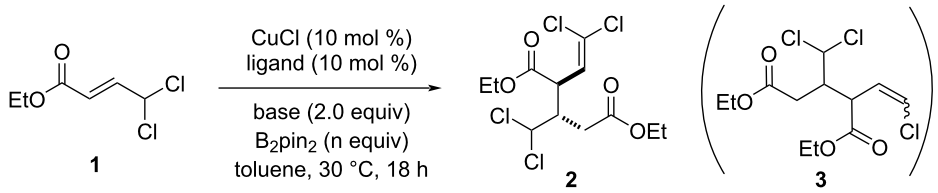

Entry[a]	Base	B_2pin_2 (equiv)	Ligand	Yield **2**[b]	**2** dr[c]
1	NaO*t*-Bu	2.0	SIMes	34	73:27
2	NaO*t*-Bu	1.0	SIMes	56	70:30
3	NaO*t*-Bu	0.5	SIMes	8	n.d.
4	NaO*t*-Bu[d]	1.0	SIMes	22	72:28
5	LiO*t*-Bu	1.0	SIMes	49	>95:5
6	KO*t*-Bu	1.0	SIMes	27	92:8
7[e]	LiO*t*-Bu	1.0	SIMes	20	93:7
8[f]	LiO*t*-Bu	1.0	SIMes	41[g]	92:8
9	LiO*t*-Bu	1.0	IMes	35	>95:5
10	LiO*t*-Bu	1.0	IPr	50	>95:5
11	LiO*t*-Bu	1.0	SIPr	60	>95:5
12	LiO*t*-Bu	1.0	DPEphos	57	>95:5
13	LiO*t*-Bu	1.0	Xantphos	39	>95:5
14	LiO*t*-Bu	1.0	PCy_3	51	>95:5

[a]Reactions run on a 0.2 mmol scale. [b]Yield of isolated product. [c]Diastereomeric ratio determined by GC analysis of reaction crude (structure of major diastereomer shown). [d]1.0 equiv of NaO*t*-Bu. [e]THF used as solvent. [f]CH_2Cl_2 used as solvent. [g]Product **3** was also obtained in 15% yield as a 1:1 mixture of *Z*:*E* isomers.

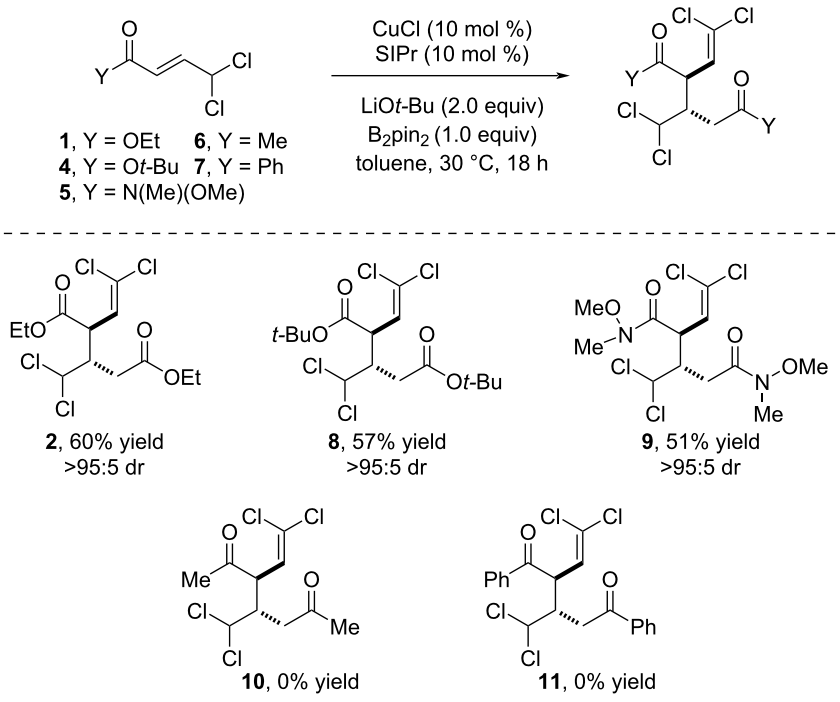

Scheme 2: Cu-Bpin-mediated dimerization of 4,4-dichoro-2-butenoic acid derivatives.

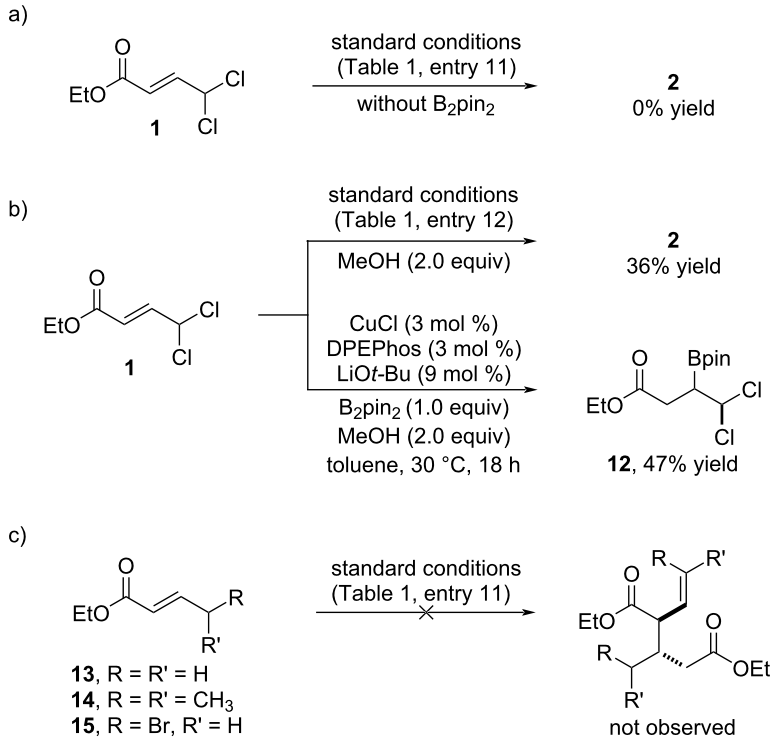

Scheme 3: Control experiments.

metathesis reaction of Cu(I) alkoxides with B_2pin_2 and the reactivity of the resulting Cu–Bpin complex towards α,β-unsaturated esters and hydrocarbons [8-15], we hypothesized that the first step of the reaction may deal with the insertion of the copper–boron bond into **1**. The dual functionality of this substrate imposed a question related to the regioselectivity of the Cu–Bpin insertion since it can potentially behave as an α,β-unsaturated ester or an allylic substrate [16-19]. To shed some light into this issue, we ran the reaction in the presence of MeOH in order to trap the potential copper intermediate by protonation. When 2 equiv of MeOH were used, we still obtained the dimerization product **2**. Nevertheless, when a catalytic amount of base was used, we only observed the formation of β-borylation product **12** (Scheme 3b). This result suggests that Cu–Bpin insertion into **1** generates a copper enolate which may engage in further steps for the formation of the dimerization product. The presence of the two chlorine atoms was found to be key for the outcome of the reaction. No dimerization product was observed when the reaction was carried out under standard conditions with ethyl crotonate derivatives bearing a methyl group, hydrogen or bromine atoms at the γ position. Either β-borylation or decomposition products were obtained in those cases (Scheme 3c).

On the basis of our experimental results, we propose the following mechanism for the copper-catalyzed diastereoselective dimerization of 4,4-dichoro-2-butenoic acid derivatives (Scheme 4). Initially, the LCu–pin complex generated through reaction between LCu–O*t*-Bu and B_2pin_2 undergoes coordination and regioselective insertion into **1** giving rise to β-borylated organocopper species **A** which is in equilibrium with the Cu–O enolate **B** [11]. In the presence of excess of LiO*t*-Bu, a salt metathesis reaction between this base and intermediate **B** generates lithium enolate **C** and LCuO*t*-Bu to close the copper catalytic cycle. The formation of a lithium enolate is consistent with the different diastereoselectivity observed when other bases featuring different metal cations were used (Table 1, entry 2 vs entry 5), and the absence of any significant stereochemical influence from the copper complex (Table 1, entries 9–14). Lithium enolate **C** would then undergo a diastereoselective conjugate addition to a second molecule of **1**. Given the negative results observed for other crotonate derivatives (Scheme 3c), coordination between the Li cation and the two chlorine atoms via proposed transition state **D** may be crucial not only for diastereoselective control but also for the viability of this step. Finally, the new enolate **E** evolves through intramolecular proton abstraction and elimination of boryllithium [20,21]. The formation of side product **3** observed when dichloromethane was used as a solvent could be explained by protonation of intermediate **A**, followed by transmetalation of the resulting organoboron compound with CuO*t*-Bu and subsequent S_N2'-selective allylic alkylation of **1**.

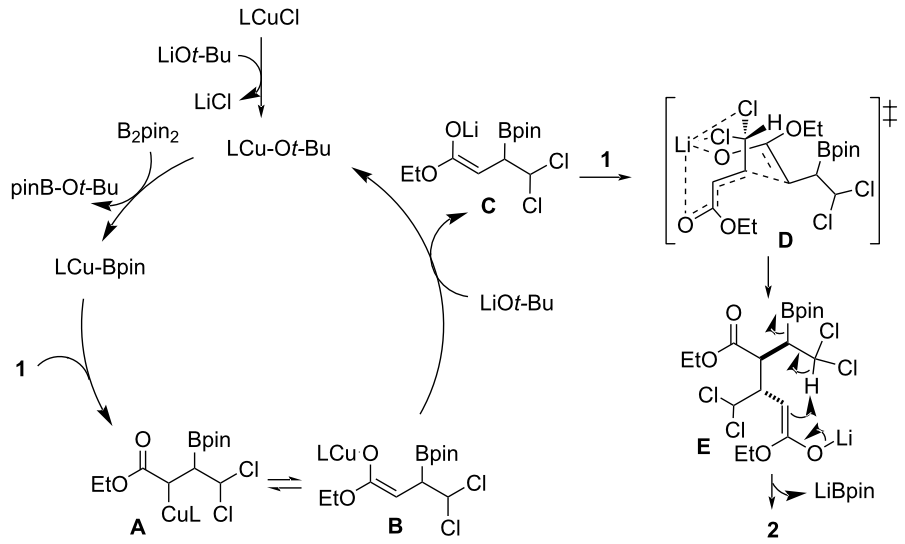

Scheme 4: Proposed mechanism for the Cu-catalyzed dimerization of 4,4-dichoro-2-butenoic acid derivatives.

The densely functionalized structure of these dimerization products offers a versatile synthetic handle for further chemoselective functionalization. Considering the presence of two enolizable esters together with the aliphatic *gem*-dichloride, we explored the feasibility of a base-mediated formation of chlorocyclopropanes (Table 2).

Evaluation of bases such as metal *tert*-butoxides, phosphates, acetates, and organic amines resulted in either low conversion or decomposition of **2** (see Supporting Information File 1 for details). In contrast, the use of CsF in dioxane at 70 °C proved to be efficient and selectively provided cyclopropane **9** in good yield, albeit with no diastereoselectivity (Table 2, entry 1). Cs_2CO_3 was also selective for this cyclization and provided a slight increase in diastereoselectivity, although still far from satisfactory (Table 2, entry 2). A major improvement was observed when TBAF was used as base. At 70 °C, product **16** was obtained with good diastereoselectivity (80:20 dr), although in

Table 2: Synthesis of densely functionalized (2,2-dichlorovinyl)cyclopropanes by base-promoted intramolecular cyclization.

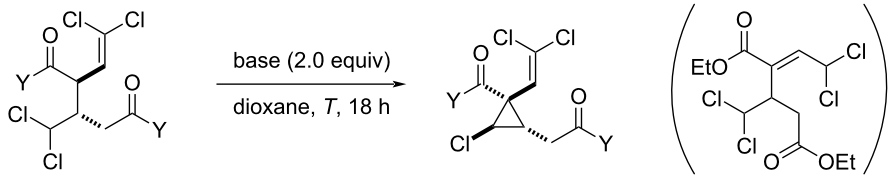

2, Y = OEt
8, Y = O*t*-Bu
9, Y = N(Me)OMe

16, Y = OEt
17, Y = O*t*-Bu
18, Y = N(Me)OMe

19

Entry[a]	Y	Base	*T* (°C)	Product, yield (%)[b]	dr[c]
1	OEt	CsF	70	**16**, 80	50:50
2	OEt	Cs_2CO_3	70	**16**, 55	61:39
3	OEt	TBAF	70	**16**, 32[d]	80:20
4	OEt	TBAF	50	**16**, 70	83:17
5	O*t*-Bu	TBAF	50	**17**, 61	81:19
6	N(Me)(OMe)	TBAF	50	**18**, –	–

[a]Reactions run on a 0.1 mmol scale. [b]Yield of isolated product. [c]Diastereomeric ratio determined by ^{1}H NMR analysis of reaction crude. [d]Product **19** was also obtained in 23% yield.

low yield mainly due to the formation of side product **19**. However, **16** could be obtained as a single product in 70% yield with 83:17 dr by decreasing the reaction temperature to 50 °C (Table 2, entry 4). Under the same optimal conditions, compound **8** could be transformed into cyclopropane **17** in 61% yield with 81:19 dr (Table 2, entry 5). It is important to note that (2,2-dichlorovinyl)cyclopropanes represent an important class of compounds present in a range of bioactive compounds such as permethrin or alpha-cypermethrin, which are commonly used as insecticides [22,23]. The present transformation provides access to densely functionalized (2,2-dichlorovinyl)cyclopropanes, thus representing a potential platform for the synthetic diversification on these important scaffolds.

Surprisingly, when the TBAF-mediated cyclization was attempted on bisamide **9** the corresponding cyclopropane **18** was not formed (Table 2, entry 6). The use of other mild bases at different temperatures also resulted unproductive. However, when the reaction was carried out with KO*t*-Bu, we observed the selective conversion of **9** into product **20** featuring a different cyclopropane scaffold. Slight modification of the reaction conditions allowed us to obtain product **20** in 56% yield as a single diastereomer (Scheme 5a). Taking advantage of the twofold utility of KO*t*-Bu, we explored the formation of this new cyclopropane structure directly from *gem*-dichloride **5**. By using this base under standard conditions, product **20** was selectively obtained in similar yield, albeit with diminished diastereoselectivity (Scheme 5b).

Conclusion

In summary, we have discovered an unanticipated Cu–Bpin-promoted diastereoselective dimerization of 4,4-dichloro-2-butenoic acid derivatives. The reaction occurs via initial Cu–Bpin insertion followed by keto–enol isomerization and salt metathesis to generate a lithium enolate which is then trapped by a second molecule of the 4,4-dichloro-2-butenoic acid derivative. We have observed that the use of lithium as base metal cation is key to achieve excellent levels of diastereoselectivity. Our study also highlights, how the dimerization products can be selectively converted into different densely functionalized cyclopropane scaffolds depending on the nature of the carboxylic acid derivative.

Supporting Information

Supporting Information File 1

Experimental procedures, characterization data and copies of NMR spectra.
[https://www.beilstein-journals.org/bjoc/content/supplementary/1860-5397-21-71-S1.pdf]

Funding

Financial support from the AEI (PID2020-118237RB-I00), European Research Council (863914), Xunta de Galicia (ED431C 2022/27; Centro de investigación do Sistema univer-

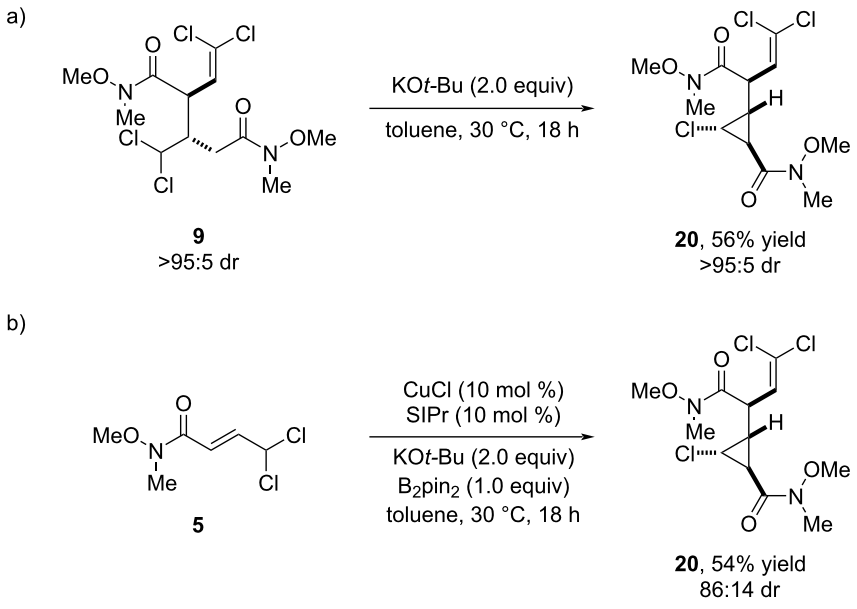

Scheme 5: a) KO*t*-Bu-mediated intramolecular cyclization of **9**. b) Direct formation of cyclopropane **20** from *gem*-dichloride **5** using KO*t*-Bu as base.

sitario de Galicia accreditation 2023–2027, ED431G 2023/03) and the European Regional Development Fund (ERDF) is gratefully acknowledged.

Author Contributions

Patricia Gómez-Roibás: investigation; methodology; writing – review & editing. Andrea Chaves-Pouso: investigation; methodology. Martín Fañanás-Mastral: conceptualization; formal analysis; funding acquisition; project administration; resources; supervision; writing – original draft; writing – review & editing.

ORCID® iDs

Martín Fañanás-Mastral - https://orcid.org/0000-0003-4903-0502

Data Availability Statement

All data that supports the findings of this study is available in the published article and/or the supporting information of this article.

References

1. Rivera-Chao, E.; Fañanás-Mastral, M. *Angew. Chem., Int. Ed.* **2018,** *57,* 9945–9949. doi:10.1002/anie.201806334
2. Rivera-Chao, E.; Mitxelena, M.; Varela, J. A.; Fañanás-Mastral, M. *Angew. Chem., Int. Ed.* **2019,** *58,* 18230–18234. doi:10.1002/anie.201910707
3. Chaves-Pouso, A.; Álvarez-Constantino, A. M.; Fañanás-Mastral, M. *Angew. Chem., Int. Ed.* **2022,** *61,* e202117696. doi:10.1002/anie.202117696
4. Pérez-Saavedra, B.; Velasco-Rubio, Á.; Rivera-Chao, E.; Varela, J. A.; Saá, C.; Fañanás-Mastral, M. *J. Am. Chem. Soc.* **2022,** *144,* 16206–16216. doi:10.1021/jacs.2c07969
5. Piñeiro-Suárez, M.; Álvarez-Constantino, A. M.; Fañanás-Mastral, M. *ACS Catal.* **2023,** *13,* 5578–5583. doi:10.1021/acscatal.3c00536
6. Álvarez-Constantino, A. M.; Chaves-Pouso, A.; Fañanás-Mastral, M. *Angew. Chem., Int. Ed.* **2024,** *63,* e202407813. doi:10.1002/anie.202407813
7. Vázquez-Galiñanes, N.; Sciortino, G.; Piñeiro-Suárez, M.; Tóth, B. L.; Maseras, F.; Fañanás-Mastral, M. *J. Am. Chem. Soc.* **2024,** *146,* 21977–21988. doi:10.1021/jacs.4c07188
8. Ito, H.; Yamanaka, H.; Tateiwa, J.-i.; Hosomi, A. *Tetrahedron Lett.* **2000,** *41,* 6821–6825. doi:10.1016/s0040-4039(00)01161-8
9. Takahashi, K.; Ishiyama, T.; Miyaura, N. *J. Organomet. Chem.* **2001,** *625,* 47–53. doi:10.1016/s0022-328x(00)00826-3
10. Mun, S.; Lee, J.-E.; Yun, J. *Org. Lett.* **2006,** *8,* 4887–4889. doi:10.1021/ol061955a
11. Dang, L.; Lin, Z.; Marder, T. B. *Organometallics* **2008,** *27,* 4443–4454. doi:10.1021/om8006294
12. Lillo, V.; Bonet, A.; Fernández, E. *Dalton Trans.* **2009,** 2899–2908. doi:10.1039/b819237e
13. Neeve, E. C.; Geier, S. J.; Mkhalid, I. A. I.; Westcott, S. A.; Marder, T. B. *Chem. Rev.* **2016,** *116,* 9091–9161. doi:10.1021/acs.chemrev.6b00193
14. Hemming, D.; Fritzemeier, R.; Westcott, S. A.; Santos, W. L.; Steel, P. G. *Chem. Soc. Rev.* **2018,** *47,* 7477–7494. doi:10.1039/c7cs00816c
15. Das, K. K.; Mahato, S.; Hazra, S.; Panda, S. *Chem. Rec.* **2022,** *22,* e202100290. doi:10.1002/tcr.202100290
16. Ito, H.; Kawakami, C.; Sawamura, M. *J. Am. Chem. Soc.* **2005,** *127,* 16034–16035. doi:10.1021/ja056099x
17. Guzman-Martinez, A.; Hoveyda, A. H. *J. Am. Chem. Soc.* **2010,** *132,* 10634–10637. doi:10.1021/ja104254d
18. Gao, P.; Yuan, C.; Zhao, Y.; Shi, Z. *Chem* **2018,** *4,* 2201–2211. doi:10.1016/j.chempr.2018.07.003
19. Akiyama, S.; Kubota, K.; Mikus, M. S.; Paioti, P. H. S.; Romiti, F.; Liu, Q.; Zhou, Y.; Hoveyda, A. H.; Ito, H. *Angew. Chem., Int. Ed.* **2019,** *58,* 11998–12003. doi:10.1002/anie.201906283
20. Segawa, Y.; Yamashita, M.; Nozaki, K. *Science* **2006,** *314,* 113–115. doi:10.1126/science.1131914
21. Segawa, Y.; Suzuki, Y.; Yamashita, M.; Nozaki, K. *J. Am. Chem. Soc.* **2008,** *130,* 16069–16079. doi:10.1021/ja8057919
22. Li, N.; Xu, H.-H.; Liu, Z.-Y.; Yang, Z.-H. *J. Photochem. Photobiol., B* **2009,** *96,* 170–177. doi:10.1016/j.jphotobiol.2009.06.002
23. Walker, K. J.; Williams, C. T.; Oladepo, F. O.; Lucas, J.; Malone, D.; Paine, M. J. I.; Ismail, H. M. *Sci. Rep.* **2022,** *12,* 9715. doi:10.1038/s41598-022-13768-z

License and Terms

BEILSTEIN JOURNAL OF ORGANIC CHEMISTRY

Microwave-enhanced additive-free C–H amination of benzoxazoles catalysed by supported copper

Andrei Paraschiv[1], Valentina Maruzzo[1], Filippo Pettazzi[1,2], Stefano Magliocco[3], Paolo Inaudi[1], Daria Brambilla[4], Gloria Berlier[3], Giancarlo Cravotto[1] and Katia Martina[*1]

Full Research Paper

Open Access

Address:
[1]Department of Drug Science and Technology, University of Turin, Via Pietro Giuria 9, 10125 Turin, Italy, [2]Present address: R&D Department, Farmabios S.P.A., Via Pavia 1, Gropello Cairoli, Italy, [3]Department of Chemistry, NIS Interdepartmental Centre and INSTM Reference Centre, University of Turin, Via Pietro Giuria 7, 10125 Turin, Italy and [4]Cube Labs Spa V. Giulia Caccini 1, 00198 Roma, Italy

Email:
Katia Martina[*] - katia.martina@unito.it

* Corresponding author

Keywords:
aerobic oxidation; copper; grafted silica; heterogeneous catalysis; microwave

Beilstein J. Org. Chem. **2025,** *21,* 1462–1476.
https://doi.org/10.3762/bjoc.21.108

Received: 03 March 2025
Accepted: 18 June 2025
Published: 15 July 2025

This article is part of the thematic issue "Copper catalysis: a constantly evolving field".

Guest Editor: J. Yun

Abstract

The C2-amination of benzoxazole offers wide-ranging potential for substrate expansion and the functionalisation of bioactive compounds. This study presents a green and efficient C–H amination, catalysed by CuCl and $CuCl_2$, in acetonitrile without acidic, basic or oxidant additives that is accelerated by microwave (MW) irradiation and is completed in 1.5–2 h. A solid Cu(I) catalyst supported on aminated silica made the process cost-effective and heterogeneous, thus simplifying work-up and minimising free copper in solution. The catalyst was found to be regeneratable and reusable for up to eight cycles. The optimised method facilitated the synthesis of various benzoxazole derivatives, demonstrating its versatility and practical applicability.

Introduction

2-Aminoazoles are nitrogenous heterocyclic compounds of high relevance due to their biological and pharmaceutical activity and their importance within the materials sciences [1,2]. 2-Aminobenzoxazoles, in particular, are important building blocks in the development of new bioactive compounds that can be useful as therapeutic agents with antibacterial [3], antiviral, antifungal [4], anticancer [5-7] and anti-inflammatory activity [8]. Moreover, they can be applied in disorders of the central nervous system, such as insomnia and Alzheimer's disease [9,10].

The preparation of 2-aminobenzoxazoles classically proceeds via cyclocondensation reactions from pre-functionalised precursors, or via the C2-amination of benzoxazoles by transition-metal-catalysed reactions that traditionally involve aryl halide scaffolds [11-14]. However, these procedures entail disadvan-

tages that need to be overcome if green chemistry criteria are to be met; high temperatures, long reaction times, the need for ligands, and the huge overall economic impact of these processes.

Inspired by the logic behind cross-dehydrogenative C–C-coupling methods [15], the direct C–H amination has been developed as a more straightforward, economical and environmentally friendly reaction, compared to its counterparts (such as the classical Buchwald–Hartwig amination reaction [16] or the Ullman reaction [17,18]) which require pre-functionalisation steps and harsh conditions [19].

Many protocols for C–H aminations have been applied to heteroaromatic compounds, mainly 5-membered heteroarenes, and a great deal of attention has been devoted to benzoxazoles. When applied to benzoxazole, the reaction is catalysed by transition metals such as Ag(I) [20], Mn(II) [21], Fe(III) [22,23], Co [24], Ni(II) [25] and Fe(III) [26]. However, the use of Cu(II) has increased thanks to its high tolerance towards several functional groups, high environmental abundance, low cost and low overall toxicity. A wide range of aminating reagents have been utilised, including nitrogen electrophiles and amines in the presence of external or internal oxidants [27], in many types of copper-catalysed synthetic protocols. The direct copper-catalysed C–H amination of azoles was pioneered by Mori [28], Schreiber [29], and Zhao [30]. However, high reaction temperatures and a large amount of base or acid dramatically decrease atom economy (the percentage of reactant atoms incorporated into the desired product) and functional-group tolerance, while the use of an oxidant considerably impacts upon the sustainability of the process because it involves toxic reagents, generates hazardous by-products, increases the overall reaction cost and increases waste production [30-32]. In subsequent years, other base-catalysed protocols have been developed for the reaction of azolic substrates, but here the amines and the ligands are still used in excess and auxiliary oxidants are occasionally employed [33-35]. Although electrophilic amines, such as chloroamines [36,37], hydroxylamine [38-40], acylated hydroxylamine (with a wider reaction scope) [41-44] and sulfamoyl chlorides [32] can perform the coupling under basic conditions, the need for the activation of the amine as an electrophilic agent generates additional waste. This reduces atom economy and indicates lower reaction efficiency.

Acid-catalysed protocols have also been specifically developed for the amination of oxazoles, with many of them utilizing aerobic oxidation to improve the sustainability of the process. Indeed, in 2011, Guo et al. [45] developed a protocol for the direct C–H amination of benzoxazoles and oxadiazoles, under an O_2 atmosphere using 20 mol % of a Cu(II) catalyst, that still required high temperatures, but the excess of amine (2 equiv) was lowered and only a catalytic amount of acid was utilised. Similar acidic protocols were subsequently developed by Li et al. [46], in which benzoxazoles were reacted with secondary amines and amides, with higher temperature being applied when reacting amides to achieve their decarbonylation. In 2014, Cao et al. [47] reported the amination of benzoxazole with a secondary amine either in air or an O_2 atmosphere, lowering the catalyst amount and the reaction temperature.

In 2020, a study by De Vos and co-workers [48] focused on developing a new additive-free protocol, catalysed by a copper catalyst supported on acidic zeolites that efficiently catalysed C2-benzoxazole amination in the presence of a perfluorinated solvent (hexafluoroisopropanol) as a source of mobile protons. Despite the significant interest in this area, to the best of our knowledge, this study represents one of the few examples of a heterogeneous catalysed copper-mediated C–H amination of benzoxazole.

The pursuit for greener methodologies in organic synthesis and transitioning from traditional homogeneous catalysis to the use of heterogeneous catalysts for direct C–H amination processes could be a significant breakthrough in optimising these reactions. Despite recent progress in site-selective C–H functionalisation [49], most reactions have remained reliant on homogeneous catalysis due to its molecularly defined nature. By contrast, the development of heterogeneous catalysis has faced challenges, due to uncertainties around catalytic sites, aggregation, and the leaching of active species during reactions. The use of a heterogeneous catalyst can greatly simplify the work-up process, as the catalyst can be easily removed via simple filtration. Additionally, using supported metals instead of metal salts can prevent the formation of chelates, which might otherwise impact the efficiency of the procedure. Moreover, this approach can provide bifunctional catalysis as the support itself contributes to the catalyst's reactivity, thus enhancing its overall efficiency. In the context of the C2 amination of azoles, to the best of our knowledge, only a few studies [48,50] have explored this approach, suggesting significant opportunities for further development and improvement. Building on our previous experience in the preparation and characterisation of supported copper(II) catalysts on covalently modified silica [51,52], we have set out to develop a new heterogeneous catalyst with atomically distributed active sites for the mild and efficient C–H amination of benzoxazole. This approach was chosen because the silica derivatisation and copper deposition methods are simple, inexpensive and scalable, making the catalyst reliable and suitable for large scale production. This study aims to optimise an efficient, user-friendly and heterogeneously catalysed procedure that enables the rapid synthesis of 2-aminobenzoxa-

zole derivatives. A key focus is leveraging microwave irradiation to enhance the protocol's efficacy. The non-thermal effects and unique ability of MW irradiation to promote reactions catalysed by solid-supported metals have already been demonstrated [53]. As shown in Scheme 1, our research is in line with earlier studies that highlight the advantages of heterogeneous catalysis, but compared to other approaches, we aimed at eliminating the presence of bimetallic catalysts, the addition of a base [50], and the use of costly perfluorinated protic solvents [48]. In addition, this approach offers improved performance compared to photochemical C–H amination reactions of benzoxazole, which, although metal-free, are still limited in versatility and require photocatalysts such as eosin Y and a tightly controlled O_2 atmosphere [54]. The objective of the present study aims to provide a rapid, additive-free and convenient alternative to existing approaches in this field, which have attracted considerable interest over the years.

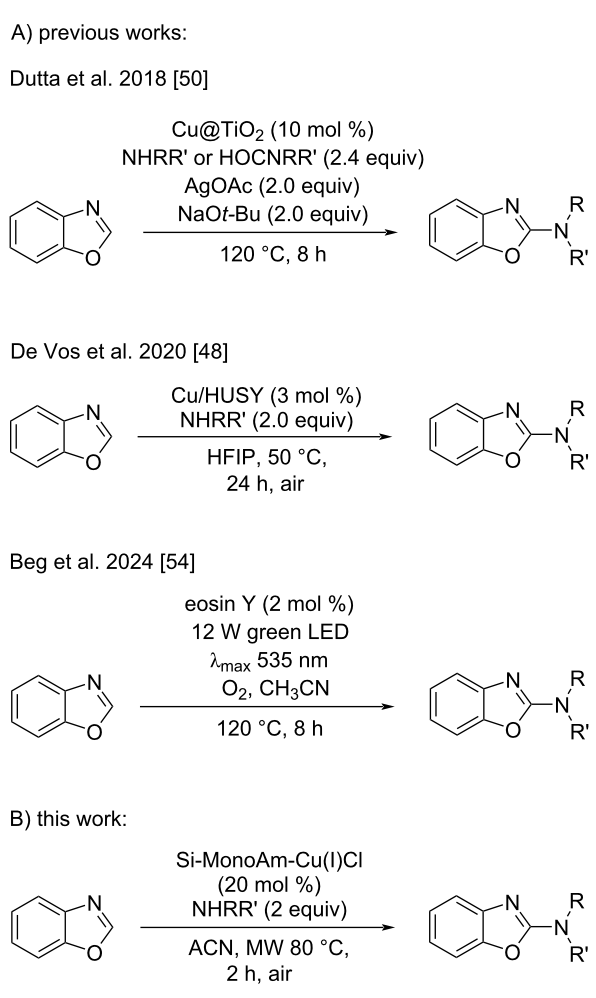

Scheme 1: Representative synthetic routes for the C–H amination of benzoxazole using supported copper catalysts.

Results and Discussion

Inspired by the extensive literature on C2-benzoxazole amination, we initially began our optimisation by studying a homogeneous procedure in the presence of piperidine, which was used as amine component to identify mild conditions for the Cu-catalysed aerobic C–H amination in absence of acid, base or co-catalyst additives. As described in Table 1, we explored the effects of different solvents and copper species, and preliminary reactions were conducted with Cu(II) salts, with reference to reaction conditions already reported in the literature for aerobic protocols. As shown in Table 1, entries 1–3, we compared xylene, toluene, and acetonitrile as solvents. According to Bhanage and Wagh [13], Cu(II) catalyses the C–H amination in xylene at 140 °C for 14 hours under oxygen. We tested the reaction in refluxing toluene with 20 mol % of $CuCl_2$ and observed a significantly decreased product yield (Table 1, entry 2). As Cao et al. [47] already have reported, acetonitrile improved the reaction efficiency, resulting in an increase in product yield to 78% when the reaction was performed at 80 °C. Interestingly, reflux conditions did not improve reaction conversion, as shown in entries 3 and 4 (Table 1) and we consistently observed a decrease in reaction yield. This effect is likely due to the lower solubility of O_2 in the refluxing solvent, which may negatively impact the reaction outcome. As previously demonstrated, adding acetic acid enabled the reaction to proceed with even lower catalyst loading [47]. To avoid the use of acid and to minimise the amount of the amine, we repeated the reaction with 1.5 equivalents of piperidine, and compared different Cu(II) and Cu(I) salts. Both Cu(I) and Cu(II) chloride demonstrated good product conversion and selectivity without the need to perform the reaction under oxygen, while $Cu(OAc)_2$ was slightly less efficient. When the catalyst loading was reduced to 15 mol %, the reaction yield decreased to approximately 75% for both copper salts. However, reducing the reaction time to 6 hours, with a catalyst loading of 20 mol %, resulted in complete conversion and high selectivity, comparable to the results obtained from an overnight reaction. Notably, decreasing the reaction temperature to 60 °C still yielded excellent results with both catalysts after an overnight reaction and after 6 hours, although conversion was still proceeding after 4 hours of reaction. Both catalysts performed comparably, with $Cu(OAc)_2$ consistently showing slightly lower efficiency (Table 1, entries 14–20).

We then focused on studying the efficiency of MW-irradiation-promoted reactions, which, as reported in numerous green protocols, offer significant advantages over the use of conventional heating. The goal was to utilise selective, volumetric dielectric heating to save time and energy, enable selective catalysis and generally achieve higher selectivity and yields [53,55,56]. Building on the improvements made using conven-

Table 1: C2-Amination of benzoxazole with piperidine via homogeneous catalysis.

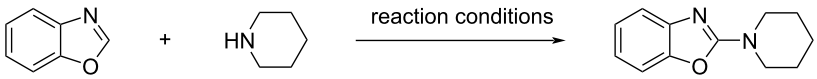

2a

Entry	Catalyst (mol %)	Amine (equiv)	Conditions[a]	Conversion (%)[b]	Yield (%)[b]
1	$Cu(acac)_2$ (20)	2	xylene, 140 °C, 14 h, O_2	>99	88, ref [13]
2	$CuCl_2$ (20)	2	toluene, reflux, o.n.	82	28
3	$CuCl_2$ (20)	2	acetonitrile, 80 °C, o.n,	96	78
4	$CuCl_2$ (20)	2	acetonitrile, reflux, o.n.	83	49
5	$CuBr_2$ (10)	1.2	2 equiv CH_3COOH, acetonitrile, 50 °C, o.n.	>99	95, ref [47]
6	$CuCl_2$ (20)	1.5	acetonitrile, 80 °C, o.n.	92	81
7	$Cu(OAc)_2$ (20)	1.5	acetonitrile, 80 °C, o.n.	96	74
8	CuCl (20)	1.5	acetonitrile, 80 °C, o.n.	>99	83
9	$CuCl_2$ (15)	1.5	acetonitrile, 80 °C, o.n.	89	75
10	CuCl (15)	1,5	acetonitrile, 80 °C, o.n.	96	74
11	$CuCl_2$ (20)	1.5	acetonitrile, 80 °C, 6 h	90	83
12	CuCl (20)	1.5	acetonitrile, 80 °C, 6 h	96	87
13	CuCl (10)	1.5	acetonitrile, 80 °C, 6 h	83	36
14	$CuCl_2$ (20)	1.5	acetonitrile, 60 °C, o.n.	96	91
15	$Cu(OAc)_2$ (20)	1.5	acetonitrile, 60 °C, o.n.	99	77
16	CuCl (20)	1.5	acetonitrile, 60 °C, o.n.	95	88
17	$CuCl_2$ (20)	1.5	acetonitrile, 60 °C, 6 h	97	90
18	CuCl (20)	1.5	acetonitrile, 60 °C, 6 h	93	86
19	$CuCl_2$ (20)	1.5	acetonitrile, 60 °C, 4 h	78	65
20	CuCl (20)	1.5	acetonitrile, 60 °C, 4 h	77	57

[a]Reaction conditions: benzoxazole (0.1 mmol), piperidine (see table), Cu catalyst, solvent (1 mL). [b]Conversion and yield were measured by ^{1}H NMR spectroscopy.

tional methods, we tested the reaction under MW irradiation (see Table 2).

Two different pieces of equipment were evaluated: a flexible MW oven (Microsynth by Milestone) for traditional glassware synthesis and a MW reactor (SynthWave by Milestone) capable of handling any reaction temperature and gas pressure (up to 300 °C and 200 bar). The SynthWave reactor also allows multiple gases to be loaded, including both inert and reactive gases. As shown in Table 2, MW irradiation significantly reduced reaction times from 6 hours to 2 hours under atmospheric air conditions. At 60 °C with 20 mol % of $CuCl_2$, an 87% product yield was obtained, while the use of CuCl enhanced reactivity, providing a nearly quantitative yield of 98% (Table 2, entries 1 and 2).

When the reaction was conducted in the SynthWave reactor, pressurised with 5 bar of nitrogen, the yield of desired product dropped to 13%, highlighting the importance of oxygen/air in the oxidative aromatisation of the benzoxazole ring. Reducing the reaction time to 1 hour or lowering the catalyst loading to 15 mol % resulted in decreased yields of 75% and 71%, respectively.

The reaction was also carried out in Anton Paar equipment with the vessel pressurised under nitrogen (Table 2, entry 7). Under these conditions, the yield was 58%, demonstrating the superiority of an open vessel in a multimode cavity for this reaction.

Since Cu salts facilitate both the nucleophilic attack of piperidine on benzoxazole to form the intermediate open derivative, and the subsequent ring oxidation upon closure (as shown in the mechanism in Scheme S1 (Supporting Information File 1), the reaction mixture may contain the desired 2-substituted benzoxazole **2a** together with its open-form precursor **2a-o**. The latter can be hydrolysed to give *N*-formylpiperidine and aminophenol (**2a-o-hydrol**) (see Figure 1a). To better understand the influence of the reaction conditions on product distribution, we

Table 2: Microwave-promoted C2-amination of benzoxazole with piperidine.

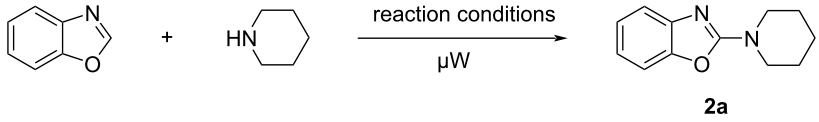

2a

Entry	Catalyst (mol %)	Conditions[a]	Conversion (%)[b]	Yield (%)[b]
1	$CuCl_2$ (20)	60 °C, 2 h, open vessel, MW[c]	87	85
2	CuCl (20)	60 °C, 2 h, air, MW[c]	>99	98
3	CuCl (20)	60 °C, 2 h, N_2 5 bar, MW[d]	77	13
4	CuCl (20)	60 °C, 1 h, air, MW[c]	81	75
5	CuCl (15)	60 °C, 2 h, air, MW[c]	75	71
6	CuCl (10)	60 °C, 2 h, air, MW[c]	63	45
7	CuCl (20)	60 °C, 2 h, closed vial, MW[e]	79	58

[a]Reaction conditions: benzoxazole (0.1 mmol), piperidine (0.2 mmol), Cu catalyst, acetonitrile (1 mL); [b]conversion and yield were measured by NMR spectroscopy; [c]Microsynth MW oven; [d]SynthWave MW reactor; [e]Anton Paar Monowave.

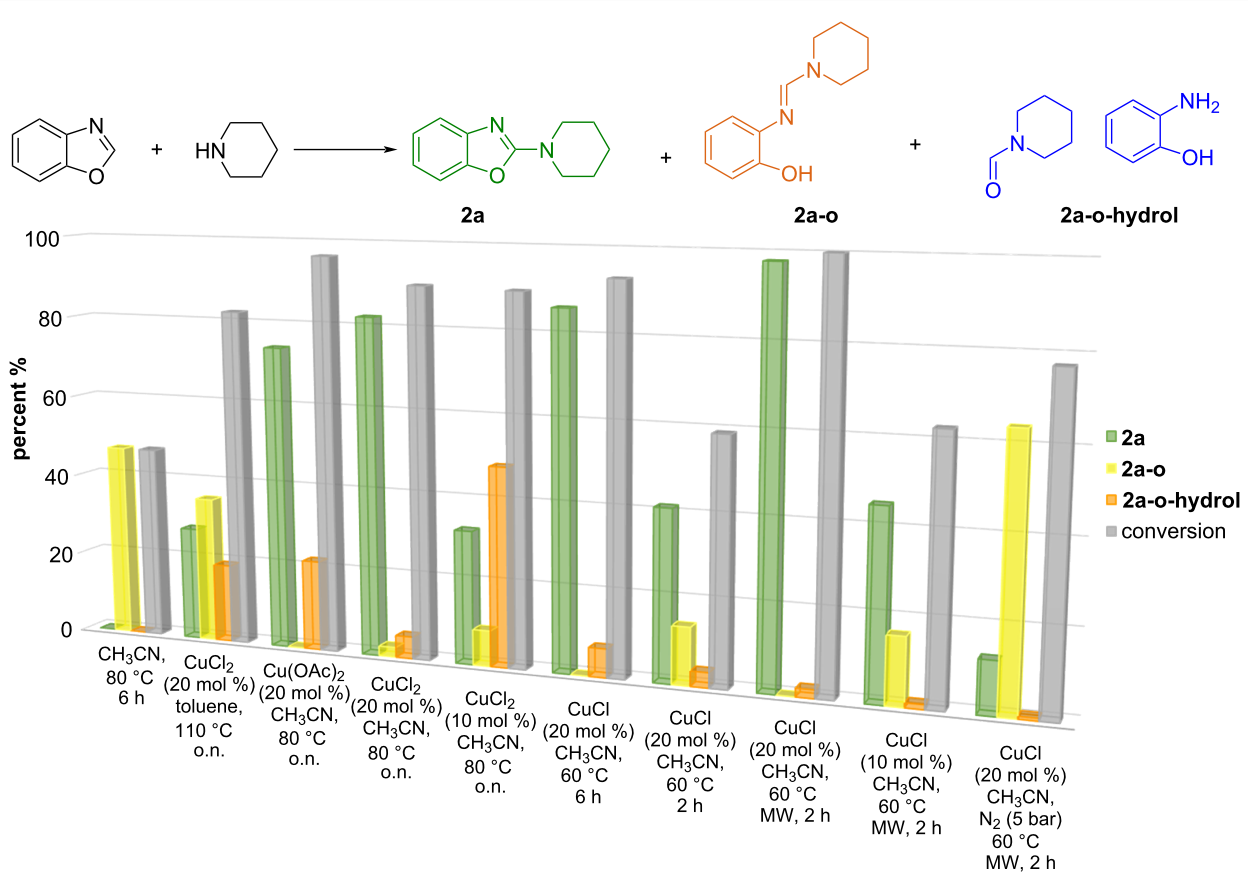

Figure 1: Reaction of benzimidazole with piperidine. a) Reaction scheme including intermaidates and b) conversion and selectivity plot of the C2-amination of benzoxazole with piperidine. Reaction conditions: benzoxazole (0.1 mmol), piperidine (0.15 mmol), copper catalyst, solvent (1.0 mL). Conversion was measured by NMR spectroscopy (see Figure S1 in Supporting Information File 1 for an example).

plotted conversion versus selectivity in Figure 1b. Crudes were analysed by ^{1}H NMR spectroscopy, as shown in Figure S1 (Supporting Information File 1), to determine the percentage composition of starting material and products **2a**, **2a-o** and **2a-o-hydrol**. The reaction was perfectly reproducible and no other derivatives were observed.

As shown in Figure 1b, when the reaction was conducted without a catalyst, only ring opening was observed, accounting for 47%. By contrast, the presence of Cu facilitated the conversion of the intermediate to the desired aromatic benzoxazole **2a**, demonstrating copper's dual role as a Lewis acid in enhancing nucleophilic attack, and as an efficient catalyst for ring-closing oxidative rearomatisation.

Of the conditions tested, the use of $CuCl_2$ in toluene showed limited effectiveness, achieving 82% conversion but only a 28% yield of the final product. The remaining resulting mixture included 35% of the intermediate **2a-o** and 19% of the hydrolysed product **2a-o-hydrol**. However, the reaction performance in acetonitrile improved significantly, with $CuCl_2$ yielding 82% of the desired product, alongside 2.4% of **2a-o** and 5.4% of **2a-o-hydrol**. Reducing the catalyst amount from 20 mol % to 10 mol % did not affect conversion, but resulted in a lower yield of **2a** and increased production of **2a-o-hydrol** to 48%, indicating that insufficient catalyst at 80 °C overnight favours side reactions, compromising selectivity.

When using CuCl (20 mol %), an excellent selectivity was observed at 60 °C. Although conversion was only 59% after 2 hours, full reaction completion was observed in 6 hours. MW irradiation enhanced both the reaction rate and selectivity, with the reaction being completed after 2 hours at 60 °C affording a 98% yield of the desired product. We observed only trace amounts of **2a-o-hydrol** (1.2%) even at a reduced catalyst amount of 10 mol % CuCl. We hypothesise that, under MW, the hydrolysis side reaction is mitigated due to the mild reaction conditions both in terms of temperature and time, as observed using a lower catalyst amount. This assumption was confirmed when the reaction was performed in a MW reactor under 5 bar of N_2; in this environment, the copper catalyst cannot regenerate because of the absence of oxygen (see mechanism Scheme S1 in Supporting Information File 1). The ^{1}H NMR spectrum of the crude showed that the starting material was almost completely converted (by 77.4%), that the intermediate **2a-o** was recovered in the mixture at 64% and that the side product was detected at only 0.7%.

To more deeply understand the influence of MW irradiation in the enhancement of the reaction rate for the CuCl-catalysed reaction, we carried out the model reaction in parallel, using both an oil bath and MW irradiation at 60 °C. Figure 2 clearly shows that MW irradiation drives the reaction to completion in 2 hours. By contrast, the conventional method results in a slower rate for the conversion of the starting benzoxazole to the open intermediate **2a-o**, and the subsequent ring closing aromatisation to product **2a**. As can be seen in Figure 2, a complete conversion is achieved in 6 hours under conventional conditions. Our observations indicate that MW irradiation enhances the catalytic activity of Cu toward the oxidative aromatisation of **2a-o**, leading to the fast and complete conversion of the starting material to the desired 2-(piperidine-1-yl)benzoxazole (**2a**). Since both reactions were conducted at the same temperature, this experiment confirms that MW irradiation activates the catalyst independently of bulk temperature, as reported in previous studies [57,58]. We can hypothesise that MW heating is likely associated with the generation of hot spots on metal sites, resulting in an accelerated reaction rate and improved selectivity for the desired product.

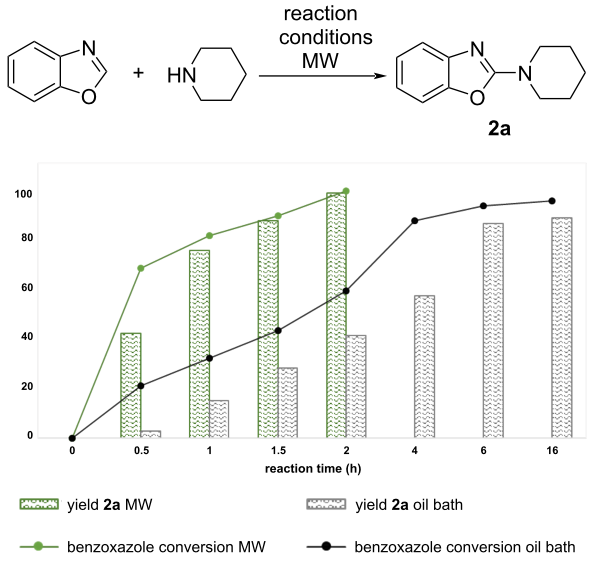

Figure 2: Reaction rate comparison between conventional (oil bath) and MW heating. Reaction conditions: benzoxazole (0.1 mol), piperidine (0.15 mmol), copper catalyst 20 mol %, solvent (1.0 mL). Conversion was measured by ^{1}H NMR spectroscopy.

Despite the advantages of the developed protocol, the homogeneously catalysed procedure negatively impacted the purification and recovery of the products because of the presence of copper salts and complexes. We observed that multiple aqueous washes of the reaction crude are required to remove copper salts, and aqueous ammonia has been used to improve the efficacy of liquid–liquid extraction (see Supporting Information File 1 and experimental procedure). This issue made liquid–liquid extraction time-consuming and wasteful, while chromatographic column purification is also required to obtain a pure final product.

To overcome this problem, a heterogeneous catalytic approach has been developed in which copper is anchored on an aminated silica support. Given that ammonia, amino derivatives and other nitrogen-containing compounds form strong coordination complexes with transition metals like copper [59,60], we decided to

graft an amino derivative onto the surface of silica, based on our previous experience [51,52]. This covalently modified support was then used to stably bind Cu(I) and Cu(II) species (see Scheme 2).

Silica SIPERNAT 320 (Evonik) was selected because of its moderate absorption capacity and specific surface area (SSA), measured at 164 m^2/g using the BET surface area analysis, and because it can be efficiently derivatised with a trialkoxysilane amino derivative as recently reported [61]. A previously optimised ultrasound-promoted synthetic protocol was employed to efficiently graft either 3-aminopropyltriethoxysilane (MonoAm) or 3-(2-aminoethylamino)propyltrimethoxysilane (DiAm) (Scheme 2) [51], and the efficiency of derivatisation was measured by thermogravimetric analysis (TGA) as showed in Figure 3. TGA curves were all normalised to 150 °C to circumvent any possible solvent influence on yield calculations and both Si-MonoAm and Si-DiAm showed a high degree of derivatisation; 9.9 and 21 wt %, respectively, which correspond to 738 and 1090 µmol/g. The first derivative peak temperatures that indicate the point of the greatest rate of change in the weight-loss curve were consistent in both samples and detected to be 446 °C in Si-MonoAm and 448 °C in Si-DiAm.

Both Si-MonoAm and Si-Diam were loaded with either CuCl or $CuCl_2$ by exposing the derivatised silica to a solution of the corresponding Cu salt in THF, following a procedure previously reported in the literature [62,63]. The suspension was stirred magnetically for 6 hours at room temperature, resulting in the formation of a blue-coloured catalyst. We aimed to vary the amount of copper loaded onto the silica surface to achieve different catalyst loadings (Cu wt %) and compared their catalytic activities. The Cu salts reacted with the amino groups grafted onto the silica surfaces of Si-MonoAm and Si-DiAm, resulting

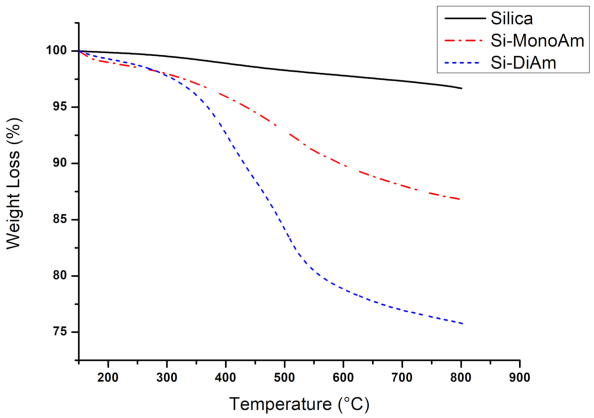

Figure 3: TGA profiles of SIPERNAT silica and Si-MonoAm and Si-DiAm.

in a theoretical copper content of 3, 5 and 9 wt % on the surface at the end of the reaction (see Table S1 in Supporting Information File 1).

The supported catalysts were subsequently tested and we performed preliminary reactions with Cu(I or II) 5 wt % supported on Si-MonoAm and Si-DiAm. We observed that the solid-supported catalysts consistently achieved complete conversion at 80 °C with Si-MonoAm and produced a good-to-quantitative yields of the desired product (see Table 3, entries 3 and 4). The Si-MonoAm support demonstrated superior efficiency over Si-DiAm, and supported Cu(I) performed better than Cu(II) (see Table 3, entries 3–6). At 60 °C, the reaction mixture contained the **2a-o** intermediate, and the yield was lower (see Table 3, entries 1 and 2). As expected, higher temperatures were generally required for the heterogeneous catalytic reactions due to them having higher activation barriers than the homogeneous procedures. As reported in Table 3 (entry 3), excellent results

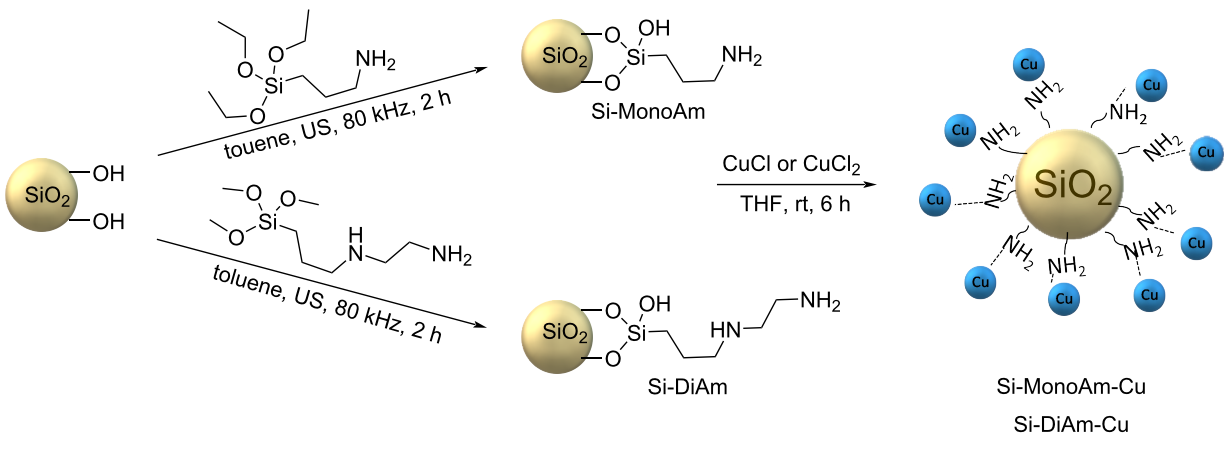

Scheme 2: Graphical representation of Si-MonoAm-Cu(I) and Si-DiAm-Cu(I) preparation.

Table 3: Efficacy of silica-supported Cu(I) and Cu(II) in promoting the C2-amination of benzoxazole with piperidine.

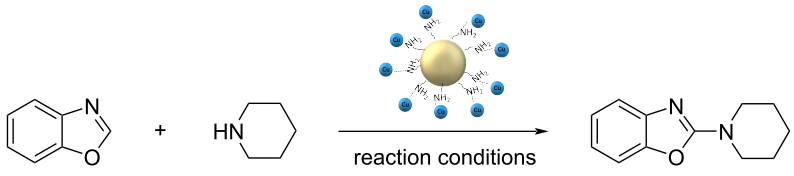

2a

Entry	Catalyst (20 mol %)[a]	Reaction conditions[b]	Yield[c]	Conversion[c]
1	Si-MonoAm-Cu (I) 5 wt %	60 °C, 6 h	75	>99
2	Si-MonoAm-Cu(II) 5 wt %	60 °C, 6 h	63	89
3	Si-MonoAm-Cu(I) 5 wt %	80 °C, 6 h	98	>99
4	Si-MonoAm-Cu(II) 5 wt %	80 °C, 6 h	81	88
5	Si-DiAm-Cu(I) 5 wt %	80 °C, 6 h	22	89
6	Si-DiAm-Cu(II) 5 wt %	80 °C, 6 h	53	88
7	Si-MonoAm-Cu(I) 3 wt %	80 °C, 6 h	83	98
8	Si-DiAm-Cu(I) 9 wt %	80 °C, 6 h	86	>99
9	Si-DiAm-Cu(II) 3 wt %	80 °C, 6 h	69.2	86
10	Si-DiAm-Cu(II) 9 wt %	80 °C, 6 h	72	92.8
11	silica	80 °C, 6 h	n.d.	89
12	–	80 °C, 6 h	n.d.	47
13	Si CuCl	80 °C, 6 h	48	90
14	Si-MonoAm-Cu(I) 5 wt %	60 °C, 2 h, air 5 bar, MW	67	77
15	Si-MonoAm-Cu(I) 5 wt %	70 °C, 2 h, air 5 bar, MW	71	81
16	Si-MonoAm-Cu(I) 5 wt %	80 °C, 2 h, air 5 bar, MW	99	>99
17	Si-MonoAm-Cu(I) 5 wt %	80 °C, 1,5 h, air 5 bar, MW	99	>99
18	Si-MonoAm-Cu(I) 5 wt %	80 °C, 1 h, air 5 bar, MW	87	95
19	Si-MonoAm-Cu(II) 5 wt %	80 °C, 2 h, air 5 bar, MW	77	90

[a]The loading is theoretical considering a complete reaction of copper salt; [b]reaction conditions: benzoxazole (0.4 mmol), piperidine (0.8 mmol), copper catalyst theoretical 20 mol %, CH_3CN (4 mL); [c]yield and conversion measured by ^1H NMR.

were observed with the silica-supported catalyst when the reaction was performed at 80 °C for 6 hours in the presence of Si-MonoAm-Cu(I) 5 wt %. Under these conditions, the yield was quantitative, and NMR analysis confirmed the exclusive formation of the desired product. No improvements were observed when the catalyst was loaded at 3 or 9 wt % (Table 3, entries 7–10). For comparison, the reaction was also tested in the absence of both the catalyst and the support, as well as in the presence of bare silica (Table 3, entries 11 and 12). These conditions resulted in 47% to 89% conversion to **2a-o**, respectively. These results highlight the influence of silica in promoting the conversion to the open form **2a-o** and underscore the critical role of copper in catalysing the synthetic process (Table 3, entries 11 and 12). We believe that the exceptional performance of the solid-supported copper catalyst, which was even superior to homogeneous CuCl in terms of product purity and conversion, can be attributed to the heterogeneous nature of the catalyst. Metal–support interactions likely play a critical role in tuning the catalytic behaviour of the supported copper species, further enhancing their efficiency. An additional experiment was conducted using a catalyst prepared by adsorbing CuCl onto silica without the aminopropyl ligand. Under these conditions, only 48% of the product was obtained (Table 3, entry 13). This result demonstrates that the activity of the Cu catalyst is significantly influenced by the surrounding ligands. The amino ligand not only stabilises the catalyst, by ensuring stronger binding to the metal, but also positively influences its reactivity.

The influence of MW irradiation on reducing the reaction time was investigated using the SynthWave MW reactor, and reactions were performed under 5 bar of air to avoid the evaporation of the solvent at 80 °C, with this also potentially being beneficial to increasing the amount of dissolved oxygen. As shown in Table 3, MW irradiation effectively accelerated the reaction rate. Complete conversion was achieved at 80 °C within 2 hours using Si-MonoAm-Cu(I). These excellent results, obtained conventionally within 6 hours, were replicated

under MW irradiation in less than a third of the time, with the product obtained in pure form without the need for chromatographic purification.

A further reduction in reaction time to 1.5 hours was possible at 80 °C, while incomplete conversion was observed after 1 hour (Table 3, entries 17 and 18). When using Si-MonoAm-Cu(II), the reaction reached 90% conversion and 77% yield after 2 hours of MW irradiation, with the **2a-o** intermediate still present (Table 3, entry 19). This confirms the lower reactivity of the solid-supported Cu(II) salt compared to both the homogeneous catalyst and the supported Cu(I) derivative.

Next, the scope of the optimised heterogeneous MW-assisted protocol was tested with a set of 16 different secondary amines (Scheme 3). This set included linear, branched aliphatic, and cyclic amines, both commercially available and ad-hoc synthesised derivatives (see Supporting Information File 1 for the syntheses of derivatives **1k**, **1m**–**s**).

Encouragingly, all 16 amines were successfully converted to the corresponding 2-aminobenzoxazole derivatives with yields greater than 50%. Beyond piperidine, other cyclic amines, such as morpholine, piperazine, and pyrrolidine, also reacted efficiently, affording good-to-excellent yields. The Boc-protecting group proved to be stable under the reaction conditions, underlining the importance of avoiding the addition of acidic additives. Steric hindrance exerted a moderate influence on the reaction, and branched aliphatic amines yielded the products **2o**, **2r** and **2s** in the range of 61–87%. The protocol demonstrated compatibility with more lipophilic amines, such as **1n**, and also tolerated amine **1q** containing an allyl substituent.

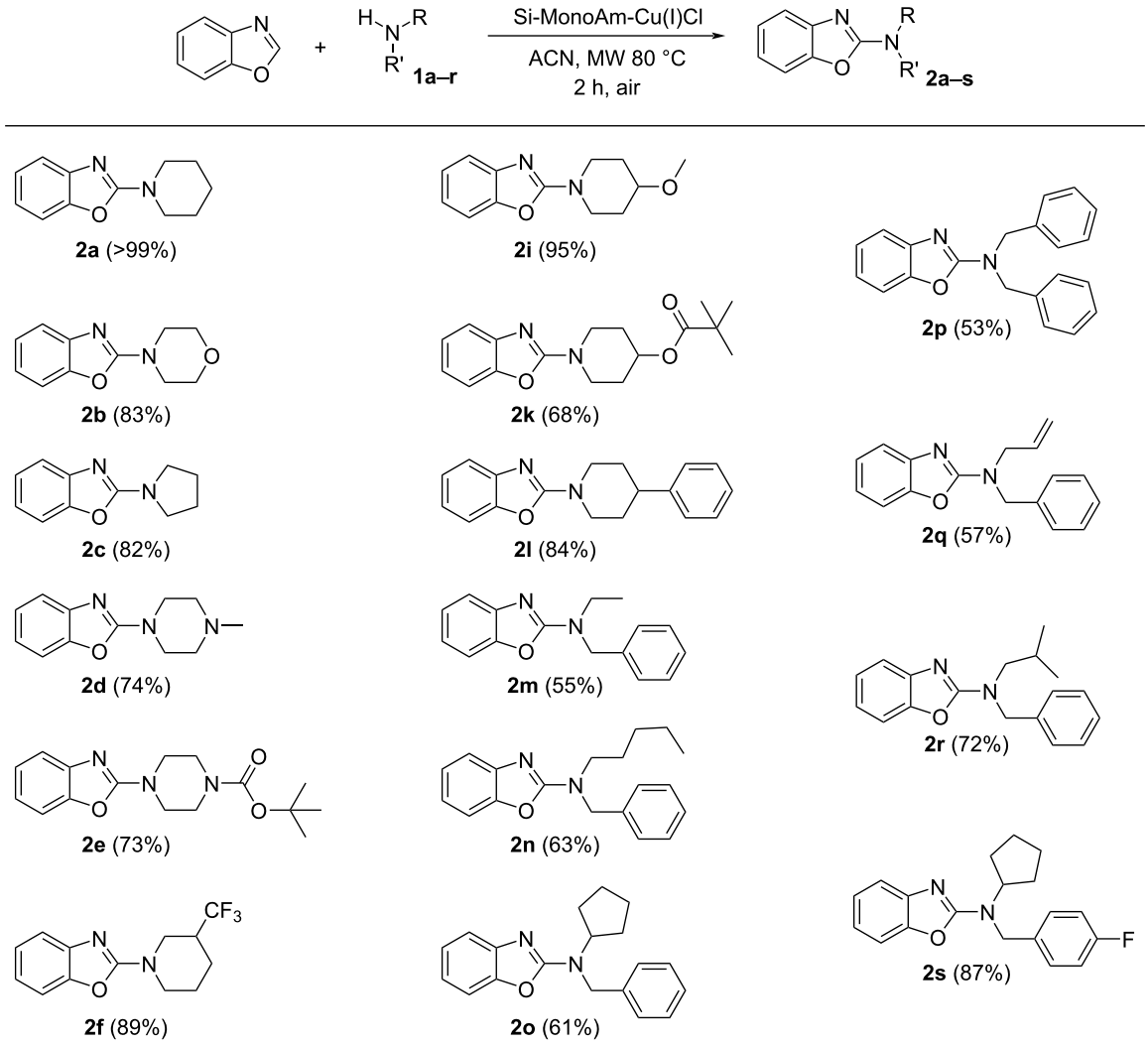

Scheme 3: Scope of the MW-promoted C2-amination of benzoxazole catalysed by Si-MonoAm-Cu(I). Reaction conditions: benzoxazole (1.0 mmol), amine (2 mmol), Cu(I) catalyst (0.2 mmol), acetonitrile (1 mL), MW 80 °C, 2 h, 5 bar air; yields refer to isolated compounds.

When the reaction was carried out using substituted benzoxazoles (see Scheme 4), their reactivity with piperidine was confirmed, as observed with the unsubstituted starting material. However, a slight decrease in the yield of 6-chlorobenzoxazole was noted.

To investigate the heterogeneity of the Si-MonoAm-Cu(I) catalyst, a hot leaching test was carried out. As shown in Figure 4, it was observed that the removal of the solid catalyst after 1 h stopped the reaction. Conversely, when the reaction was allowed to continue in the presence of the catalyst, aerobic oxidation proceeded to completion. This result supports the conclusion that the process operates via true heterogeneous catalysis.

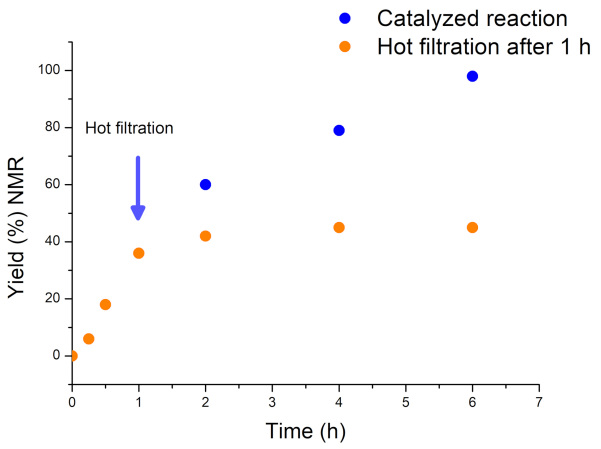

Figure 4: Hot filtration test for the Si-MonoAm-Cu(I)-catalysed C2-amination of benzoxazole with piperidine in acetonitrile at 80 °C. Si-MonoAm-Cu(I) was filtered off after 60 min using a hot filter.

Given the optimal performance of the silica-supported Si-MonoAm-Cu(I) 5 wt % catalyst, we proceeded to measure the amount of copper present using ICP analysis. The catalyst was prepared by reacting silica with CuCl in quantities that, if fully bound to the amino groups, would result in a Cu(I) loading of 5 wt %. The analysis showed that 4.42 ± 0.07 wt % Cu(I) was anchored to the Si-MonoAm support, corresponding to 6.88% CuCl. Similarly, when Si-MonoAm-Cu(II) was analysed, 4.22 ± 0.22 wt % Cu(II) was supported, corresponding to 8.92% $CuCl_2$. These results indicate that the lower activity observed with the supported Cu(II) catalyst is not due to a lower amount of copper on the solid surface, but rather to the intrinsic reactivity of Cu(II) itself. ICP analysis was also carried out on all the prepared catalysts to compare their activity. As shown in Table 4, the loading is consistently about 80% of the amount of copper used in the preparation (theoretical loading). This suggests that optimum catalyst distribution and activity is achieved with 5 wt % supported CuCl.

Table 4: Copper-supported catalysts.

Entry	Product	Theoretical loading (wt %)[a]	Loading by ICP (wt %)[b]
1	Si-MonoAm-Cu(I)	3	2.47 ± 0.09
2	Si-MonoAm-Cu(I)	5	4.42 ± 0.07
3	Si-DiAm-Cu(I)	3	2.42 ± 0.08
4	Si-DiAm-Cu(I)	5	4.21 ± 0.06
5	Si-DiAm-Cu(I)	9	7.63 ± 0.09
6	Si-MonoAm-Cu(II)	5	4.22 ± 0.22
7	Si-DiAm-Cu(II)	5	4.09 ± 0.04
8	Si-DiAm-Cu(II)	9	7.01 ± 0.07

[a]The theoretical loading considers a complete reaction of Cu(I or II) chloride with amino silica derivatives and it refers to wt % Cu (see Table S1 in Supporting Information File 1 for reaction conditions); [b]the loading is measured by ICP analysis and it refers to wt % of Cu.

The two catalysts were also characterised by FTIR and DR UV–vis spectroscopy, to obtain information about the grafted aminopropyl ligand and inserted copper functionality, respectively.

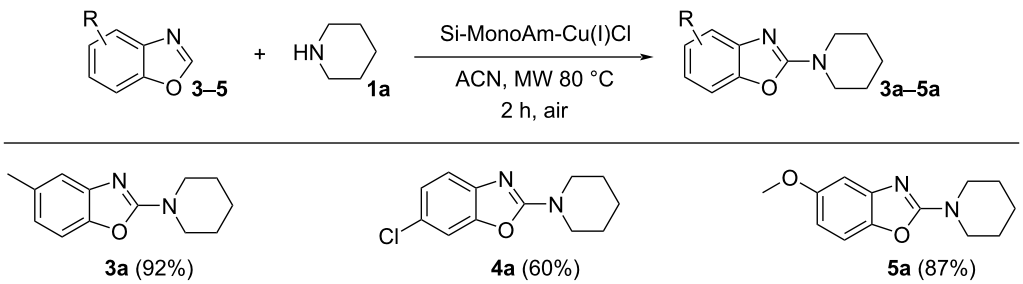

Scheme 4: C2-Amination of substituted benzoxazoles. Reaction conditions: benzoxazole (1.0 mmol), piperidine (2 mmol), Cu(I) catalyst (0.2 mmol), acetonitrile (1 mL), MW 80 °C, 2 h, 5 bar air; yields refer to solated compounds.

Figure 5 shows the FTIR spectra measured on the silica support functionalised with the aminopropyl group, and the subsequent insertion of copper. The successful grafting of the amino ligand is testified by the characteristic stretching and bending modes of the NH_2 group (νNH_2 and δNH_2, at around 3370, 3300 and 1596 cm^{-1}, respectively) and by the νCH_2 and δCH_2 vibrations (curve a) [64,65]. The broad absorption in the high frequency region is characteristic of hydrogen bonding between Si–OH and NH_2 groups in functionalised silica materials. After insertion of Cu(I), small changes in the position and shape of the νNH_2 and δNH_2 bands are observed, which are an indirect indication of the interaction of the amino group with the metal (curve b) [51]. On the other hand, major changes are observed in the spectrum of 5 wt % Si –MonoAm-Cu(II) (curve d). These are particularly informative in the low frequency range, where two new broad bands are observed at 1610 and 1515 cm^{-1}, which are compatible with the presence of $–NH_3^+$ groups (antisymmetric and symmetric bending modes, respectively) [66,67].

The study also aimed to characterise the catalyst Si-MonoAm-Cu(I) after usage in optimised conditions (80 °C, MW, 2 h) with both techniques (curves c in Figure 5). The fingerprints of the aminopropyl groups are still observable in the FTIR spectrum, but new bands are formed at 1660 cm^{-1} and below 1500 cm^{-1}, with a minor component around 1700 cm^{-1}, which could be related to the adsorption of an imino derivative, and, more specifically, νC=N (1660 with shoulder around 1700 cm^{-1}) and δN–H (1590 cm^{-1}, overlapping with the δNH_2 of the aminopropyl groups) in –C=N–H (Figure 5). According to the literature, copper species may contribute to the partial oxidation of amino groups to imino groupds [68], while still retaining the ability of a Schiff base to efficiently bind transition metals, including copper [69].

An advantage of using a heterogeneous catalyst, beyond the easy filtration from the reaction mixture, lies in its possible reuse, multiple times, directly or after performing regeneration. Thus the exhausted Si-MonoAm-Cu(I) catalyst was therefore reused, but, unfortunately, reduced efficiency and selectivity were detected (85% conversion and 60% yield).

For this reason, catalyst regeneration was performed by suspending the catalyst in a solution containing CuCl in THF. Based on optimisation, we observed that the amount of CuCl required for regeneration was lower than in the preparation step; the addition of only 50% of the CuCl amount used for the preparation of the fresh catalyst was required to achieve comparable performance.

The regenerated catalyst was then used in the optimised microwave conditions, which confirmed that its selectivity to the desired product had been restored, as reported in Figure 6. Reuse was performed eight times without observing consistent catalytic deactivation.

FESEM images of Si-MonoAm-Cu(I) before and after usage were also acquired to demonstrate the dispersion of Cu and possible alterations of morphology.

As reported in Figure 7, the silica support is characterised by irregular micrometre-sized agglomerates of nanometre-sized particles. This morphology is not modified after the use of the Si-MonoAm-Cu(I) catalyst in the reaction, as can be seen by

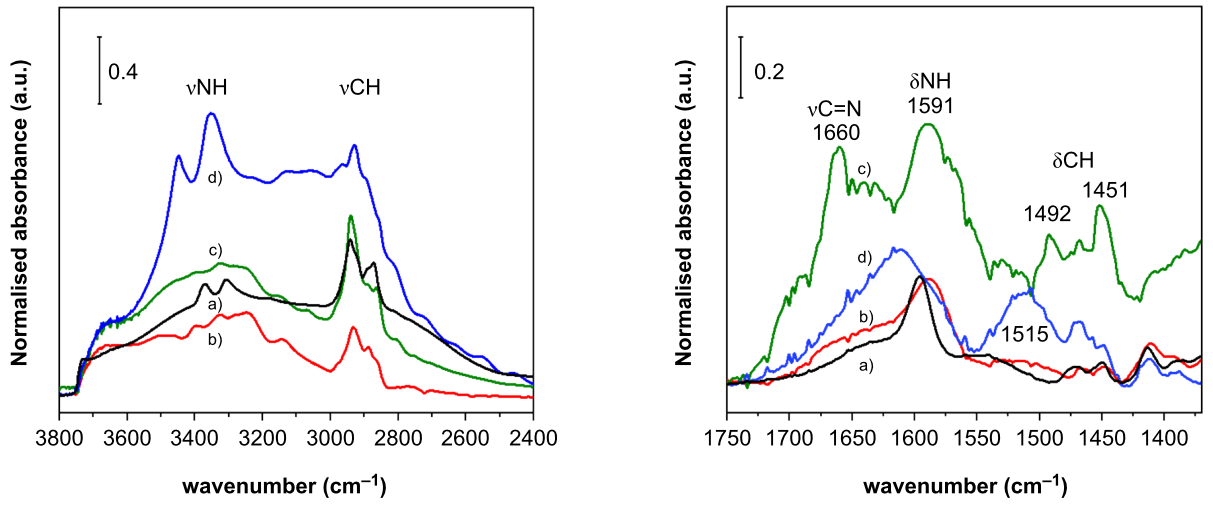

Figure 5: FTIR spectra of samples on the left 3800–2400 cm^{-1} wavenumber on the right 1750–1350 cm^{-1} wavenumber; a) Si-MomoAm, b) 5% Si-MonoAm-Cu(I), c) Si-MonoAm-Cu-used and d) 5% Si-MomoAm-Cu(II).

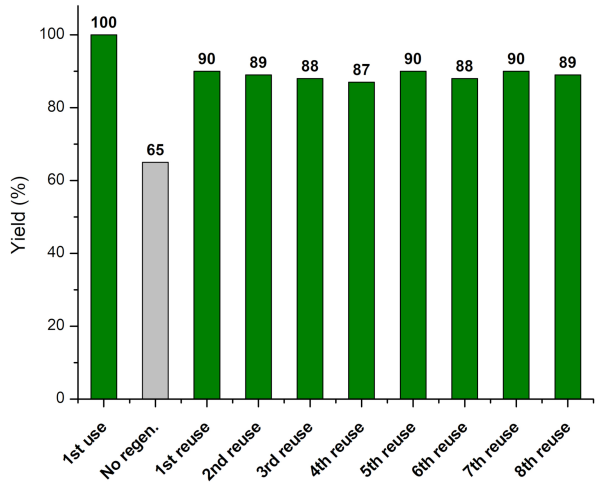

Figure 6: Si-MonoAm-Cu(I) catalyst reuse.

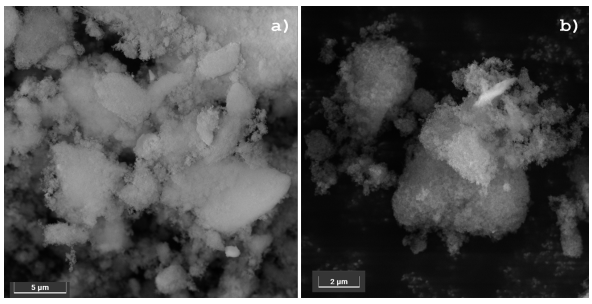

Figure 7: FESEM images of sample a) Si-MonoAm-Cu(I) 5 wt % and c) Si-MonoAm-Cu(I) 5 wt % used.

comparing the corresponding FESEM images of the fresh and used catalyst (see Figure 7a and b). EDS maps show a homogeneous dispersion of copper on the catalyst with this dispersion being maintained after the catalysts is used (panels a and b of Figure 8).

Conclusion

The study demonstrates that the efficient and green direct C–H amination of benzoxazoles can be catalysed by copper chlorine salts in acetonitrile in the absence of any acidic, basic, or oxidising additives. Both CuCl and $CuCl_2$ have been found to be highly efficient in promoting the reaction, on the base of their activity as Lewis acids and weak oxidants. MW irradiation has led to a significant enhancement in reaction rate with the reaction running to completion in only 1.5–2 h.

The derivatisation of silica with pendent primary amino groups has granted it the capability to stably support copper(I) and (II) in a cheap and efficient MW-promoted procedure that has been optimised with solid-supported Cu(I). The heterogeneous process dramatically simplified the work-up of the reaction, allowing the catalyst to be removed from the reaction mixture via simple filtration. Moreover, it led to an increase in the amount of recovered products and to a decrease in the amount of free copper in solution. Catalyst reuse has been explored, and it has been confirmed that reuse up to eight times is possible after proper regeneration. A wide library of derivatives has been easily synthesised with the optimised procedure by reacting benzoxazole and its 5- or 6-substituted derivatives with a variety of cyclic, alkyl and branched secondary amines, probing the protocol's versatility and confirming its potential usefulness.

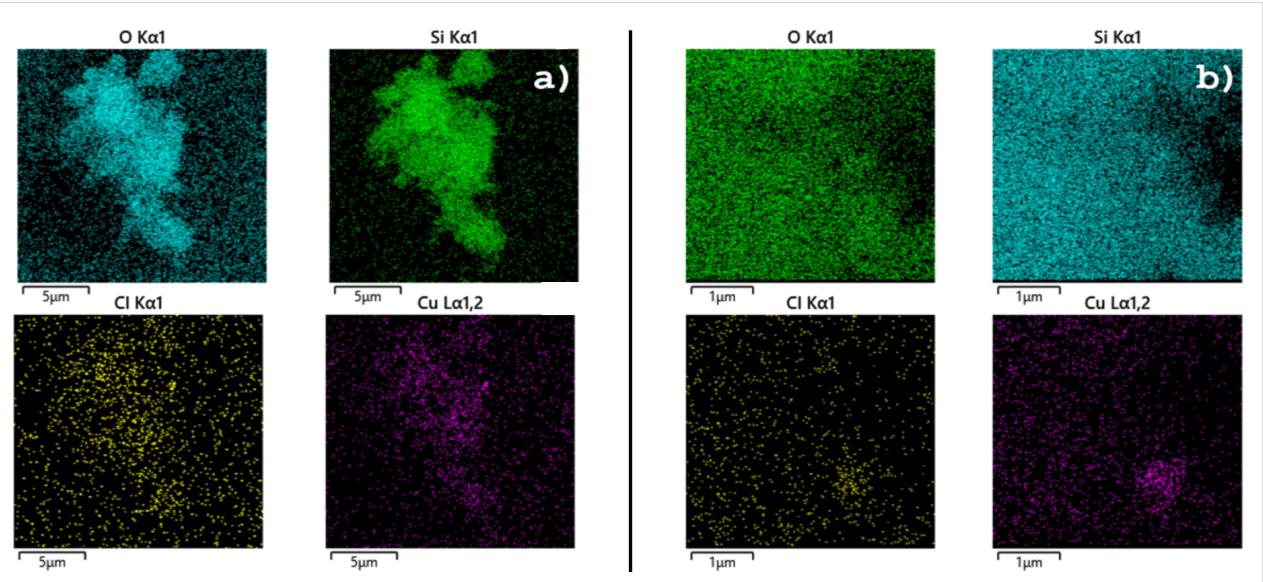

Figure 8: EDS maps of a) Si-MonoAm-Cu(I) and b) Si-MonoAm-Cu(I) used.

This study provides the basis for the application of the protocol in continuous flow systems, such as a continuous heterogeneous reactor known as a packed bed reactor, enabling the production of 2-aminobenzoxazoles at scales ranging from large laboratory batches to pilot scale operations.

Experimental

Materials and methods

All chemicals were purchased from Sigma-Aldrich (Milan, Italy) and used without further purification. SIPERNAT 320 amorphous silica was supplied by Evonik. Reactions were monitored by TLC on Merck 60 F254 (0.25 mm) plates (Milan, Italy), which were visualised by UV inspection and/or by heating after spraying with 0.5% ninhydrin in ethanol or phosphomolybdic acid. Homogeneously catalysed reactions were performed in a professional MW oven (MicroSynth MLS GmbH, Milestone S.r.l.), while heterogeneously catalysed reactions were carried out in a professional MW reactor SynthWave (MLS GmbH, Milestone S.r.l.). The SynthWave MW cavity was filled with 5 bar of air.

The syntheses of amino compounds **1k** and **1m**–**s** and of substituted benzoxazoles **3**–**5** and characterisation of products and solid-supported copper catalysts are reported in Supporting Information File 1.

General procedure for the preparation and regeneration of Si-MonoAm-Cu(I) 5 wt %

Silica SIPERNAT 320 (1 g) was added to a solution of 3-aminopropyltriethoxysilane (2 mmol) in toluene (10 mL). The suspension was sonicated for 2 h in an US bath (Power 200 W, Frequency 80 kHz). The resulting silica was then filtered, washed with toluene and chloroform, and dried under vacuum at room temperature for 12 hours. The derivatised silica was characterised by means of TGA and FTIR.

Si-MonoAm (200 mg) and 16 mg of Cu(I)Cl were dispersed in 4 mL of THF. The mixture was stirred at room temperature for 4 hours, filtered under reduced pressure, and the powder was washed with THF and $CHCl_3$. The resulting product was then kept in a desiccator overnight and fully characterised.

When undergoing regeneration, 200 mg of the exhausted Si-MonoAm-Cu(I) and 8 mg of CuCl were dispersed in 4 mL of THF. The reaction mixture was treated as described for the preparation of the fresh catalyst.

General procedure for synthesis of derivative **2a** by means of homogeneous catalysis

Benzoxazole (0.4 mmol), piperidine (0.63–0.8 mmol), and Cu catalyst (CuCl or $CuCl_2{\cdot}2H_2O$ 0.08 mmol, 20 mol %) were dissolved in CH_3CN (4 mL). The reaction mixture was heated to 60–80 °C for 6 h, after which the solvent was evaporated under reduced pressure. The resulting residue was dissolved in 10 mL of $CHCl_3$, and the organic phase was extracted with 3.5 M aqueous ammonia solution (1 × 10 mL) and distilled water (2 × 10 mL). The organic phase was washed with brine, dried over sodium sulphate, and filtered. The solvent was removed under reduced pressure to obtain a pure product. Where required, the residue was purified by flash chromatography over basic alumina, using a PE/EtOAc 7:3 mixture as the eluent.

When the reaction was performed in a MW oven, the MicroSynth instrument (Milestone) was used. The reaction was performed in an open round-bottomed flask that was heated to 60 °C for 2 h (see Supporting Information File 1 for details on MW procedure setup).

Synthesis of derivatives **2a–s**, **3a**, **4a**, **5a** with Si-MonoAm-Cu(I)

Benzoxazole (0.4 mmol), amine (0.8 mmol) and Si-MonoAm-Cu(I) 5 wt % (100 mg, 0.08 mmol, 20 mol %) were dispersed in CH_3CN (4 mL). The reaction mixture was heated in an oil bath to 80 °C for 6 h, and the catalyst was then removed by filtration and recovered where required. The solvent was evaporated under reduced pressure. The resulting residue was dissolved in 10 mL of $CHCl_3$, and the organic phase was extracted with distilled water (2 × 10 mL). The organic phase was washed with brine, dried over sodium sulphate and filtered. The solvent was removed under reduced pressure. When required, the residue was purified by flash chromatography over basic alumina, using a PE/EtOAc 7:3 mixture as the eluent.

When performed under MW irradiation, the reaction was heated at 80 °C for 2 h. Before the reaction started, the reactor was pressurized with 5 bar of air (for experimental MW setup see Supporting Information File 1).

Supporting Information

Supporting Information File 1

Experimental procedures, compound characterization data, and copies of NMR spectra.
[https://www.beilstein-journals.org/bjoc/content/supplementary/1860-5397-21-108-S1.pdf]

Funding

The University of Turin is warmly acknowledged for its financial support (Rilo 2022).

Author Contributions

Andrei Paraschiv: data curation; investigation; validation; writing – original draft. Valentina Maruzzo: investigation; validation; writing – original draft. Filippo Pettazzi: investigation; methodology; validation. Stefano Magliocco: formal analysis; investigation. Paolo Inaudi: formal analysis; investigation. Daria Brambilla: project administration; resources. Gloria Berlier: data curation; formal analysis; writing – review & editing. Giancarlo Cravotto: project administration; resources; supervision; writing – review & editing. Katia Martina: conceptualization; data curation; supervision; validation; writing – original draft; writing – review & editing.

ORCID® iDs

Andrei Paraschiv - https://orcid.org/0009-0006-5082-9601
Valentina Maruzzo - https://orcid.org/0009-0002-6809-5598
Stefano Magliocco - https://orcid.org/0009-0004-6721-8415
Paolo Inaudi - https://orcid.org/0000-0001-8321-8109
Gloria Berlier - https://orcid.org/0000-0001-7720-3584
Katia Martina - https://orcid.org/0000-0003-2256-5021

Data Availability Statement

All data that supports the findings of this study is available in the published article and/or the supporting information of this article.

Preprint

A non-peer-reviewed version of this article has been previously published as a preprint: https://doi.org/10.3762/bxiv.2025.14.v1

References

1. Abdullahi, A.; Yeong, K. Y. *Med. Chem. Res.* **2024,** *33,* 406–438. doi:10.1007/s00044-024-03190-7
2. Zhang, H.-Z.; Gan, L.-L.; Wang, H.; Zhou, C.-H. *Mini-Rev. Med. Chem.* **2017,** *17,* 122–166. doi:10.2174/1389557516666160630120725
3. Shanbhan, G. S.; Bhargava, A.; Singh, G. P.; Joshi, S. D.; Chundawat, N. *Turk. J. Chem.* **2023,** *47,* 263–279. doi:10.55730/1300-0527.3535
4. Fan, L.; Luo, Z.; Yang, C.; Guo, B.; Miao, J.; Chen, Y.; Tang, L.; Li, Y. *Mol. Diversity* **2022,** *26,* 981–992. doi:10.1007/s11030-021-10213-7
5. Gadakh, S.; Aghav, B.; Teraiya, N.; Prajapati, D.; Kamdar, J. H.; Patel, B.; Yadav, R. *Bioorg. Med. Chem.* **2025,** *122,* 118142. doi:10.1016/j.bmc.2025.118142
6. Huang, G.; Cierpicki, T.; Grembecka, J. *Bioorg. Chem.* **2023,** *135,* 106477. doi:10.1016/j.bioorg.2023.106477
7. Fuentes-Aguilar, A.; Merino-Montiel, P.; Montiel-Smith, S.; Meza-Reyes, S.; Vega-Báez, J. L.; Puerta, A.; Fernandes, M. X.; Padrón, J. M.; Petreni, A.; Nocentini, A.; Supuran, C. T.; López, Ó.; Fernández-Bolaños, J. G. *J. Enzyme Inhib. Med. Chem.* **2022,** *37,* 168–177. doi:10.1080/14756366.2021.1998026
8. Bano, S.; Nadeem, H.; Zulfiqar, I.; Shahzadi, T.; Anwar, T.; Bukhari, A.; Masaud, S. M. *Heliyon* **2024,** *10,* e30102. doi:10.1016/j.heliyon.2024.e30102
9. Sun, L.-Q.; Chen, J.; Takaki, K.; Johnson, G.; Iben, L.; Mahle, C. D.; Ryan, E.; Xu, C. *Bioorg. Med. Chem. Lett.* **2004,** *14,* 1197–1200. doi:10.1016/j.bmcl.2003.12.052
10. Hussain, R.; Rahim, F.; Rehman, W.; Khan, S.; Rasheed, L.; Maalik, A.; Taha, M.; Alanazi, M. M.; Alanazi, A. S.; Khan, I.; Shah, S. A. A. *Arabian J. Chem.* **2023,** *16,* 105244. doi:10.1016/j.arabjc.2023.105244
11. Hili, R.; Yudin, A. K. *Nat. Chem. Biol.* **2006,** *2,* 284–287. doi:10.1038/nchembio0606-284
12. Šlachtová, V.; Chasák, J.; Brulíková, L. *ACS Omega* **2019,** *4,* 19314–19323. doi:10.1021/acsomega.9b02702
13. Wagh, Y. S.; Bhanage, B. M. *Tetrahedron Lett.* **2012,** *53,* 6500–6503. doi:10.1016/j.tetlet.2012.09.064
14. Basak, S.; Dutta, S.; Maiti, D. *Chem. – Eur. J.* **2021,** *27,* 10533–10557. doi:10.1002/chem.202100475
15. Li, C.-J.; Li, Z. *Pure Appl. Chem.* **2006,** *78,* 935–945. doi:10.1351/pac200678050935
16. Heravi, M. M.; Kheilkordi, Z.; Zadsirjan, V.; Heydari, M.; Malmir, M. *J. Organomet. Chem.* **2018,** *861,* 17–104. doi:10.1016/j.jorganchem.2018.02.023
17. Goldberg, I. *Ber. Dtsch. Chem. Ges.* **1906,** *39,* 1691–1692. doi:10.1002/cber.19060390298
18. Sambiagio, C.; Marsden, S. P.; Blacker, A. J.; McGowan, P. C. *Chem. Soc. Rev.* **2014,** *43,* 3525–3550. doi:10.1039/c3cs60289c
19. Jiao, J.; Murakami, K.; Itami, K. *ACS Catal.* **2016,** *6,* 610–633. doi:10.1021/acscatal.5b02417
20. Cho, S. H.; Kim, J. Y.; Lee, S. Y.; Chang, S. *Angew. Chem., Int. Ed.* **2009,** *48,* 9127–9130. doi:10.1002/anie.200903957
21. Pal, P.; Giri, A. K.; Singh, H.; Ghosh, S. C.; Panda, A. B. *Chem. – Asian J.* **2014,** *9,* 2392–2396. doi:10.1002/asia.201402057
22. Wang, J.; Hou, J.-T.; Wen, J.; Zhang, J.; Yu, X.-Q. *Chem. Commun.* **2011,** *47,* 3652–3654. doi:10.1039/c0cc05811d
23. Xu, D.; Wang, W.; Miao, C.; Zhang, Q.; Xia, C.; Sun, W. *Green Chem.* **2013,** *15,* 2975–2980. doi:10.1039/c3gc41206g
24. Kim, J. Y.; Cho, S. H.; Joseph, J.; Chang, S. *Angew. Chem., Int. Ed.* **2010,** *49,* 9899–9903. doi:10.1002/anie.201005922
25. Li, Y.; Liu, J.; Xie, Y.; Zhang, R.; Jin, K.; Wang, X.; Duan, C. *Org. Biomol. Chem.* **2012,** *10,* 3715–3720. doi:10.1039/c2ob25425e
26. Ibrahim, K.; Saranya, P. V.; Anilkumar, G. *ChemistrySelect* **2022,** *7,* e202200601. doi:10.1002/slct.202200601
27. Louillat, M.-L.; Patureau, F. W. *Chem. Soc. Rev.* **2014,** *43,* 901–910. doi:10.1039/c3cs60318k
28. Monguchi, D.; Fujiwara, T.; Furukawa, H.; Mori, A. *Org. Lett.* **2009,** *11,* 1607–1610. doi:10.1021/ol900298e
29. Wang, Q.; Schreiber, S. L. *Org. Lett.* **2009,** *11,* 5178–5180. doi:10.1021/ol902079g
30. Zhao, H.; Wang, M.; Su, W.; Hong, M. *Adv. Synth. Catal.* **2010,** *352,* 1301–1306. doi:10.1002/adsc.200900856
31. Cao, K.; Wang, J.-L.; Wang, L.-H. *Synth. Commun.* **2015,** *45,* 1471–1475. doi:10.1080/00397911.2015.1015035
32. Chen, S.; Zheng, K.; Chen, F. *Tetrahedron Lett.* **2012,** *53,* 6297–6299. doi:10.1016/j.tetlet.2012.09.044
33. Mitsuda, S.; Fujiwara, T.; Kimigafukuro, K.; Monguchi, D.; Mori, A. *Tetrahedron* **2012,** *68,* 3585–3590. doi:10.1016/j.tet.2012.03.001
34. Wang, X.; Sun, K.; Lv, Y.; Ma, F.; Li, G.; Li, D.; Zhu, Z.; Jiang, Y.; Zhao, F. *Chem. – Asian J.* **2014,** *9,* 3413–3416. doi:10.1002/asia.201403052
35. Oda, Y.; Hirano, K.; Satoh, T.; Miura, M. *Org. Lett.* **2012,** *14,* 664–667. doi:10.1021/ol203392r

36. Kawano, T.; Hirano, K.; Satoh, T.; Miura, M. *J. Am. Chem. Soc.* **2010,** *132,* 6900–6901. doi:10.1021/ja101939r
37. Liu, X.-Y.; Gao, P.; Shen, Y.-W.; Liang, Y.-M. *Org. Lett.* **2011,** *13,* 4196–4199. doi:10.1021/ol201457y
38. Matsuda, N.; Hirano, K.; Satoh, T.; Miura, M. *Org. Lett.* **2011,** *13,* 2860–2863. doi:10.1021/ol200855t
39. Zhou, S.; Yang, Z.; Chen, X.; Li, Y.; Zhang, L.; Fang, H.; Wang, W.; Zhu, X.; Wang, S. *J. Org. Chem.* **2015,** *80,* 6323–6328. doi:10.1021/acs.joc.5b00767
40. Yotphan, S.; Beukeaw, D.; Reutrakul, V. *Tetrahedron* **2013,** *69,* 6627–6633. doi:10.1016/j.tet.2013.05.127
41. Tan, Y.; Hartwig, J. F. *J. Am. Chem. Soc.* **2010,** *132,* 3676–3677. doi:10.1021/ja100676r
42. McDonald, S. L.; Hendrick, C. E.; Wang, Q. *Angew. Chem., Int. Ed.* **2014,** *53,* 4667–4670. doi:10.1002/anie.201311029
43. Yoon, H.; Lee, Y. *J. Org. Chem.* **2015,** *80,* 10244–10251. doi:10.1021/acs.joc.5b01863
44. Lee, S.; Lee, Y. *Eur. J. Org. Chem.* **2019,** 3045–3050. doi:10.1002/ejoc.201900335
45. Guo, S.; Qian, B.; Xie, Y.; Xia, C.; Huang, H. *Org. Lett.* **2011,** *13,* 522–525. doi:10.1021/ol1030298
46. Li, Y.; Xie, Y.; Zhang, R.; Jin, K.; Wang, X.; Duan, C. *J. Org. Chem.* **2011,** *76,* 5444–5449. doi:10.1021/jo200447x
47. Cao, K.; Wang, J.-L.; Wang, L.-H.; Li, Y.-Y.; Yu, X.-H.; Huang, Y.; Yang, J.; Chang, G. *Synth. Commun.* **2014,** *44,* 2848–2853. doi:10.1080/00397911.2014.919402
48. Henrion, M.; Smolders, S.; De Vos, D. E. *Catal. Sci. Technol.* **2020,** *10,* 940–943. doi:10.1039/c9cy02153a
49. Aneeja, T.; Neetha, M.; Afsina, C. M. A.; Anilkumar, G. *RSC Adv.* **2020,** *10,* 34429–34458. doi:10.1039/d0ra06518h
50. Dutta, P. K.; Sen, S.; Saha, D.; Dhar, B. *Eur. J. Org. Chem.* **2018,** 657–665. doi:10.1002/ejoc.201701669
51. Calsolaro, F.; Martina, K.; Borfecchia, E.; Chávez-Rivas, F.; Cravotto, G.; Berlier, G. *Catalysts* **2020,** *10,* 1118. doi:10.3390/catal10101118
52. Martina, K.; Calsolaro, F.; Zuliani, A.; Berlier, G.; Chávez-Rivas, F.; Moran, M. J.; Luque, R.; Cravotto, G. *Molecules* **2019,** *24,* 2490. doi:10.3390/molecules24132490
53. Petricci, E.; Cini, E.; Taddei, M. *Eur. J. Org. Chem.* **2020,** 4435–4446. doi:10.1002/ejoc.202000092
54. Beg, M. Z.; Singh, P. K.; Singh, P. P.; Srivastava, M.; Srivastava, V. *Mol. Diversity* **2024,** *28,* 61–71. doi:10.1007/s11030-022-10595-2
55. Ahmad, H.; Hossain, M. K. *Mater. Adv.* **2022,** *3,* 859–887. doi:10.1039/d1ma00840d
56. Martina, K.; Cravotto, G.; Varma, R. S. *J. Org. Chem.* **2021,** *86,* 13857–13872. doi:10.1021/acs.joc.1c00865
57. Li, H.; Zhang, C.; Pang, C.; Li, X.; Gao, X. *Front. Chem. (Lausanne, Switz.)* **2020,** *8,* 355. doi:10.3389/fchem.2020.00355
58. Muley, P. D.; Wang, Y.; Hu, J.; Shekhawat, D. Microwave-assisted heterogeneous catalysis. In *Catalysis;* Spivey, J.; Han, Y.-F.; Shekhawat, D., Eds.; The Royal Society of Chemistry: London, UK, 2021; Vol. 33, pp 1–37. doi:10.1039/9781839163128-00001
59. Crestani, M. G.; Manbeck, G. F.; Brennessel, W. W.; McCormick, T. M.; Eisenberg, R. *Inorg. Chem.* **2011,** *50,* 7172–7188. doi:10.1021/ic2007588
60. Velásquez-Yévenes, L.; Ram, R. *Cleaner Eng. Technol.* **2022,** *9,* 100515. doi:10.1016/j.clet.2022.100515
61. Martina, K.; Baricco, F.; Berlier, G.; Caporaso, M.; Cravotto, G. *ACS Sustainable Chem. Eng.* **2014,** *2,* 2595–2603. doi:10.1021/sc500546e
62. Li, H.; Yang, M.; Zhang, X.; Yan, L.; Li, J.; Qi, Y. *New J. Chem.* **2013,** *37,* 1343–1349. doi:10.1039/c3nj41006d
63. Sung, S.; Braddock, D. C.; Armstrong, A.; Brennan, C.; Sale, D.; White, A. J. P.; Davies, R. P. *Chem. – Eur. J.* **2015,** *21,* 7179–7192. doi:10.1002/chem.201405699
64. Iliade, P.; Miletto, I.; Coluccia, S.; Berlier, G. *Res. Chem. Intermed.* **2012,** *38,* 785–794. doi:10.1007/s11164-011-0417-5
65. Musso, G. E.; Bottinelli, E.; Celi, L.; Magnacca, G.; Berlier, G. *Phys. Chem. Chem. Phys.* **2015,** *17,* 13882–13894. doi:10.1039/c5cp00552c
66. Meng, M.; Stievano, L.; Lambert, J.-F. *Langmuir* **2004,** *20,* 914–923. doi:10.1021/la035336b
67. Long, D. A. *J. Raman Spectrosc.* **2004,** *35,* 905. doi:10.1002/jrs.1238
68. Patil, R. D.; Adimurthy, S. *Adv. Synth. Catal.* **2011,** *353,* 1695–1700. doi:10.1002/adsc.201100100
69. Cozzi, P. G. *Chem. Soc. Rev.* **2004,** *33,* 410–421. doi:10.1039/b307853c

License and Terms